KChIP4a: a biophysical modulator of learning from disappointment

Dissertation for obtaining a doctorate degree in natural sciences
presented to the
Faculty of Biosciences of Goethe University

by

Kauê Machado Costa

from Belém do Pará, Brazil

Frankfurt am Main (2017)

(D 30)

Accepted by the Faculty of Biosciences
of Goethe University as a PhD dissertation

Dean: Prof. Dr. Sven Klimpel

1st expert assessor: Prof. Dr. Manfred Kössl

2nd expert assessor: Prof. Dr. Jochen Roeper

3rd expert assessor: Prof. Dr. Amparo Acker-Palmer

4st expert assessor: Prof. Dr. Bernd Grünewald

Date of disputation: 19.04.2018

“Exploration is in our nature. We began as wanderers, and we are wanderers still.”

— Carl Sagan, Cosmos

Acknowledgements

I would like to express my enduring gratitude to:

- **Prof. Dr. Jochen Roeper** for providing unwavering, outstanding and continuous support, trust, motivation, funding and fun during my stay in his lab.
- **Prof. Dr. Gilles Laurent** for having me in his lab as a rotation student and for providing very instructive comments and support as a member of my thesis committee.
- **Prof. Dr. Manfred Kössl** for being my official PhD thesis supervisor at the Biological Sciences Faculty and for providing insightful comments as a member of my thesis committee.
- **Prof. Dr. Gaby Schneider** for the highly profitable, illuminating and friendly collaboration over the entire course of my thesis.
- **Prof. Dr. Eleanor Simpson** and **Prof. Dr. Eric Kandel** for, in a short conversation in Columbia, providing me with the crucial yet often forgotten insight that neuroscience always needs a solid grounding in behavior.
- **Dr. Mahalakshmi Subramaniam** for teaching me *in vivo* neuronal recordings.
- The other institute PIs, **Dr. Torfi Sigurdsson** and **Dr. Sevil Duvarci** for comments on my project during lab seminars.
- Our workshop team, **Charly Winter**, **Thomas Wulf** and **Hans-Peter Günster** for the assistance with setting up crucial hardware and software for my study.
- **Günther Amrhein** for the excellent support in caring for our animals, and for helping me practice my (still atrocious) German.
- **Maren Baier** and **Dr. Arjan Vink** for all the help and patience with handling my move to Germany and (many) visa renewals.
- **Regina Giegerich** for helping me navigate the treacherous world of German university bureaucracy and making sure we always got what we needed.

- **Carolin Stoffer** for assistance with the German summary.

- **Beatrice Fisher** for providing incredible technical support to my project, helping me write my German summary and for steering our lab with outstanding competence, discipline and care.

- Our technicians **Jasmine Salmen**, **Maria Cristina Giardino** and **Felicia Müller-Braun** for their distinguished technical support.

- My current and former labmates **Navid Farassat**, **Josef Shin**, **Lora Kovacheva**, **Somanath Jaganath, Kanako Otomo, Strahinja Stojanovic, Dennis Schneider, Dr. Poonam Thakur, Alois Kreuzer** and **Sylvie Kutterer** for making my time in the lab highly collaborative, fun and productive.

- My institute colleagues **Pascal Voguel**, **Sebastian Betz** and **Johannes Hahn** for all the fruitful discussions and all the help over the years.

- **Brian Rummel** for providing important suggestions when I was setting up the behavior equipment, and the shared conversations and beers over the course of the years.

- **Ivaylo Borislavov Iotchev**, for being a good friend and always inspiring wild, challenging discussions about basically everything. Our conversations in front of the building are deeply missed.

- **Raquel de Brito Lima**, for the love and companionship over the last two years. I am always learning from and being inspired by you.

- My parents **Jessé Carvalho Costa** and **Silvia Nadia Lopes Machado**, for giving me an amazing childhood, supporting me in everything I always wanted and instilling in me a love for science, knowledge and literature. I am very happy with the opportunities you have provided me and I hope to always make the best use of them.

Table of Contents

List of figures

List of tables

List of abbreviations

A2a: adenosine type 2a receptors

AC1: Ca^{++}/calmodulin–dependent adenylyl cyclase 1

AIS: axonal initial segment

AMPA: α-amino-3-hydroxy-5-methyl-4-isoxazolepropionic acid

AMPAR: α-amino-3-hydroxy-5-methyl-4-isoxazolepropionic acid receptor

AP: action potential

APW: action potential width

ArchT: archaerhodopsin, a light gated proton pump, used for experimental neuronal hyperpolarization

BK: big conductance Ca^{++}-activated K^+ channels

BNST: bed nucleus of the stria terminalis

Ca^{++}: calcium

cAMP: cyclic adenosine monophosphate

CeA: central amygdala

ChR2: channelrhodopsin, a light gated cationic channel used for experimental neuronal depolarization

Cl^-: chloride

CS: conditioned stimulus

CTRL: control

CV: coefficient of variation

D1/D5R: dopamine type 1 and 5 receptor family

D1R: dopamine type 1 receptor

D2/D3/D4R: dopamine type 2, 3 and 4 receptor family

D2R: dopamine type 2 receptor

D3R: dopamine type 3 receptor

D4R: dopamine type 4 receptor

D5R: dopamine type 5 receptor

DA: dopamine

DAT: dopamine transporter

DAT KD: DAT knockdown

DAT KO: full DAT knockout

DNA: deoxyribonucleic acid

DOPA: 3,4-dihydroxyphenylalanine

DRN: dorsal raphe nucleus

dSTR: dorsal striatum

EAG : “ether-a-go-go” family of K^+ channels

EPSP: excitatory post-synaptic potential

EGTA: ethylene glycol-bis(β-aminoethyl ether)-N,N,N',N'-tetraacetic acid

Ex3: exon 3 of the KChIP4 gene

Ex3d: deletion of exon 3 of the KChIP4 gene
Flox: flanked by loxP sites
GABA: γ-aminobutyric acid
GP: globus pallidus
GPe: globus pallidus external capsule
GPi: globus pallidus internal capsule
HCN: hyperpolarization-activated cyclic nucleotide–gated
I_A: A-type K^+ current
I_D: D-type K^+ current
I_h: hyperpolarization-activated depolarizing currents
IL1- α: interleukin 1 α
IP3: inositol 1,4,5-trisphosphate
IPSP: inhibitory post-synaptic potential
K^+: potassium
KChIP: voltage-gated potassium channel interaction protein
KChIP1: voltage-gated potassium channel interaction protein type 1
KChIP2: voltage-gated potassium channel interaction protein type 2
KChIP3: voltage-gated potassium channel interaction protein type 3
KChIP4: voltage-gated potassium channel interaction protein type 4
KChIP4a: voltage-gated potassium channel interaction protein isoform 4a
KCNIP4: alias for the voltage-gated potassium channel interaction gene
KD: knock-down
KI: knock-in
KISD: potassium channel inactivation suppression domain
KO: knock-out
Kv: voltage-gated potassium channel
LDTg: laterodorsal tegmental nucleus
LH: lateral hypothalamus
LHb: lateral habenula
loxP: locus of X-over P1
LTD: long term depression
LTP: long term potentiation
M1: area 1 of motor cortex
M1R: muscarinic type 1 receptors
M2: area 2 of motor cortex
mAHP: medium afterhyperpolarization
MFB: medial forebrain bundle
mGluR: metabotrobic glutamate receptor
MHb: medial habenula
MSN: medium spiny neuron

mRNA: messenger RNA

Na^+: sodium

NAcc: nucleus accumbens

ncRNA: non-coding RNA

NhPR: halorhodopsin, a light gated chloride pump, used for experimental neuronal hyperpolarization

NMDA: N-methyl-D-aspartate

NMDAR: N-methyl-D-aspartate receptor

OFC: orbitofrontal cortex

PAG: periaqueductal gray

PBS: phosphate buffered saline

PCR: polymerase chain reaction

PD: Parkinson's disease

PFA: paraformaldehyde

PKA: protein kinase A

PKC: protein kinase C

PPTg: pedunculopontine tegmental nucleus

RGS: robust Gaussian surprise

RMTg: rostromedial tegmental nucleus

RNA: ribonucleic acid

S1: area 1 of somatosensory cortex

SEM: standard error of mean

SFB: spikes fired in bursts

SK: to small conductance Ca^{++}- activated K^+ channels

SNc: substantia nigra pars compacta

SNr: substantia nigra pars reticulata

STDP: spike timing-dependent plasticity

STN: subthalamic nucleus

STR: striatum

US: unconditioned stimulus

V: associative strength parameter in the Rescorla-Wagner model

V_0: initial associative strength parameter in the Rescorla-Wagner model

V_{max}: maximal associative strength parameter in the Rescorla-Wagner model

V_{min}: minimal associative strength parameter in the Rescorla-Wagner model

VP: ventral pallidum

VTA: ventral tegmental area

WT: wildtype

English Summary

Inhibition of midbrain dopamine (DA) neurons codes for negative reward prediction errors, and causally affects conditioning learning. DA neurons located in the ventral tegmental area (VTA) display two-fold longer rebound delays from hyperpolarizing inhibition in comparison to those in the substantia nigra (SN). This difference has been linked to the slow inactivation of Kv4.3-mediated A-type currents (I_A). One known suppressor of Kv4.3 inactivation is a splice variant of potassium channel interacting protein 4 (KChIP4), KChIP4a, which has a unique potassium channel inactivation suppressor domain (KISD) that is coded within exon 3 of the KChIP4 gene. Previous *ex vivo* experiments from our lab showed that the constitutive knockout of KChIP4 (KChIP4 KO) removes the slow inactivation of I_A in VTA DA neurons, with marginal effects on SN DA neurons. KChIP4 KO also increased firing pauses in response to phasic hyperpolarization in these neurons. Here I show, using extracellular recordings combined with juxtacellular labeling in anesthetized mice, that KChIP4 KO also selectively changes the number and duration spontaneous firing pauses by VTA DA neurons *in vivo*. Pauses were quantified with two different statistical methods, including one developed in house. No other firing parameter was affected, including mean frequency and bursting, and the activity of SN DA neurons was untouched, suggesting that KChIP4 gene products have a highly specific effect on VTA DA neuron responses to inhibitory input.

Following up on this result, I developed a new mouse line (KChIP4 Ex3d) where the KISD-coding exon 3 of KChIP4 is selectively excised by cre-recombinase expressed under the dopamine transporter (DAT) promoter, therefore disrupting the expression of KChIP4a only in midbrain DA neurons. I show that these mice have a highly selective behavioral phenotype, displaying a drastic acceleration in extinction learning, but no changes in acquisition learning, in comparison to control littermates. Computational fitting of the behavioral data with a modified Rescorla-Wagner model confirmed that this phenotype is congruent with a selective increase in learning from negative prediction errors. KChIP4 Ex3d also had normal open field exploration, novel object preference, hole board exploration and spontaneous alternation in a plus maze, indicating that exploratory drive, responses to novelty, anxiety, locomotion and working memory were not affected by the genetic manipulation. Furthermore semi-quantitative IHC revealed that KChIP4 Ex3d mice have increased Kv4.3 expression

in TH^+ neurons, suggesting that the absence of KChIP4a increases the binding of other KChIP variants, which known to increase surface expression of Kv4 channels.

Furthermore, in the course of my experimental study I identified that the most used mouse line where cre-recombinase is expressed under the DAT promoter (DAT-cre KI) has a different behavioral phenotype during conditioning in relation to WT littermate controls. These animals displayed increased responding during the initial trials of acquisition and delayed response latency extinction, consistent with an increase in motivation, which is in line with a decrease in DAT function.

I propose a working model where the disruption of KChIP4a expression in DA neurons leads to an increase in binding of other KChIP variants to Kv4.3 subunits, promoting their increased surface expression and increasing I_A current density; this then increases firing pauses in response to synaptic inhibition, which in behaving animals translates to an increase in negative prediction error-based learning.

Short German Summary

Die Inhibierung von dopaminergen (DA) Mittelhirn-Neuronen kodiert einen negativen Belohnungserwartungsfehler und beeinflusst das konditionelle Lernen. DA Neuronen in ventralen Tegmentalen Regionen (VTA) zeigen im Vergleich zu denen in der Substantia Nigra (SN) zweifach längere Rebound-Verzögerungen nach Hyperpolarisierungsinhibition. Dieser Unterschied wurde mit der langsamen Inaktivierung von Kv4.3-vermittelten A-Typ-Strömen (I_A) in Verbindung gebracht. Ein bekannter Suppressor der Kv4.3-Inaktivierung ist die Spleißvariante des Kaliumkanal-Wechselwirkungsproteins 4 (KChIP4), KChIP4a, das eine einzigartige Kaliumkanalinaktivierungs-Suppressordomäne (KISD) aufweist, die durch das Exons 3 des KChIP4-Gens (KCNIP4) kodiert ist. Vorangegangene Ex-vivo-Experimente aus unserem Labor zeigten, dass das konstitutive Knockout von KChIP4 (KChIP4 KO) die langsame Inaktivierung von I_A in DA-Neuronen der VTA aufhebt mit marginalen Auswirkungen auf SN-DA-Neuronen. KChIP4 KO erhöhte auch die Aktivitätspausen als Reaktion auf phasische Hyperpolarisation in diesen Neuronen. Hier zeige ich unter Verwendung extrazellulärer Aufnahmen, kombiniert mit einer juxtazellulären Markierung bei anästhesierten Mäusen, dass KChIP4 KO auch selektiv die Anzahl und Dauer spontaner Aktivitätspausen durch VTA DA-Neuronen in vivo verändert. Die Pausen wurden mit zwei verschiedenen statistischen Methoden quantifiziert, darunter eine die in unseren Labor etabliert wurde. Kein anderer Aktivitätsparameter wird beeinflußt, einschließlich der Durchschnittsfrequenz und der schnellen phasischen Entladungen (sog. Bursts). Auch die Aktivität der SN DA-Neuronen bleibt unangetastet, was darauf hindeutet, daß KChIP4-Genprodukte einen spezifischen Effekt auf VTA-DA-Neuron haben, welche für den inhibitorischen Input verantwortlich sind.

Im Anschluss an diese Ergebnisse charakterisierte ich eine neue Mauslinie (KChIP4 Ex3d), in der das KISD-kodierende Exon 3 von KChIP4 selektiv durch eine Cre-Rekombinase unter Kontrolle des Dopamin-Transporter (DAT)-Promotors herausgeschnitten wurde. Somit wurde das Exon 3 nur in dopaminergen Mittelhirn Neuronen eliminiert. Ich zeigte, dass dieses Mausmodell einen hochselektiven Verhaltensphänotyp aufweist, der sich in einer drastischen und selektiven Beschleunigung des Extinktionslernen zeigt. Der zeitliche Verlauf der Verhaltensdaten wurde erfolgreich durch ein modifiziertes Rescorla-Wagner-Modell

beschrieben, was die Aussage bestärkt, dass dieser Phänotyp durch einen selektiven Anstieg des Lernens in Folge negativer Vorhersagefehler verursacht wird. KChIP4 Ex3d Mäuse zeigen dagegen eine normale Offenfeld Exploration, sowie Präferenz für neuartige Objekte, und unverändertes Verhalten im Lochplattentest und beim spontanen Wechsel in einem Plus-Labyrinth-Test. Dies deutet darauf hin, dass sowohl die explorative Motivation, wie auch die Reaktionen auf Neuheit und Angstzustände, Fortbewegung sowie Arbeitsgedächtnis durch die genetische Manipulation nicht beeinflusst wurden. Darüber hinaus zeigte die semi-quantitative immunohistologische Experimente, dass KChIP4 Ex3d-Mäuse eine erhöhte Kv4.3-Expression in TH^+-Neuronen aufweisen, was darauf hindeutet, dass die Abwesenheit von KChIP4a die Bindung anderer KChIP-Varianten erhöht, von denen bekannt ist, dass sie die Oberflächenexpression von Kv4-Kanälen erhöhen.

Außerdem konnte im Rahmen dieser experimentellen Studie festgestellt werden, dass die am häufigsten verwendete Mauslinie, bei der die Cre-Rekombinase unter dem DAT-Promotor exprimiert wird (DAT-cre KI), einen veränderten Verhaltensphänotyp bei der Konditionierung in Vergleich zu Wildtyp-Geschwisterkontrollen aufweist. Diese Tiere zeigen verstärkte Reaktionen während der anfänglichen Versuche des Erwerblernens und eine Verzögerung in des Latenz der Extinktion. Diese Beobachtungen stimmen mit der Zunahme der Motivation überein, die wiederum durch die Reduktion des DAT Funktion im cre-Modell verursacht sein könnte. Ich schlage zusammenfassend ein Arbeitsmodell vor, bei dem die Störung der KChIP4a-Expression in DA-Neuronen zu einer Erhöhung der Bindung anderer KChIP-Varianten an Kv4.3-Untereinheiten führt, was eine erhöhte Oberflächenexpression fördert und die I_A-Stromdichte erhöht. Dadurch erhören sich die Aktivitätspausen als Reaktion auf synaptische Hemmung, welche selektiv das Lernen durch negative Vorhersagefehler verstärkt.

Detailed German Summary

Der katecholaminerge Neurotransmitter Dopamin reguliert die Erregbarkeit und Plastizität von Synapsen durch seine Wirkung an zwei Rezeptor Hauptklassen: D1-Typ Rezeptoren (D1R), die überwiegend exzitatorisch sind, und die primär inhibitorischen D2-Typ Rezeptoren (D2R). In Säugetieren befinden sich die meisten DA Neuronen im Mesencephalon, im ventralen Tegmentum (VTA) und in der Subtantia Nigra (SN), die vor allem postsynaptischen Dopaminrezeptoren finden sich in hoher Konzentration vor allem im Striatum. Störungen des dopaminergen Systems sind ausschlaggebend für einige neurologische und psychiatrische Erkrankungen. Aktivität in striatalen dopaminergen Zielregionen hängt kausal mit Lernprozessen zusammen, insbesondere mit Konditionierungen und Lernen durch Belohnung, d.h. Lernprozesse durch die ein Verhalten mit einem sensorischen Reiz (klassische Konditionierung) oder einer Handlung (operante Konditionierung) assoziiert wird. Dopaminerge Neuronen kodieren die Differenz zwischen erwarteten und tatsächlich erlebter Belohnung (verursacht durch Reize oder eigene Handlungen). Dieser sogenannte Belohnungserwartungsfehler stellt ein zentrales Lernsignal im Gehirn dar.

Dopaminerge Neuronen sind spontanaktive Schrittmacher. Unerwartete Belohnungen (d.h. positiven Belohnungserwartungsfehler) führen zu schnellen phasischen Entladungen (sog. Bursts;), während das Ausbleiben einer erwarteten Belohnung (d-h. negativen Belohnungserwartungsfehler) zur Hemmung von dopaminerger Aktivität führt (sog. Pausen); Diese Pausen sind kausal relevant für das Lernen aus enttäuschten Belohnungserwartungen. Insbesondere wird davon ausgegangen, dass phasisch zunehmende, dopaminerge Aktivität von niederaffinen striatalen D1R Rezeptoren detektiert wird, während striatale D2R Rezeptoren in Folge von Aktivitätspausen deaktiviert werden. Das Erlernen von Assoziationen zwischen Belohnungen und vorangehenden Stimuli zeigt sich durch eine Verstärkung des konditionierten Verhaltens und eine vermehrte Suche nach der erwarteten Belohnung. Das Ausbleiben einer erwarteten Belohnung führt hingegen zu einer Reduktion des konditionierten Verhaltens und wird Extinktion genannt.

Die biophysikalischen Eigenschaften dopaminerger Neuronen bestimmen, wie diese auf verhaltens-relevante Exzitation und Inhibition reagieren. Verschiedene dopaminerge Subpopulationen exprimieren verschiedene Ionenkanäle, was dadurch

unterschiedliche Arten von synaptischer Integration ermöglicht. Wie diese Diversität intrinsicher Erregbarkeit durch molekulare Mechanismen definiert wird und welche verhaltensrelevanten Konsequenzen sie nach sich zieht, ist jedoch nicht ausreichend geklärt. Die vorliegende Studie untersucht wie eine alternative Spleißvariante einer auxilären K^+ Kanal Untereinheit, die möglicherweise für inhibitorische Integration zuständig ist, die Dynamik des Lernens aus Enttäuschung reguliert.

Inspiriert wurde die Studie durch die Beobachtung, dass dopaminerge Neuronen in der ventralen tegmentalen Regionen (VTA) im Vergleich zu denen in der Substantia Nigra (SN) zweifach längere Rebound-Verzögerungen nach Inhibition zeigen. Dieser Unterschied wurde mit der langsamen Inaktivierung von Kv4.3-vermittelten A-Typ-Strömen (I_A) in Verbindung gebracht. Ein bekannter Suppressor der Kv4.3-Inaktivierung ist die Spleißvariante A des Kaliumkanal-Interaktionsproteins 4 (KChIP4a), welches eine besondere Kaliumkanalinaktivierungs-Suppressordomäne (KISD) enthält, die durch das Exons 3 des KChIP4-Gens (KCNIP4) kodiert ist. Vorangegangene Ex-vivo-Experimente aus unserem Labor zeigten, dass das komplette Knockout von KChIP4 (KChIP4 KO) die langsame Inaktivierung von I_A in DA-Neuronen der VTA aufhebt, während sich die I_A Ströme in den DA-Neuronen der SN nur unwesentlich verändern. In Folge waren auch in vitro die post-inhibitorischen Aktivitätspausen bei DA VTA Neuronen in KChIP4 KO Mäusen im Vergleich zu Wildtypen verlängert.

Hier zeige ich unter Verwendung extrazellulärer Aufnahmen, kombiniert mit einer juxtazellulären Markierung und post-hoc histologischer Zell Identifikation, in Isofluran anästhesierten Mäusen, dass KChIP4 KO auch selektiv die Anzahl und Dauer von in vivo Aktivitätspausen von VTA DA-Neuronen im Vergleich zu Wildtyp Mäusen verändert. Die Pausen wurden mit zwei verschiedenen statistischen Methoden quantifiziert: zum einen, die „Robust Gaussian Surprise“ (RGS) Methode und zum anderen einen Algorithmus, den ich speziell zur Pausendetektion in diesen Datensätzen entwickelt habe. Letzerer beruht den nicht-parametrischen Eigenschaften der Verteilungen von inter-spike Intervalen (ISI). Die Reduktion der Pausen konnte auch durch die Messung der maximal Werte, der Schiefe und der Kurtosis der ISI Verteilung aufgezeigt werden; verglichen mit Wildtyp Mäusen waren all diese Werte kleiner. Kein anderer Aktivitätsparameter wurde beeinflusst, einschließlich der Durchschnittsfrequenz und der schnellen phasischen Entladungen.

Die Aktivität von SN Neuronen war ebenfalls unverändert. Dies weist darauf hin, dass die Gen Produkte des KChIP4 einen spezifischen Effekt auf die Wirkung von inhibitorischen Input auf VTA Zellen haben.

Im Anschluss an diese Ergebnisse charakterisierte ich eine neue Mauslinie (KChIP4 Ex3d), in der das KISD-kodierende Exon 3 von KChIP4 selektiv durch eine Cre-Rekombinase unter Kontrolle des Dopamin-Transporter (DAT)-Promotors herausgeschnitten wurde. Somit wurde das Exon 3 nur in dopaminergen Mittelhirn Neuronen eliminiert. Diese Tiere und ihre Kontroll Wurfgeschwister wurden einem Lernprotokoll unterzogen, wobei ein Ton als Prädiktor für eine Belohnung mit Zuckerwasser diente. Um die Stärke der Assoziation von Prädiktor und Belohnung zu quantifizieren, wurde zum einen die Zeit gemessen, welche die Maus mit ihrer Schnauze im Flüssigkeitsspender verbrachte, zum anderen die Latenz mit der die Maus nach dem Ton den Flüssigkeitsspender aufsucht. Um die Extinktion zu testen, wurde den Tieren der Ton ohne darauffolgende Belohnung präsentiert. Die KChIP4 Ex3d Mäuse wiesen eine selektive Beschleunigung des Extinktions-Lernens auf, zeigten jedoch keine weiteren Unterschiede für andere Lernformen und Verhaltensweisen. Der Extinktionsphänotyp der KChIP4 Ex3d Mäuse manifestierte sich erst nach dem ersten Ausbleiben der Belohnung, so dass es sich in der Tat um eine selektive Veränderung des Lernverhaltens und nicht um eine grundsätzliche Störung der Motivation handelt.

Eine detaillierte Analyse des Verhaltens der Mäuse zeigte zudem, dass nur die Anzahl der Besuche des Flüssigkeitsspenders, nicht aber deren jeweilige Dauer bei den KChIP4 Ex3d Mäusen abgenommen hatte. Dies bedeutet, dass diese Mäuse sich seltener entscheiden in der Extinktionspause den Belohnungsbereich aufzusuchen.

Zusätzlich wurde von mir eine modifizierte Variante des Rescorla-Wagner Models auf die experimentellen Daten angepasst. Dies ermöglichte eine unabhängige Abschätzung der positiven und negativen Belohnungserwartungsfehler. Diese Analyse bestärkte die These, dass der beobachtete Phänotyp durch eine selektive Steigerung des Lernens durch negative Belohnungserwartungsfehler verursacht wurde, da bei den modellierten Daten lediglich die Lernrate für den negativen Belohnungserwartungsfehler für die KChIP4 Ex3d Mäuse erhöht war. Wichtig ist hier anzumerken, dass die Qualität der Modelanpassung für beide Genotypen gleich gut war.

Der Knockout der 3. Exons von KChiP4 hatte dagegen keinerlei Auswirkungen auf spontane, Dopamin-abhängige Verhaltensweisen. Die KChIP4 Ex3d Mäuse verhielten sich normal bei der Exploration eines Offenfeldes, bei der Präferenz für neue im Vergleich zu bereits bekannten Objekten, sowie bei der Exploration eines Lochbrettes und der Nutzung des Arbeitsgedächtnisses. Desweiteren zeigte eine semi-quantitative, immunohistologische Untersuchung der Kv4.3 Kanaluntereinheit, dass deren Expression in den dopaminergen Neuronen der KChIP4 Ex3d Mäusen zugenommen hatte. Dies könnte bedeuten, dass die Abwesenheit von KChIP4a die Expression und das Trafficking von Kv4.3 Kanalkomplexen erhöhte.

Außerdem konnte im Rahmen dieser experimentellen Studie festgestellt werden, dass eine häufig verwendete cre-Mauslinie zur selektive Expression in dopaminergen Mittelhirnneuroen, bei der die Cre-Rekombinase unter dem DAT-Promotor exprimiert wird (DAT-cre KI), einen im Vergleich zu Wildtyp-Geschwisterkontrollen veränderten Verhaltensphänotyp bei der Konditionierung aufweist. Diese DAT-cre KI Tiere zeigen verstärkte Reaktionen zu Beginn des Belohnungslernens und Verzögerungen beim Extinktionslernen. Diese Beobachtungen sind im Einklang mit der Annahme einer bei diesem Genotyp erhöhten Motivation, die Folge eines hyperdopaminergen Phänotyps nach Reduktion der DAT Funktion sein könnte. Dieser Befund sollte die genauere Erforschung von Physiologie und Verhalten dieser Mauslinie anregen. Es wäre ins besondere wichtig zu testen, wie diese Tiere auf DAT-blockierende Stimulanten, wie Kokain, reagieren und dazu die Expressions Muster von DAT und dopaminerger Rezeptoren in verschiedenen Arealen des Striatums zu bestimmen.

Ich schlage zusammenfassend ein Arbeitsmodell vor, bei dem der Verlust der KChIP4a-Expression in DA-Neuronen zu einer Erhöhung der Bindung anderer KChIP-Varianten an Kv4.3-Untereinheiten führt, was eine erhöhte Oberflächenexpression des Kanalkomplexes und damit eine erhöhte I_A-Stromdichte nach sich ziehen könnte. In Folge, wären verlängerte Aktivitätspausen nach synaptischer Hemmung zu erwarten. Dies würde selektiv das Lernen durch negative Vorhersagefehler verstärken, so wie es in dieser Studie beobachtet wurde . Die genauen zellulären und molekularen Veränderungen, die sich aus dem Verlust von KChip4a ergeben, sollten in zukünftigen Studien detaillierter untersucht werden, u.a. mit ex vivo elektrophysiologischen Methoden, Einzelzell-RT-PCR, proteomischer Analysen und Elektronenmikroskopie. Der KChIP4a-abhängige Mechanismus könnte

auch andere zelluläre Prozesse für Dopamin-abhängiges Lernen, wie z.B. die synaptische Plastizität dopaminerger Neuronen und verändern. Des Weiteren, haben genomweite Assoziationsstudien verschiedene KCNIP4-Varianten mit einer Vielzahl psychiatrischer Erkrankungen in Verbindung gebracht (ADHS, Depressionen und Drogenabhängigkeit). Es wäre hier interessant zu untersuchen, ob KChIP4 Ex3d Mäuse charakteristische Reaktionen auf krankheitsrelevante Stressfaktoren zeigen und ob krankheitsassoziierte Varianten des menschlichen KCNIP4 Gens die relative Expression von KChIP4a beeinträchtigen können.

1. Introduction

Dopamine (DA) was first described by George Barger and Henry Dale (1910) as a sympathomimetic, epinephrine-like monoamine compound. This compound remained in relative obscurity, believed to be a mere precursor of norepinephrine, for the next four decades, until its neurotransmitter function was discovered by Arvid Carlsson and collaborators, a landmark finding that earned Carlsson the 2000 Nobel Prize in Physiology and Medicine (Carlsson et al., 1957, 1958; Benes, 2001). Currently, DA is known to have an essential role in nearly all cognitive functions, including motor control, motivation and learning (Schultz et al., 1997; Redgrave et al., 2010; Berridge, 2012). Dysfunctions in DA neurotransmission are a hallmark of several psychiatric and neurological disorders and pharmacological modulation of DA synthesis and DA receptors are today widely used in clinical practice (Grace, 1992, 2016; Hornykiewicz, 2002a). DA is also one of the oldest neurotransmitters; its function is extremely conserved across multiple species, regulating similar motivational and learning processes from roundworms and flies to man (Hills, 2006; Strausfeld and Hirth, 2013; Yamamoto and Seto, 2014).

1.1. The midbrain dopamine system

1.1.1. Chemistry and biosynthesis of dopamine

DA is a catecholamine, i.e. a monoamine with a catechol group (benzene with two hydroxyl side groups at carbons 1 and 2). It comprises 80% of the catecholamine content in the brain, making it the predominant neurotransmitter of its kind (Vallone et al., 2000). DA is derived from the amino acid tyrosine and is biochemically related to other monoamine transmitters like norepinephrine and octopamine (Barron et al., 2010). The chemical structure of DA and its full biosynthesis pathway are illustrated in Figure 1.1. The rate-limiting enzyme for DA production is tyrosine-hydroxylase (TH), which forms the catechol group by adding a hydroxyl group to tyrosine, converting it to 3,4-dihydroxyphenylalanine (DOPA). In mammals, only the left-handed chiral form, L-DOPA, is synthetized. L-DOPA is converted into DA by DOPA-decarboxylase, which removes the carboxyl group and converts it into a monoamine. DA can also be converted to norepinephrine in the presence of dopamine-β-hydroxylase, which means that both neurotransmitters share the TH and DOPA-decarboxylase pathways.

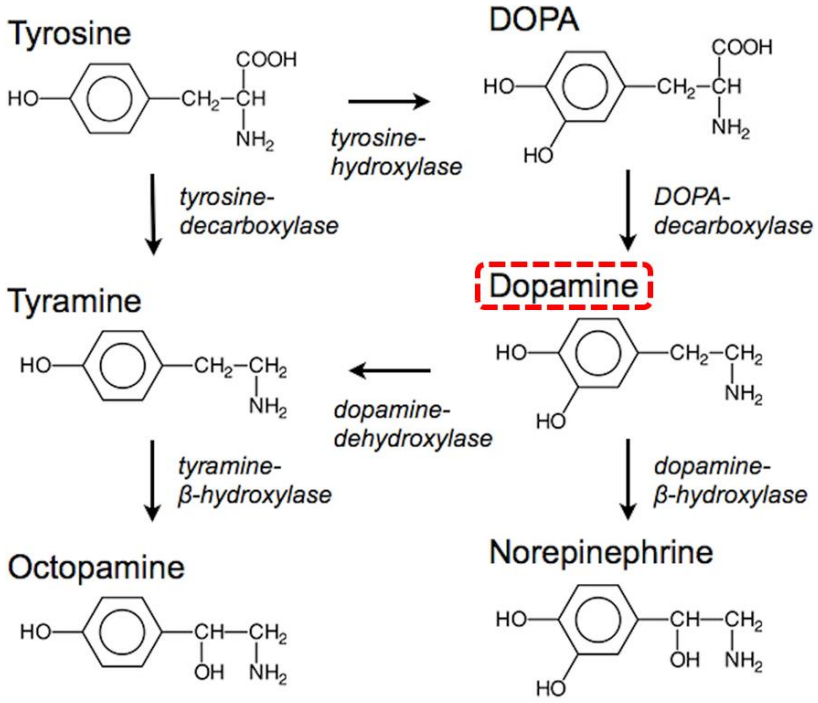

Figure 1.1. Biosynthetic pathway of DA production.
DA is derived from DOPA through the action of DOPA-decarboxylase, and is structurally similar to the neurotransmitters norepinephrine and octopamine. TH catalyzes the conversion of tyrosine to DOPA and is the rate limiting enzyme for DA production. Note that TH is part of the synthetic pathway of both DA and norepinephrine. Adapted from Barron et al. (2010).

1.1.2. Dopamine receptors

Once synthesized, DA is packaged into vesicles by the vesicular monoamine transporter 2 (VMAT2) and transported to their cellular release sites (Iversen et al., 2010). Once released from the pre-synaptic neuron, DA interacts with at least five different metabotropic G-protein coupled receptor subtypes: D1, D2, D3, D4 and D5 receptors. These five subtypes can be divided in two major families based on their biochemical properties: the D1R family, composed of D1 and D5, are coupled to G_s, G_q or G_{Olf} and have a relatively longer third cytoplasmic loop and carboxyl tail; and the D2R family, composed of D2, D3 and D4, are coupled to G_i or G_o and have a shorter third cytoplasmic loop and carboxyl tail (Jackson and Westlind-Danielsson, 1994; Vallone et al., 2000; Seamans and Yang, 2004; Beaulieu and Gainetdinov, 2011). D1 family receptors increase cyclic adenosine monophosphate (cAMP) production by adenylyl cyclase, while D2 family receptors decrease cAMP levels. The D1 and D2 receptors (D1R and D2R, respectively) have the highest and most extensive expression patterns of all the DA receptors in the brain, and as a consequence are the best understood receptor subtypes (Vallone et al., 2000).

With respect to binding of dopamine, both, D1Rs and D2Rs display high, nanomolar, and low, micromolar, affinity states, which can be controlled by the binding of exogenous guanine nucleotides (Richfield et al., 1989). *In vivo*, most D2Rs (≈ 75%) exist in the high-affinity state, binding to DA with a dissociation constant (K_D) in the range of 10-50 nM. D1Rs, on the other hand, are mainly (≈ 80%) in the low-affinity state, with DA K_D in the range of 1-5 µM. This means that the effective DA affinity of D2Rs is nearly 100-fold greater than that of D1Rs. Consequently, D1R need much larger DA concentrations for effective activation (Missale et al., 1998; Iversen et al., 2010). Because of this disparity in DA affinity, it is thought that D2Rs are preferentially sensitive to tonic, low nanomolar concentrations of DA and therefore constitutively activated by baseline levels of extracellular DA, as well as deactivated only by transient decreases in DA levels. D1Rs, on the other hand, are not activated by baseline levels of DA, but require phasic micromolar-range increases in extracellular DA concentration to be activated (Dreyer et al., 2010; Dodson et al., 2016). It is important, however, to emphasize that this functional dichotomy is neither absolute nor static; for example, there is evidence that some D2R-expressing MSN that are sensitive to tonic DA levels are also phasically inhibited by fast increases in DA concentration, likely due to the presence of D2Rs with different affinity states within the same cell (Marcott et al., 2014)

1.1.3. Anatomy of the midbrain dopamine system

In mammals, DA neurons are found in the retina, hypothalamus, olfactory bulb, brainstem and reticular formation, but the majority of DA neurons cluster in the ventral midbrain within the substantia nigra (SN), especially the pars compacta (SNc) subregion, and the ventral tegmental area (VTA), also called areas A9 and A10 respectively (Dahlstroem and Fuxe, 1964; German and Manaye, 1993). These neurons comprise a population of around 135 thousand in the SN and 40 thousand in the VTA of humans, and 5-10 thousand in the SN and 8-15 thousand in the VTA of mice (Hirsch et al., 1988; Nelson et al., 1996; Zaborszky and Vadasz, 2001). Midbrain DA neurons have been found to be essential to the control of movement, motivation, learning and cognition. In order to understand how their physiology relates to these behavioral components it is crucial to understand their anatomical connectivity. These neurons send dense projections to multiple forebrain regions via the medial forebrain bundle (MFB); they are densely innervated by long-range

projections and their activity is controlled by the combined excitatory glutamatergic and inhibitory γ-aminobutyric acid (GABA) inputs of several brain regions, including the prefrontal cortex (PFC), the lateral habenula (LHb), the rostromedial tegmental nucleus (RMTg) and others (Figure 1.2).

In addition, DA neuron activity is strongly regulated by neuromodulatory inputs; these include norepinephrine input from the pontine locus coeruleus (LC); serotonin input from the dorsal raphe nucleus (DRN); cholinergic input from the laterodorsal tegmental (LDTg) and pedunculopontine tegmental (PPTg) nuclei; neuropeptidergic input from among others the hypothalamus (e.g. oxytocin, neurotensin, orexin) as well as modulation by peripheral hormones such as insulin, leptin or ghrelin (Simon et al., 1979; Oakman et al., 1995; Korotkova et al., 2003; Abizaid, 2009; Watabe-Uchida et al., 2012; Ogawa et al., 2014; Beier et al., 2015; Dautan et al., 2016; Ogawa and Watabe-Uchida, 2017; Xiao et al., 2017). These neuromodulatory inputs are thought to act as mediators of state-specific changes in DA signaling. For example, orexin and ghrelin receptors in VTA DA neurons are thought to change feeding-related DA signals according to the animal's hunger levels and nicotinic cholinergic receptors in VTA DA neurons may mediate the rewarding effects of expected uncertainty in unstable environments (Abizaid, 2009; Moorman and Aston-Jones, 2010; Cone et al., 2014; Naude et al., 2016). Given their role in state-dependent adaptation, these neuromodulatory mechanisms may play essential roles in homeostasis and disease. As an example, a recent study has suggested that norepinephrine inputs to VTA DA neurons contribute to the behavioral adaptations to chronic stress (Isingrini et al., 2016).

Midbrain DA neurons are crucial nodes of the basal ganglia (BG) and limbic systems (Kandel et al., 2000; Iversen et al., 2010; Redgrave et al., 2010). The BG are a group of interconnected subcortical nuclei in the forebrain that includes the striatum, globus pallidus (GP), ventral pallidum (VP), subthalamic nucleus (STN) and SN pars reticulata (SNr). The limbic system is composed by structures involved in motivational and emotional control, including the hippocampus, amygdala and hypothalamus (Kandel et al., 2000; Ikemoto et al., 2015). The region with the densest DA innervation is the striatum, which is divided in two main sub-compartments. The ventral striatum, comprised of the nucleus accumbens (NAcc) and the olfactory tubercle, is involved primarily in the motivation of goal-directed behaviors, learning

and emotional control and receives dense inputs from limbic structures such as the amygdala and hippocampus and cortical regions involved in executive control, such as the PFC and OFC. The NAcc is further subdivided in three main regions, the NAcc core, medial shell and lateral shell, which have distinct functional connectivity and behavioral roles (Ambroggi et al., 2011; Saddoris et al., 2015). For example, blocking D1Rs and D2Rs in the NAcc core, but not the medial shell, selectively impairs the acquisition of cue-reward associations (Di Chiara, 2002; Ito and Hayen, 2011). The dorsal striatum (which in primates is further subdivided in the caudate and putamen) is involved primarily in motor control, action selection and habit formation, and is connected mainly to the motor cortex and BG nuclei.

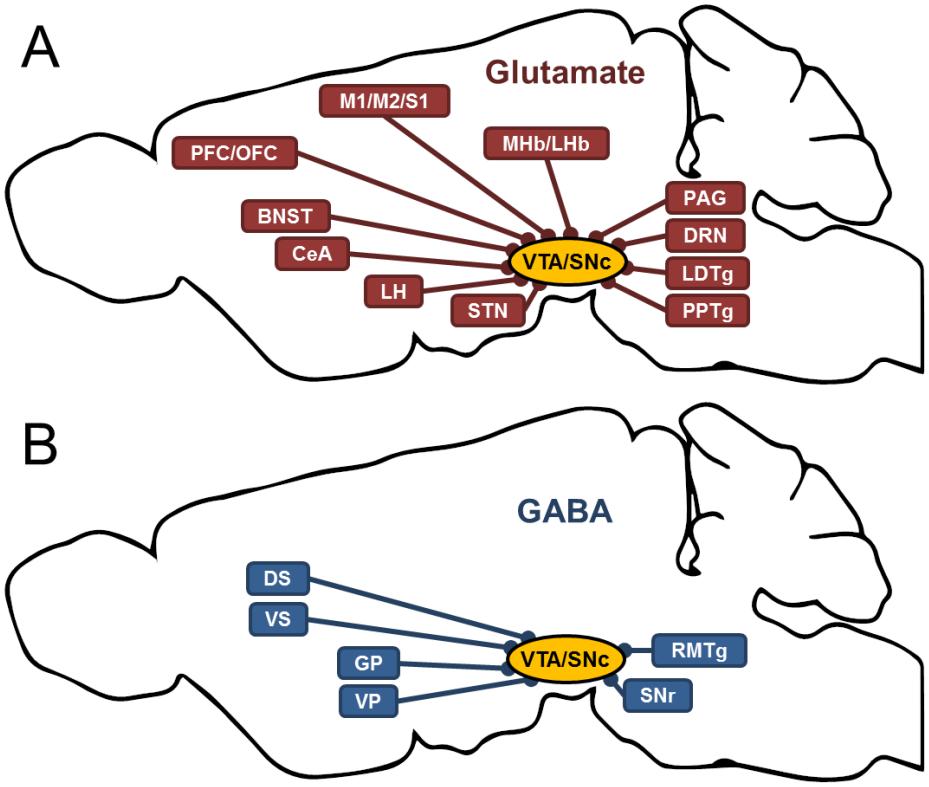

Figure 1.2. Major excitatory and inhibitory afferents to midbrain DA neurons.
A: Summary of major brain areas that send direct glutamatergic projections to VTA and SN DA neurons. B: Summary of major brain areas that send direct GABAergic projections to VTA and SN DA neurons. BNST: bed nucleus of the stria terminalis; CeA: central amygdala; DRN: dorsal raphe nucleus; DS: dorsal striatum; GP: globus pallidus; LDTg: laterodorsal tegmental nucleus; LH: lateral hypothalamus; M1: area 1 of motor cortex; M2: area 2 of motor cortex; MHb: medial habenula; OFC: orbitofrontal cortex; PAG: periaqueductal gray; PPTg: pedunculopontine tegmental nucleus; RMTg: rostromedial tegmental nucleus; S1: area 1 of somatosensory cortex; SNc: substantia nigra pars compacta; SNr: substantia nigra pars reticulata; STN: subthalamic nucleus; VP: ventral pallidum. VTA: ventral tegmental area. References for anatomical connections from Carr and Sesack, 2000; Georges and Aston-Jones, 2002; Balcita-Pedicino et al., 2011; Watabe-Uchida et al., 2012; Kempadoo et al., 2013; Qi et al., 2014.

Importantly, striatal DA projections are topographically organized, with more medial regions of the midbrain projecting to more medial and ventral areas of the striatum and, conversely, more lateral areas of the midbrain projecting to more lateral and dorsal striatal regions. Therefore, VTA DA neurons project primarily to the ventral striatum, forming the mesolimbic pathway, while SNc DA neurons project primarily to the dorsal striatum, forming the nigrostriatal pathway (Iversen et al., 2010; Howe and Dombeck, 2016). It has been proposed that behaviorally-relevant activity in these pathways follows a functional hierarchy. This model, initially proposed by Suzanne Haber and collaborators, and consequently known as the “Haber spiral”, was founded on the anatomical findings in primates that ventromedial striatal neurons project back to a large number of DA cells but receive a relatively smaller DA input, while more dorsolateral striatal regions receive larger DA input but project to a smaller subset of DA neurons in the SNc (Nauta et al., 1978; Haber et al., 2000; Haber, 2014). This architecture led to the proposition of an ascending hierarchy of control, where “the (NAcc) shell influences the core, the core influences the central striatum, and the central striatum influences the dorsolateral striatum” (Haber et al., 2000). Since its initial proposal, there has been an accumulation of functional evidence in line with this model, including the demonstration that the recruitment of striatal DA signaling during habit formation (particularly habitual drug use) follows a temporal progression from ventromedial to dorsolateral striatum (Belin and Everitt, 2008; Willuhn et al., 2012). In addition to these topographically organized ventral and dorsal striatal projections, VTA DA neurons project to the amygdala, the hippocampus, cerebellum and cortex, and SNc DA neurons also project to the cortex and the amygdala (Lindvall et al., 1974; Loughlin and Fallon, 1984; Ikai et al., 1992; Lammel et al., 2008).

The vast majority (95%) of striatal neurons are medium spiny neurons (MSNs), which are GABAergic projection neurons with large dendrites densely covered with spines (Kandel et al., 2000; Iversen et al., 2010). MSNs in the ventral and dorsal striatum are divided in two major groups: those belonging to the direct, or striatonigral, pathway, which project directly to the internal GP (GPi) and SNr, and express exclusively D1R, and those belonging to the indirect, or striatopallidal, pathway, which project to the external GP (GPe) and express only D2R receptors (Redgrave et al., 2010).The classical functional model of BG function in motor control, developed in the 1980s, proposes that these nuclei act as a go/no-go

selection gate of cortical motor commands (Albin et al., 1989; Chevalier and Deniau, 1990). The principal output nuclei of the BG are the GPi and SNr, which keep the thalamic nuclei under tonic inhibition. The thalamus serves as a gateway for cortical motor commands; when inhibited, the thalamus precludes the execution of cortical motor commands; release from this inhibition allows cortical activity to be translated into behavior. When direct pathway MSNs increase their firing, they directly inhibit the GPi and SNr, thus disinhibiting the corticothalamic circuit and promoting motor output. Indirect pathway MSNs, on the other hand, inhibit GABAergic neurons of the GPe, which exert tonic inhibitory control over glutamatergic STN neurons that project to the GPi and SNr. Therefore, increased firing in indirect pathway MSNs disinhibits the STN, which excites the GPI and SNr and inhibits the thalamus, blocking cortical motor output. In this classical framework, movement occurs when there is a relative dominance of the direct versus the indirect pathway, while stopping an action sequence or inhibiting the initiation of a motor response involves a relative predominance of the indirect pathway.

The real architecture of BG circuits is, of course, more complex than what is proposed in standard models. Importantly, there are a number of anatomically identified pathways that are not taken into account by this framework (Figure 1.3A). For example, D1R-expressing MSNs, STN, GPi and SNr neurons also have a direct projection back to SNc DA neurons, whose function is not yet fully understood within an integrated functional model (Redgrave et al., 2010). In addition, recent findings have shown that direct and indirect pathway neurons are both activated during the execution of voluntary movements, challenging a cornerstone proposal of the classical model (Cui et al., 2014b; Jin et al., 2014). Recent critiques of the available evidence suggest that instead of relying on a binary functional segregation of “go” and “no-go” signals, action selection in BG circuits may involve the recruitment of action-specific engrams, i.e. the execution of a specific action would require both the activation of neuronal populations associated with that movement by the direct BG pathway and the inhibition of neuronal populations associated with alternative behaviors by the indirect pathway (Jin and Costa, 2015). Likewise, “stopping” a movement (“no-go” signals) can be further subdivided into specific action components; for example, pausing an ongoing movement sequence for a limited time and fully cancelling a behavior seems to involve the activation of different neuronal populations (Schmidt and Berke, 2017).

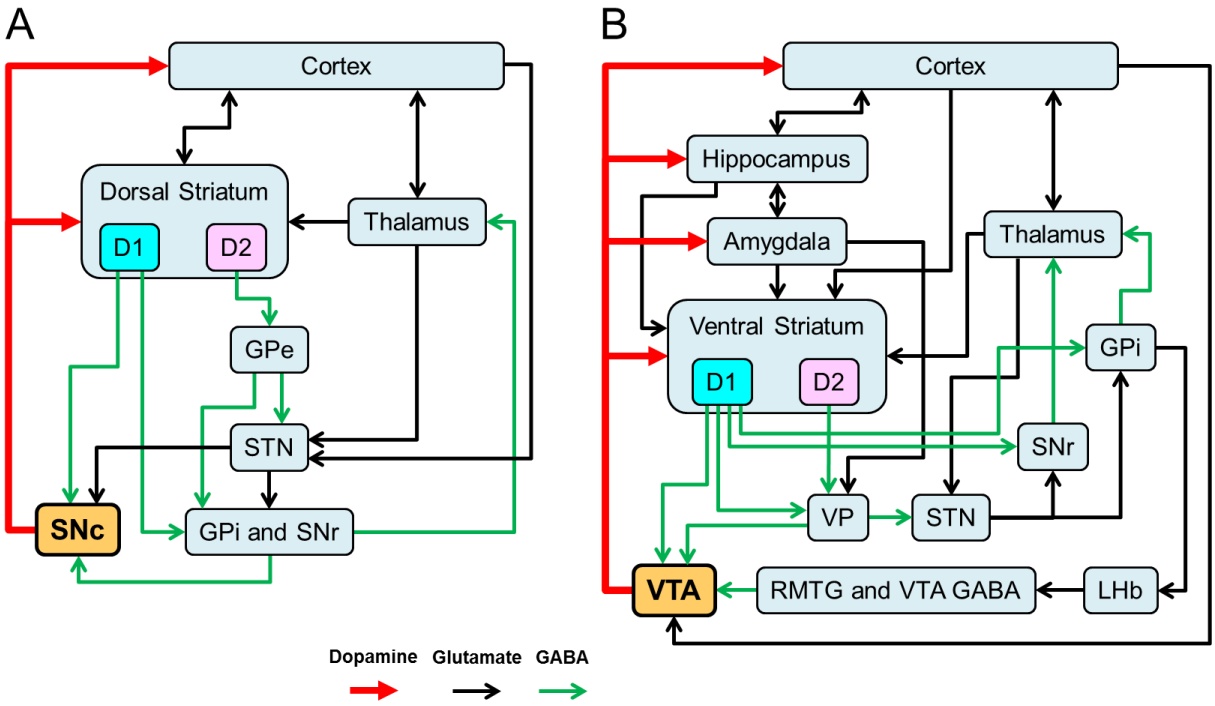

Figure 1.3. General schematic of midbrain DA neurons within cortico-BG-limbic circuits. A: Classical representation of the BG circuit for motor control. SNc DA neurons project mainly to the dorsal striatum (but also to the cortex), and are involved in the direct/indirect pathway control of motor output. B: VTA DA neurons have widespread projections in the limbic system, ventral striatum and cortex, and control learning, emotion and decision making. For the sake of simplicity, some known connections in cortico-BG-limbic circuits are not represented in these schematic drawings. GPe: external globus pallidus; GPi: internal globus pallidus; RMTg: rostromedial tegmental nucleus; SNc: substantia nigra pars compacta; SNr: substantia nigra pars reticulata; STN: subthalamic nucleus; VP: ventral pallidum; VTA: ventral tegmental area; VTA GABA: GABAergic neurons of the VTA. Based on data from Gerfen et al., 1982; Loughlin and Fallon, 1984; Robertson and Jian, 1995; Grace et al., 2007; Redgrave et al., 2010; Sesack and Grace, 2010; Shabel et al., 2012; Hosp and Luft, 2013; Overton et al., 2014; Ikemoto et al., 2015; Kupchik et al., 2015.

While the classical BG model provides a useful heuristic for dorsal striatal connections, current evidence suggests that it does not reflect the functional connectivity and behavioral relevance of ventral striatal pathways (Figure 1.3B). While many ventral striatal D1R-expressing MSNs project to SNr and GPi (similar to the dorsal striatum D1R MSNs), ventral striatal D2R-expressing neurons project to the VP; furthermore, a large proportion of ventral D1R MSNs also project to the VP, partially overlapping with D2R MSNs projections (Robertson and Jian, 1995; Kupchik et al., 2015; Kupchik and Kalivas, 2017). In addition, NAcc MSNs receive inputs mainly from frontal association cortices, such as the PFC, and from limbic regions such as the ventral hippocampus and amygdala, and synaptic potentiation of these

inputs have been implicated in the control of reward seeking, but not locomotion (Grace et al., 2007; Sesack and Grace, 2010; Ikemoto et al., 2015; Creed et al., 2016). One interpretation of ventral striatal pathways proposes that the VP neurons have a similar functional segregation as the GP, but without the anatomical segregation observed in this region (GPe versus GPi). Therefore, distinct subpopulations of VP neurons would represent analogues of GPi- (direct pathway) and GPe-projecting (indirect pathway) neurons, with VP→STN neurons representing the indirect pathway and VP→VTA GABA neurons representing the indirect pathway (Sesack and Grace, 2010; Ikemoto et al., 2015; Creed et al., 2016; Knowland et al., 2017).

A similar analogy has been proposed for the architecture of the SN and the VTA, given that both nuclei are composed primarily of long-range projecting DA neurons and GABA neurons that connect to neighboring DA neurons and send long-range projections. However, the SN has a clear division, with the majority of DA neurons located in the SNc and the majority of GABA neurons in the SNr, while in the VTA these two populations are intermingled. One interpretation of these findings is that functionally distinct midbrain and BG circuits may have evolved from the expansion or duplication of a prototypical GABA/DA circuit, which has specialized for different functions (exaptation) over the course of vertebrate evolution; in this manner, this circuit module whose original function might have been action selection might duplicate and adapt to serve other roles, such as emotional regulation (Stephenson-Jones et al., 2011; Ericsson et al., 2013). A similar hypothesis has been proposed for the evolution and development of cortical circuits, which share canonical anatomical and physiological features (e.g. layered structure, cell type subdivision) but participate in different functions (e.g. sensory processing, memory storage, emotional regulation) and have region- and function-specific adaptations (e.g. different inputs and outputs or number of layers) across multiple species. One implication of this hypothesis is that the cortical expansion observed in mammals is the result of the successive replication and adaptation of a simpler primordial cortical circuit (Shepherd, 1974, 2011; Smith et al., 1980; Northcutt and Kaas, 1995; Douglas and Martin, 2004; Fournier et al., 2015).

A crucial aspect of the BG circuits involved in limbic processing is the excitatory projection from the GPi (or entopeducunlar nucleus, in rodents) to the LHb, which

inhibits VTA DA neurons by exciting VTA GABA neurons and the RMTG (Christoph et al., 1986; Ji and Shepard, 2007; Hong and Hikosaka, 2008; Omelchenko et al., 2009; Brinschwitz et al., 2010; Bromberg-Martin et al., 2010c; Balcita-Pedicino et al., 2011; Hong et al., 2011; Stephenson-Jones et al., 2013, 2016). This pathway has been extensively investigated in recent years, as it has been shown to be conserved throughout the vertebrate lineage and essential for the evaluation of negative feedback and aversive motivation (see Section 1.3).

1.1.4. Electrophysiological properties and diversity of DA neurons

The electrophysiological properties of nigrostriatal DA neurons were described by the seminal work of Grace and Bunney in the 1980s using intracellular recordings of – in some instances – neurochemically and otherwise functionally identified DA neurons in the SN of anesthetized rats, in some cases with confirmed dorsal striatal projections (Grace and Bunney, 1980, 1983a, 1983b, 1983c, 1984a, 1984b, 1986). In a series of landmark studies, the authors demonstrated that nigrostriatal DA neurons display tonic pacemaker (also called single-spike) firing interspersed with visually identified spontaneous bursts and pauses (Figure 1.4). Average firing frequency in these neurons is relatively low, never exceeding 10 Hz, except during bursts. These cells had broad action potentials (APs), exceeding 2 ms, non-linear responses to hyperpolarizing current pulses, which were later attributed to hyperpolarization-activated depolarizing currents (I_h), and large medium afterhyperpolarizations (mAHPs), which were later linked to small conductance Ca^{++}- activated K^+ (SK) channels. These characteristics quickly became the standard for identifying putative DA neurons in intracellular and extracellular recordings without neurochemical identification across multiple species (Schultz, 1986; Ungless et al., 2004; Zaghloul et al., 2009; Ungless and Grace, 2012).

Grace and Bunney also defined a heuristic criterion for separating burst firing from the underlying single-spike firing (Grace and Bunney, 1984b). By observing the patterns of these transient increases in firing, which were typically associated with excitatory post-synaptic potentials (EPSPs), the authors noticed that bursts were generally composed of a series of two to ten high frequency (>12 Hz) spikes with progressively decreasing amplitudes and increasing AP widths and inter-spike

intervals (ISIs). Based on these empirical observations, Grace and Bunney established what is now referred to as the template method of burst identification, where a burst is defined by having an onset when the ISI is below 80 ms and offset when the ISI within the burst is over 160 ms (Grace and Bunney, 1984b). Importantly, they also showed that buffering intracellular Ca^{++} with ethylene glycol-bis(β-aminoethyl ether)-N,N,N',N'-tetraacetic acid (EGTA) abolished burst firing, and that intracellular Ca^{++} injections as well as blockade of K^{+} channels with extracellular iontophoresis of barium or intracellular injection of tetraethylammonium bromide increased burst firing, therefore demonstrating that bursts were dependent on intracellular Ca^{++} concentrations and could be controlled by K^{+} conductances.

Pacemaker firing in midbrain DA neurons is cell autonomous, i.e. persists in the absence of synaptic input (Sanghera et al., 1984). When recorded *ex vivo*, this is the only form of spontaneous activity that DA neurons display, although burst firing can be elicited *ex vivo* with stimulation or simulation of synaptic input and pharmacological manipulations of glutamatergic receptors and ion channels (Overton and Clark, 1992; Wolfart and Roeper, 2002; Deister et al., 2009). DA neurons are also particularly sensitive to depolarization block, i.e. they quickly cease firing if they are active at high firing rates (Grace, 1992; Seutin and Engel, 2010; Tucker et al., 2012; Qian et al., 2014). This might be related to the properties of voltage gated Na^{+} channels in these neurons, which have a smaller density and more positive mid-point potential of steady-state inactivation than those in most other neuronal subtypes (Kuznetsova et al., 2010; Seutin and Engel, 2010; Ding et al., 2011). The susceptibility of these neurons to depolarization block is thought to be functionally related to the control of pacemaker frequency (Tucker et al., 2012; Qian et al., 2014).

Because of their high sensitivity to depolarization block, midbrain DA neurons cannot achieve high frequency firing through linear-conductance depolarizations alone, such as those created by α-amino-3-hydroxy-5-methyl-4-isoxazolepropionic acid receptor (AMPAR) activation (Grace and Bunney, 1983a). Indeed, a notable feature of these neurons is that they require the activation of non-linear conducting N-methyl-D-aspartate receptors (NMDAR) for bursting (Overton and Clark, 1992, 1997, Zweifel et al., 2008, 2009; Deister et al., 2009). This dependence has been proposed to be due to the special voltage dependency of NMDAR currents (at negative membrane potentials, the pore of NMDARs is blocked by a Mg^{++} ion) - in combination

with voltage-gated Ca^{++} channels - which create a high frequency oscillation in depolarized potentials that recover Na^{++} channels, thereby allowing high frequency firing (Deister et al., 2009).

Nigrostriatal DA neurons have other striking physiological and anatomical properties that set them apart from most mammalian neurons. The axonal arborization of a single DA neuron in the striatum can approximate one meter in length and form almost 30 thousand synapses with MSNs in rats, and is estimated to reach ten times those numbers in humans, making these neurons some of the largest in the brain (Matsuda et al., 2009; Bolam and Pissadaki, 2012). They also display large back-propagating spikes (APs that propagate up the dendrites from the soma); these are accompanied by strong dendritic Ca^{++} waves, which are thought to modulate the gain of periodic synaptic inputs (Häusser et al., 1995; Wilson and Callaway, 2000; Chan et al., 2007; Hage and Khaliq, 2015). It is important to note that, in these DA neurons, pacemaking activity (and presumably backpropagating APs) can be decoupled from dendritic Ca^{++} oscillations by blocking L-type ("long-lasting") Ca^{++} channels or buffering intracellular Ca^{++}, suggesting that the former causes, and is relatively independent of, the latter (Chan et al., 2007; Guzman et al., 2009). These neurons also have their axonal initial segment (AIS) initiating from a dendrite, not the soma, which means they have a distinct form of dendritic integration, where inputs to the AIS-bearing dendrite likely have a greater influence on AP initiation in relation to other inputs (Grace and Bunney, 1983a, 1983b; Häusser et al., 1995).

DA neurons also display a striking form of auto-regulatory control by expressing pre-synaptic D2Rs, a.k.a. D2 autoreceptors, in both the axonal and somatodendritic compartments (Ford, 2014). In DA neurons, D2R activation produces a profound inhibition of spontaneous firing, due to the activation of G-protein-activated inwardly rectifying potassium channels (GIRK), which means that DA release inhibits DA neuron activity (Beckstead et al., 2004; Lammel et al., 2008; Dragicevic et al., 2014; Ford, 2014). In the striatum, axonal D2 autoreceptors are major regulators of DA release on multiple time scales; following phasic axonal DA release, activation of D2 autoreceptors can decrease the probability of DA release to subsequent presynaptic stimulations for hundreds of milliseconds up to several seconds (Benoit-Marand et al., 2001; Phillips et al., 2002; Schmitz et al., 2002). DA neurons also display

somatodendritic DA release, i.e. DA is released not only from axonal terminals but also from dendrites (Geffen et al., 1976; Cheramy et al., 1981). This form of DA release has been proposed to act not only as a form of autoinhibitiory feedback, but also as a local signal for the regulation of neighboring DA and non-DA neurons (Rice and Patel, 2015). For example, dendritically released DA activate D1Rs on the terminals of striatonigral (direct pathway) MSN axons in the SNr, enhancing GABA release and amplifying SNr inhibition (Miyazaki and Lacey, 1998; Rice and Patel, 2015).

Since the seminal work of Grace and Bunney, it has been consistently confirmed that DA neurons in both the SN and VTA display the same three major modes of firing when recorded *in vivo*, either in anesthetized or awake states, across multiple mammalian species (Bayer et al., 2007; Morikawa and Paladini, 2011; Schiemann et al., 2012; Paladini and Roeper, 2014). The patterns of pacemaker firing, bursts and pauses relate directly to different patterns of DA release and the occupancy of D1 and D2 receptors in striatal MSNs (Figure 1.4). Within the framework of the classical BG model, the slow pacemaker firing of DA neurons maintains the tonic baseline levels of DA in the target regions, which constitutively and selectively activates D2Rs, thus keeping the indirect pathway “silent”. Bursts transiently increase extracellular DA, which binds to D1Rs and activates the direct pathway (both by increasing excitability and promoting synaptic plasticity on cortico-striatal synapses), facilitating behavior (Shen et al., 2008; Cohen and Frank, 2009). Pauses in firing transiently decrease DA levels, releasing indirect pathway MSNs from D2R-mediated inhibition and thus decreasing the probability of behavior.

However, despite this relative homogeneity in firing patterns *in vivo*, and the initial assumption that the physiological properties of nigrostriatal DA neurons were generalized to all DA neurons, it is now known that midbrain DA neurons display a large diversity of biophysical properties, gene expression profiles, afferent and efferent synaptic connectivity and cell morphology (Watabe-Uchida et al., 2012; Roeper, 2013; Lammel et al., 2014; Beier et al., 2015). A recently described general feature of neuronal systems is that similar functional firing patterns can be achieved with different ion channel expression profiles by homeostatic tuning of gene expression; however, different functional combination of ion channels impose unique constraints on the variability of neuronal activity and specific vulnerabilities to

physiological and pathological challenges (Marder and Goaillard, 2006; O'Leary et al., 2013, 2014). Congruently, distinct subpopulations of midbrain DA neurons have been shown to have different behavioral roles and specific functional phenotypes in disease states (Yamada et al., 1990; Liss et al., 2005; Lammel et al., 2012; Schiemann et al., 2012; Krabbe et al., 2015; Lerner et al., 2015).

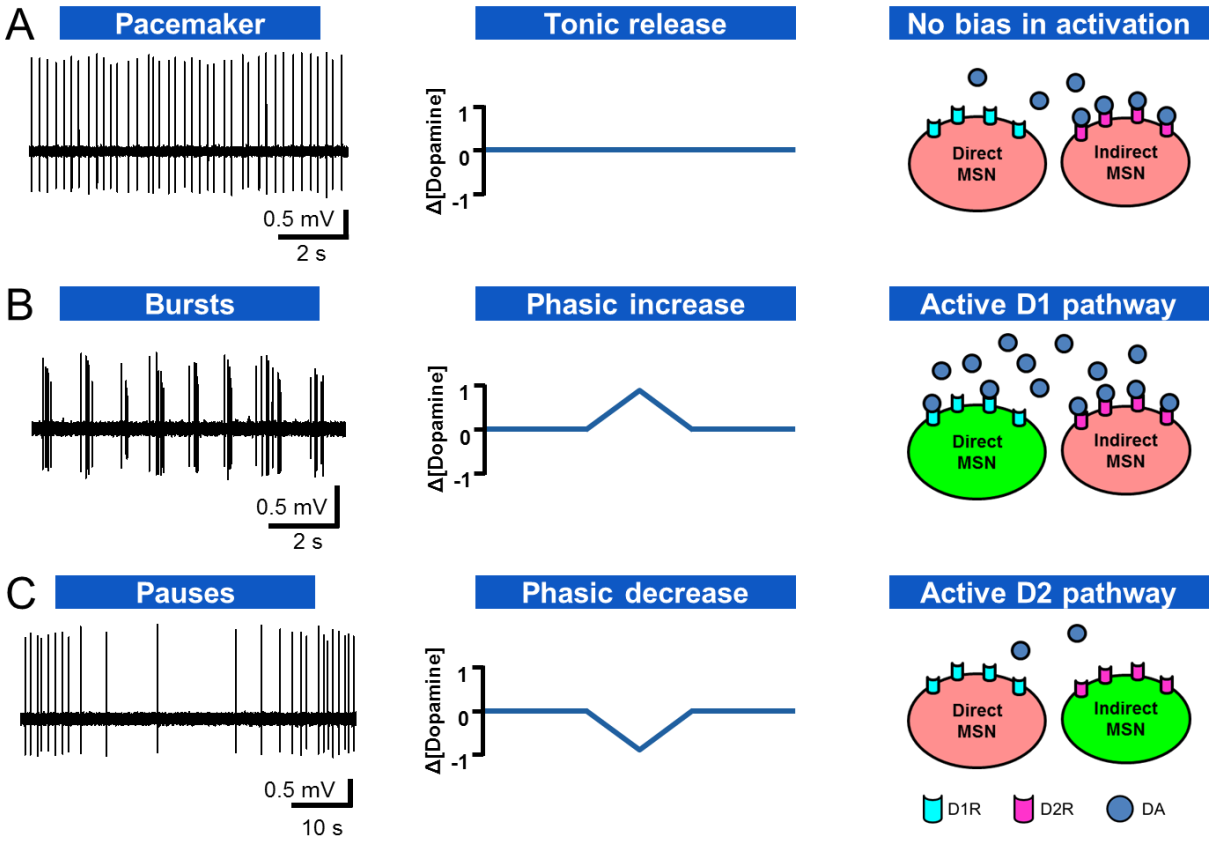

Figure 1.4. Major *in vivo* firing modes of midbrain DA neurons and their postsynaptic effects. In both anesthetized and awake states, DA neurons display three major modes of firing which determine the release of DA in the axonal projection targets. A: Pacemaker, or single-spike, firing. This pattern maintains the tonic levels of DA release in the target regions, maintaining a constitutive activation of inhibitory D2Rs in indirect MSN but not activating D1Rs in direct MSN. B: Burst firing. Characterized by transient increases in activity (onset when ISIs is >80 ms and offset when ISI >160 ms), this form of firing is related to phasic surges in DA release which have been proposed to activate D1Rs in direct pathway MSNs (indicated by the green color), while maintaining DA binding to D2Rs. C: Pauses in firing. These pauses typically interrupt pacemaker firing or immediately following intense bursts, and can last for multiple seconds. When DA neurons synchronously stop firing, there is a decrease in DA levels in target regions, which release D2Rs from their constitutive activation (green color), thus releasing the indirect pathway from inhibition (see section 1.3).

One major differentiating feature of DA neuron populations is their post-synaptic projection target. Work from our laboratory and others have shown that DA neurons that project to different forebrain regions have different biophysical, synaptic and molecular properties and are involved in distinct behaviors (Lammel et al., 2008, 2012; Margolis et al., 2008; Lerner et al., 2015; Tarfa et al., 2017). Performing whole-cell patch-clamp recordings of projection-identified DA neurons in brain slices, Lammel et al. (2008) showed that midbrain DA neurons can be classified in two major groups. The first group corresponds to the classically described nigrostriatal DA neurons and those that project to the lateral shell of the NAcc (mesolimbic lateral shell), which are located in the medial SNc and lateral VTA (with the highest density in the parabrachial nucleus). The second group, also called “atypical” DA neurons, is composed of neuronal populations located in the VTA. This group included neurons that project to the amygdala (mesoamygdaloid), PFC (mesocortical) and the core and medial shell of the NAcc (mesolimbic core and mesolimbic shell, respectively). Mesocortical and mesolimbic medial shell neurons have their highest density in the paranigral nucleus in the ventral portion of the VTA, mesolimbic core and mesoamygdaloid neurons are distributed across the ventral and dorsal VTA in both the paranigral and parabrachial nuclei, and mesolimbic lateral shell neurons are almost exclusively located in the parabrachial nucleus, in a similar ventro-medial to dorso-lateral gradient as observed in nigrostriatal projections (Lammel et al., 2008; Iversen et al., 2010). Importantly, DA neurons that project to cortical and limbic regions have markedly smaller and less complex axonal branching (Aransay et al., 2015).

Atypical DA neurons show several key differences from the classically described SN DA neurons. They are less sensitive to depolarization block, being able to reach high frequency firing with current injection alone, and have markedly reduced AHPs and I_h currents, and wider AP widths (Neuhoff et al., 2002; Lammel et al., 2008). Reduced AHP amplitudes in VTA DA neurons are related to a lower expression of SK channels (Wolfart et al., 2001; Wolfart and Roeper, 2002). Importantly, atypical VTA DA neurons have increased rebound delays, i.e. the time interval between the release from hyperpolarizing inhibition and the resuming of pacemaker firing (Lammel et al., 2008). This is due to a slower slope of depolarization following negative current injection, suggesting that this longer

rebound delay is due to a specific biophysical mechanism (Figure 1.5). A detailed account of this feature can be found in section 1.4.5.

While all midbrain DA neurons display autonomous pacemaking driven by slow depolarizing currents during single-spike ISIs, the ionic mechanisms of spontaneous firing are markedly different between classical and atypical DA neurons. In nigrostriatal DA neurons, it is thought that pacemaker firing is driven by a combination of I_h, mediated by hyperpolarization-activated cyclic nucleotide–gated (HCN) channels, and low threshold voltage-gated L-type Ca^{++} currents, mediated by Cav1.3 channels (Wilson and Callaway, 2000; Chan et al., 2007; Puopolo et al., 2007; Guzman et al., 2009; Putzier et al., 2009; Branch et al., 2014; Poetschke et al., 2015). While there is still substantial controversy on the relative contribution of each of these currents to pacemaker drive, especially in regard to different developmental stages and within different SN regions, this is very different from what is observed in the VTA (Costa, 2014). In atypical DA neurons in the medial VTA, pacemaker firing is not driven by the same voltage-gated currents that drive pacemaking in classical DA neurons, but rather by the combined effect of a voltage-dependent tetrodotoxin-sensitive Na^+ current and a voltage-independent background Na^+ current (Khaliq and Bean, 2010).

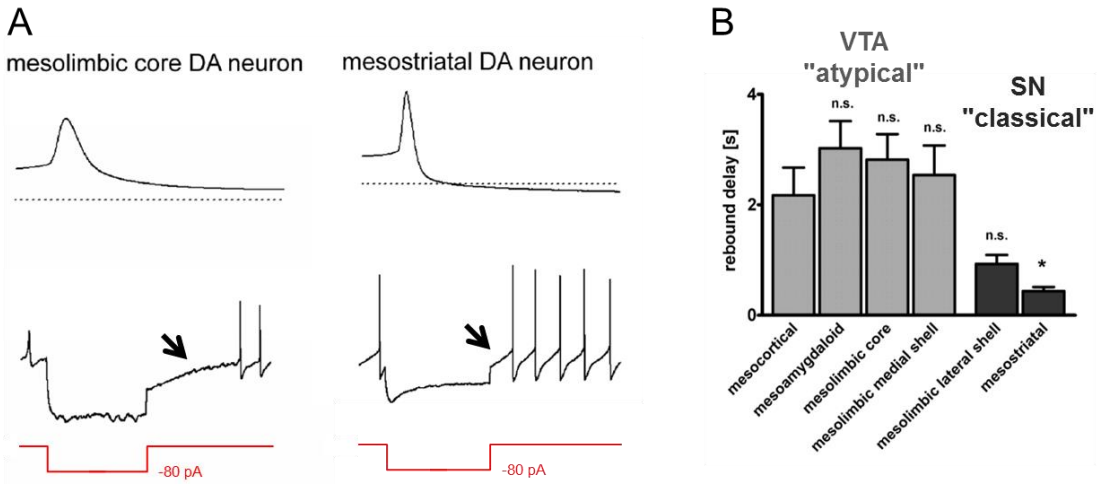

Figure 1.5. Atypical VTA DA neurons have long rebound delays.
A: example *ex vivo* patch clamp recordings of an “atypical” DA neuron, specifically a mesolimbic core DA neuron, and a “classical” nigrostriatal, or mesostriatal, DA neuron. Notice the longer rebound delay in the mesolimbic core neuron, due to a slower slope in depolarization following negative current injection. B: bar graph showing average rebound delays for different projection target-identified DA neurons. Notice that atypical VTA neurons that project to the medial shell and core of the NAcc, the amygdala and PFC differ qualitatively from the classical SN neurons that project to the dorsal striatum and lateral shell of the NAcc. Figure adapted from Lammel et al. (2008).

Within the atypical category of VTA DA neurons, mouse mesocortical neurons seem to possess particularly unique properties. In addition to the biophysical differences from classical DA neurons, they are the only ones that lack somatodendritic D2 autoreceptors and have a markedly reduced expression of DA transporter (DAT), different input connectivity and show different glutamatergic plasticity responses to aversive and appetitive stimuli (Sesack et al., 1998; Lammel et al., 2008, 2012, 2014). It is important to note, however, that there could be significant differences in the properties of DA neurons between species, as Margolis et al. has reported that mesocortical DA neurons in rats do have functional D2 receptors while mesoamygdaloid DA neurons do not, which stands in stark contrast to the results observed in mice (Margolis et al., 2008). This discrepancy has yet to be resolved, but if it is due to biological differences between species, it would mean that DA neuron properties, especially in mesocortical projection neurons, can undergo rapid evolutionary changes and have sharply distinct functional properties even in species that belong to the same taxonomical family, such as mice and rats (both belong to the Muridae family of the order Rodentia). This is a very exciting concept, as primates have a considerably more widespread DA innervation of the cortex in relation to rodents, with humans displaying a unique topographical structure of DA axons in cortical layers (Berger et al., 1991; Raghanti et al., 2008). This has led to the intriguing hypothesis that many aspects of human cognition, including cognitive flexibility and abstract reasoning, may be directly linked to species-specific adaptations in cortical DA signaling (Previc, 1999).

1.1.5. Control of extracellular DA clearance rates

The post-synaptic effects of DA are not only regulated by DA release from axonal terminals, but also by the rate of DA clearance from the extracellular space. Higher rates of clearance decrease the probability of DA receptor occupancy, while lower rates do the opposite, meaning that DA clearance can bi-directionally control DA signals. Apart from diffusion, the most important mechanism of DA clearance in striatal compartments is the uptake of this neurotransmitter into the presynaptic DA neuron by the DAT protein (Torres et al., 2003; Cragg and Rice, 2004; Vaughan and Foster, 2013). DAT belongs to the SLC6 family of transporters, which translocate solutes down the gradient of Na^+ and Cl^- ions; DAT function requires the binding and co-transport of two Na^+ ions and one Cl^- ion for each DA molecule (Torres et al.,

2003). The DAT protein is exclusively detected in midbrain DA neurons and its axons, and is to date the most selective molecular marker for this neuronal subclass (Cerruti et al., 1993; Ciliax et al., 1995, 1999; Freed et al., 1995; Maggos et al., 1997; Bäckman et al., 2006; Lammel et al., 2008).

DAT function and expression is highly plastic, and modulates DA clearance rates in response to short- and long-term physiological demands (Schmitt and Reith, 2010). Functional regulation is achieved mainly by post-translational modifications (e.g. phosphorylation and palmitoylation) and binding partner interactions (e.g. binding with syntaxin 1A). By regulating the duration and amplitude of extracellular DA transients, DAT modulates the effects of DA on post-synaptic and pre-synaptic DA receptors and thus influences behavior. For example, as discussed later in this thesis, DAT blockers like amphetamines and cocaine are used as drugs of abuse and as stimulants in clinical practice (Schmitt and Reith, 2010; Vaughan and Foster, 2013).

In terms of behavioral control, the function of DAT has been investigated in mouse lines with genetically-determined dysfunctions in DAT expression (Giros et al., 1996; Gainetdinov et al., 1999; Viggiano et al., 2003; Zhang et al., 2010; Efimova et al., 2016). The first DAT-transgenic model was the DAT knockout (DAT KO) mice; these animals were viable, but showed several developmental defects, including dwarfism and high mortality (Giros et al., 1996; Bossé et al., 1997). DAT KO mice are hyperdopaminergic, with basal striatal DA levels, as measured by microdialysis, being five-fold higher when compared to controls, and clearance of phasic extracellular DA after a single MFB pulse stimulation being up to 300 times slower in compared to controls (Giros et al., 1996; Jones et al., 1998).

These animals are constitutively hyperactive, have exacerbated and non-habituating responses to novelty, working memory deficits, severe spatial learning impairments, decreased anxiety levels, lower immobility in the forced swim test, impaired taste processing and disrupted phase synchrony across the hippocampal-prefrontal cortex pathway, among other deficits (Table 1.1.) (Giros et al., 1996; Gainetdinov et al., 1999; Costa et al., 2007; Morice et al., 2007; Dzirasa et al., 2009a, 2009b; Li et al., 2010a; Carpenter et al., 2012; Efimova et al., 2016). These animals are also insensitive to cocaine and amphetamines, and actually reduce their activity in response to these stimulants (Giros et al., 1996). DAT KO mice also show altered

patterns of consummatory licking behaviors when accessing freely available liquid rewards (Rossi and Yin, 2015). The role of DAT KO in extinction learning (see section 1.3) is controversial, as there have been reports of both accelerated and slowed extinction in this line (Hironaka et al., 2004; Rossi and Yin, 2015).

Another model for studying the behavioral role of DAT is the DAT knockdown (DAT KD) mouse, where DAT activity is reduced by 90% (Zhuang et al., 2001). These animals have similar behavioral phenotypes to DAT KO mice, but do not develop dwarfism. DAT KD mice also display a persistent hyperdopaminergic state, but not constitutive hyperactivity; they do, however, display novelty-induced hyperactivity (Zhuang et al., 2001). The performance of these animals in learning tasks has been extensively investigated (Cagniard et al., 2006a; Yin et al., 2006; Balci et al., 2010; Beeler et al., 2010; Milienne-Petiot et al., 2017). A consistent finding from these studies, across a variety of reinforcement-based learning tasks, is that DAT KD increases the motivation to work for or respond to a cue in order to obtain a reward, without affecting the rate or effectiveness of associative learning (see section 1.3). This indicates that DAT-mediated regulation of DA concentrations has a higher effect on motivation than on learning itself.

Heterozygous DAT KO mice ($DAT^{+/-}$) display a less severe (50%) loss in DAT function (Giros et al., 1996; Li et al., 2010b; Deng et al., 2015). These animals, like the DAT KD line, have normal body weight and life spans. These mice display normal baseline locomotor activity (are not hyperactive), open field exploration, novel object recognition, anxiety, movement control and spatial memory (Giros et al., 1996; Morice et al., 2007; Li et al., 2010b; Deng et al., 2015). They do, however, display specific and subtle changes in working memory, behavioral despair, trace conditioning and pattern memory, as well as attenuated responses to cocaine and amphetamine (Giros et al., 1996; Spielewoy et al., 2000b; Mead et al., 2002; Perona et al., 2008; Li et al., 2010b; Deng et al., 2015). This indicates that the effect of DAT on behavioral control is multifaceted, and is dependent on the specific degree of changes in DAT activity, with effects on motivation, stimulant responses and complex memory processes seeming to be more sensitive to decreases in DAT activity (Table 1.1).

Table 1.1. Reported behavioral phenotypes of DAT KO, KD and heterozygous KO mice.

Genotype	Behavioral phenotypes (in relation to controls)	References
DAT KO ($DAT^{-/-}$) **100% DAT loss**	- Hyperactivity, increased meandering and impaired exploratory habituation in the open field - Attenuated locomotor responses to cocaine and amphetamine - Attenuated cocaine self-administration - Exacerbated and non-habituating responses to novel environments - Attenuated locomotor responses to haloperidol and clozapine - Drastically reduced immobility and exacerbated escape behaviors (climbing, swimming and jumping) in the forced swim test - Reduced immobility in the tail suspension test - Impaired novel object preference - Increased preference and exacerbated withdrawal symptoms for morphine, with unaltered analgesic effects - Increased preference for and consumption of sucrose - Decreased negative bias for bitter tastes - Deficient working memory in the spontaneous alternation test (fewer alternations) - Reduced marble burying - Decreased maternal behaviors - Delayed acquisition and reversal learning of place navigation in the uncued Morris water maze (spatial memory formation) - Impaired performance in the cued Morris water maze (which is reversed by haloperidol, but not methylphenidate - Reduced anxiety measures in the elevated plus maze - Longer and more frequent licks when consuming sucrose, with faster cessation of licking when sucrose is no longer available (faster extinction) - Slower extinction of a food reinforced nosepoke FR5 (one pellet for five nosepokes) task	Giros et al., 1996 Rocha et al., 1998 Gainetdinov et al., 1999 Spielewoy et al., 2000a, 2000b Costa et al., 2007; Morice et al., 2007 Perona et al., 2008 Thomsen et al., 2009 Li et al., 2010a Carpenter et al., 2012 Fox et al., 2013 Rossi and Yin, 2015
DAT knockdown ≈90% DAT loss	- Hyperactivity and impaired exploratory habituation in the open field - Impaired exploratory habituation in the Y maze - Higher rates of lever pressing for rewards, but with similar acquisition and reversal learning rates (enhanced motivation) - Improved reversal learning in a probabilistic task - High reward and risk preference - Increased searching for rewards in the absence of CS in a Pavlovian task (enhanced motivation) - Anticipated responding in an interval timing task	Zhuang et al., 2001; Cagniard et al., 2006a; Yin et al., 2006; Balci et al., 2010; Beeler et al., 2010; van Enkhuizen et al., 2014; Milienne-Petiot et al., 2017
Het. DAT KO ($DAT^{+/-}$) **≈50% DAT loss**	- Attenuated locomotor responses to cocaine and amphetamine (less than controls, more than DAT KO) - Lack of exploratory habituation to novel environments - Increased climbing behavior in the forced swim test (more than controls, less than DAT KO) - Reduced immobility in the tail suspension test (similar to DAT KO) - Impaired trace fear conditioning and increased effects of distractors on trace and delay fear conditioning - Impaired working memory in a delayed non-matching-to-place version of water T-maze task - Deficits in pattern completion during spatial reference memory retrieval (reversed with haloperidol)	Giros et al., 1996 Spielewoy et al., 2000b Mead et al., 2002 Perona et al., 2008 Li et al., 2010b Deng et al., 2015

Importantly, Morice et al. (2004) demonstrated, by crossing DAT KO mice (originally developed in a mixed B6×129 background) with C57BL/6JOrl and DBA/2JOrl strains for more than 12 generations, that the intensity of the DAT KO behavioral phenotype is heavily influenced by the genetic background of the mouse (the mutation was much more deleterious in C57BL/6JOrl bred mice than in the DBA/2JOrl background), suggesting that other genes can compensate, or perhaps exacerbate, the effects of DAT loss of function.

Other regulators of extracellular DA signals include monoamine oxidase (MAO) enzymes, which degrade DA through oxidative deamination, catechol-O-methyltransferase (COMT), which inactivates DA by adding a methyl group and converting it to 3-methoxytyramine, and the norepinephrine transporter (NET), which also transports DA but with a much lower efficiency than DAT (Di Chiara et al., 1992; Youdim et al., 2006; Käenmäki et al., 2010; Sulzer et al., 2016). In the cortex, due to the relative paucity of DAT expression, the relative contribution of these clearance mechanisms is much higher than in the striatum (Carboni et al., 1990; Wayment et al., 2001; Yavich et al., 2007; Käenmäki et al., 2010). Because of this, DA transients in cortical tissue tend to have longer time scales than in the striatum, but the implications of this for cortical physiology and behavioral control are not well understood (Garris and Wightman, 1994; Sulzer et al., 2016)

1.2. Dopamine and disease

1.2.1. Parkinson's disease and aging

Perhaps the most studied disease involving the midbrain DA system is Parkinson's disease (PD), a neurodegenerative disorder characterized by the motor manifestations of akinesia, rigidity, resting tremor, hunched posture and shuffling gait (Goetz et al., 2008; Iversen et al., 2010). PD is the second most common neurodegenerative disorder after Alzheimer's disease and imposes an economic burden of approximately 30 billion dollars per year in the USA and Europe combined (Hirtz et al., 2007; Olesen et al., 2012; Ascherio and Schwarzschild, 2016).

The main pathophysiological hallmark of PD is the selective loss of nigrostriatal DA neurons, especially those located in the lateral SN (Hornykiewicz, 1963; Yamada

et al., 1990; Fearnley and Lees, 1991). Historically, basic DA research is intricately tied to the investigation of PD. Shortly after Carlsson's initial discovery that DA acts as a neurotransmitter and that 80% of DA in the brain was concentrated in basal ganglia circuits, Oleh Hornykiewicz found that patients with PD had dramatically reduced levels of striatal DA (Carlsson et al., 1957, 1958, Hornykiewicz, 1962, 1963). Shortly thereafter, Birkmayer and Hornykiewicz found that treating PD patients with L-DOPA, the biochemical precursor of DA, was highly effective in alleviating the motor symptoms of the disease, and this treatment is still used in clinical practice to this day (Birkmayer and Hornykiewicz, 1961, 1962; Hornykiewicz, 2002b; Lees et al., 2015). Studying PD patients and experimental animal models of parkinsonism have produced several insights on the behavioral role of nigrostriatal DA transmission (Kopin, 1993; Schwarting and Huston, 1996; Tieu, 2011).

It is important to note that aging is by itself also associated with a progressive loss of DA neurons even in the absence of PD or any other diagnosis of neurodegenerative disorders (McGeer et al., 1977; Gibb and Lees, 1991; Costa, 2014). It has been estimated that non-parkinsonian humans lose approximately 5% of SN DA neurons per decade after the age of 50 years, while patients with PD have a ten-fold acceleration of this DA neuron loss rate (Fearnley and Lees, 1991; Gibb and Lees, 1991; Naoi and Maruyama, 1999; Costa, 2014). Although there is some evidence that this age-related DA neuron loss may be negligible in some human populations (Muthane et al., 1998; Kubis et al., 2000; Alladi et al., 2009), this phenomenon has also been observed in non-human primates (Collier et al., 2011) and has inspired the influential hypothesis that PD could be caused by the acceleration of normal aging processes (Mann and Yates, 1982; Barbeau, 1984).

1.2.2. Schizophrenia

Schizophrenia is a relatively common, highly debilitating psychiatric disease that is also strongly linked to DA system dysfunction. Symptoms of this disease are manifold and can be divided in three major categories: 1) positive symptoms, which encompass hallucinations, delusions and thought disorder; 2) negative symptoms, including social withdrawal, lack of affect and reduced motivation; 3) cognitive symptoms, including intelligence loss and specific deficits in learning, verbal fluency and working memory (Iversen et al., 2010; Kring and Caponigro, 2010; Meier et al.,

2014; Grace, 2016). Schizophrenia is responsible for approximately 7.5% of all disability-adjusted life years (DALYs) attributed to mental disorders worldwide (Whiteford et al., 2013). Patients with schizophrenia have a staggeringly high unemployment rate of 80-90% and their life expectancy is reduced by 10-20 years, largely due to an increased risk of suicide (Marwaha and Johnson, 2004; Chesney et al., 2014).

DA neurotransmission is thought to play a key role in the clinical development and manifestation of the disease, a proposition that has been called the “dopamine hypothesis” for schizophrenia (Carlsson, 1988; Howes et al., 2017). This hypothesis was developed in the 1960s, based on the finding that early anti-psychotics, such as haloperidol and chlorpromazine, were strong D2R antagonists; currently all neuroleptic medications are still D2R antagonists at clinically relevant doses (Carlsson and Lindqvist, 1963; Kapur and Remington, 2001; Madras, 2013; Grace, 2016).

In addition, drugs that potentiate DA transmission, such as L-DOPA and amphetamines, aggravate psychotic (positive) symptoms in patients with schizophrenia and can induce schizophrenia-like symptoms in healthy individuals if given repeatedly or at high doses (Carlsson, 1988; Winton-Brown et al., 2014; Grace, 2016). Finally, patients with schizophrenia show several signs of structural and function abnormalities in DA transmission, such as higher post-mortem levels of DA and its metabolites, greater *in vivo* occupancy and post-mortem expression of D2Rs in the striatum, and dysregulated DA release and D1R occupancy in the PFC (Wong et al., 1986; Heinz and Schlagenhauf, 2010; Iversen et al., 2010; Howes et al., 2017).

It is important to note that the etiology of schizophrenia involves the dysfunction of multiple other cellular systems, including hippocampal hyperactivity and dysfunction of cortical and hippocampal parvalbumin-positive interneurons (Heckers, 2001; Lewis et al., 2005; Grace, 2012, 2016). This has led some authors to hypothesize that altered DA neurotransmission is not a primary cause of schizophrenic symptoms, but rather a consequence of dysregulated afferent inputs due to structural and functional deficits in regions upstream of midbrain DA neurons (Grace, 2012, 2016).

1.2.3. Drug abuse and addiction

The American National Institute on Drug Abuse describes drug addiction as “a chronic disease characterized by drug seeking and use that is compulsive, or difficult to control, despite harmful consequences” (NIDA, 2016). Addictive drugs include tobacco (nicotine), amphetamines, cocaine and its derivatives, nicotine, alcohol (ethanol) and opioids (such as heroin and fentanyl). While there is still a deep controversy as to the relative contribution of biological and socio-economic factors to the development and incidence of drug seeking behaviors, compulsive drug use severely impacts human health, quality of life and social stability (Alexander et al., 1981; Leshner, 1997; Alexander, 2000). In the United States alone, abuse of tobacco, alcohol, and illicit drugs exacts over 740 billion US dollars annually in costs related to crime, lost work productivity and health care, and approximately 10% of the population older than 12 years of age is addicted to some drug (Volkow et al., 2016; NIDA, 2017). In the United States, drug overdoses are the number one cause of injury-related death (Hedegaard et al., 2015). The overdose death rate in 2015 was 16.3 per 100 thousand inhabitants (52,404 deaths), of which 63.1% (33,091) involved opioid abuse (Rudd et al., 2016). These numbers represent a growing trend, as there were less than 20 thousand overdose-related deaths in the year 2000 (>160% increase in 15 years) and highlight the increasingly heavy social cost of drug abuse in modern societies (Hedegaard et al., 2015). Drug abuse also correlates with diagnosis of other mental illnesses, including schizophrenia, bipolar disorder and depression (Regier et al., 1990).

A striking common feature of all known addictive drugs is that they cause sharp increases in DA release (Volkow et al., 2016). The most established theory on the origin of addiction is that drugs of abuse function as exceptionally strong primary rewards, which reinforce behaviors and cues related to drug use; because of this abnormal form of learning, environments where drugs have been taken trigger DA surges which induce strong cravings for the conditioned drug reward (see section 1.3.). Importantly, while the repeated consumption of normal rewards, such as food and water, gradually reduced DA signals (due to reduced subjective value) and consequently the behavioral drive towards consumption, drugs circumvent this process, which increases the likelihood of developing compulsive behaviors (Wise, 2002).

1.2.4. Depression

Depression (specifically major depressive disorder or clinical depression) is a mental disorder characterized by anhedonia (inability to feel pleasure), lack of motivation, feelings of helplessness and hopelessness, cognitive deficits and, in extreme cases, psychosomatic pain and suicidal thoughts (NIMH, 2015). It is the most common mental illness, and is responsible for over 40% of all disability-adjusted life years (DALYs) attributed to mental disorders (Whiteford et al., 2013). In the United States depression imposes an annual economic burden of over 83 billion US dollars; in Germany, this cost is estimated to be over 15.5 billion Euros per year (Krauth et al., 2014; Greenberg et al., 2015).

While serotonin has been the main neurotransmitter associated with depression, due to the efficacy of selective serotonin reuptake inhibitor (SSRI) antidepressant drugs, dopaminergic dysfunction is also a hallmark of this disease (Dunlop et al., 2007; Grace, 2016). Indeed, specific symptoms of depression, particularly anhedonia and lack of motivation, appear to be directly linked to deficits in mesolimbic and mesoamygdaloid DA transmission, and some of the therapeutic effects of SSRIs are thought to be due to the effect of serotonergic modulation of DA neurons (Dunlop et al., 2007). This view is based on postmortem studies of patients with severe depression, including suicide victims, which have found reduced levels of DA and its metabolites in the cerebrospinal fluid (CSF) and brain regions linked to mood and motivation, including the NAcc (John Mann et al., 1997; Engström et al., 1999; Dunlop et al., 2007). Furthermore, antidepressant treatment was found to increase D1R receptor expression selectively in the NAcc (Bowden et al., 1997). In clinical practice, drugs that enhance DA transmission, such as nomifensine (a DAT and NET inhibitor) and amineptine (a DAT blocker), are also effective antidepressants (Dunlop et al., 2007). Finally, several neuroimaging studies report that patients with depression display reduced D1R receptor binding in the striatum and frontal cortex, increased D2R binding in the striatum and decreased DAT function (Savitz and Drevets, 2013)

1.2.5. Attention deficit hyperactivity disorder

Attention deficit hyperactivity disorder (ADHD) is a common neurodevelopmental disorder characterized by age-inappropriate high levels of

inattention, impulsivity, motoric activity and deficient executive control and decision making (Luman et al., 2010; Ziegler et al., 2016). In children and adolescents, prevalence ranges from 2 to 9% depending on diagnostic definitions, incurring in a global annual economic burden of 42.5 billion US dollars (Pelham et al., 2007). While until recently this disorder was thought to affect only children and teenagers, the current understanding is that symptoms can persist into adulthood, with ADHD now being recognized as a chronic neurobehavioral disorder (Goodman, 2007). Patients with ADHD typically have severe difficulties with academic and professional development, family interactions and social activity, leading to loss of quality of life and reduced economic prospects.

A dysfunction of the DA system is believed to be the major determinant of ADHD pathophysiology (Levy, 1991; Swanson et al., 2007; Genro et al., 2010; del Campo et al., 2011). The strongest support for this hypothesis comes from the successful clinical treatment of the disorder with methylphenidate (a DAT blocker) and amphetamines, powerful potentiators of DA transmission, which have a paradoxical calming effect in ADHD patients (Volkow et al., 2001; Swanson et al., 2007; Gonon and Al., 2009). In addition, neuroimaging studies have shown that the striatum and frontal cortical regions are smaller in ADHD patients compared to control subjects, and that ADHD-related anatomical abnormalities in the striatum are correlated with symptom severity, even resolving over time as symptoms improve with age and clinical treatment (Castellanos et al., 2002; Swanson et al., 2007). Furthermore, ADHD is associated with reduced DAT and D2R availability in subcortical regions of the left hemisphere, including the ventral and dorsal striatum and midbrain (del Campo et al., 2011). While there is clear evidence for dysregulated DA transmission in ADHD patients, there is still controversy over whether DA release is elevated or reduced in ADHD patients, and whether the reduction in DAT and D2R availability are involved in generating pathological symptoms or are compensatory adaptations (Genro et al., 2010; del Campo et al., 2011). A simple interpretation of the success of stimulant treatments would suggest that DA levels should be reduced in untreated ADHD patients; however, some authors suggest that stimulants probably exert their effects by promoting the activation of presynaptic D2 autoreceptors, gradually correcting a constitutive overactivity of the DA system (Solanto, 1998; Genro et al., 2010). Nevertheless, due to what is known on the function of the DA system, it has been proposed that different aspects of ADHD symptomatology are

related to dysfunctions in different DA pathways. For example, it is suggested that hyperactivity is linked to deficits in the nigrostriatal pathway, impulsivity is linked to deficits in the mesolimbic pathway, and deficient executive functions are linked to deficits in the mesocortical pathway (Genro et al., 2010). However, there is little evidence confirming this proposition. Given that the major drug used for treating ADHD, methylphenidate, is a DAT blocker and that DAT gene variants are associated with ADHD diagnosis, it was thought that this protein would play a clear causal role in ADHD pathophysiology. However, there are conflicting reports on DAT expression density in ADHD patients, with different studies reporting higher, lower or unchanged levels of DAT expression, which has led to the proposition that variations in DAT levels might "be plastic and vary over time, dependent on homeostatic mechanisms that operate to maintain tonic levels of synaptic or extra-synaptic DA" (Swanson et al., 2007). In summary, the mechanisms of DA dysregulation in ADHD are still not clearly understood, may be contingent on neuroplasticity processes and likely involve subtle changes to DA signaling.

1.2.6. Other disorders

Structural and functional abnormalities in in midbrain DA transmission has also been associated, either experimentally or theoretically, to several other mental disorders, including personality disorders, bipolar disorder, psychopathy, obsessive compulsive disorder and Tourette syndrome (Gelernter et al., 1997; Denys et al., 2004; Friedel, 2004; Buckholtz et al., 2010; Buse et al., 2013; Byrd et al., 2014; Ashok et al., 2017). This highlights the crucial role of forebrain DA signaling for behavioral control, and the necessity of understanding this system for developing new therapeutic strategies for mental disease. Importantly, the fact that DA neurons are involved in the pathophysiology of such a large repertoire of mental illness indicates that minor alterations in their physiology can have dramatic impacts on the behavior.

1.3. Dopamine and learning

1.3.1. Learning and conditioning: definitions

In the context of biological research, behavior can be defined as the elements of an organism's function which directly act upon the outside world (Skinner, 1938). Learning occurs when organisms change their behavior based on information acquired from previous experiences. Learned behaviors give organisms the capacity to adapt to dynamic environments within their lifetime. This means that when confronted with a major environmental change a given population can survive if each individual animal changes its behavior in order to reflect the transformations in its surroundings, instead of only going through the natural selective process where animals with suboptimal and rigid behaviors are eliminated and the median behavioral strategy shifts across multiple generations. Likewise, learning gives individual animals the capacity to adapt to unstable environments, developing increasingly more effective survival strategies within their lifetimes.

Learning can be conceptualized as the acquisition, storage and access of abstract information (such as stimulus-outcome associations and spatial maps) in the brain, and is therefore considered a prerequisite of the conscious experiences described by humans (Thorndike, 1898; Tolman, 1948; Crick and Koch, 1990). From this conceptualization rises one of the major general underlying hypotheses of all neuroscience and psychology: that understanding the origin, development and mechanisms of the human mind requires and encompasses the understanding of learning processes in other animals (Thorndike, 1898).

Conditioning is the form of learning by which a given behavior becomes associated with a specific sensory cue (classical or Pavlovian conditioning) or action (operant conditioning) depending on its outcome. A reinforcer, or reward, is an outcome that increases the frequency, intensity and/or predictability of behaviors that directly predict or directly cause its delivery or that arises in response to similarly predictive stimuli (also called conditioned stimuli, or CS). Conversely, punishments are outcomes that reduce (inhibit) behaviors associated with its delivery and promote behaviors related to its omission. Behaviors linked to the omission of a reward, or disappointment, are likewise inhibited. Rewards and punishments, as they produce intrinsic changes to behavior, are also called unconditioned stimuli (US).

Disappointment, therefore, can be considered as a form of punishment and the omission of a predicted reward is a clear negative outcome. The consistent omission of a reward following a previously reinforced behavior eventually leads to the abolishment of the reinforced behavior, a process referred to as “extinction”.

While it was initially hypothesized that conditioning was established primarily through temporal and statistical association (i.e. when a stimulus or an action is closely followed in time by a given outcome with a certain probability) it quickly became clear that association by itself is not sufficient to generate learning (Rescorla and Wagner, 1972; Rescorla, 1976; Pearce and Hall, 1980). For example, if a CS-US pairing has already been established (e.g. A→US), it drastically reduces learning of a second CS that is paired to the same US in compound to the first CS (e.g. AB→US), a phenomenon called “blocking” (Kamin, 1968). Learning therefore is only observed when an organism’s assumptions and predictions about the world are violated, i.e. when there is a discrepancy, or error, between its expectations and the experienced outcomes. In the context of conditioning, this discrepancy is referred to as a “prediction error”, and the greater this error, the more an animal learns from the experience. Current theories of conditioning conceptualize the prediction error as a teaching signal, which informs how much the organism must update its expectations on each individual action/stimulus-outcome pairing.

One influential learning model, proposed by Robert Rescorla and Allan Wagner in the 1970s, conceptualizes Pavlovian conditioning as error-guided changes in associative strength (V) between a specific CS and US as a result of a conditioning trial (Rescorla and Wagner, 1972). In the Rescorla-Wagner model, the V for a given future trial (V_{n+1}) is determined by the current V (established by previous trial experiences) added to the difference between the maximal possible associative strength of the US (R) and the current V (the prediction error term) multiplied by a single (α) or compound learning rate ($\alpha\beta$), which determines how much the V is updated per trial. In the original instantiation of the model, the learning rate constants α and β referred to the “salience” or intensity of the CS and US, respectively. This division was introduced to take into account potential differences in learning produced by variations in CS properties independently of the US. For example, rats acquire stronger contextual fear responses to the same shock intensity (US) in sensory stimuli-enriched arenas (CS) than in non-enriched boxes (Mckinzie and

Spear, 1995). However, in most practical instantiations of the Rescorla-Wagner model, the learning rate constant can be simplified to one term, particularly if the CS properties are not changed (Rescorla and Wagner, 1972; Raczka et al., 2011; Tian and Uchida, 2015).

The Rescorla-Wagner model can successfully recapitulate several phenomena of conditioning learning, such as blocking and conditioned inhibition, where an animal learns that a second CS predicts the omission of a US after the presentation of a predictive CS (e.g. A→US; AB→ no US; B thus acquires a negative V in relation to the US). Moreover, this model predicted a number of previously unknown conditioning phenomena, such as overexpectation, where animals are trained to associate two different CSs with the same type and quantity of US in separate trials. If the experimenter then presents the two CSs in combination, but does not double the US, this creates a negative prediction error, as the animal initially expects two times the US quantity it actually receives (Kremer, 1978; Rescorla, 2006, 2007).

Equation 1.1. The Rescorla-Wagner model of reinforcement learning (simplified)

$$V_{n+1} = V_n + \alpha(R - V_n)$$

where

V = associative strength between CS and US

α = learning rate parameter

R = maximal associative strength of the US

n = trial index

Another influential learning model is the temporal difference (TD) learning model. This model is inspired by psychological theory but was primarily developed for artificial intelligence applications, where it has been highly successful (Sutton and Barto, 1981, 1998; Sutton, 1988; Tesauro, 1992). The main advantage of TD learning is that, instead of being driven by the error between predicted and actual outcomes for a given conditioning trial, it is driven by the error or difference between temporally successive predictions. Therefore, learning occurs whenever there is a change in prediction over time, and specific predictions are attributed to specific time points. For example, suppose an animal is conditioned to learn that a given CS is always

followed by a US with a one second delay; with a trial-based conditioning model, one can only model the effect of the CS-US association, while with a TD approach, a prediction is formed for the exact time point of US presentation. If the US is delayed or arrives early in relation to expected time point of delivery, this also creates prediction errors that drive the update of future expectations.

In order to guide goal-directed decision making, TD reinforcement learning algorithms assume predictions of outcome value, i.e. valence-defined outcomes (Schultz et al., 1997; Sutton and Barto, 1998; Dayan and Niv, 2008; Nasser et al., 2017). Value expectation error signals act as a teaching signal that updates a value function, which keeps track of expected value at current and future time points. This is conceptually different from the association strength conceptualization of the Rescorla-Wagner model, which does not necessarily assume that the signals reflect positive valence (Rescorla and Wagner, 1972).

It is important to note, from a practical perspective, that models of reinforcement learning can shape interpretations of behavioral conditioning data by decomposing the observed behavior into quantitative parameters (Hull et al., 1940; Rescorla and Wagner, 1972; Rescorla, 1976; Pearce and Hall, 1980; Sutton and Barto, 1998; Kubis et al., 2000). By fitting model results to empirical data, they have been used experimentally to quantify behavioral parameters such as learning rates, risk seeking and exploratory drive in different behavioral contexts and across genotypes (Luksys et al., 2009; Raczka et al., 2011; Tian and Uchida, 2015; Naude et al., 2016). Leaning models have also been instrumental in providing quantitative frameworks and specific predictions for behavioral outcomes, which can further be tested experimentally (Kremer, 1978; Sharpe et al., 2017).

1.3.2. The reward prediction error theory of dopamine signaling

The first indication that DA neurotransmission is involved in reward came from the seminal work of Olds and Milner (1954), where they found that self-initiated electrical stimulation of the MFB led to persistent self-stimulation behavior. This meant that the stimulation of DA axons in itself could support operant conditioning as if it was a reward, and established intra-cranial self-stimulation as a standard paradigm for assessing the mechanisms of reward processing. Later studies confirmed that direct stimulation of the VTA and the SN was also reinforcing, and that this rewarding effect depended on intact DA neurotransmission (Crow, 1972; Corbett

and Wise, 1980; Wise, 1981; Fibiger et al., 1987). Recently, these experiments have been replicated using cell-type specific genetic approaches, and have extensively confirmed that activation of mesolimbic and nigrostriatal DA neurons, or their direct excitatory afferents, supports self-stimulation (Witten et al., 2011; Kim et al., 2012; Rossi et al., 2013; Ilango et al., 2014; Beier et al., 2015). However, despite the crucial importance of these findings, they offer limited insight as to the information that is coded by DA activity in normal behavior. For example, self-stimulation paradigms do not test whether region-specific DA signals or controls the perception of consummatory pleasure (liking), motivational salience (wanting) or cue-outcome association strength.

The selectivity of DA's role in reward was intensely investigated by Wolfram Schultz and collaborators in a series of pioneering studies in the late 1980s and early 1990s (Schultz, 1986; Ljungberg et al., 1992; Schultz et al., 1993, 1997, Mirenowicz and Schultz, 1994, 1996). Using extracellular single unit recordings of putative DA neurons in head-fixed macaques during Pavlovian conditioning, they showed that the firing patterns of 55 to 80% or recorded putative DA neurons in the primate SNc closely resembled the teaching signals used in TD learning models (Schultz et al., 1997; Sutton and Barto, 1998). More specifically, DA neurons represented reward (value-based) prediction errors, scaling their activity to the difference between expected reward values and the actual obtained rewards after a CS (Figure 1.6). DA neurons exhibited constant pacemaker-like firing in the absence of reward or CS; when the animals were exposed to an unexpected reward or a reward that was greater in value than was previously predicted (a positive prediction error) they displayed phasic increases in firing activity, i.e. bursts; when a fully predicted reward was delivered, the activity of these neurons did not change; and when an expected reward was omitted (a negative prediction error) dopamine neurons briefly ceased their firing (paused).

Since these groundbreaking first observations, the activity of DA neurons has been extensively linked to the coding of prediction errors in conditioning across multiple mammalian species, including humans, and prediction error theory has dominated the field due to its high explanatory power, formal descriptive precision and face validity (Mirenowicz and Schultz, 1996; Schultz, 1997, 2007; Schultz et al., 1997; Waelti et al., 2001; Zaghloul et al., 2009; Cohen et al., 2012). Today, this

finding is considered one of the most replicated phenomena in neuroscience, highlighting the highly conserved function of this neuronal subclass (Bromberg-Martin et al., 2010a).

An exciting interpretation of these findings is that DA neurons may code for reward value across multiple behaviorally relative dimensions, such as reward modality (food, water, sex, social interaction, etc.), probability, timing and effort (Lak et al., 2014; Stauffer et al., 2014; Schultz et al., 2015). For example, if an animal is confronted with a choice of obtaining food or water, DA neurons would compute the relative value of each reward and inform target neural circuits of which choice is optimal. Indeed, recent studies have found that DA neurons can code for formal economic utility, i.e. the subjective value of a given resource (Stauffer et al., 2014; Schultz et al., 2015).

It is important to note, however, that different model organisms and experimental preparations provide qualitatively different results, which can still be encompassed by the reward prediction error theory. One noteworthy observation is that most primate studies on reward prediction error signaling by DA neurons focus on the SNc, while rodent studies focus on the VTA (Björklund and Dunnett, 2007; Bromberg-Martin et al., 2010a). This is largely because of the different anatomical organization of the primate and rodent midbrain; the dorsal tier of the primate SNc is highly heterogeneous in comparison to rodents, and contains cells that project both to the dorsal and ventral striatum, as well as several cortical regions (Williams and Goldman-Rakic, 1998; Björklund and Dunnett, 2007; Iversen et al., 2010). This distinct anatomical organization suggests that some DA neurons in the primate SNc, especially in the dorsal tier, are functional analogues, and perhaps homologues, to DA neurons in the rodent VTA. Another difference between primate and rodent studies is the extent to which reward-related bursts are actually cancelled out by a CS-triggered prediction. In primate studies, a fully predicted reward does not generate any change in the firing of DA neurons; in rodent studies, firing rate increases associated with reward delivery are only attenuated by CS-triggered predictions, with no study reporting a full elimination of the reward response (Schultz et al., 1997; Roesch et al., 2007; Cohen et al., 2012; Menegas et al., 2017). This is often explained by the different training schedules used with primates and rodents; monkeys are usually trained for thousands of trials before DA neuron activity is

recorded, while rodents are trained in dozens or at most hundreds of trials. The interpretation is that rodents are never trained to the full extent necessary in order for the animal to consider a reward to be fully predicted by the CS, while monkeys, due to being over-trained, can indeed learn full predictions. It is still an open question whether these factors can fully explain the different results reported in the primate and rodent literature, but they alone do not challenge the fundamental concepts of the reward prediction error signaling theory.

A recent study, however, has provided evidence that DA transients might promote learning that is based not only on reward value, but on general prediction errors (PEs) formed even by unrewarded stimulus associations (Sharpe et al., 2017). In this context, DA signaling would be more similar to the general associative prediction error term expressed in the Rescorla-Wagner model, for example, than to the value-based reward prediction error assumed by TD-learning algorithms. This would mean that the prediction errors observed in DA neuron firing patterns during reward-based learning and decision making might be a particular expression of a more general function of DA neurons in signaling errors in event prediction (Sharpe et al., 2017).

While the finding that DA neurons code for prediction errors has been extensively replicated, it is crucial to note that this is not the full extent of the behavioral relevance of DA neurons. Indeed, the diversity of DA behavioral signals parallels the previously discussed biophysical and anatomical diversity of DA neurons. Some studies report that SN DA neurons display phasic increases in firing rate (on average around 6 Hz), as well as increased axonal DA calcium signals, immediately before the execution of a motor behavior regardless of its value (Jin and Costa, 2010; Howe and Dombeck, 2016). Interestingly, Dodson et al. (2016) reported finding pauses in SN DA neuron activity during initiation of locomotion. There is also evidence, from recordings of calcium transients of DA neuron axon terminals in the dorsal striatum, that suggest these neurons can display a mixed signal, representing both action selection and reward prediction error, while DA signals in the ventral striatum more closely resemble “pure” reward prediction errors (Parker et al., 2016).

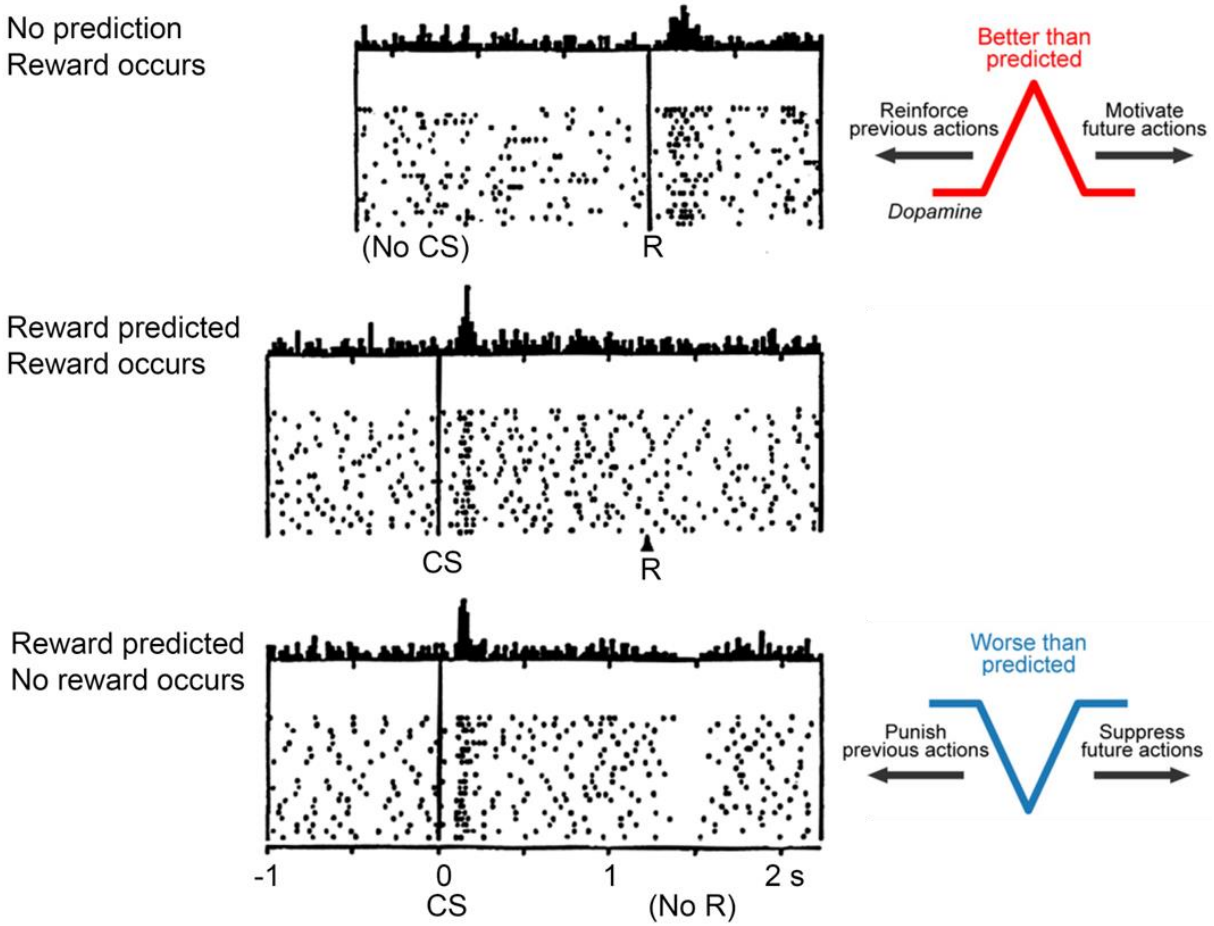

Figure 1.6. DA signal reward prediction error in Pavlovian conditioning.
If an unexpected reward is delivered, DA neurons respond with a burst, leading to increases in DA release in target regions, reinforcing behaviors that preceded reward delivery and increasing motivations. If a completely predicted reward is delivered, DA neurons no longer respond to reward delivery, but instead burst following the presentation of the cue that predicted the reward. Conceptually, this occurs because the value or the associative strength of the US is now attributed to the unexpected CS. When an expected reward is not delivered at the predicted time after a cue, DA neurons pause their firing, leading to a reduction of DA release in target regions and punishing, i.e. suppressing the execution, of behaviors that lead to the disappointment. Figure panels were adapted from Schultz et al. (1997) and Bromberg-Martin et al. (2010).

Nigrostriatal DA transmission has also been linked to other signals that cannot be fully explained by reward prediction error theory, such as the coding of action vigor, movement kinematics, exploratory drive and novelty (Schiemann et al., 2012; Barter et al., 2015; Panigrahi et al., 2015; Yttri and Dudman, 2016; Menegas et al., 2017). Mesocortical DA release, as measured with microdialysis and manipulated with optogenetics, has been linked to behavioral flexibility, working memory and stimulus discrimination (Watanabe et al., 1997; Wang et al., 2004; Popescu et al.,

2016). Importantly, some authors argue that prediction error coding by mesolimbic DA signals is a particular instantiation of a more general coding of motivational salience, both related and unrelated to value (Horvitz, 2000; Berridge, 2007; Bromberg-Martin et al., 2010a; Saunders and Robinson, 2012; Matsumoto et al., 2016; Schultz, 2016a). This is supported by multiple studies that have linked changes in DA signaling, especially of tonic DA concentrations in the NAcc, with the determination of motivational states, particularly of incentive salience, which is the drive to pursue specific outcomes independent of learned associations (Berridge, 2007, 2012; Bello et al., 2011). It has also been proposed that DA signals, particularly in the mesolimbic pathway, convey a decision variable that multiplexes these two forms of information, coding "the available reward for investment of effort, which is employed for both learning and motivational functions" (Hamid et al., 2015).

1.3.3. Learning from disappointment: dopamine negative prediction errors

The role of DA neuron inhibition in behavior and learning has recently garnered attention of the research community. A large body of evidence suggests that phasic reductions in DA neuron firing are correlated with negative reward prediction errors and the behavioral responses to reward omission. Studies with extracellular recordings in awake head-fixed primates have found that inhibition of DA neuron activity (measured with both firing rate changes or pause duration) can scale linearly with the magnitude of negative prediction errors (Nakahara et al., 2004; Tobler et al., 2005; Bayer et al., 2007). One study where DA neurons were recorded in awake primates during a paradigm of conditioned inhibition also found that a large fraction of DA neurons are inhibited (median 35% decrease from baseline) by the cue that signals reward omission, which is a powerful formal evidence that these neurons encode negative prediction errors (Tobler et al., 2003).

Similar results have also been found with extracellular recordings of genetically identified DA neurons in head-fixed rodents, where decreases in firing have also been found to scale linearly with the magnitude of negative prediction errors within an average range of 0 to -3 spikes/second in relation to baseline (Tian and Uchida, 2015). Significant decreases in DA neuron firing rate (≥10% decrease in relation to baseline) have also been observed during the extinction of an appetitive response in freely moving rats, where it preceded the full suppression of the conditioned

behavior; pauses also gradually subsided as the animals learned that the CS no longer predicts the US, indicating that it corresponded to an error in prediction (which progressively decreases with learning), and not just reward omission (Pan et al., 2008b).

Studies using cyclic voltammetry to directly measure DA release corroborate the results from electrophysiological experiments. In a very elegant study, Hart et al. (2014a) explicitly tested if the reward prediction error-associated changes in DA release complied with the formal neuroeconomic axioms of “consistent prize ordering” (larger signals for larger rewards given similar reward probabilities), “consistent lottery ordering” (larger signals for rewards obtained under lower probabilistic expectations, given similar reward sizes) and “no surprise equivalence” (in a fully deterministic task, signals should be the same for all reward sizes). They showed that phasic decreases in dopamine release in the NAcc core of freely moving rats correlated with the magnitude of the formal negative prediction errors in a probabilistic choice task, complying with the axiomatic definition. Importantly, the decreases in DA release in response to negative prediction errors mirrored the increases in DA release in response to positive prediction errors, indicating that the coding of prediction errors by phasic changes in DA concentration in the NAcc core is quantitatively symmetrical across valence representations. Other studies with freely moving rodents have shown similar patterns, with greater than expected rewards (positive prediction errors) being represented by phasic increases in NAcc core DA signals, and lower than expected rewards (negative prediction errors) being represented with decreases in DA concentration (Sugam et al., 2012; Sunsay and Rebec, 2014; Saddoris et al., 2015). This pattern also holds true for initial sessions of extinction learning, where reward-related negative prediction errors are quickly accompanied by a reduction in cue-related positive prediction error signals, even though these signals quickly become hard to quantify as the animals learn that the CS-US pairing is no longer valid and stop responding to the CS or initiating operant behaviors (Sunsay and Rebec, 2014; Saddoris et al., 2015). Notably, some studies found only trend (not statistically significant) decreases in NAcc core DA signals in response to reward omission, but this seems to be dependent on task structure parameters, such as the average reinforcement history preceding omission trials (Hart et al., 2014a, 2015). It is important to note that the properties of this signal can vary significantly depending on the specific projection target within the striatum. For

example, negative prediction error-associated decreases in DA release are not observed in the neighboring medial shell of the NAcc, where DA release seem to be better correlated to stimulus salience (Saddoris et al., 2015). Indeed, decreases in DA release in response to expected reward omissions, and especially during extinction, seem to be selective to the NAcc core. This has also been confirmed by microdialysis measurements of DA concentrations in the NAcc core and medial shell over multiple minutes in extinction sessions (Biesdorf et al., 2015). The relevance of this apparent functional specialization of the NAcc core for the general circuitry of reward processing and the control of goal-directed behaviors is not well understood.

Recently, a technique called fiber photometry (aka fluorometry) has been used to record bulk Ca^{++} transient-related fluorescent signals from DA neurons or DA axons embedded in their target regions (Gunaydin et al., 2014; Lerner et al., 2015; Kim et al., 2016; Parker et al., 2016; Menegas et al., 2017). Signals recorded with this method represent the population activity of multiple genetically-specified cells or axonal compartments. Despite not having the spatial resolution of carbon-fiber cyclic voltammetry, and therefore being unable to resolve between difference accumbal regions, photometry recordings have consistently shown that DA axon Ca^{++} signals in the NAcc decrease in response to the omission of an expected reward or an aversive stimulus (Kim et al., 2016; Parker et al., 2016; Menegas et al., 2017). Again, however, there is a large diversity in the nature of the response depending on the striatal projection target, as similar recordings in the dorsal striatum reveal a mixture of prediction error and action-related signaling, while in the posterior (tail) striatum DA signals seem to reflect stimulus novelty (Parker et al., 2016; Menegas et al., 2017).

There is also increasing evidence that pauses in dopamine neurons have a causal role in promoting learning from negative prediction errors. Overriding pauses in dopamine neurons with channelrhodopsin (ChR2) stimulation (optogenetic excitation) at the time of expected reward delivery during consistent reward omission slows down extinction learning (Steinberg et al., 2013). Even more convincingly, inducing brief (two second) pauses with halorhodopsin (NhPR) stimulation (optogenetic inhibition) during reward presentation mimics negative prediction error effects (Chang et al., 2015). This was tested using a modified Pavlovian overexpectation task. Chang et al. (2015) modified the classical paradigm, in which animals receive less than expected rewards, by matching reward delivery to the

animal's expectations (providing twice the unitary reward amount during compound CS presentation), but optogenetically inhibiting DA neurons during the consumption of the second reward. This did not change the consummatory behavior during US presentation, but did accelerate the subsequent extinction of the response to the CS paired with US delivery and optogenetic inhibition of DA neurons (similarly to what is observed in true unmatched "overexpectation") thus demonstrating that brief pauses in DA neuron activity drive the behavioral effects of learning from negative prediction errors.

In tasks where animals have to choose between a small/certain and larger/risky rewarded levers, stimulation of the LHb or RMTG (inhibiting DA neurons) during reward presentation after choosing one option redirected bias toward the alternative option, as would be expected if the positive prediction errors were diminished, while stimulation of the VTA during reward omission after choosing the risky option increased risky choices, as would have been expected is negative prediction errors were overridden (Stopper et al., 2014). Chronic electrical stimulation of the LHb also facilitates the extinction of sucrose- and cocaine-reinforced lever pressing, consistent with an increase in learning from negative prediction errors (Friedman et al., 2010, 2011). Lesioning the LHb (removing a source of disynaptic inhibition for DA neurons), on the other hand, decreases DA neuron inhibition during reward omission, strongly reduces learning from negative prediction errors and prevents the extinction of sucrose- and cocaine-reinforced operant behaviors (Friedman et al., 2010; Tian and Uchida, 2015). Finally, from a post-synaptic perspective, pharmacological blockade of $GABA_A$ receptors with bicuculline in the VTA completely prevents the extinction of an appetitive response (Pan et al., 2008b). In summary, generating pauses in DA neuron firing with direct optogenetic inhibition or by triggering inhibitory GABAergic input from upstream circuits facilitates extinction learning and biases choices from reward omission; blocking pauses, either with direct optogenetic or electrical excitation, lesioning upstream inhibitory regions or pharmacological blockade of GABAergic receptors, impairs learning from reward omission (Table 1.2).

Recent studies have investigated the mechanisms of how VTA DA neurons calculate negative prediction errors via the integration of inhibitory input. The two major afferent circuits that provide crucial information for this computation are local VTA GABA neurons and the GPi-LHb-RMTg pathway. One influential hypothesis

postulates that the expectation of reward is coded by inhibitory input to DA neurons, while information about the reward value itself is transmitted via excitatory inputs; the DA prediction error is then calculated by a direct subtraction of the expected value (inhibition) and experienced reward value (excitation) within DA neurons (Schultz et al., 1997; Joel et al., 2002; Cohen et al., 2012; Eshel et al., 2015). Neural correlates of an expectation signal have indeed been found in the activity of local GABA neurons in the VTA, which gradually increase their activity after CS presentation, peaking at the precise time of expected reward delivery (Cohen et al., 2012). In a follow up study, Eshel et al. (2015) established that the activity of VTA GABA neurons causally mimics an expectation signal, as selective excitation of these neurons with ChR2 subtracts from positive reward prediction error-related firing rate increases in putative VTA DA neurons, while their selective inhibition with archaerhodopsin (ArchT) increases the magnitude of positive prediction error signals in VTA DA neurons. Importantly, optogenetic excitation of VTA GABA neurons was sufficient to bias behavior; post-training stimulation of these neurons with a pattern that mimicked their natural ramping expectation signal during CS-US pairing trials markedly reduced anticipatory licking during the interval between CS and US presentation, which is akin to the effect of disappointment, i.e. receiving less reward than expected. This was also not an acute motor effect, but rather a form of learning, as the animals had to re-learn the previous association in subsequent training sessions where there was no inhibition of VTA GABA neurons.

LHb neurons, unlike VTA GABA neurons, code reward-related prediction errors directly, but in an inverse manner as DA neurons, being excited during punishment or reward omission, and being inhibited by reward delivery (Matsumoto and Hikosaka, 2007, 2009a; Bromberg-Martin and Hikosaka, 2011; Hong et al., 2011). Importantly, LHb neurons signal prediction errors with shorter sensory latencies than DA neurons, indicating that they calculate these errors before DA neurons and transfer this signal to them (Hong et al., 2011). Activity of LHb neurons can also reflect temporal expectation of rewards and stimulus salience, but their strongest changes in phasic activity during conditioning is linked to reward value (Matsumoto and Hikosaka, 2007; Bromberg-Martin et al., 2010b). Signals related to negative motivational value are at least partly transmitted to the LHb by excitatory projections from the GPi, and these signals are further transmitted from LHb excitatory synapses to the RMTg and VTA GABA neurons, which then inhibit the majority of DA neurons (Christoph et al., 1986;

Ji and Shepard, 2007; Hong and Hikosaka, 2008; Omelchenko et al., 2009; Brinschwitz et al., 2010; Bromberg-Martin et al., 2010c; Balcita-Pedicino et al., 2011; Hong et al., 2011; Stephenson-Jones et al., 2016).

There is also some evidence that prediction error-related information could be transmitted to the LHb from the VP and striatum, but this is not a well-established finding (Hong and Hikosaka, 2013). Inhibition of DA neurons by the GPi-LHb-RMTg pathway is important for controlling the tonic levels of DA neuron firing and the calculation of both positive (through disinhibition) and negative (through inhibition) prediction errors, as determined by the effects of LHb lesions (Tian and Uchida, 2015). However, the effect of disrupting this pathway on behavior and DA firing patterns is much more severe for negative prediction error calculation, suggesting that this pathway is most important for providing direct negative prediction error information to DA neurons (Tian and Uchida, 2015). In summary, the representation of negative prediction errors by DA neurons is a composite of at least two (and potentially many more) afferent inputs which convey information about both expected value and prediction errors calculated by other neuronal circuits (Tian and Uchida, 2015; Tian et al., 2016). It is important first to note that phasic inhibition of VTA DA neurons also induces immediate aversive responses in certain contexts. Direct inhibition of DA with optogenetic methods, or stimulation of upstream inhibitory circuits such as the LHb (which leads to the disynaptic inhibition of DA neurons), RMTG and VTA GABA interneurons, leads to real-time place aversion, the interruption of consummatory behaviors and blocks the animal's innate preference for dark environments (Lammel et al., 2012; Stamatakis and Stuber, 2012a; van Zessen et al., 2012; Danjo et al., 2014).

Table 1.2. Causal evidence that DA neuron inhibition codes for negative prediction errors.

Finding	Methods	Reference
Overriding pauses in DA neuron activity during consistent reward omission slows extinction learning	- Optogenetic excitation of DA neurons with ChR2 - Operant conditioning with sucrose reward in freely moving rats	Steinberg et al., 2013
Introducing pauses in DA neuron activity during reward presentation in acquisition accelerates the subsequent extinction of the conditioned response	- Optogenetic inhibition of DA neurons with NhPR - Sucrose pellet-rewarded Pavlovian overexpectation task in freely moving rats	Chang et al., 2015
Lesioning the LHb (an upstream region that disynaptically inhibits DA neurons) reduces DA neuron firing rate decreases in response to reward omission and impairs learning from negative prediction errors	- Electrolytic lesions of the LHb - *In vivo* extracellular recordings of identified DA neurons in awake animals - Pavlovian conditioning with sucrose reward in head-fixed mice	Tian and Uchida, 2015
Chronic stimulation of the LHb facilitates extinction of cocaine self-administration, and lesioning the LHb impairs extinction of the reinforced response	- Electrical stimulation of the LHb - Quinolinic acid lesions of the LHb - Operant conditioning with cocaine reward in freely moving rats	Friedman et al., 2010
Chronic stimulation of the LHb facilitates extinction of sucrose-conditioned behavior, and lesioning the LHb impairs extinction of the reinforced response	- Electrical stimulation of the LHb - Quinolinic acid lesions of the LHb - Operant conditioning with sucrose reward in freely moving rats	Friedman et al., 2011
Time-locked stimulation of the LHb or RMTG during reward presentation biases operant behavior in a manner that is congruent with diminished positive prediction errors, while VTA stimulation during reward omission biases behavior in a manner that is congruent with diminished negative prediction errors	- Electrical stimulation of the LHb, RMTG and VTA - Risky decision making task with sucrose reward in freely moving rats	Stopper et al., 2014
Pharmacological blockade of $GABA_A$ receptors in the VTA prevents the extinction of a conditioned response	- *In vivo* local VTA infusion of bicuculline - Pavlovian conditioning with sucrose reward in freely moving rats	Pan et al., 2008b
Excitation of local inhibitory inputs to VTA DA neurons subtracts from positive reward prediction error representations and reduces anticipatory reward seeking. Inhibition of these inputs, on the other hand, increases positive prediction error signals in VTA DA neurons.	- *In vivo* extracellular recordings of identified DA neurons in awake animals - Optogenetic excitation of VTA GABA neurons with ChR2 - Optogenetic inhibition of VTA GABA neurons with ArchT - Pavlovian conditioning with sucrose reward in head-fixed mice	Eshel et al., 2015

The distinct mechanisms by which DA neurons respond to direct punishment, as opposed to reward omission or mismatched expectations, are not as well understood. There is a strong contention as to whether primary rewards and punishments are processed by dopamine neurons across the same dimension of value. Consistently with reward prediction error theory, the majority of DA neurons studied across different mammalian species respond to acute painful (foot shocks or toe pinches) and distressing (air-puffs, bitter tastes) stimuli with transient decreases in firing (Ungless et al., 2004; Brischoux et al., 2009; Brown et al., 2009; Matsumoto and Hikosaka, 2009b; Cohen et al., 2012; Matsumoto et al., 2016).

These results are often interpreted within the reward prediction error framework, with aversive stimuli being considered a form of disappointing outcome, i.e. violating the animal's expectations of the world. This form of coding is, however, not homogenous, as some DA neuron populations, specifically those located in the ventromedial VTA of rodents and the dorsolateral SNc of primates, have been found to preferentially respond to aversive stimuli with transient excitation (Brischoux et al., 2009; Matsumoto and Hikosaka, 2009b). In addition, most studies to not quantify control for different subjective perceptions of aversive versus appetitive stimuli.

The quantitative opposition of reward prediction error and aversiveness has been elegantly investigated in a series of studies by Fiorillo and collaborators (Fiorillo, 2013; Fiorillo et al., 2013a, 2013b). In these studies the intensity of aversive stimuli, including air puffs and foul tasting solutions, were carefully titrated in order to match the absolute value of competing appetitive stimuli. Before recordings, animals underwent a series of choice tasks where it was determined how much juice reward they were willing to sacrifice in order to avoid an aversive stimulus. The response of DA neurons to each individual stimuli and each combination of aversive and appetitive stimuli was then recorded. They found that DA neurons were not significantly inhibited by the presentation of aversive stimuli nor excited by their omission. Presentation of aversive stimuli also did not subtract from the value representation of concurrently presented rewards unless it physically impeded reward evaluation (as in the concurrent delivery of sweet juice and bitter denatonium solution). These results led the authors to conclude that DA neurons are insensitive to changes in intensity of aversive outcomes, which must be represented by

alternative neural systems, an interpretation that had been previously proposed in theoretical studies (Daw et al., 2002; Fiorillo, 2013).

However, Matsumoto et al. (2016) have recently suggested the coding of primary aversive stimuli depends on behavioral context. Recording genetically identified DA neurons in head-fixed mice, they showed that VTA DA neurons displayed purely inhibitory responses to air-puffs when in low-reward contexts, and a combination of a short-latency excitation and delayed inhibition in response to the same stimulus in high-reward contexts (Matsumoto et al., 2016). The latter finding suggests that the differences in DA neuron responses to aversive stimuli reported by different labs, including the Fiorillo studies, could be due to different contextual estimates of general reward availability in each task. Nevertheless, this response diversity is not easily explained by the classical reward prediction error theory and the mechanisms and behavioral relevance of these DA signals remains poorly understood.

Interestingly, DA signals for the prediction of aversive events seem, in some conditions, to fit well to the reward prediction error theory. For example, the duration of inhibitory pauses in VTA DA neurons has been shown to scale linearly with the breathing rate responses to a shock-predicting CS after fear conditioning, suggesting that pauses in DA neurons also code for expected painful stimuli (Mileykovskiy and Morales, 2011). This interpretation is corroborated by the consistent findings that shock-predicting CS after fear conditioning promote a marked decrease in DA release in the NAcc core (but not the medial shell), while the successful avoidance of a painful stimulus promotes increased DA release in both regions (Badrinarayan et al., 2012; Oleson et al., 2012; Gentry et al., 2016)

There are also controversies on the symmetry of prediction error coding by DA neurons. Some authors argue that dopamine neurons do not have the necessary dynamic range to code for negative predictions errors with the same resolution that they code for positive prediction errors (Bayer et al., 2005; Niv et al., 2005; Dayan and Niv, 2008; Glimcher, 2011). This proposition derives mainly from the observation that DA neurons typically fire regularly *in vivo* at approximately 3-6 Hz, achieve 25-30 Hz during burst firing (≈20 Hz change), but can only reduce their firing to zero. This means that the range, measured as absolute instantaneous rate change, for coding positive prediction errors is much higher than the range for coding negative prediction

errors (Niv et al., 2005). Taken at face value, this could mean that DA signals are not ideally suited for reporting symmetrically positive and negative formal prediction errors.

However, these ongoing issues can potentially be elucidated by considering three interlinked findings in the field. First, some studies demonstrate that the duration of inhibitory pauses provide a more accurate estimate of negative reward prediction error coding than instantaneous absolute rate changes in firing rate (Bayer et al., 2005, 2007; Dreyer et al., 2010; Mileykovskiy and Morales, 2011). Dreyer et al. (2010) elegantly demonstrated with computational modeling of DA neuron activity, post-synaptic DA release and DA receptor occupancy that, while the degree of D1R increases in occupancy is linearly related with the **frequency** of bursting activity, decreases in D2R occupancy scale with the **duration** of pauses in DA neuron activity. Indeed, in two studies from the Glimcher lab where the same dataset (DA neuron recordings in awake primates performing a delay-sensitive operant conditioning task) were analyzed with the two different methods, it was shown that only pause duration was quantitatively related to negative prediction error magnitude (Bayer et al., 2005, 2007).

These incongruities in data analysis and interpretation is likely related to two properties of the DA system discussed previously in this dissertation: 1) DA release in not linearly linked to AP frequency and 2) the mechanisms of post-synaptic readout of pauses and bursts by D2Rs and D1Rs, respectively, are not dependent on absolute firing rate. This would mean that while the absolute range of firing frequency is not symmetrical in DA neurons, the post-synaptic effects could still represent a symmetrical opponent signal in its post-synaptic readout.

An important potential exception to the classical reward prediction error coding theory in relation to the processing of aversive/negative events is the case of mesocortical DA neurons. As discussed before, this atypical population of DA neurons has been proposed to signal aversion. In addition to their genetic and biophysical peculiarities, mesocortical DA neurons receive direct excitatory inputs from the LHb and only display synaptic plasticity (as measured by changes in the AMPA/NMDA ratio) in response to aversive, but not rewarding, stimuli (Lammel et al., 2011, 2012, 2014). In addition, optogenetic activation of mesocortical DA neurons results in real-time place aversion, suggesting that increases in PFC DA levels are

intrinsically aversive (Lammel et al., 2012). This interpretation has been further corroborated by fiber photometry recordings of DA axons in the PFC during the presentation of unexpected rewards and tail shocks, which showed that Ca^{++} transients in these axons were only observed in response to the latter (Kim et al., 2016).

However, several other studies from multiple labs over the course of the last three decades have reported radically different findings and interpretations on PFC DA signals. A recent study, also using fiber photometry recordings of DA axons in the PFC, showed that mesocortical DA axon activity transiently increased in response to rewards and reward prediction CSs, and that the reward response were reduced with increasing reward probability, as expected within the reward prediction error theory framework (Ellwood et al., 2017). However, stimulation of these axons was neither reinforcing or aversive, which is strikingly different from the results of direct VTA DA neuron stimulation (Witten et al., 2011; Steinberg et al., 2013; Ellwood et al., 2017; Sharpe et al., 2017). Instead, optogenetic stimulation of DA axons in the PFC regulated behavioral flexibility, with tonic stimulation promoting perseverance, even in the absence of reward, and phasic stimulation facilitating behavioral adaptation to task variations (Ellwood et al., 2017).

Several other studies also suggest that mesocortical DA signaling acts more by modulating cognitive representations in cortical circuits. For example, Popescu et al. (2016) found that phasic optogenetic stimulation of PFC DA axons was also not reinforcing or aversive, but instead increased stimulus discrimination in both rewarding and aversive contexts. Microdialysis studies have also reported increases in tonic PFC DA concentrations (measured across seconds), in response to changes in reward probability and in the execution of a working memory task (Watanabe et al., 1997; St Onge et al., 2012). DA iontophoresis into the PFC has also been shown to increase neuronal activity related to delayed responding, and disruption of DA signaling in the PFC with DA receptor antagonists can impair several cognitive functions, including working memory and delay responding (Sawaguchi et al., 1990; Wang et al., 2004). A more comprehensive review of the role of PFC DA in cognition can be found elsewhere (Iversen et al., 2010; Floresco, 2013), but there is not yet a clear functional model of how DA signals in frontal cortices relate both to cognition and aversion/reward processing in a unified framework.

1.3.4. Pauses and the synaptic mechanisms of learning in VTA DA neurons

Long term potentiation (LTP) and depression (LTD) of synaptic inputs are thought to be widespread subcellular substrates of learning and memory in the brain (Bliss and Lomo, 1973; Pignatelli and Bonci, 2015). Persistent potentiation of inputs to VTA DA neurons has been proposed as candidate cellular mechanism for the learning of CS-reward pairings. Three major forms of inducing LTP have been identified in midbrain DA neurons in *ex vivo* preparations. The first one was discovered by adapting classical LTP induction protocols from the hippocampal literature, i.e. by pairing the stimulation of glutamatergic inputs with postsynaptic depolarization (Bonci and Malenka, 1999; Overton et al., 1999). These protocols induce persistent LTP of excitatory post-synaptic currents (EPSCs) or EPSPs in both voltage and current clamp by increasing AMPAR conductances (AMPAR-LTP). This form of LTP is dependent on NMDAR activation, but does not change NMDAR current amplitudes; because of this, its induction can be inferred post-hoc by measuring the ratio of AMPAR and NMDAR currents in a given cell. This proxy measure has been used to demonstrate that this form of synaptic plasticity is induced by *in vivo* exposure to different drugs of abuse and stress (Ungless et al., 2001; Saal et al., 2003; Dong et al., 2004; Lammel et al., 2011). A second form of inducing AMPAR LTP is by applying spike timing-dependent (STD) protocols. From a cellular point of view, this form of plasticity appears to be the physiologically plausible variant to the classical LTP induction described above (NMDAR-dependent, mediated by increasing AMPAR conductance). Its induction is achieved by repeatedly pairing glutamatergic input stimulation with single post-synaptic spikes, in which the onset of each stimulated EPSP precedes the peak of the postsynaptic spike by ~5 ms (Liu et al., 2005; Luu and Malenka, 2008). Like classical LTP, STDP is facilitated by exposure to drugs of abuse. STDP protocols are thought to represent a more physiological form of synaptic plasticity, i.e. a more accurate facsimile of *in vivo* phenomena, in relation to LTP induced by post-synaptic depolarization (Pignatelli and Bonci, 2015).

A third form of LTP involves the potentiation of NMDAR conductances (NMDAR-LTP); it can be achieved by pairing sustained glutamatergic input stimulation with post-synaptic unclamped AP bursts in the voltage clamp configuration (Cui et al., 2007; Harnett et al., 2009). *In vivo* exposure to drugs of

abuse also amplifies the magnitude of this form of LTP (Bernier et al., 2011; Degoulet et al., 2016). This process is also modulated by repeated social defeat and fear learning (Stelly et al., 2016; Pignatelli et al., 2017). NMDAR-LTP in DA neurons is DA- and AMPAR-independent, but requires the activation of NMDAR, metabotropic glutamate receptor 1 (mGluR1), inositol 1,4,5-trisphosphate (IP3), protein kinase C (PKC) and L-type Ca^{++} channels. Furthermore, NMDAR-LTP is only induced if a post-synaptic burst is induced in a time window of 0.5-1.5 seconds after the onset of pre-synaptic glutamatergic terminal stimulation. Activating pre-synaptic terminals without a post-synaptic burst pairing not only fails to induce novel NMDAR-LTP but actually reverses NMDAR-LTP that might have been induced by previous stimulation-burst pairings (Harnett et al., 2009). Importantly, this does not induce LTD of NMDAR currents (only reversal of previously induced NMDAR-LTP) and triggering a single post-synaptic AP during input stimulation is enough to block NMDAR-LTP reversal, even though pairing with single APs cannot induce NMDAR-LTP in neurons that have not been subjected to synaptic plasticity protocols.

The NMDAR-LTP reversal phenomenon calls forth the prediction that suppression of burst firing after a CS presentation would potentially lead to the progressive abolition of DA neuron representations of, and consequently the behavioral responses to, CS-US pairings, which is a hallmark of extinction learning (Pan et al., 2008b; Harnett et al., 2009; Degoulet et al., 2016). It is important here to remember that extinction learning is likely composed of two processes: the fast formation of a new form of inhibitory learning (the CS now indicates the omission of the US) and the slow unlearning of the original CS-US association, with NMDAR-LTP reversal likely only being directly implicated in the latter (Pan et al., 2008b).

The activity dependency of NMDAR-LTP induction is thought to mimic, at a synaptic level, the observed *in vivo* patterns of DA neuron burst activity promoting learning, tonic single spike activity not promoting learning but also not driving extinction, and pausing of DA neuron activity promoting extinction. While to my knowledge this hypothesis has not been fully experimentally tested, it has been proposed that prediction error-related excitation of DA neurons, through promotion of bursting, leads to NMDAR-LTP induction and the negative prediction error-related inhibition of DA neurons, through its suppression of firing activity, could lead to NMDAR-LTP reversal. There is some experimental evidence to this effect, as *in vivo*

pharmacological blockade of mGluR1 and L-type Ca^{++} channels in the VTA, which are essential for the induction and maintenance of NMDAR-LTP *ex vivo*, prevent the learning and reinstatement of drug-induced conditioned place preference (Degoulet et al., 2016). Likewise, L-type Ca^{++} channel blockade *ex vivo* facilitates NMDAR-LTP reversal and, concordantly, accelerates extinction of drug-seeking behavior *in vivo*.

Another type of persistent synaptic plasticity observed in DA neurons than could be related to the processing of negative prediction errors is the LTD of AMPAR conductances (AMPAR-LTD), i.e. a persistent reduction of AMPAR-mediated post-synaptic currents. This form of plasticity has been induced by two different protocols, being mediated by different intracellular pathways. One form of induction is achieved by pairing low-frequency (1 Hz) glutamatergic input stimulation while maintaining the post-synaptic neuron at -40mV in voltage clamp (Jones et al., 2000; Gutlerner et al., 2002). This form of LTD does not depend on NMDAR or mGluR1 activation, but is dependent on increased intracellular Ca^{++} levels and can be completely blocked by D2R activation. It's regulation by D2R is thought to be the reason why it can be blocked by acute amphetamine exposure *ex vivo* (Jones et al., 2000). Another form of AMPR-LTD can be induced by pairing high-frequency (66 Hz) glutamatergic input stimulation while maintaining the post-synaptic neuron at -50 mV in voltage clamp (Bellone and Lüscher, 2005, 2006; Mameli et al., 2007). This form of LTD is also not dependent on NMDAR activation, but is dependent on mGluR1 activation and is mediated by membrane insertion of low-conductance, GluR2-lacking AMPARs. Interestingly, AMPAR-LTD can reverse AMPAR-LTP induced by cocaine exposure *in vivo* (Bellone and Lüscher, 2006; Mameli et al., 2007).

Finally, LTP can also be observed in GABA-ergic synapses onto DA neurons (GABA-LTP), which is characterized by a persistent increase in the amplitude of GABAergic IPSCs. Like with AMPAR-LTD, different forms of GABA-LTP co-exist in DA neurons (Nugent et al., 2007; Kodangattil et al., 2013; Simmons et al., 2017). The first identified form of GABA-LTP was inferred from the observation that ethanol exposure *in vivo* increased the probability of release in GABAergic synapses on DA neurons, and that this effect was dependent on and could be reproduced by pre-synaptic adenylyl cyclase activation (Bonci and Williams, 1997; Melis et al., 2002). The second, and better characterized, form of GABA-LTP can be induced by high frequency (100 Hz) stimulation of synaptic afferents (both GABAergic and

glutamatergic) with the post-synaptic cell in current clamp (without additional current injection) (Nugent et al., 2007; Nugent and Kauer, 2008). This process is heterosynaptic and dependent on NMDAR activation in glutamatergic synapses on the DA neuron; this induces the production of nitric oxide, which activates guanylate cyclase in GABAergic axonal terminals and increases release probability. Interestingly, guanylate cyclase-dependent GABA-LTP is blocked by multiple drugs of abuse and stress, i.e. the opposite effect to what is observed with glutamatergic LTP in these neurons (Niehaus et al., 2010). GABA-LTP also follows STDP rules. Kodangattil et al. (2013) systematically paired pre-synaptic afferent stimulation with current injection-triggered bursts of post-synaptic APs. They found that, following classical Hebbian plasticity rules, stimulation of afferents preceding (by 15 ms) AP bursts induced guanylate cyclase-dependent GABA-LTP, while stimulation after (by 5 ms) AP bursts induced LTD of IPSCs.

Recently, Simmons et al. (2017) demonstrated that both adenylyl cyclase- and guanylate cyclase-dependent GABA-LTP on DA neurons can be recruited with high frequency stimulation of mixed afferent inputs, and that the expression of these different forms of plasticity is differentially distributed among identified inhibitory input pathways. Specifically, both adenylyl cyclase- and guanylate cyclase-dependent GABA-LTP following high frequency stimulation could be observed in IPSCs triggered by optogenetic stimulation of identified GABAergic afferents from the NAcc and local VTA GABA neurons, but RMTG afferents only expressed the adenylyl cyclase-dependent form of GABA-LTP, suggesting that different GABA inputs to DA neurons have distinct synaptic plasticity mechanisms.

Importantly, in general terms, both AMPAR-LTP and NMDAR-LTP depend on the pairing of pre-synaptic excitatory input stimulation with slightly delayed or concurrent post-synaptic depolarization, spiking or burst firing, while AMPAR-LTD and NMDAR-LTP reversal depend on the pairing of pre-synaptic excitatory input stimulation with slightly delayed or concurrent post-synaptic hyperpolarization or absence of spiking. This implies the existence of a general Hebbian rule where excitatory synaptic inputs to DA neurons (which *in vivo* may reflect CS presentations) are enhanced when paired with increased post-synaptic activity (which *in vivo* may reflect reward presentation) and are decreased when paired with decreased post-synaptic activity, i.e. “pauses” (perhaps related to expected reward omission).

Likewise GABA-LTP induction protocols suggest that inhibitory inputs to DA neurons that are concurrently activated with glutamatergic inputs and a delayed post-synaptic burst tend to be potentiated, which could be a mechanism for strengthening inhibitory inputs that should override excitatory cue or reward-related signals (which perhaps can control the representation of negative prediction errors, if one assumes a separate circuit mechanism for the evaluation of the validity of reward associations).

The combination of these synaptic rules is therefore thought to underlie the transference of reward value to the CS during learning (Bonci and Malenka, 1999; Harnett et al., 2009; Pignatelli and Bonci, 2015). It is still not clear how these different forms of plasticity interact during naturalistic learning in behaving animals; they may be (at least in part) recruited in parallel and synergistically regulate synaptic transmission in a given neuron, or perhaps they are each recruited differentially depending on factors such as the timing of CS-US presentation or the identity of the post-synaptic and pre-synaptic neurons. For example, there is evidence that the expression of AMPAR-LTP is recruited by specific events in distinct neuronal populations, suggesting that this form of plasticity is expressed in select DA neuron populations depending on the behavioral context (Lammel et al., 2011). Likewise, the distribution of the two forms of GABA-LTP is input-specific, opening the possibility that different forms of synaptic plasticity in DA neurons are also heterogeneously expressed in input pathways with distinct functions, e.g. tonic inhibitory control versus phasic reward omission signals (Simmons et al., 2017). It is therefore possible that the coordinated expression of these forms of plasticity in specific synapses may underlie DA neuron correlates of associative learning, such as the transference of burst responses to reward-predicting cues and the suppression of excitatory responses to expected rewards. However a quantitative theory for the integration of multiple forms of synaptic plasticity in DA neurons, especially within the context of associative learning, has not yet been proposed (Costa et al., 2017).

1.3.5. Pauses and the synaptic mechanisms of learning in MSNs

As discussed in section 1.1, DA modulates activity in striatal MSNs depending on its extracellular concentration and whether the MSN expresses D1Rs or D2Rs. A crucial feature of this neuromodulatory control is that DA also regulates synaptic plasticity in MSNs. Dopaminergic gating of long term changes in synapses from

cortical afferents on MSNs has been proposed as a cellular underpinning of striatum-dependent learning, including conditioning and motor learning (Reynolds et al., 2001; Surmeier et al., 2007; Kreitzer and Malenka, 2008; Grueter et al., 2012). The most well characterized form of MSN plasticity is LTD, which in these neurons is most often induced by pairing post-synaptic depolarization (from -70 to -50 mV holding potentials) with high frequency (10-100 Hz) stimulation of pre-synaptic glutamatergic afferents (Kreitzer and Malenka, 2005; Surmeier et al., 2009). Alternatively, LTD can be induced with STDP protocols by stimulating glutamatergic afferents with a 10 ms delay after a burst of post-synaptic APs in current clamp (Shen et al., 2008). In both D1R- and D2R-expressing MSN populations, this form of plasticity relies on post-synaptic Cav1.3 channels and mGluRs, which trigger the release of endocannabinoids and consequently reduce pre-synaptic glutamate release.

MSNs have also been shown to express a form of LTP; however, this form of plasticity is less well understood. The initial protocols for inducing LTP on MSNs were highly non-physiological, and required high frequency stimulation in the absence of extracellular Mg^{++} (Calabresi et al., 1992). This form of LTP requires NMDA receptors, but it is not clear why conventional post-synaptic depolarization is not sufficient to reveal it, as is seen in other brain regions (Kreitzer and Malenka, 2008; Park et al., 2014). Nevertheless, STDP protocols, i.e. stimulating glutamatergic afferents 5 ms before a burst of post-synaptic APs in current clamp, can also induce LTP in both direct and indirect pathway MSNs in physiological extracellular Mg^{++} concentrations (Shen et al., 2008; Thiele et al., 2014). This indicates that both direct and indirect MSNs display Hebbian synaptic plasticity, with synapses that are activated before post-synaptic spikes being potentiated and synapses activated after post-synaptic spikes being depressed.

Importantly, DA modulates MSN LTD and LTP in diametrically opposite ways depending on whether they express D1Rs or D2Rs (Shen et al., 2008). In indirect pathway MSNs, LTD expression is strongly modulated by the activation of D2Rs, while in direct pathway MSNs it is not affected by D1R stimulation. In D2R-expressing MSNs, spike-timing dependent LTD can be completely blocked by the bath application of a D2R antagonist. Furthermore, D2R blockade does not affect the expression of LTP in indirect pathway MSNs; in these neurons, LTP expression is modulated by adenosine acting on post-synaptic adenosine 2a receptors (A2a).

Conversely, D1R activation in direct pathway MSNs is crucial for the expression of spike-timing dependent LTP, but not LTD. In summary, tonic levels of DA release are thought to create a state where LTD in cortico-striatal synapses on D2R-expressing MSNs is facilitated. Phasic increases in DA release either do not affect or further facilitate LTD in D2R-expressing MSNs while facilitating the induction of LTP in D1R-expressing MSNs. Finally, decreases in striatal DA concentrations would inhibit the induction of LTP in D1R-expressing MSNs and facilitate the induction of LTP in D2R-expressing MSNs.

This framework outlines a cellular mechanism that, like the plasticity rules observed in DA neurons, is a putative substrate for the forms of DA-dependent learning observed in intact animals. Learning from positive outcomes, which induces DA release in the striatum, can be thought of as a result of increased synaptic transmission between cortical and direct pathway striatal neuron ensembles that represent the actions, sensory cues or internal states associated with reward delivery, while at the same time inducing a LTD of transmission between cortical and indirect pathway neuronal ensembles associated with the rewarding event. This presumably would increase the probability that the motor actions that led to reward delivery will be repeated in the future, i.e. the behavioral manifestation of learning (Surmeier et al., 2011; Schultz, 2016b). Conversely, negative outcomes such as reward omission, which lead to pauses in DA neuron firing and consequent reduction of DA release and reduced activation of D2Rs, would decrease LTP of cortico-D1R MSN synapses and LTD of cortico-D2R MSN synapses.

There are still some important features of learning that are not fully explained by this theory. One of the most prominent is the so called “credit assignment” or “distal reward” problem, and is que question of how can DA release potentiate synapses that were activated multiple seconds in the past. This is not immediately clear from most *ex vivo* results, which usually study DA modulation of synaptic plasticity by changing the overall concentration of DA in the bath and use STDP protocols with time delays in the order of milliseconds. However, a recent study using STDP protocols by Yagishita et al. (2014) demonstrated that phasic DA signals indeed do potentiate excitatory synapses (as measured by structural spine changes) in D1R-expressing MSNs that were activated seconds in the past (with the maximum effect being observed within a 0.5 to 1 second delay). This effect was dependent on the

dynamics of post-synaptic Ca^{++}/calmodulin–dependent adenylyl cyclase 1 (AC1) priming of activity. With this priming, increases in cAMP induced by D1R could induce a PKA-dependent enlargement of activated spines. This is a prime candidate for a cellular "eligibility trace" on which DA signals can act upon. This finding had been somewhat predicted in the computational studies of Izhikevitch (2007) and Florian (2007), which demonstrated that the distal reward problem could be solved, in theory, by a time-decaying synapse-specific eligibility trace that keeps a memory of the relationships between recent pre- and postsynaptic spike pairs which could determine the extent of a DA dependent synaptic potentiation.

Despite this very valuable insight, however, it is not clear if this cellular eligibility trace mechanism also applies to the processing of negative prediction errors, which would be carried primarily by a reduction D2R-dependent suppression of cAMP levels. Similarly, the mechanisms of how A2a-dependent LTP in D2R-expressing neurons is involved in striatal-dependent learning is not well understood, aside from the findings that genetically deleting these receptors impairs habit formation and that activating them suppresses goal-directed behavior (Yu et al., 2009; Li et al., 2016). There is also no cogent model explaining how these different forms of synaptic plasticity are expressed *in vivo* in specific cortico-striatal synapses between in select neuronal ensembles of at least two different cell types (D1R- or D2R-expressing MSNs), especially during tasks that require the evaluation of positive and negative prediction errors, such as foraging and risk-based decision making.

It should also be noted that the mechanisms of LTD expression in direct pathway MSNs is still a controversial topic, as different labs report opposing results depending on the stimulation protocols and experimental preparations. Specifically, studies that used "macro-stimulation" (large bipolar concentric electrodes that stimulate a wide area) found a D2R-independent LTD of excitatory synapses in direct pathway neurons, while studies that used "micro-stimulation" (small glass pipette electrodes that stimulate a restricted area) could not replicate this finding (Wang et al., 2006; Kreitzer and Malenka, 2007, 2008; Surmeier et al., 2007). One potential explanation for this dichotomy is that the D2-independent LTP in direct pathway MSNs requires a reduction in activation of muscarinic type 1 receptors (M1Rs) in these neurons, which is accomplished with macro-stimulation by the concurrent activation of D2Rs in striatal cholinergic interneurons. However, it is not yet clear how

these different mechanisms are integrated in physiological conditions. What are agreed upon are the mechanisms for LTD induction in indirect MSNs.

1.3.6. Negative prediction errors and disease

Negative prediction error-based learning is disrupted in several psychiatric disorders. There is extensive clinical evidence that patients with depression tend to overvalue negative feedback and show increased loss-related neural signals (Beats et al., 1996; Elliott et al., 1996, 1997; Steffens et al., 2001; Murphy et al., 2003; Pizzagalli et al., 2006; Taylor Tavares et al., 2008; Beard et al., 2015; Huys et al., 2015; Ubl et al., 2015). Interestingly, patients with depression tend to normalize (albeit not fully) their abnormal responses to negative feedback with psychiatric treatment and clinical recovery (Elliott et al., 1996, 1997). These clinical observations support the hypothesis that learning from disappointment, including the representation of negative prediction errors by DA neurons, is directly related to the symptomatology of depression (Huys et al., 2015).

Patients with drug addiction, on the other hand, show reduced learning from, and neural representations of, negative prediction errors (Parvaz et al., 2015; Ersche et al., 2016; García-García et al., 2017), which is thought to be related to their persistent drug use despite the negative physical and social consequences of their behaviors. Individuals with psychopathic and antisocial traits are notoriously slow to learn from punishments and negative social outcomes, which is thought to be a crucial element in the development of criminal and socially disruptive behaviors (Byrd et al., 2014). Insensitivity to negative feedback has been observed in patients with ADHD (Sagvolden et al., 1998; Johansen et al., 2002). Indeed, a consistent hallmark of ADHD is precisely a resistance to extinction of conditioned responses (Sagvolden et al., 2005a). It has been argued that this resistance to extinction is a contributing factor to the other symptoms of ADHD, especially hyperactivity, as deficient extinction processes would lead to excess motor activity following the disruption of previously acquired CS-US pairing contingencies (Johansen et al., 2002). Interestingly, this learning phenotype seems to be dissociated from the hedonic reactions to reward omission, as children with ADHD react with greater frustration to the loss of anticipated rewards (Douglas and Parry, 1994).

Clinical manifestations in Parkinson's disease (PD) reveal an interesting dual effect of DA neuron loss this form of learning: untreated PD patients (hypodopaminergic state) have increased learning from negative feedback (Frank et al., 2004; Frank, 2005), while those undergoing DA replacement therapies (hyperdopaminergic state) show reduced learning from negative outcomes (Frank et al., 2004, 2007; Frank, 2005; Cools et al., 2006; García-García et al., 2017). This is consistent with an enhanced deactivation of the pause-sensitive D2R-expressing indirect pathway in untreated PD, which would lead to a potentiated read-out of pause-related signals (phasic DA decreases) in the striatum, and an obverse inhibition of this pathway after L-DOPA treatment, which then reduces striatal processing of DA neuron pauses.

Importantly, not all brain disorders are associated with the disruption of negative prediction errors. Current evidence suggests that schizophrenic patients have disrupted learning from rewarding events, deficits in forming predictions of desired outcomes and attenuated neural responses to positive prediction errors (features that correlate with the severity of negative symptoms), but learning and neural representation of reward omission is relatively unchanged (Moran et al., 2008; Waltz et al., 2009; Gradin et al., 2011; Maia and Frank, 2017). There are reports that patients with schizophrenia display reduced behavioral responses to, and neural correlates of, aversive conditioning (learning to predict aversive events, such as the display of a loud sound or disturbing image), however it is not clear to which extent this could represent a selective disruption in certain features of negative prediction error-based learning or a deficit in salience attribution (Jensen et al., 2008; Romaniuk et al., 2010). The case of schizophrenia highlights that pathological enhancement or attenuation of negative prediction error processing in the brain constitutes a specific feature of the symptomatology of certain brain diseases.

Given the importance of deficient negative prediction error processing in several mental diseases, understanding the mechanisms of learning from disappointment could potentially elucidate the origin of learning deficits in these diseases and how they relate to other clinical symptoms, thus providing insights for the development of novel therapeutic strategies.

1.4. Kv4 channels and KChIP4a

1.4.1. Kv4 channel alpha and beta subunits: structure and function

Ion channels are transmembrane pore-forming structures that allow the flow of ions between the intracellular and extracellular space (Hille, 2001; Gouaux and Mackinnon, 2005). They are integral components of living cells, and control their membrane potential by selectively regulating transmembrane ion movement. In addition, they contribute to the electrolyte flow necessary for volume regulation and interact with intracellular signaling pathways by controlling the transmembrane flow of some ions, notably Ca^{++}. Ion channels are typically oligomeric protein complexes, generally composed of several subunits. They have three main functional domains: the ion conducting pore (an aqueous pathway that only allows the passage of specific ions), gates (which can open and close the pore) and sensors (stimuli detectors that respond to chemical or electrical signals and modulate the open probability of the gates). In neuronal cells, ion channels determine the dynamic changes in electric potential that define neuronal communication, e.g. spikes and post-synaptic potentials.

Ion channels that are selectively permeable to K^+ ions constitute one of the main families of these proteins. K^+ channels share a common evolutionary origin, having essentially the same pore structure – including the highly conserved "K^+ channel signature sequence" (TVGYG) – across all known organisms (Heginbotham et al., 1994; Doyle et al., 1998; Rudy et al., 2009; Moran et al., 2015). These channels conduct K^+ ions near the diffusion limit, yet remarkably select for K^+ over Na^+ by a factor of over 1000:1. Voltage gated (or voltage dependent) K^+ channels (Kvs) are opened by membrane depolarization, and have very important roles in controlling neuronal excitability and signal processing (Miller, 2000; Rudy et al., 2009). Kv subunits assemble in tetrameric configurations in order to form a functional K^+ channel; each one consists of six membrane-spanning domains (S1-S6) flanked by intracellular N- and C- terminal sequences of variable lengths. The pore is formed by the S5 and S5 domains, and voltage dependent activation is enabled by the presence of positively charged residues at every third position in S4 (voltage sensor), which move outwards in response to changes in membrane potential, causing a conformational shift that opens the pore. Because of their widespread distribution

across all phylogenetic groups, Kvs are thought to have been the first voltage gated ion channels to have evolved (Moran et al., 2015). The first sequence of a Kv channel was identified in the late 1980s in *Drosophila melanogaster*, based on the sequence of the *Shaker* locus (so named because fruit flies with mutations on this locus would shake under ether anesthesia and show aberrant movements), and was rapidly followed by the identification of three other *Drosophila* Kv families (S*hal*, *Shaw* and *Shab*) and their mammalian homologues (Tempel et al., 1987; Pongs et al., 1988; Butler et al., 1989; Wei et al., 1990; Pak et al., 1991; Salkoff et al., 1992).

The pore-forming subunits of mammalian Kvs are classified into three groups based on sequence similarity (Rudy et al., 2009; Moran et al., 2015). The first group includes the Kv1–Kv6, Kv8, and Kv9 subfamilies (collectively called “KvF family” for “fast activating Kvs”); these channels are functionally characterized by their fast activation upon membrane depolarization. The second group is formed by the Kv7 subfamily (or KCNQ family for the genes that encode these channels), which is composed of subunits with slow activation and deactivation kinetics (Brown and Passmore, 2009). The third group is composed of the Kv10–Kv12 subfamilies (also known as the EAG family for “ether-a-go-go”, name given because the fruit flies with mutations on this channel would shake their legs under ether anesthesia), composed of channels with slow activation kinetics, little to no inactivation and a characteristic slowing down of activation by negative pre-pulses and by increased Mg^+ and H^+ concentrations (Bauer and Schwarz, 2001).

Each subfamily of Kvs conducts currents with distinct properties. One current of particular importance is the subthreshold A-type K^+ current (I_A), mediated in mammals mainly by the Kv4 channel subfamily (homologues of the invertebrate *Shal* channels). The cloning and characterization of the first *Shal* gene from *Drosophila melanogaster* was reported in 1990 (Wei et al., 1990). Within one year, the first mammalian homologues, the Kv4 family, were also identified, cloned and characterized (Baldwin et al., 1991; Pak et al., 1991). Shortly thereafter, the first evidence that these channels were modulated by auxiliary subunits was published (Chabala et al., 1993). Kv4 channels mediate depolarization-activated, transient, potassium outward currents and require hyperpolarization of the membrane potential to recover from inactivation. The name “A-type” derives from its kinetics, which are characterized by a fast activation and, typically, fast inactivation; this results in K^+

current traces, when recorded in voltage clamp, that resemble in shape the letter “A” (Figure 1.7). This shape differentiates Kv4 currents from other voltage-gated K^+ currents, like for example the fast activating but slowly inactivating D-type (I_D) currents (Figure 1.7), which are mediated mainly by Kv1 (a.k.a. Shaker) channels, or fast-activating and non-inactivating delayed rectifier K^+ currents (e.g. Kv2, Kv7 channels) (Storm, 1988; Rudy et al., 2009).

The mammalian Kv4 channel family includes three pore forming alpha subunits: Kv4.1, Kv4.2 and Kv4.3 (coded by the genes KCND1, KCND2 and KCND3, respectively) (Rudy et al., 2009). The KCND1 and KCND2 genes code for a single protein each, while the KCND3 gives rise to two alternative splice variants: Kv4.3S and Kv4.3L (short and long, respectively). Kv4.1 is expressed very weakly in the brain, and only in a few sparse neuronal populations; Kv4.2 and Kv4.3, on the other hand, are abundantly expressed across the brain. These channels are functionally differentiated by their kinetics, with Kv4.1 channels generally having slower inactivation kinetics than Kv4.2 and Kv4.3, and Kv4.3 typically having slower inactivation kinetics than Kv4.2 (Rudy et al., 2009).

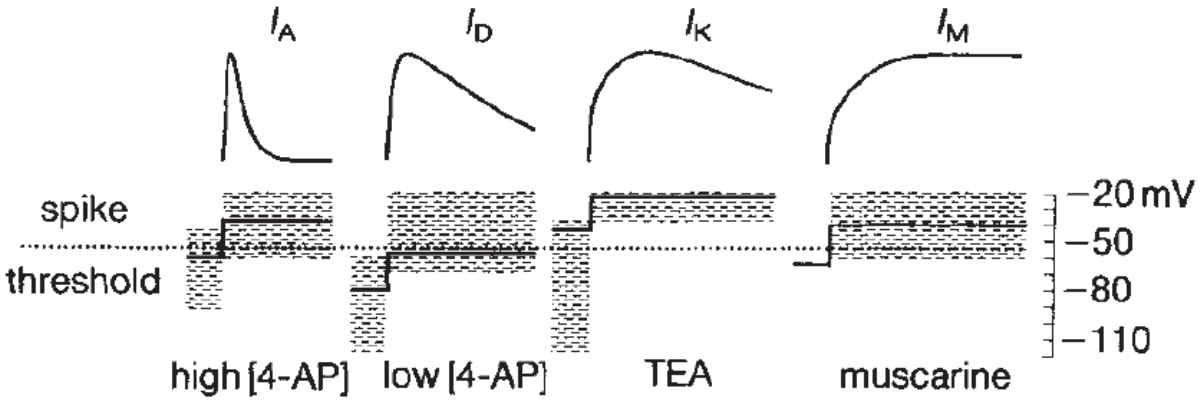

Figure 1.7. Comparison between different voltage gated K+ currents.
Drawings represent the idealized kinetics of four different voltage gated K+ currents: A-type (I_A), D-type (I_D), delayed rectifier current (I_K) and the M current (I_M). Traces below the drawings indicate the typical voltage steps used to elicit each current, as well as the approximate voltage ranges of activation and inactivation (shaded areas) and their effective blocking agents. Adapted from Storm, 1988.

These channels can also form heteromeric complexes, with each channel being composed of different Kv4 types (e.g. Kv4.2 and Kv4.3). However, native Kv4 channels are not only composed of pore-forming alpha-subunits but also contain different types of auxiliary subunits (see below). Nevertheless, Kv4 channels exclusively mediate somatodendritic low-threshold activating I_A currents. Other fast I_A currents, such as Kv1.4 or Kv3.3, are activated at higher membrane voltages and are mainly expressed in axonal compartments (Birnbaum et al., 2004; Covarrubias et al., 2008).

Kv4 channels display two types of inactivation mechanisms (Birnbaum et al., 2004). The first is called N-type inactivation, a.k.a. “ball and chain” inactivation, in which a tethered N-terminus of the Kv4 protein or an auxiliary subunit (the “ball”) binds to the intracellular entrance of the pore (Hoshi et al., 1990; Gebauer et al., 2004). This type of inactivation occurs only when the channel is open, has fast kinetics, and is dependent on the pore-blocking N-terminus. The second form is called C-type inactivation, which involves the collapse, or “pinching”, of the channel pore due to a structural reconfiguration of the tetramer subunits (Choi et al., 1991; Liu et al., 1996). This type of inactivation is typically slower than N-type inactivation and can occur even when the channel is closed (closed-state inactivation) (Bähring and Covarrubias, 2011).

Notably, the properties of native Kv4 channel complexes are strongly modulated by their two classes of integral auxiliary beta subunits and are might be further modulated by other interacting proteins and post-translational modifications (Birnbaum et al., 2004). The two classes of Kv4 modulatory beta subunits are the extracellular dipeptidyl aminopeptidase-like proteins (DPLPs) and the intracellular K^+ channel interacting proteins (KChIPs). DPLPs are transmembrane proteins belonging to the S9B family of serine proteases; they markedly accelerate Kv4 channel activation and inactivation gating, and shift the voltage dependence of activation and inactivation to more hyperpolarized potentials (Jerng and Pfaffinger, 2014). While they exert a highly important role in Kv4 channel function, this dissertation will focus on the role of KChIPs on I_A modulation.

1.4.2. The KChIP family

KChIPs are cytosolic calbindin-like auxiliary beta subunits that bind to pore-forming Kv4 alpha subunits and modulate biophysical gating properties as well as plasma membrane delivery (i.e. trafficking) of channel protein complexes (An et al., 2000; Shibata et al., 2003; Jerng et al., 2004; Jerng and Pfaffinger, 2008, 2014). There are four isoforms of mammalian KChIPs (KChIP1-4), each coded by their own gene (a.k.a. KCNIP1-4, respectively), but with several different alternative splicing-defined isoforms. The first evidence that KChIPs acted as auxiliary subunits to Kv4 channels was published in the year 2000, with the functional characterization of KChIP1-3 (An et al., 2000). KChIPs belong to the neuronal Ca^{++} sensor (NCS) superfamily, exhibiting four Ca^{++}-binding EF hand motifs. All KChIPs have a conserved core domain, which contains the EF hands and binds to the Kv4 subunits. The binding of the core domain to the N-terminus of Kv4 proteins masks an endoplasmatic reticulum (ER) retention motif, allowing the assembly and transport of KChIP-Kv4 tetrameric complexes, and ultimately forming functional membrane-bound Kv4 channels (Figure 1.8A); thus, KChIP-binding is essential for membrane expression of functional Kv4 channels (Shibata et al., 2003).

The different KChIP isoforms are defined by their variable N-termini (Figure 1.8B). In general, most KChIP isoforms, including the common KChIP1a, KChIP2a and KChIP3a, increase the surface channel density (by reducing ER-retention), and, by modulating C-type inactivation, speed up recovery from inactivation (Jerng et al., 2004; Covarrubias et al., 2008; Jerng and Pfaffinger, 2014). All KChIPs slow down N-type inactivation due to their binding to, and consequent sequestration of, the Kv4 N-terminus (Patel et al., 2002). The biophysical properties of Kv4 channels are tuned stoichiometrically according to the relative expressions of different KChIP proteins (Tang et al., 2013; Kitazawa et al., 2014; Zhou et al., 2015). This is because KChIP proteins compete for the binding site of each of the four pore-forming Kv4 alpha subunits of the channel tetramer. Therefore, differential expression or alternative splicing of functionally distinct KChIPs could potentially fine tune I_A gating properties and density in order to adapt to different cellular contexts, such as inflammatory challenges or oxidative stress.

KChIPs, akin to the pore forming Kv4 subunits, are highly evolutionarily conserved proteins. The oldest known KChIP-like proteins are NCS-4, NCS-5 and

NCS-7 from the nematode *Caenorhabditis elegans*, which have been found to modulate SHL-1 channels, an orthologue of mammalian Kv4 channels (Chen et al., 2015). Already in *C. elegans*, KChIP-like proteins are essential for the expression of functional I_A and strongly modulate their kinetics. More specifically, NCS-4, NCS-5 and NCS-7 all increase peak current densities, slow down inactivation kinetics of SHL- channels and shift the voltage dependency of activation to more hyperpolarized potentials. In the chordate lineage, the oldest known form of KChIP protein in the *Ciona*KChIP, found in the tunicate *Ciona intestinalis* (Salvador-Recatalà et al., 2006). This organism only expresses this KChIP protein, which binds to *Ciona*Kv4 channels, increasing peak current, markedly slowing down inactivation, shifting the voltage dependency of activation and inactivation to more hyperpolarized potentials and slowing recovery from inactivation. The structure and function of KChIP proteins is so highly conserved that even artificial expression of human KChIP1 in lobster neurons is capable of modulating *Shal* I_A channels in a physiologically relevant manner, despite over 500 million years of divergent evolution between these two organisms (Zhang et al., 2003). This underscores the pivotal role of these proteins for survival and the regulation of the nervous system.

1.4.3. KChIP4a and the KIS domain

The mouse KChIP4 gene (i.e. KCNIP4) is located on chromosome 5 (B3, 48.39 – 49.52 Mb), is 1135 kb in length and has 14 exons, with ATG translation initiation codons in exons 1, 2, 3, 5, and 8, and the STOP codon located in exon 14 (National Library of Medicine (US); National Center for Biotechnology Information, 2017). It has 92.7% homology with the human KCNIP4, located on chromosome 4 (4p15.31-p15.2, 20.73 – 21.95 Mb). The different exons in KCNIP4 (Figure 1.8B) contains at least six alternative splice variants which, like with other KChIPs, share a conserved C-terminus but display functionally distinct N-termini (Pruunsild and Timmusk, 2005; Jerng and Pfaffinger, 2008, 2014). The roles of KChIP4 gene products in I_A modulation were first reported only in 2002, two years later than for KChIP1-3 (Holmqvist et al., 2002; Morohashi et al., 2002). While other KChIP proteins can be found in several tissues, such as heart, lung and testis, KChIP4 gene products are found exclusively in the brain (Holmqvist et al., 2002; Morohashi et al., 2002; Pruunsild and Timmusk, 2005; Jerng and Pfaffinger, 2014).

KChIP4a (a.k.a. KChIP4.4) is a 229 amino acid protein that corresponds to the alternative splicing of exons 3 through 8b of KChIP4 (Holmqvist et al., 2002; Deng et al., 2005). This isoform stands out from all other mammalian KChIPs, as it reduces the surface expression of Kv4 complexes, in sharp contrast to the canonical roles of most other KChIPs. It also substantially slows down the inactivation kinetics of Kv4 channels (Holmqvist et al., 2002; Baranauskas, 2004; Jerng and Pfaffinger, 2008, 2014; Lin et al., 2010; Norris et al., 2010; Tang et al., 2013). KChIP4a also promotes closed state inactivation, resulting in delayed recovery from inactivation (Tang et al., 2013). Finally, when bound to Kv4.3 channels, KChIP4a also shifts the voltage dependency of activation to more depolarized potentials (Jerng and Pfaffinger, 2008). These properties are determined by the presence of a K-channel inactivation suppression domain (KISD), a specialized transmembrane N-terminus (Figure 1.8C) coded by exon 3 of KCNIP4 (Holmqvist et al., 2002; Jerng and Pfaffinger, 2008; Liang et al., 2009), and an additional ER-retention motif, also located in the N-terminal domain (Tang et al., 2013). Because of the combined effects on reducing amplitude, surface expression and slowing inactivation, KChIP4a is sometimes called the "*inhibitory KChIP*" (Shibata et al., 2003; Tang et al., 2013).

KChIP4a is the only KChIP4 isoform that contains the KISD. The KChIP4 gene code for six splice variants in total: KChIP4a; KChIP4b, KChIP4bL, KChIP4c (only predicted from gene structure; not yet detected in brain), KChIP4d and KChIP4e (Figure 1.8B) (Jerng and Pfaffinger, 2014). Besides KChIP4a, only two other KChIP4 isoforms, KChIP4bL and KChIP4e, have been characterized from a functional perspective. These splice variants, in contrast to KChIP4a, act like conventional KChIPs by increasing surface expression of Kv4 channel complexes and accelerate recovery from inactivation (Holmqvist et al., 2002; Jerng and Pfaffinger, 2008; Jerng et al., 2012; Pruunsild and Timmusk, 2012; Zhou et al., 2015); due to these properties, KChIP4bL and KChIP4e are sometimes called the "*canonical KChIP4 variants*" (Massone et al., 2011). This finding also highlights the importance of the unique N-terminus of KChIP4a for its biophysical effect. Importantly, like with other KChIPs, the effect of KChIP4a is dependent on its relative level of expression in relation to other KChIPs within the cell (Holmqvist et al., 2002; Kitazawa et al., 2014; Tang et al., 2014; Zhou et al., 2015). Tang et al. (2013) elegantly demonstrated this principle by co-expressing Kv4.3, KChIP1and KChIP4a proteins at different ratios (Figure 1.9A). They achieved this by co-injecting varying amounts of KChIP4a

complementary ribonucleic acids (cRNAs) with a fixed amount of Kv4.3 and KChIP1 cRNAs into *Xenopus laevis* oocytes. As expected, they found that increasing relative amounts of KChIP4a gradually slowed the macroscopic open-state inactivation and decreased the peak amplitude of Kv4.3 currents. A follow up study from the same group demonstrated that this effect is also valid for the competition of KChIP4a and KChIP4bL (Figure 1.9B), demonstrating that splice variants of the KChIP4 gene can compete between themselves for binding sites on Kv4 subunits (Zhou et al., 2015). Importantly, when Kv4 subunits outnumber KChIP4a proteins, the biophysical effects of the modulatory subunit are reduced, demonstrating that the "dose dependency" of KChIP4a effects is stoichiometric (Figure 1.9). Therefore, the net macroscopic effect on a cell's I_A depends on the co-expression of Kv4 variants with KChIP1-3 isoforms and other KChIP4 splice variants.

How does a cell decide which splice variant will be expressed at a given time? The mechanism of alternative splicing of the KChIP4 gene has been partially elucidated and is, to some extent, based on the up-regulation of 38A, a small RNA polymerase III–transcribed non-coding RNA (ncRNA) (Massone et al., 2011). The 38A ncRNA is coded within intron 1 of the KChIP4 gene, and acts as an anti-sense RNA to canonical KChIP4 variants, increasing the relative expression of KChIP4a in relation to other KChIP4 isoforms, e.g. KChIP4bL. Interestingly, 38A expression is increased by interleukin-1-α (IL1- α), a pro-inflammatory cytokine, which indicates that differential splice variant expression of KChIP might be a dynamic and regulated phenomenon, potentially in response to immune challenges.

Two other KChIP variants, namely KChIP2x and KChIP3x, also possess a KISD and promote a slowdown of inactivation; however, only KChIP4a has the combined effect of slowing inactivation, reducing surface expression and promoting closed state inactivation (Jerng and Pfaffinger, 2008, 2014). Interestingly, KChIP4a function closely resembles the ancestral *Ciona*KChIP found in tunicates, which also increase the inactivation time constant of I_A and slow down recovery from inactivation. The N-terminus of *Ciona*KChIP also contains a sequence that strongly approximate the KISD of KChIP4a (Salvador-Recatalà et al., 2006). This indicates that KChIP4a, with its unique combination of biophysical effects, is actually an ancient and highly conserved protein within the chordate and vertebrate lineage, suggesting that it may play a crucial, and hard to offset, role in survival.

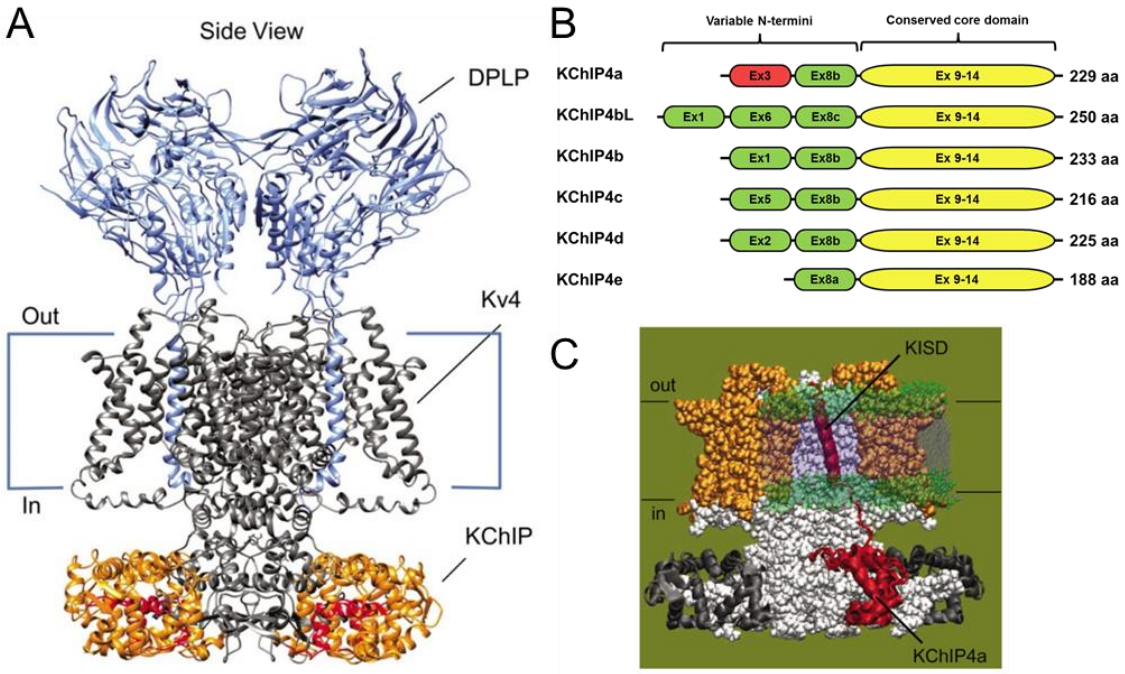

Figure 1.8. General structure of Kv4 subunits and KChIP4a.
A: Structure of Kv4 pore forming subunits and their binding to extracellular DPLPs and intracellular KChIP subunits. B: KChIP4 splice variants have a conserved core C-terminal domain. Each splice variant is defined by different N-terminal exons and have a different number of amino acids. C: The effects of KChIP4a on Kv4 channel properties are dependent on the KISD located on its transmembrane N-terminus. Adapted from Tang et al., 2013 and Jerng and Pfaffinger, 2014.

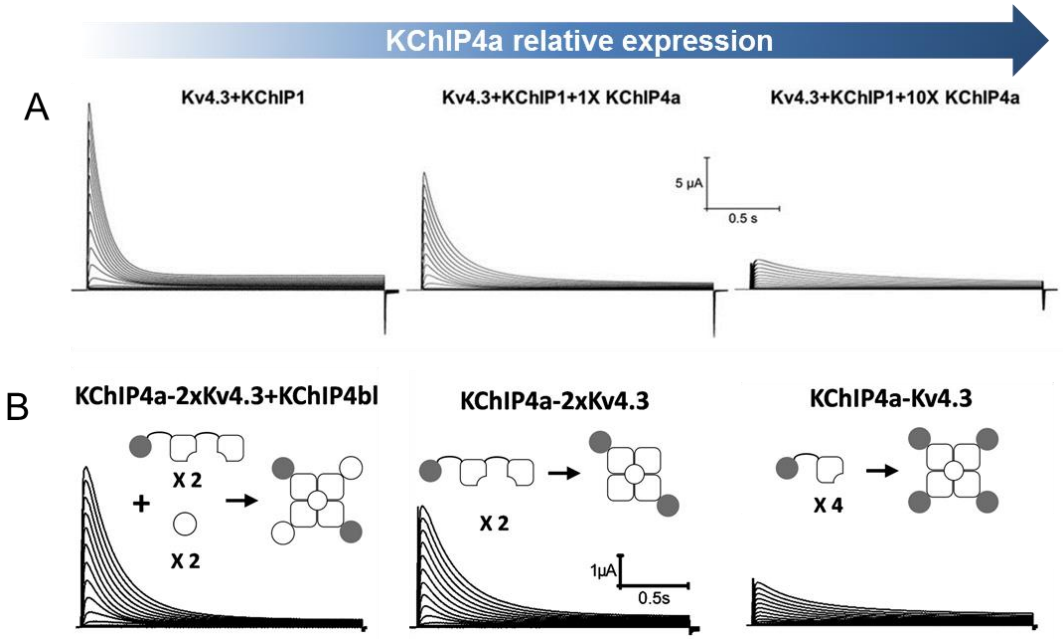

Figure 1.9. KChIP4a effects on Kv4.3 channel properties.
A: Example I_A recordings from heterologous systems expressing different ratios of Kv4.3, KChIP1 and KChIP4a. Adapted from Tang et al., 2013. B: Example I_A recordings from heterologous systems expressing different ratios of Kv4.3, KChIPbL (white circles) and KChIP4a (gray circles). Cartoons indicate the competitive binding of KChIP4 variants to Kv4.3 subunits. Adapted from Tang et al., 2013. In both A and B, a higher relative KChIP4a expression results in smaller I_A current density and slower inactivation.

1.4.4. KChIP4 and disease

Understanding the function of KChIP4 in the brain has potential clinical relevance, as variations in the KChIP4 gene identified by genome wide association studies (GWAS) have been linked to several brain diseases. A summary of the main known genetic variants, including single nucleotide polymorphisms (SNPs), in the KChIP4 gene associated to mental and neurological diseases, drug abuse and personality disorders can be seen in Tables 1.2, 1.3 and 1.4 respectively. Some of the strongest statistical associations between KChIP4 gene variants and disease a seen in ADHD (Lasky-Su et al., 2008; Neale et al., 2008; Weißflog et al., 2013). KChIP4 gene variants are also associated with abuse of a wide variety of drugs, including nicotine, suggesting that this genetic factor acts on a common mechanism of all drugs of abuse, which would include the control of the midbrain DA system (Uhl et al., 2008; Han et al., 2013).

Table 1.3. Associations between KChIP4 gene SNPs and mental and neurological diseases

Disease	SNP or gene region	P value	Reference
ADHD	rs4697192	0.0166	Weißflog et al., 2013
	rs16870771	0.0349	Weißflog et al., 2013
	rs13110425	0.0092	Weißflog et al., 2013
	rs1349384	0.0490	Weißflog et al., 2013
	rs7356396	0.0138	Weißflog et al., 2013
	rs12646862	0.0147	Weißflog et al., 2013
	rs876477	<0.0001	Lasky-Su et al., 2008
	rs876477	<0.0001	Neale et al., 2008
Depression	rs4697267	0.0242	Ripke et al., 2013
	rs358592	<0.0001	Perroud et al., 2012
Schizophrenia	rs6447982 - rs10016449	0.0160	Brennan and Phillips, 2009
	rs1380272	<0.0001	Sullivan et al., 2008
Bipolar disorder	rs1425328	<0.0001	Xu et al., 2014
	rs6847752	0.0002	Sklar et al., 2008
Autism	Full gene	0.0260	Hussman et al., 2011
Alzheimer's Disease	rs6817475	<0.0001	Shulman et al., 2013
Stroke	rs4697177	0.0120	Domingues-Montanari et al., 2010
	rs4697177	<0.0001	Matarin et al., 2007

Table 1.4. Associations between KChIP4 gene SNPs and personality disorders

Disease	SNPs or gene region	P value	Reference
Cluster B personality disorders	rs16871892 rs11726872 rs1425326 rs6448034 rs983071 rs7356396 rs12646862	0.0109 0.0264 0.0091 0.0356 0.0437 0.0339 0.0191	Weißflog et al., 2013
Cluster C personality disorders	rs2291530 rs1425326 rs7356396 rs12646862	0.0331 0.0355 0.0043 0.0085	Weißflog et al., 2013
Anxiety disorder	rs4697192 rs1388321 rs6850182 rs983071 rs16870771	0.0201 0.0169 0.0383 0.0358 0.0305	Weißflog et al., 2013
Mood disorder	rs4697192 rs6448034 rs17455886 rs13110425	0.0244 0.0067 0.0172 0.0471	Weißflog et al., 2013
Substance abuse personality disorder	rs4697192	0.0095	Weißflog et al., 2013

Interestingly, KChIP4 gene SNPs are associated with specific personality disorders, and even specific personality traits, suggesting this subunit play a crucial role in behavioral control (Weißflog et al., 2013). Personality disorders are classified into clusters A, B, and C (Angstman and Rasmussen, 2011). Cluster A includes schizoid, schizotypal, and paranoid personality disorders, which share aspects of dissociation from reality and distorted thinking. Cluster B includes borderline, histrionic, antisocial, and narcissistic personality disorders; the common aspects of these disorders are disregard for negative social feedback, impulsivity and engagement in risky behavior. Cluster C disorders are more prevalent and include avoidant, dependent and obsessive-compulsive personality disorders, all of which involve high levels of fear, anxiety and risk aversion. Specific KChIP4 gene SNPs are associated with cluster B and C personality disorders, indicating that the effects of KChIP4 on behavioral variables are not only strong but also selective.

Table 1.5. Associations between KChIP4 gene SNPs and drug abuse

Relation to drug use	SNPs or gene region	P value	Reference
Alcoholism	rs16869946	0.0340	Han et al., 2013
	rs13129008	0.0493	Han et al., 2013
	rs16869959	0.0185	Han et al., 2013
	rs1157616	0.0315	Han et al., 2013
	rs10022151	0.0055	Han et al., 2013
	rs9884923	0.0293	Han et al., 2013
	rs1459270	0.0062	Han et al., 2013
	rs10012055	0.0012	Han et al., 2013
	rs12513338	0.0019	Han et al., 2013
	rs7697475	0.0019	Han et al., 2013
	rs6448072	0.0076	Han et al., 2013
	rs1380270	0.0080	Han et al., 2013
	rs717531	0.0066	Han et al., 2013
	rs12646630	0.0094	Han et al., 2013
	rs1868744	0.0024	Han et al., 2013
	rs7668222	0.0406	Han et al., 2013
	rs10009391	0.0440	Han et al., 2013
	rs9995524	0.0351	Han et al., 2013
	rs727633	0.0445	Han et al., 2013
	rs10938866	0.0379	Han et al., 2013
	rs13109656	0.0108	Han et al., 2013
	rs1913332	0.0214	Han et al., 2013
	rs4697249	0.0360	Han et al., 2013
	rs4325996	0.0319	Han et al., 2013
	rs17520130	0.0152	Johnson et al., 2011
Illegal substance use	rs13316480	0.0094	Johnson et al., 2011
Cannabis dependence	Full gene	<0.0001	Gizer et al., 2017
Smoking cessation	2-6 SNP clusters	0.0169	Uhl et al., 2008b

In addition to the statistical associations with disease proposed by GWAS, the fact that KChIP4a expression might be driven by an IL1-α-dependent mechanism suggests that this particular splice variant is involved in neuroinflammatory processes. In addition, KChIP4a, unlike alternative KChIP4 variants, cannot interact with the γ-secretase complex, resulting in modification of γ-secretase activity, amyloid precursor protein processing, and increased secretion of β-amyloid, a protein involved in Alzheimer's disease (AD) pathogenesis (Massone et al., 2011). This finding, combined with a known statistical association of KChIP4 SNPs with AD diagnosis in humans, suggests that KChIP4 could have a role in the etiology and progression of AD (Massone et al., 2011; Shulman et al., 2013).

1.4.5. Kv4.3 channels and KChIP4 in DA neurons

In midbrain DA neurons I_A is mediated only by Kv4.3 channels (Serôdio and Rudy, 1998; Liss et al., 2001; Dufour et al., 2014). In classical SN DA neurons, Kv4.3 channels have a very specific function: they open after each AP and regulate the slope of the slow depolarization that generates pacemaker firing, thus finely tuning single-spike firing frequency. This has been experimentally demonstrated by a previous study from our laboratory, which showed that pacemaker frequency of SN DA neurons *ex vivo* was inversely correlated with I_A charge density and the messenger RNA (mRNA) levels for Kv4.3 and KChIP3a (Liss et al., 2001). Our group has recently demonstrated that the effects of I_A amplitude on pacemaker frequency is also valid in vivo and plays an important role in disease states. Specifically, in a mutant alpha-synuclein overexpression mouse model of pre-symptomatic PD, Kv4.3 channels in SN DA neurons are rendered inactive by oxidative stress, which causes an increase in *in vivo* firing frequency in these neurons (Subramaniam et al., 2014a). Importantly, the reduced function of Kv4.3 channels did not affect other aspects of *in vivo* firing in these cells, including bursting and pacemaker variability. This is despite theoretical and experimental evidence suggesting that low I_A-driven increases in excitability could potentially increase responses to synaptic input (Yang et al., 2001; Putzier et al., 2008). Plastic changes of Kv4.3 modulation of DA neurons has also been observed after chronic haloperidol treatment, which increased the expression of this channel and the amplitude of I_A (Hahn et al., 2003). Therefore, Kv4.3 channels can have highly specific effects on the firing properties of midbrain DA neurons and are dynamically regulated in response to homeostatic challenges.

But what is the role of Kv4.3 and I_A in atypical VTA DA neurons? The group of Zayd Khaliq had elegantly established that I_A in VTA DA neurons is only recruited with depolarization rates above 10 mV/s (Khaliq and Bean, 2008). Recently, the same group has demonstrated that hyperpolarizing pauses, such as those generated by GABAergic synaptic input, neurons are post-synaptically amplified by Kv4.3-mediated I_A in mesolimbic VTA DA (Tarfa et al., 2017; Figure 1.10). This amplification was correlated with slower inactivation kinetics of these currents in VTA dopamine neurons, compared with neighboring DA neurons in the SN. These results also confirm the subtype differences in rebound delays described initially by Lammel et al. (2008). Curiously, our laboratory was developing a similar project and came to the same conclusions (Kashiotis, 2013). However, in addition to establishing that this biophysical amplification of hyperpolarizing pauses is dependent on I_A, it was also found that these different biophysical properties of I_A in VTA dopamine neurons depend on KChIP4. This was demonstrated with a mouse line where the KCNIP4 gene was constitutively knocked out from the genome (KChIP4 KO). In wildtype (WT) SN DA neurons, I_A kinetics are close to those expected in the presence of canonical KChIP subunits, with a fast activation and inactivation; however, in the VTA a majority of neurons displayed very slowly inactivating I_A, as would be expected as a result of KChIP4a expression (Figure 1.11). In KChIP4 KO mice, the I_A properties of VTA DA neurons were similar to currents recorded in SN DA neurons, which demonstrated that the atypical I_A of VTA DA neurons was determined by the differential expression of KChIP4 gene products.

Furthermore, KChIP4 KO dramatically reduced the duration of hyperpolarizing pauses in VTA neurons recorded *ex vivo* (Figure 1.12). This confirmed that the atypical I_A properties in VTA DA neurons acted as a biophysical modulator of inhibition integration and controlled the duration of firing pauses in response to phasic hyperpolarization. There preliminary results strongly indicated that KChIP4, and more specifically KChIP4a, could play a relevant role in the control of VTA DA neuron firing patterns and behaviors that were linked to the phasic inhibition of DA neurons, such as learning from negative prediction errors (Schultz et al., 1997; Chang et al., 2015).

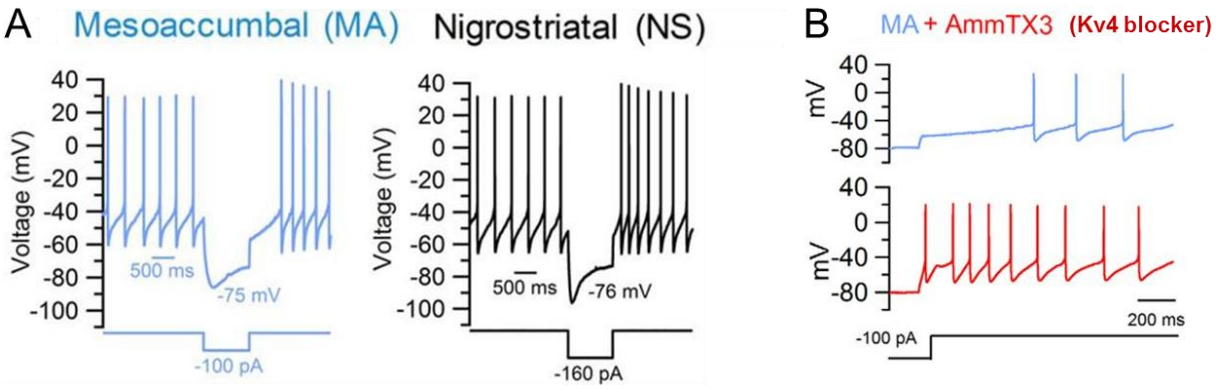

Figure 1.10. Rebound delay duration in atypical DA neurons is controlled by Kv4.3 channels. A: in the study of Tarfa et al. (2017), mesoaccumbal DA neurons recorded with whole cell patch clamp *ex vivo* show significantly longer rebound delays in relation to nigrostriatal DA neurons, recapitulating the results of Lammel et al. (2008). B: The long rebound delay in mesoaccumbal DA neurons is eliminated by bath application of the scorpion toxin AmmTX3, a selective Kv4 channel blocker, demonstrating that these neurons display a Kv4-dependent biophysical amplification of inhibition. Adapted from Tarfa et al., 2017.

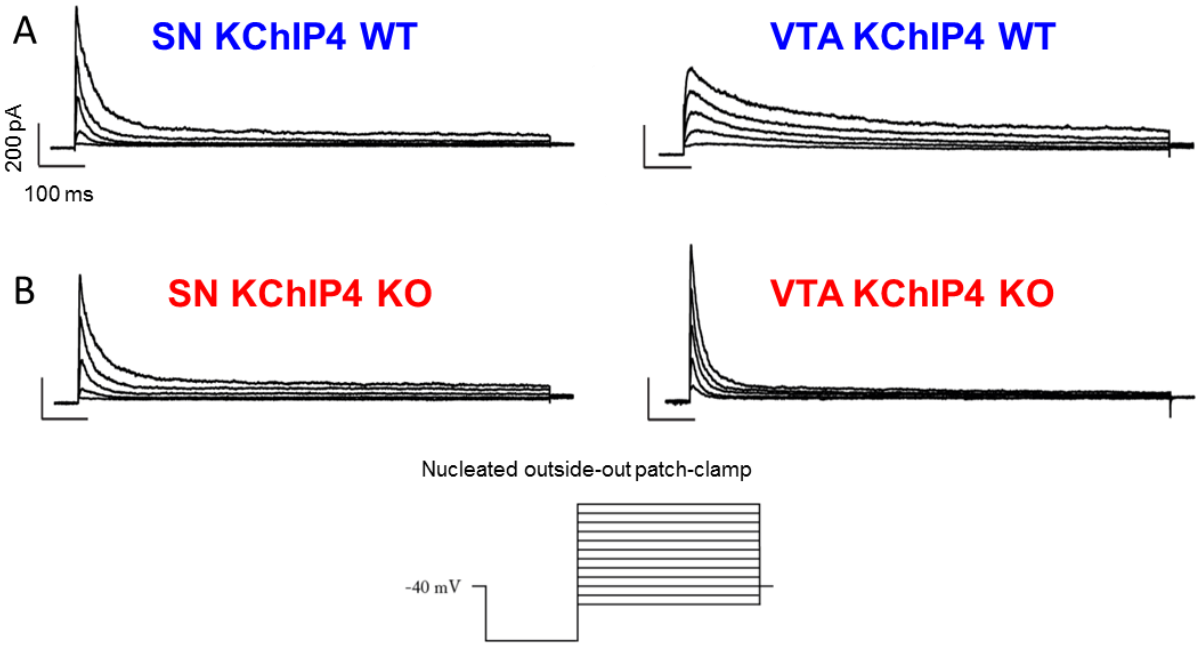

Figure 1.11. KChIP4 determines the time constant of I_A in atypical VTA neurons.
A: Nucleated outside-out voltage clamp recordings of WT SN and VTA DA neurons with successively incrementing holding voltages preceded by a negative potential pre-pulse. This protocol reveals A-type currents. Observe that I_A in SN DA neurons have faster inactivation time constants than those in VTA DA neurons. B: in mice without the KChIP4 gene, I_A in SN and VTA DA neurons have fast inactivation, suggesting that the expression of KChIP4 proteins determines the slow inactivation of VTA DA neurons. Adapted from Kashiotis, 2013.

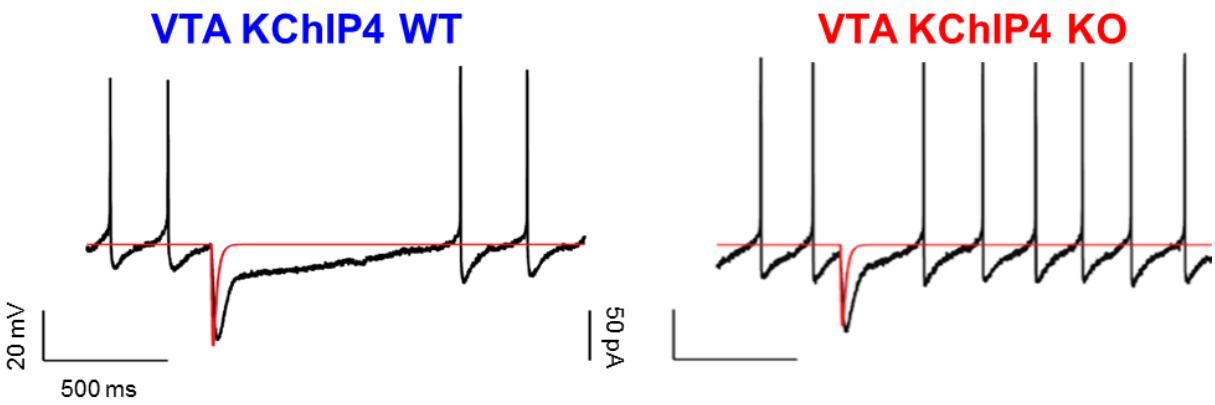

Figure 1.12. KChIP4 expression controls rebound delays in VTA DA neurons.
Current clamp recordings of VTA DA neurons from WT and KChIP4 KO mice. Note that in WT VTA DA neurons a single short hyperpolarizing pulse leads to long pauses in firing, which does not occur in KChIP4 KO DA neurons, suggesting that KChIP4 expression determines the integration of inhibition in VTA DA neurons. Adapted from Kashiotis, 2013.

1.5. Study question and objectives

Given the promising results of the *ex vivo* experiments in KChIP4 KO mice from our laboratory, I decided to investigate the in vivo role of KChIP4 gene products on DA neuron activity, and whether alternative splicing of this gene could regulate DA-dependent behavior.

The questions addressed by the current dissertation can be summarized as:

1: Does KChIP4 KO affect the firing pattern of VTA DA neurons *in vivo*? Is this effect specific for pausing?

2: Does the selective disruption of KChIP4 alternative splicing in midbrain DA neurons, specifically inhibiting the expression of KChIP4a, modulate learning that depends on the DA neuron pauses, i.e. learning from negative prediction errors?

2. Methods

2.1. Ethical standards of animal experimentation

All animal procedures described in this thesis were approved by the German Regierungspräsidium Gießen and Darmstadt (license numbers: V54-19c20/15-F40/29 and V54-19c20/15-FU/1100). C57BL/6N mice were obtained from Charles River laboratories (Germany). Transgenic mice were bred at MFD diagnostics (Germany). Animals were housed in transparent acrylic cages (35 x 19 x 13.5 cm) and for a few weeks throughout duration of the experiments they were kept on site in scantainers (Scanbur A/S, Denmark; 23-26 °C and 30-50% relative humidity). Animals were maintained under a 12 h dark/light cycle (lights on at 8 a.m.) and housed in groups of two to four animals, except when they underwent water restriction. Food (R/M-keeping, Ssniff, Germany) and tap water were available *ad libitum*, except during water restriction. Nesting material and a red acrylic glass shelter (mouse house, Tecniplast, Germany) were used as enrichment. Cages were exchanged once per week by a trained technician or by the experimenter himself when the animals were undergoing long term behavioral experiments.

2.2. The KChIP4-KO mouse line

The KChIP4-KO mouse line was previously generated by Lexicon Pharmaceuticals (USA). The KChIP4 targeting vector was derived using the lambda KOS system, based on the yeast homologous recombination machinery (Wattler et al., 1999) using specific primers for KChP4 exons 6 and 7. The PCR-positive phage pools were plated and screened by filter hybridization using the 654 bp amplicon derived from primers KChIP4-16 and KChIP4-9 as a probe. Four pKOS genomic clones, pKOS-7, pKOS-54, pKOS-88, and pKOS-89 were isolated from the library screen and confirmed by sequence and restriction analysis.

The targeting vector was electroporated into 129/SvEvBrd (129S5;Lex-1) embryonic stem (ES) cells. G418/FIAU-resistant ES cell clones were isolated and recombination was confirmed by southern blot screenings. Two targeted ES cell clones were identified and microinjected into C57BL/6J (albino) blastocysts to generate chimeric animals. Males with over 50% chimerization were bred to C57BL/6 (albino) females, and the resulting heterozygous offspring were interbred to produce

homozygous KChIP4 deficient mice. Mouse genotyping was performed by screening DNA from tail biopsy samples using quantitative PCR for the neo cassette. This enabled the identification of zero, one, or two gene disruptions representing $KChIP4^{+/+}$, $KChIP4^{+/-}$, and $KChIP^{-/-}$ (KChIP4-KO, or simply KO) mice, respectively. KChIP4-KO mice were then backcrossed for over six generations to the C57BL/6N background. Only KChIP4-KO animals, maintained by homozygous breeding pairs, were used in my experiments, and they were compared with WT C57BL/6N mice.

2.3. Anesthesia and general surgical procedures for *in vivo* recordings

Before surgeries, animals were injected intraperitoneally with 50 µL of atropine (details on chemicals and solutions can be found in Table 2.1.) 20-30 minutes before being anesthetized. Initial anesthesia was induced by placing the mice in a small Plexiglas chamber which had been flooded with a flow of isoflurane 4% in 0.35 l/min of O_2 for at least 20 minutes. As soon as the animal lost spontaneous locomotion and righting reflexes, and the respiratory frequency decreased to below 1 Hz, it was removed and placed on the stereotaxic apparatus (Kopf, USA). In the apparatus, anesthesia was maintained via an inhalation mask delivering a stable flow of isoflurane 2% (in 0.35 l/min of O_2) until the craniotomy was performed. After the craniotomy, isoflurane levels were decreased between 1 and 1.8%. This final anesthesia level was individually adjusted to each animal in order to maintain stable breathing at 1 to 2 Hz with no heavy sighs. Stable *in vivo* preparations could be maintained for at least 10 hours, but usually experiments did not last more than six hours.

During surgeries, lidocaine gel (2% lidocaine hydrochloride; Emla™, AstraZeneca, Germany) was applied on the skin before incisions as a local anesthetic. Eye cream (Vidisic, Bausch & Lomb, Germany) was applied to avoid corneal dehydration, being reapplied when necessary. Animals were laid upon an electronic heating bed coupled to a rectal probe (custom built in house) that maintained body temperature at 36°C. Incisions were made to the animals scalp with surgical scissors, and the bone was thoroughly cleared of the periosteum with surgical forceps and saline solution. Craniotomies were performed with an electric drill (0.8 mm diameter drill bit, Kopf, Germany) performed bilaterally above the SN or

the VTA (coordinates found in Table 2.2.). The drill was advanced 0.4 mm (estimated bone thickness) into the skull for each discrete craniotomy. Antero-posterior (AP or Y) coordinates were individually adjusted according to skull size using an empirically derived and validated formula (Equation 2.1.; Schiemann et al., 2012). Immediately after the craniotomies were made, 1 mL of glucose was injected subcutaneously in order to maintain physiological blood glucose concentrations and hydration throughout the experiment.

Table 2.1. Chemicals and solutions used throughout this thesis.

Solution	Description	Supplier	Origin
Electrode solution (*in vivo* recordings)	1.5% neurobiotin, 0.5 M NaCl, 10 mM HEPES pH = 7.4 with NaOH/HCl	Vector labs Sigma-Aldrich	USA Germany
Atropine	50 mg/mL in distilled water	Braun	Germany
Isoflurane	Isoflurane, pure when liquid - variable concentration during experiments	Abbvie	Germany
Saline	0.9% NaCl dissolved in distilled water	Braun	Germany
Glucose	5% glucose dissolved in 0.9% NaCl	Braun	Germany
Phosphate buffered saline (0.01 M PBS)	137mM NaCl, 2.7mM KCl, 10mM NaH_2PO_4, 10mM Na_2HPO_4, in deionized water pH = 7.4 with NaOH/HCl	Sigma-Aldrich	Germany
Paraformaldehyde (PFA)	4% paraformaldehyde, 15% picric acid, in 0.1M PBS	Sigma-Aldrich	Germany
Pentobarbital	0.16g/mL sodium pentobarbital (Narcoren™)	Merial	Germany
Storing solution	10% sucrose, 0.05% NaN_3, in 0.01 M PBS pH = 7.4 with NaOH/HCl	Sigma-Aldrich	Germany
Carrier solution	0.2% bovine serum albumin, 1% horse serum 0.5% TritonX-100™ in 0.01 M PBS pH = 7.4 with NaOH/HCl	Vector labs Sigma-Aldrich	USA Germany
Blocking solution	0.2% bovine serum albumin, 10% horse serum 0.5% TritonX-100™ in 0.01 M PBS pH = 7.4 with NaOH/HCl	Vector labs Sigma-Aldrich	USA Germany
Reward solution	10% sucrose in tap water	Sigma-Aldrich	Germany

Equation 2.1. Correction of stereotaxic coordinates according to skull size.

$$y_{adjusted} = \frac{y_{atlas}}{4.2} * BL + 0.2$$

where

BL = empirical distance between bregma and lambda

4.2 = bregma-lambda distance according to the mouse brain atlas

y_{atlas} = antero-posterior coordinates according to the mouse brain atlas

$y_{adjusted}$ = adjusted antero-posterior coordinates actually used during experiments

Table 2.2. Stereotaxic coordinates used for in vivo electrophysiology.

Target brain region	Atlas coordinates		
	Medio-lateral (x)	Anterior-caudal (y)	Dorso-ventral (z)
Substantia Nigra	0.8 – 1.4	-3.08	3.6 - 4.8
VTA	0.25 – 0.75	-3.08	3.8 - 5

2.4. *In vivo* extracellular single-unit recordings with juxtacellular labeling

All in vivo electrophysiological recordings were performed on adult male mice, either KChIP4 KO or WT (C57B/6N, non-littermates), weighing between 25-45g.

2.4.1. Extracellular recordings of dopamine neurons in vivo

Spontaneous, single unit electrical activity of DA neurons were recorded with glass microelectrodes (G120F-4, outer/inner diameter: 1.2/0.69 mm, respectively; with microfilament on the inner wall, Harvard Apparatus, USA) with long shanks (at least 7 mm in length) and resistances of 12-25 MΩ. Glass electrodes were made with a horizontal puller (DMZ-Universal Puller, Zeitz, Germany). They were backfilled with a buffered saline solution with neurobiotin (Table 1) using a microfil syringe adapter (WPI, Germany) and attached to attached to an electrode holder (Harvard Apparatus, USA) with a chlorided silver wire (Ag^+/AgCl) and connected to a pre-amplifier headstage (D-71.732, NPI electronics, Germany). Recordings were made with an extracellular amplifier (ELC-03M, NPI electronics, Germany) connected via an A/D

board (HEKA, Germany) to a computer. Electrode positioning was controlled using a semi-automated micromanipulator (SM-6, Luigs and Neumann, Germany). Signals were amplified 1000-fold via the headstage and the main amplifier.

The entire surgical setup, as well as the micromanipulator and headstage was positioned on a pneumatic table (Newport Corporation, USA) for minimizing mechanical noise and covered with a custom-built faraday cage for shielding against electrical noise. The headstage ground was connected to a chlorided silver wire and positioned under the scalp incision close to the nape.

For recordings, electrode resistance was assessed periodically, first when the electrode contacted the brain surface and then in 0.5 mm steps as it advanced through the brain, until the tip reached the ventral midbrain. Resistance was tested by applying square 1 nA current pulses. Within the range of 12-25 MΩ, single unit spikes from putative DA neurons were detected with a signal to noise ratio of at least 5:1, with spike amplitudes often reaching 1 mV. When electrode tips got clogged (resistance increased to >25 MΩ) during descent, a “buzz” circuit was activated, which generated high frequency oscillations through the capacitance compensation system and mechanically unclogged the pipette tip. No resistance tests or “buzz” circuit activations were conducted while the electrode was within the target anatomical regions in order to avoid unspecific electrophoresis of neurobiotin into the tissue.

Descent through the brain until the target regions was performed at 10 µm/s, with periodic pauses for resistance tests. Once the electrode tip was in the area of interest, the tip was lowered in slow steps of 2-5 µm, in order to search for single unit activity. Signals were reproduced on an oscilloscope (HM1008-2, Hameg Instruments, Germany) and an audio speaker (AUDIS-01, NPI electronics, Germany) for visual and auditory identification of spikes during the search. Once a single unit was detected, the electrode was further lowered very slowly, in steps of 1 µm, with the micromanipulator hand wheel in order to approach the neuron and increase recorded spike amplitude and achieve a signal to noise ratio of at least 5:1 and AP amplitudes of ≈1 mV or higher (indicating close proximity to the cell membrane). Importantly, cells where signal amplitudes did not increase with electrode lowering and cells that were not putatively dopaminergic (AP width <1.1 and firing rates > 10 Hz) were not recorded (Figure 2.1 A). Cells that passed these criteria were recorded

for at least 10 minutes with a sampling rate of 12.5 kHz (for spike train analyses), and then for another minute with a sampling rate of 20 kHz (for better resolving AP waveforms). Recorded signals were notch- (50 Hz) and bandpass-filtered at 0.3 – 5 kHz online (single-pole, 6dB/octave, DPA-2FS, NPI electronics).

2.4.2. Juxtacellular labeling of recorded neurons

The juxtacellular labeling technique was first developed by Pinault (1996) as a method to combine high resolution extracellular recordings with anatomical features of neurons. Initially validated in thalamic reticular nucleus neurons, the technique was first applied to DA neurons by Ungless et al. (2004), where, combined with immunohistochemistry (IHC) staining for TH, it was used to confirm the neurochemical identity and morphology of VTA DA neurons. The principle of this method is to use positive current pulses to simultaneously eject neurobiotin from the pipette and electroporate the plasma membrane of the recorded cell. Neurobiotin is then taken into the recorded cell and serves as a histological marker for post-hoc identification of the recorded neuron.

This is possible because neurobiotin is a positively charged biotin-derivate (N-(2-aminoethyl) biotinamide hydrochloride, or biotin coupled to an E-amino group of lysine) and thus highly soluble in aqueous solutions and amenable to electrophoresis (Kita and Armstrong, 1991; Huang et al., 1992). Biotin (also known as vitamin B7 or vitamin H) is degraded relatively rapidly by metabolic processes once inside a living cell (≈24-72 hours). Thus, biotin metabolism limits post-labelling survival times, unless biotinase-resistent variant are used (which does not apply to this study). Biotin has a high affinity to avidin and streptavidin (an avidin homologue produced by the bacterium *Streptomyces avidinii*), forming highly stable conjugates that can be used for histological detection (Weber et al., 1989; Huang et al., 1992). Indeed, the biotin-streptavidin bond is one of the strongest non-covalent interactions observed in nature, with a dissociation constant (K_d) in the order of 10^{-15} M (Weber et al., 1989; González et al., 1999; Chivers et al., 2011). This makes the biotin-streptavidin interaction practically irreversible and the resulting conjugates relatively resistant to changes in pH and temperature, which justifies its widespread use in cellular research and diagnostics (Weber et al., 1989; González et al., 1999).

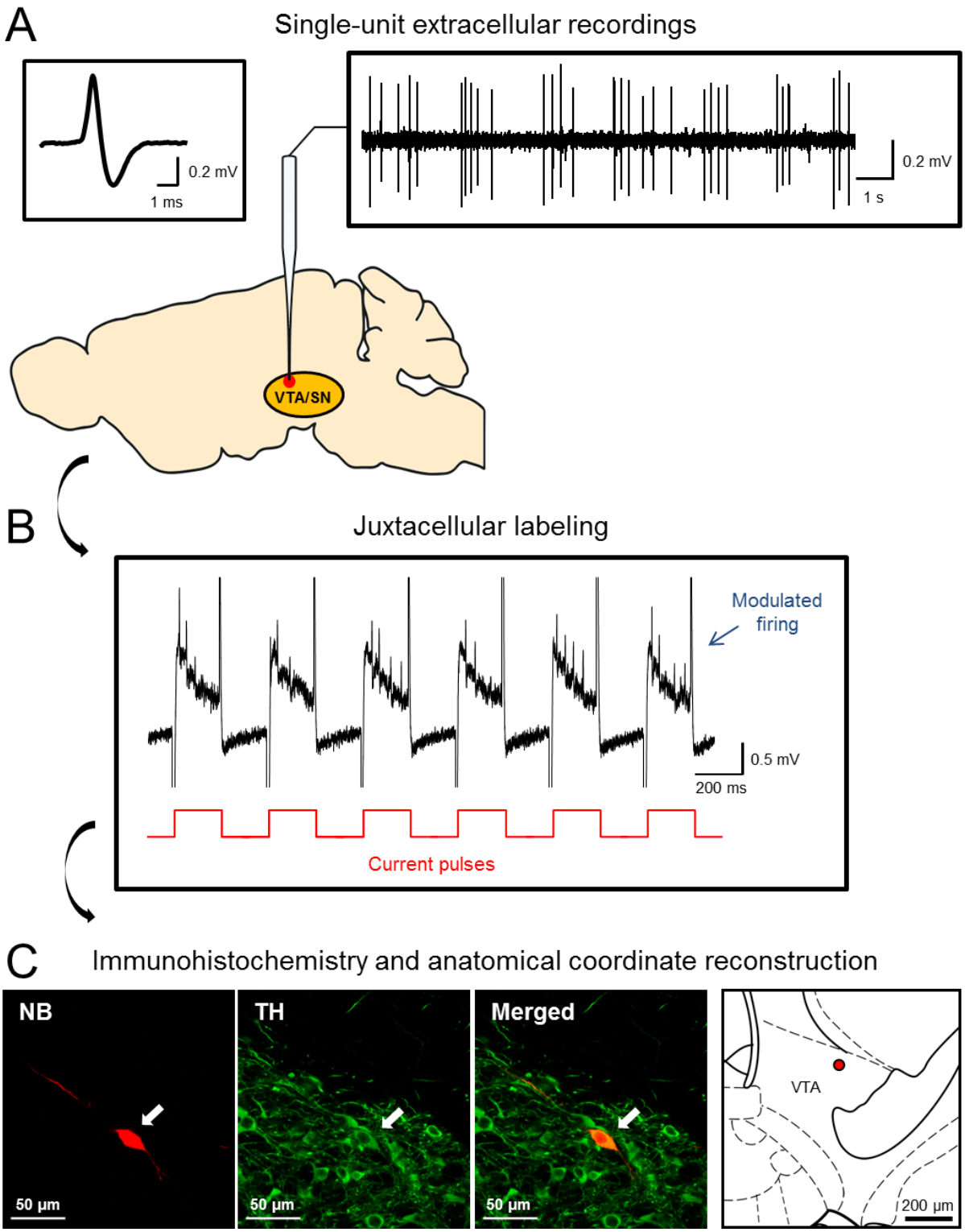

Figure 2.1. Procedures for *in vivo* recording, labeling and identification of DA cells.
A: Single-unit recordings were performed in the VTA or SN using glass micropipettes filled with saline solution and NB. Only cells that displayed >10 Hz average firing rates and AP width >1.1 ms were selected. B: After recordings, cells were juxtacellularly labeled with positive current pulses. C: following labeling, animals were perfused and the brains were processed for TH IHC and NB detection. Anatomical positions of identified cells were reconstructed with the assistance of custom MatLab® code.

After the recordings, which followed the previously specified criteria, positive current pulses (1-10 nA, 200 ms long square on/off pulses) were applied via the recording electrode with careful and continuous monitoring of the single-unit activity. Pulse currents were increased slowly until the limit of 10 nA; if cells still did not respond, the pipette was lowered by 1-2 µm and the process repeated. Electrode resistance and capacitance artifacts were corrected for to a level that allowed consistent cell monitoring at each step with the bridge balance and capacitance compensation circuits of the amplifier. Passing a current through a recording electrode creates a shift in the recorded voltage signal that is proportional to the electrode resistance and the applied current; the bridge balance circuit allows the correction of this artifact by creating an adjustable counter-acting voltage signal that is subtracted from the recorded signal, canceling out the voltage-shift artifact (Park et al., 1983). Similarly, the glass of the electrode pipette also acts as a capacitor, which is charged and discharged according to the current flow, creating capacitance artifacts in the recorded signal whenever a square labeling pulse was initiated and terminated; the capacitance compensation circuit corrects for this artifact by charging a second capacitor with adjustable gain according to the voltage output; the signal created by this is subtracted from the recorded signal, cancelling out capacitance transients (Wilson and Park, 1989).

Successful electroporation was immediately identifiable by an increase in membrane noise and modulation of firing rate (spiking activity locked to the “on” phase of the pulses; Figure 2.1 B). Once electroporation was achieved, the current was quickly reduced by approximately half to avoid cellular damage, and the modulated activity was monitored for at least 30 seconds (often exceeding one minute if the cell showed no signs of instability, such as decreased spike amplitude, increases in AP width or very high firing rates). Once this protocol was complete, the current amplitude was slowly decreased and cell activity was monitored for at least another minute. Electroporated neurons often resumed firing once the stimulation was terminated, and this was always a sign of a successful labeling. In some occasions, neurons did not resume firing immediately after labeling, but were still identifiable in histological processing (27/56 occasions, or ≈46%).

2.4.3. Perfusion and tissue fixation

Immediately after the electrophysiological experiments, and without awakening from inhalational anesthesia, animals were injected with a lethal dose (0.2 mL) of pentobarbital and pinned to a Styrofoam surgical board. The thoracic cavity was opened with surgical scissors and the heart exposed. The descending abdominal aorta was clamped with hemostatic forceps and 50 µL of heparin was injected directly into the left ventricle. The right atrium was ruptured with rat tooth (i.e. surgical) forceps and ice cold 4% PFA-PBS solution was perfused through the left ventricle for at least 6 minutes. The brain was subsequently removed and stored in 10 mL vials filled with PFA-PBS solution overnight, before being transferred to storing solution (see Table 2.1) until further histological processing.

2.4.4. Histological identification of recorded dopamine neurons

After the fixation procedure, the midbrain regions (containing the VTA and SN) of brains from recorded animals were sectioned in 60 µm sections on a microtome (VT1000S, Leica, Germany). Sections were then washed in PBS four times for ten minutes and then incubated in blocking solution for one hour. The blocking solution has a high protein content, which saturates unspecific binding sites, thus reducing the binding of antibodies with unspecific epitopes. After blocking, sections were incubated overnight at room temperature in carrier solution with an anti-tyrosine hydroxylase polyclonal rabbit primary antibody (1:1000) on a 3D shaker. Both the blocking and carrier solutions contained the detergent TritonX-100™ (0.5%), which permeabilizes lipid membranes and allows the antibodies to diffuse efficiently into the tissue and reach intracellular targets, where they interact with intracellular epitopes. Primary and secondary antibodies used in this study are summarized in Table 2.3. and 2.4. After primary antibody incubation, sections were again washed four times in PBS and incubated for at least six hours in carrier solution with AlexaFluor® streptavidin 568 (1:750), a fluorescent probe which binds to neurobiotin, and an anti-rabbit 488 secondary antibody (1:750). Following this step, sections were again washed four times in PBS, sorted according to their rostral-caudal orientation and placed on glass microscope slides (76 x 26 mm, Menzel, Germany). Sections were allowed to dry at room temperature and then covered with Vectashield® mounting medium and glass coverslips, sealed with nail polish and stored at -4 °C until visualization.

For fluorescent confocal microscopy, fluorescent stainings of the processed sections were observed with a laser-scanning microscope (Eclipse 90i, Nikon, Japan). Fluorescent microscopy in general is dependent on the capacity of certain photosensitive molecules, called fluorophores, to absorb photons of specific wavelengths, called excitation wavelengths, and in response emitting another photon of lower energy, or longer wavelength, called emission wavelength. Using sequential excitation with different wavelengths and filtering of the subsequent emission signal, different fluorophores present in the same section can be visualized selectively. Confocal imaging is based on point illumination with lasers and the selection of a focal plane with a pinhole, which spatially filters out light from outside the desired focal plane, thus creating high resolution pictures with low blur and high contrast (Paddock, 2000). The name “confocal” derives from the fact that only the emission from fluorophores positioned on both the focal plane of the laser point illumination and the pinhole are detected. In our system, sequential fluorophore excitation can be performed with four different monochromatic lasers: Argon-laser 488nm (emission filter bandpass 505-530 nm); Helium-Neon-laser 543nm (adjustable emission filter 580-625 nm); Helium-Neon-laser 647nm (high-pass emission filter 650 nm); and a laser-diode 405nm (emission filter 430-475 nm).

For detection of neurobiotin-filled TH-positive (i.e. dopaminergic) cells that were recorded *in vivo*, I used the 488 and 568 nm laser-filter configurations for visualizing streptavidin 568 and anti-rabbit 488 secondary antibodies. In this procedure, digital gain and signal offsets were optimized for each cell. Other optical configurations are summarized in Table 6. Only visually identified cells where both the neurobiotin and TH signals were co-localized (Figure 2.1 C), meaning that they were both dopaminergic and successfully labeled *in vivo*, were analyzed for their anatomical position (located in the VTA or the SN) and further studied regarding their AP waveforms and spike train properties. Classification of cells as VTA or SN DA neurons was determined by overlaying their respective anatomical positions onto the corresponding coordinates on the mouse brain atlas (Franklin and Paxinos, 2012). A custom Matlab® (MathWorks, USA) code was written for performing this overlay, as well as quantifying the cell’s distance from midline and plotting analyzed cell properties over their anatomical location symbols.

Table 2.3. Primary antibodies used for IHC.

Antibody	Dilution	Species	Supplier	Origin
Anti-tyrosine hydroxylase (polyclonal)	1:1000	rabbit	Calbiochem	Germany
Anti-tyrosine hydroxylase (monoclonal)	1:1000	mouse	Millipore	USA
Anti-Kv4.3 (polyclonal)	1:1000	rabbit	Alomone labs	Israel
Anti-KChIP4 (monoclonal)	1:500	mouse	Neuromab	USA

Table 2.4. Secondary antibodies used for IHC.

Antibody	Abbreviation	Dilution	Species	Supplier	Origin
AlexaFluor® 488 anti-rabbit	Anti-rabbit 488	1:750	goat	Invitrogen	USA
AlexaFluor® 488 anti-mouse	Anti-mouse 488	1:750	goat	Invitrogen	USA
AlexaFluor® 568 anti-rabbit	Anti-rabbit 568	1:750	goat	Invitrogen	USA
AlexaFluor® 568 anti-mouse	Anti-mouse 568	1:750	goat	Invitrogen	USA

2.4.5. Analysis of spike train properties

Recorded electrophysiological data were exported into IgorPro® (WaveMetrics, USA), thresholded for extraction of spike time stamps. Thresholds were set according to the signal to noise ratio of each recording and detection events were confirmed through visual inspection. Spike time vectors were then exported to Matlab® and analyzed using custom written code. ISIs were extracted by differentiating spike time vectors. Firing frequency was defined as the average number of spikes fired per second over the 10 minute recording period. ISI variability was quantified by the coefficient of variation (CV), defined as the ratio of the standard deviation and the mean of the recorded ISIs over the entire recording. Bursting was quantified according to the template method established by Grace and Bunney (1984), where ISIs below 80 ms define a burst onset and ISIs above 160 ms define a burst offset. After identifying bursts, the percentage of spikes fired in bursts (SFB) and intraburst statistics (e.g. mean spikes per burst, mean burst length, percentage of bursts with 2, 3 and >3 spikes) were calculated.

The asymmetry around the sample mean of recorded ISI distributions was quantified by measuring their skewness (see Equation 2.2). Skewness of a sample distribution is calculated as the ratio of the third moment (the sum of the differences to the mean cubed, divided by the number of elements in the sample) and the square root of the second moment (a.k.a. the variance, or the sum of the differences to the mean squared, divided by the number of elements in the sample) cubed (Fisher, 1930; Cramér, 1946). In finite samples of non-Gaussian distributions, this measure needs to be corrected for limited sample size by an added term (Joanes and Gill, 1998). The larger the skewness value, the more asymmetrical is the distribution of the data (a Gaussian distribution has a skewness of 0); a negative skewness value imply that the data are spread out more to the left of the mean, and a positive skewness values imply that the data are spread out more to the right. The relative presence of outliers in ISI distributions was quantified by measuring their kurtosis (see Equation 2.3). Kurtosis of sample distribution is defined as the ratio of the fourth moment (the sum of the differences to the mean elevated to the fourth power, divided by the number of elements in the sample) and the second moment squared (Fisher, 1930; Cramér, 1946). Like with the skewness measure, kurtosis values are adjusted for bias in finite samples from non-Gaussian distributions (Joanes and Gill, 1998). Kurtosis values indicate the degree to which a distribution is outlier-prone (a Gaussian distribution, for example, has a kurtosis of 3).

Equation 2.2. Skewness of a sample distribution

$$Skewness = \frac{\sqrt{n(n-1)}}{n-2} \frac{\frac{1}{n}\sum_{i=1}^{n}(x_i - \bar{x})^3}{\left(\sqrt{\frac{1}{n}\sum_{i=1}^{n}(x_i - \bar{x})^2}\right)^3}$$

where

x_i = sample element value

$\bar{x}$ = sample mean

n = number of elements in sample

Blue = sample correcting term

Equation 2.3. Kurtosis of a sample distribution

$$Kurtosis = \frac{n-1}{(n-2)(n-3)}\left((n+1)\left(\frac{\frac{1}{n}\sum_{i=1}^{n}(x_i-\bar{x})^4}{\left(\frac{1}{n}\sum_{i=1}^{n}(x_i-\bar{x})^2\right)^2}\right)-3(n-1)\right)+3$$

where

x_i = sample element value

$\bar{x}$ = sample mean

n = number of elements in sample

Blue = sample correcting term

For analysis of general spike patterns, raster plots and autocorrelation histograms (ACH, 1 ms bins, smoothed with a 20 ms Gaussian filter) were plotted using R (The R Project for Statistical Computing; https://www.r-project.org/). R codes were provided by our collaborator Prof. Gaby Schneider (Institute of Computer Science and Mathematics, Goethe-University Frankfurt). Based on the visual analysis of the ACH (Wilson et al., 1977; Paladini et al., 2003; Bingmer et al., 2011; Schiemann et al., 2012), spike trains were classified in four major categories (Figure 2.2), a procedure that has been previously performed and validated in our lab (Bingmer et al., 2011; Schiemann et al., 2012; Subramaniam et al., 2014a, 2014b):

- Regular single spike: ACH displayed three or more equidistant peaks with decreasing amplitudes, which reflects ISIs that are very similar in duration and with low variability, and no large peak around zero, which reflects the absence of burst ISIs.
- Irregular single spike: less than three peaks, potentially without peaks, increasing from zero. The absence of repetitive peaks indicates a higher variability and lower stationarity of ISIs in relation to the regular single spike pattern.
- Regular bursting: a sharp, high amplitude peak close to zero, due to intraburst spikes, followed by a clear through and at least one clear peak, reflecting long regular interburst ISIs.
- Irregular bursting: a sharp, **high amplitude** peak close to zero that is not followed by another peak, indicating that the bursts are not periodic.

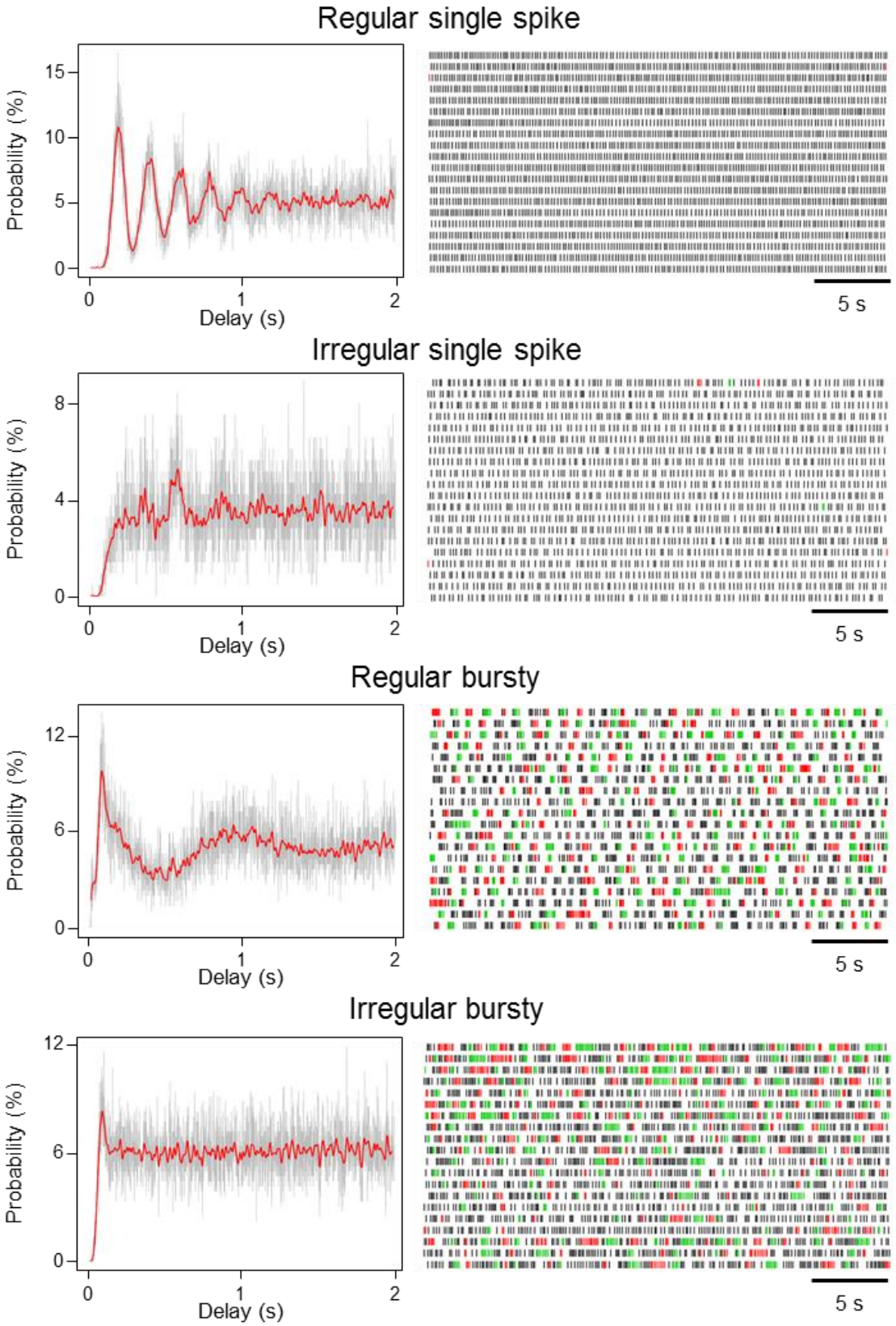

Figure 2.2. ACH-based classification of in vivo DA neuron spike patterns**.**
Representative ACHs and raster plots of neuronal spike trains for each class are displayed. Red and green spikes on the raster plots indicate detected bursts according to the template method (Grace and Bunney, 1984b). Note the sharp peak close to zero for bursty patterns, the peaks that characterize the regular patterns and the flat regions of the ACH that determine the irregular patterns.

2.4.6. Action potential waveform analyses

Single AP waveforms recorded during the 10 minute spike train recording were aligned according to their peak amplitude and overlaid using custom written IgorPro® code and the NeuroMatic extension for IgorPro® (made freely available by Jason Rothman; http://www.neuromatic.thinkrandom.com/). Consistency of AP waveforms was done with visual inspection, and ratified *post-hoc* that the same cell was always recorded throughout the experiment (Figure 2.3). Even when cells exhibited long pauses (>5 seconds), AP waveforms did not vary drastically in shape (as determined by visual inspection), indicating that there was no misidentification of any of the 86 recorded single unit spike trains.

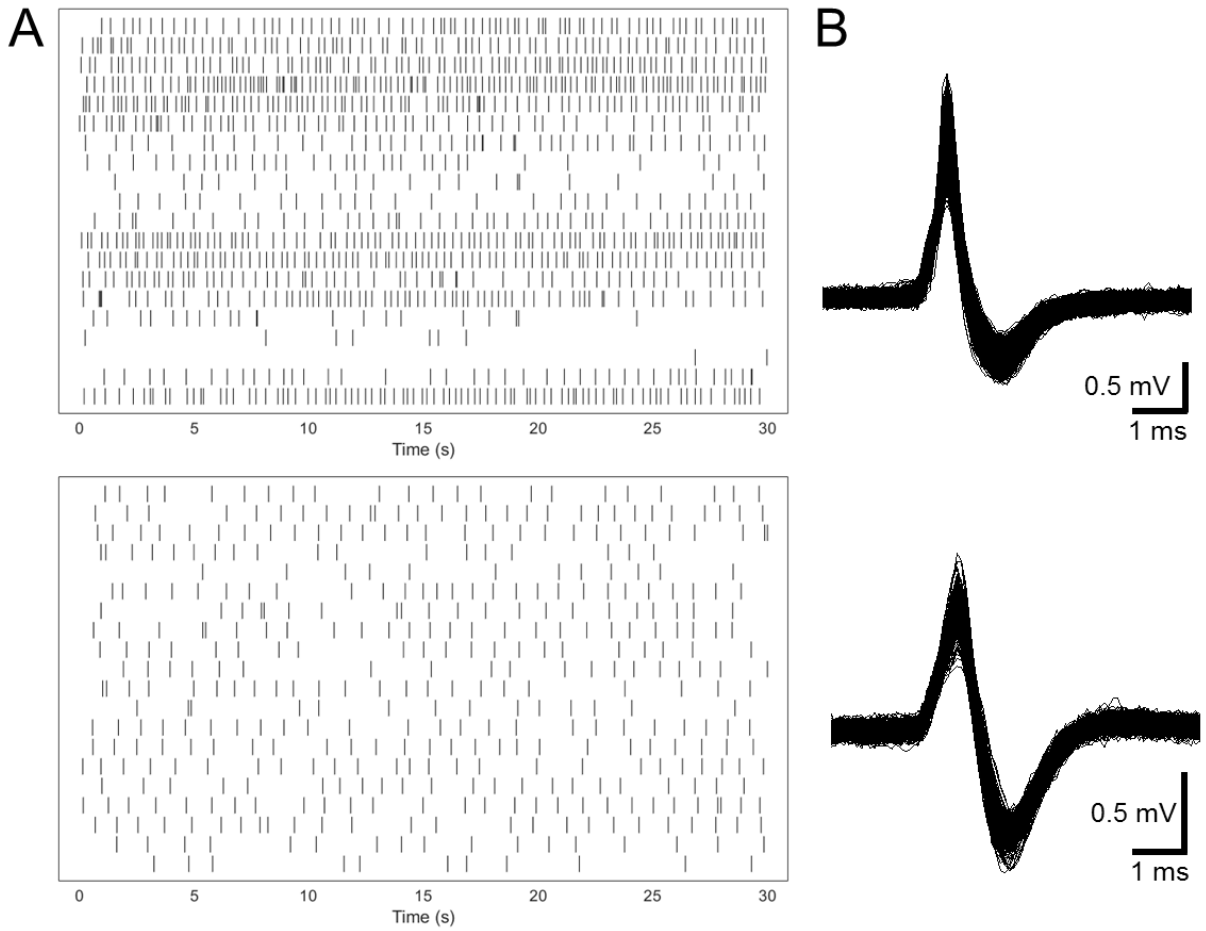

Figure 2.3. Long pauses in WT DA neuron spike trains are not due to cell misidentification. A: Raster plots of spike trains from representative DA neurons recorded in the VTA and SN. Note the presence of pauses that extend for over ten seconds. B: Overlay of all the recorded AP waveforms from the cells whose spike trains are displayed in panel A. Note that the waveform of the APs is virtually identical throughout the entire experiment, indicating that the gaps in the raster plots are indeed due to the pause in firing of a single cell.

For construction of high-resolution averaged waveforms, the first 20 APs recorded after the initial 10 minute spike train recording (at a 20 kHz sampling rate) were aligned according to their peak amplitude, overlaid and averaged. Importantly, due to my bandpass filter settings (0.3 – 5 kHz), recorded AP waveforms were broad and biphasic, unlike the triphasic AP waveforms reported with narrower bandpass limits (Grace and Bunney, 1980, 1983b; Brown et al., 2009; Schiemann et al., 2012; Ungless and Grace, 2012). For an example waveform, see Figure 2.4. In this figure, identified inflection points correspond to the AP threshold (a), spike peak (b), spike through (c) and return to baseline (d). Biophysically, the extracellular action potential approximates the first time derivative of the intracellular action potential (Grace and Bunney, 1983b). Therefore, the a→b segment corresponds to the depolarization phase of the AP, and the b→d segment corresponds to the repolarization phase. AP width was defined as the a→c segment duration and compared between groups (Ungless et al., 2004; Schiemann et al., 2012).

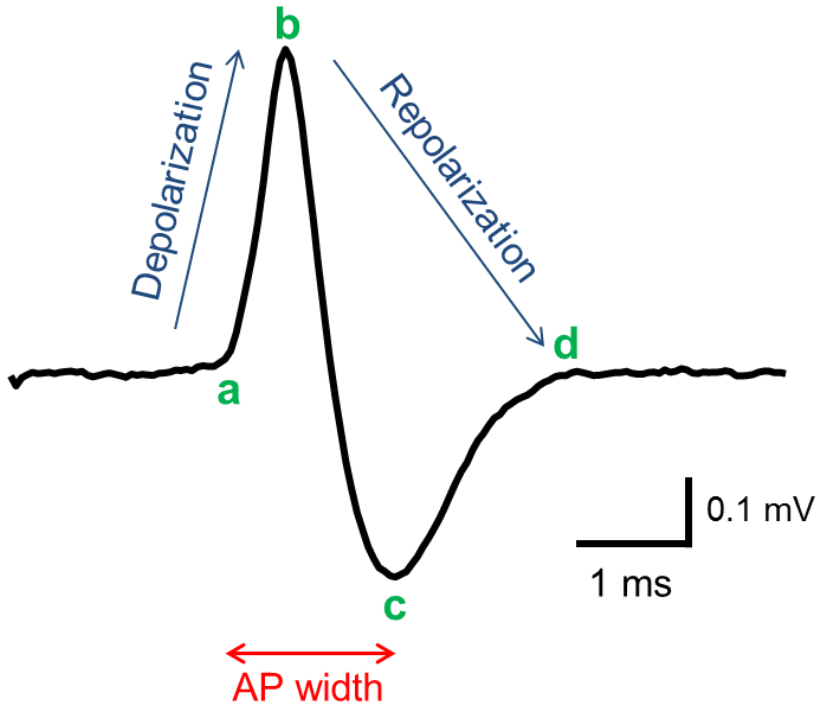

Figure 2.4. Analysis of DA cell mean AP waveforms.
Trace is an average of 20 APs from a DA cells recorded *in vivo*. Inflection points correspond to the AP threshold (a), spike peak (b), spike through (c) and return to baseline (d).

2.4.7. Detecting firing pauses in spontaneous dopamine neuron activity

Given the initial hypothesis of this study, it was crucial to establish a method to detect transient pauses in firing in DA neuron spike trains. Unlike burst detection with the template method, where there is an empirically derived static criterion with reasonable face validity, biophysical correlates and that can be applied uniformly across different DA neuron subtypes, discriminating a putative “pause” from other ISIs in a wide distribution is much more challenging. At least three issues make the identification of pauses particularly confounding: 1) the difference between a visually identified “pause” and a longer pacemaker ISI is not well defined; 2) pauses are often rare events in a recorded ISI vector by their very definition (being interruptions of firing in a cell type that is intrinsically active); 3) the detection of a pause is highly sensitive to the frequency and variability of the background single spike firing, as a neuron with low mean firing rate and high CV would be expected to have longer ISIs just from the properties of the underlying distribution. Because of this, pause detection thresholds must be adjusted according to the statistical properties of individual spike trains.

In this study, three different measures were used to identify a potential effect on pausing. Firstly, the quantification of the maximum ISI, and its ratio to the mean ISI, in each spike train. Secondly, the Robust Gaussian Surprise (RGS) method was applied (Ko et al., 2012). This method was explicitly developed for the detection of pauses and bursts in DA neuron spike trains and is based on identifying ISIs that are longer than would be expected given the distribution of ISIs immediately before it. It is predicated on the following algorithm: 1) transform all ISIs to log(ISI)and normalize the distribution to around 0 by subtracting an estimated central location parameter, 3) apply an overlapping moving window to the normalized log(ISI) vector that selects 41 values at a time and estimate a Gaussian distribution from each selection, 4) from set a pause threshold, proposed to be 99.5^{th} percentile of the central distribution of the moving window, 5) calculate a *P*-value to estimate the certainty of detection (level of significance for detection was $P < 0.01$) and correct for multiple comparisons with the Bonferroni method. For details on the definition of each parameter, see Ko et al. (2012).

While the RGS method was useful in confirming a phenotypical difference between groups (see Results section), it had a high false positive detection rate and

high variability in detection rates between spike trains, with the number of RGS pauses varying within two orders of magnitude (see Results section). Additionally, this method is extremely sensitive to changes in detection parameters such as moving window size, central estimation parameters, pause threshold and level of significance. In order to avoid this confound, I developed a simpler, custom method of detecting pauses based on the Tukey outlier identification algorithm (Tukey, 1977). This method relies on setting a non-parametric pause threshold that is adjusted to each cell but applied across the entire spike train. The pause threshold is the 75th percentile added to a factor *w* (set as 3 in this study) multiplied by the interquartile range (Equation 2.4.).

Importantly, this method only has one free parameter (*w*), which determines the stringency of pause detection and was applied similarly to all spike trains. The outlier detection algorithm was more robust and produced estimates of pausing properties that were less variable across different neuronal firing patterns (see Results section). Furthermore, because post-burst pauses in DA neurons might have distinct biophysical causes (e.g. SK channel activation, depolarization block) compared to those generated by increased inhibitory input, an additional criterion was added (Ping and Shepard, 1999; Tucker et al., 2012; Paladini and Roeper, 2014). Pauses preceded by template method-identified bursts were considered as putatively non-GABAergic and were excluded from the analysis. Examples of these pauses are shown in Figures 2.5 and 2.6.

Equation 2.4. Pause detection based on outlier identification.

$$P_{thr} = q_3 + w(q_3 - q_1)$$

where

P_{thr} = pause threshold

q_3 = 75th percentile

q_1 = 25th percentile

w = multiplicative parameter that defines outlier estimation

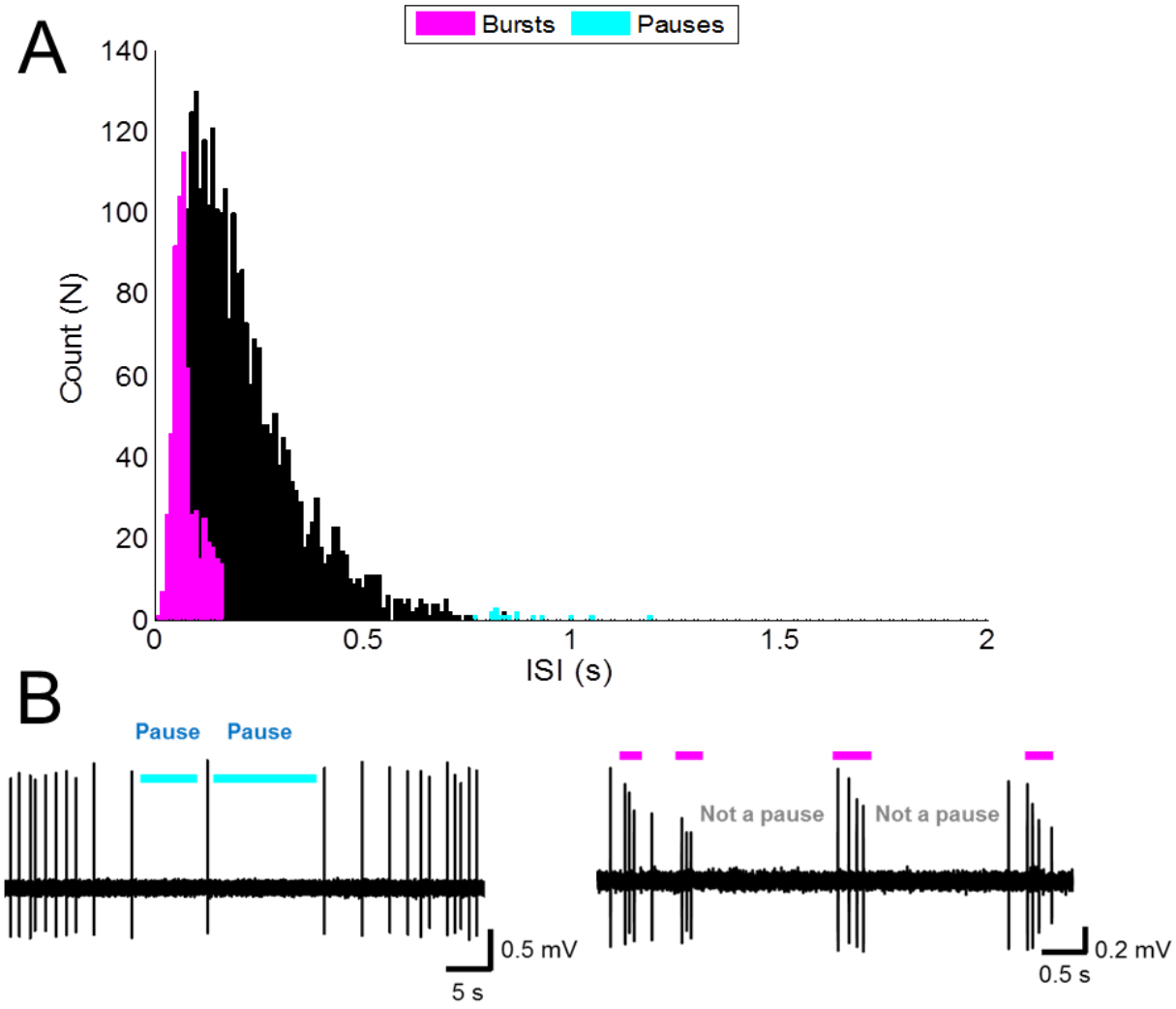

Figure 2.5 Identification of pauses using an outlier detection method.
A: Frequency histogram of ISIs in a representative spike train. ISIs in bursts and outlier pauses are identified in magenta and cyan, respectively. B: Raw traces with identified bursts and pauses, with representative ISIs that were marked as outlier pauses, highlighting the point that long ISIs that were preceded by bursts were not counted as pauses.

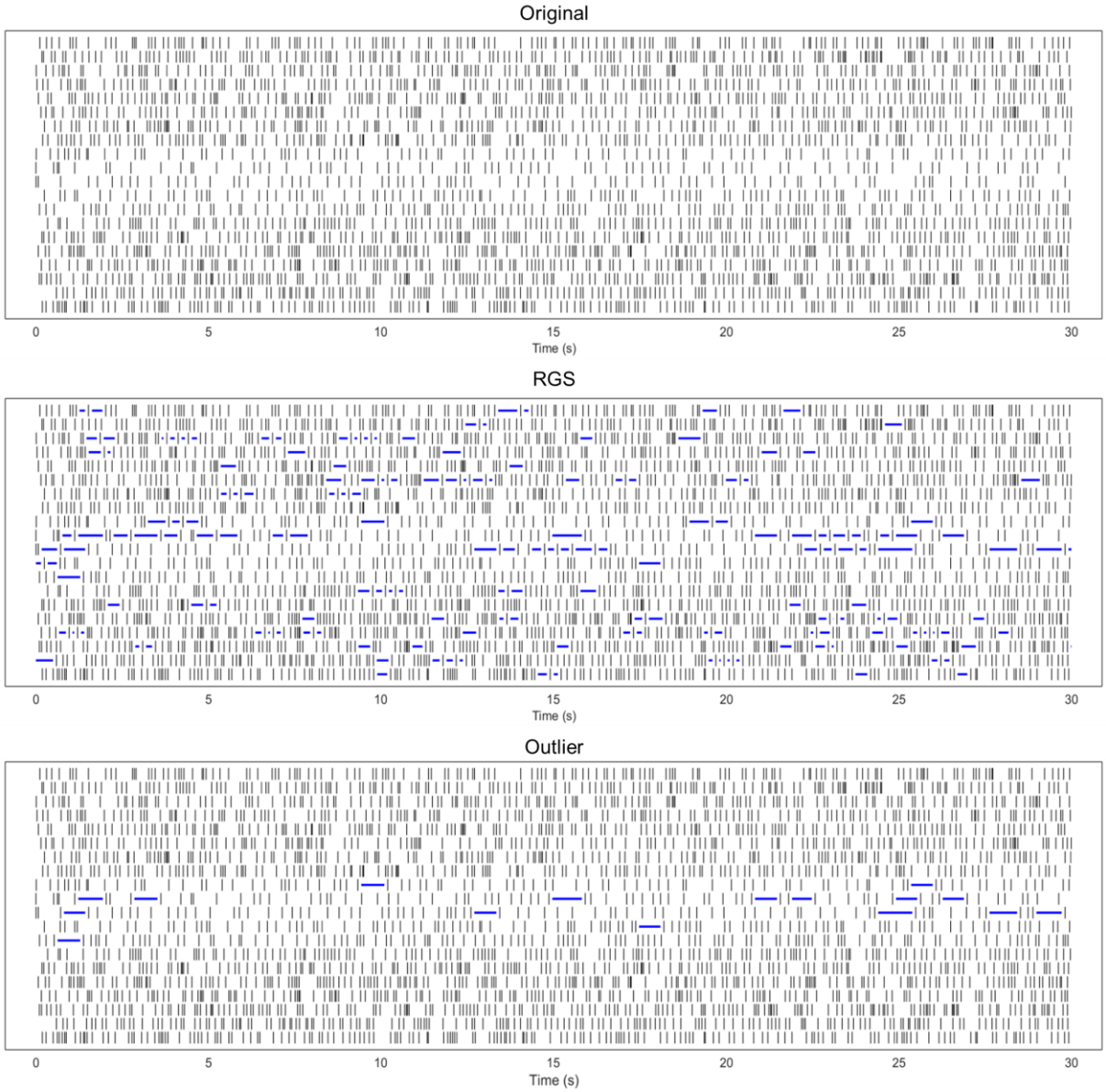

Figure 2.6 Example of identified pauses in a DA neuron spike train.
Raster plots of the same VTA DA neuron, without any markers and with pauses (blue traces) identified with the RGS and outlier algorithms. Notice the higher number and frequency of RGS pauses in comparison to outlier pauses.

2.5. Conditional exon-deletion mouse lines for assessing KChIP4a function

In collaboration with genOway (France), two new transgenic mouse lines were developed for assessing the specific function of the KIS domain of KChIP4a using the cre-lox system (Sauer, 1987; Sauer and Henderson, 1988). The fundament of this method is to flank the exon 3 of the KChIP4 gene (specific and determinant of the KChIP4a isoform) with *loxP* sites (floxing). Posteriorly, one can to induce conditional, cre-recombinase dependent, knockout of this exon in specific neuronal subtypes by breeding this line with another line where the cre enzyme is expressed under a

specific promoter (Figure 2.7). Cre-recombinase cuts out a sequence of DNA base pairs depending on the relative orientation of short, directional DNA sequences (Sauer, 1987; Sauer and Henderson, 1988; Tronche et al., 2002; Saunders et al., 2012). When two lox sites are oriented in the same direction, cre recognizes the sequence and excises the DNA flanked by the lox sites, leaving behind a single lox site and not modifying the rest of the genome (Saunders et al., 2012).

For the first line, the objective was to have a cre-dependent conditional deletion line for exon 3 of KChIP4. The KChIP4 exon 3-targeting vector was designed to display two homology regions in a C57BL/6N genetic background, including a short homology region of 1795 bp and a long region of 5858 bp, an insertion of two loxP sites flanking KChIP4 exon 3, a positive selection FRT-flanked neo cassette (neomycin resistance gene flanked by FRT sites, which are detect by the Flp recombinase enzyme, in a similar manner as the cre/lox system) and a the diphtheria Toxin A (DTA) negative selection marker. The quality of the resulting final targeting vector was controlled using sequencing of the coding exon, the junctions between the homology arms and selection cassettes, the positive and negative selection cassettes, the junctions between the homology arm and the plasmid backbone, and the distal *loxP* site. This vector was electroporated into C57BL/6N ES cells. G418 - resistant ES cell clones were isolated and recombination was confirmed with PCR and southern blot screenings.

Selected clones were injected into C57BL/6J (albino) blastocysts, which were then re-implanted into OF1 pseudo-pregnant females and allowed to develop to term. Chimeric offspring were born after approximately three weeks and the contribution of the recombinant ES cells to each individual was assessed using coat color markers. Males that displayed chimerism rates of over 50% were bred with female C57BL/6 Flp-deleter mice to excise the neo selection cassette and to generate heterozygous mice carrying the neo-excised conditional deletion allele (first generation, F1). Upon reaching sexual maturity, F1 males were bred with C57BL/6 wild-type females to generate additional animals of this type (F2). The F2 mice were then interbred with each other to generate the homozygous conditional deletion line (KChIP4-Ex3$^{lox/lox}$).

Genetic identity of all KChIP4-Ex3$^{lox/lox}$ mice was confirmed with polymerase chain reaction (PCR) genotyping throughout the breeding process. For detecting the conditional deletion allele, the following primers were used:

5-TAG TTA TGA CAA GAC AGG AGC TAG TAC CAC TAA GC-3

and

5-GAA CTG GAC TGA AGC AAA ACA AAA CAC G-3.

These primers target the flanking region of the FRT site and the PCR product lengths were 385 bp for the WT allele and 477 bp for the conditional deletion allele. The PCR was run with 1 cycle at 94 °C for 120s (denaturing), 35 cycles of 94 °C for 30s (denaturing), 65 °C for 30s (annealing) and 68°C for 30s (extension), followed by 1 cycle at 68 °C for 480s (completion).

In order to achieve robust midbrain DA neuron-specific deletion of KChIP4-Ex3, homozygous KChIP4-Ex3-flox mice were crossed with a line with heterozygous cre expression under the DAT promoter – the DAT-cre knock-in (DAT-cre$^{+/-}$ or DAT-cre KI) mouse line (Bäckman et al., 2006). DAT is to date the most reliable genetic marker for midbrain DA neurons (Lorang et al., 1994; Lammel et al., 2015). While TH is commonly used as a genetic identifier of DA neurons, especially for immunohistochemical labeling, this enzyme is also expressed in noradrenergic neurons and mouse lines that express cre under the TH promoter have been found to be non-selective for DA neurons within the VTA (Lammel et al., 2015). Genetic identity of DAT-cre KI mice was also confirmed with PCR genotyping. For detecting the conditional DAT-cre KI allele, the following primers were used:

5-TCC ATA GCC AAT CTC TCC AGT C-3, 5-GTT GAT GAG GGT GGA GTT GGT C-3

and

5- GCC GCA TAA CCA GTG AAA CAG C-3.

The PCR product lengths were ≈400 bp for the WT allele and ≈600 bp for the KI allele. The PCR was run with 1 cycle at 94 °C for 60s (denaturing), 3 cycles of 94 °C for 15s (denaturing), 56 °C for 15s (annealing) and 72°C for 15s (extension), 5 cycles of 94 °C for 15s (denaturing), 50 °C for 15s (annealing) and 72°C for 15s (extension) followed by 1 cycle at 72 °C for 600s (completion) and slow cool down until 10 °C.

In the subsequent F1 generation, half of the litter is heterozygous for the floxed KChIP4-Ex3 and the DAT-cre KI, while the other half is heterozygous for the floxed

KChIP4-Ex3 and WT for the DAT-cre KI (Figure 2.8). These two genotypes were then bred with each other, leading to an F2 generation with mice that are homozygous for the KChIP4-Ex3-flox and heterozygous for the DAT-cre KI, i.e. with DA cell specific excision of KChIP4 exon 3 (*DAT-cre*$^{+/-}$ / *KChIP4-Ex3*$^{-/-}$, or KChIP4-DAT-Ex3d), WT for the KChIP4-Ex3-flox and heterozygous for the DAT-cre KI, i.e. with DA cell specific expression of cre but no excision of KChIP4 exon 3 (DAT-cre$^{+/-}$ / *KChIP4-Ex*$^{WT/WT}$, or just DAT-cre KI), WT for the KChIP4-Ex3-flox and WT for the DAT-cre KI, i.e. with neither the DA cell specific excision of KChIP4 exon 3 or cre expression (*DAT-cre*$^{-/-}$ / *KChIP4-Ex3*$^{WT/WT}$, or DAT-cre WT) In addition, animals with other genotypes (*DAT-cre*$^{+/-}$ / *KChIP4-Ex3*$^{WT/-}$, *DAT-cre*$^{-/-}$ / *KChIP4-Ex3*$^{flox/flox}$ or *KChIP4-Ex3*$^{WT/flox}$) were produced but not used in this study. The genetic identity of all mice was confirmed with PCR genotyping before experiments (Figure 2.8 B).

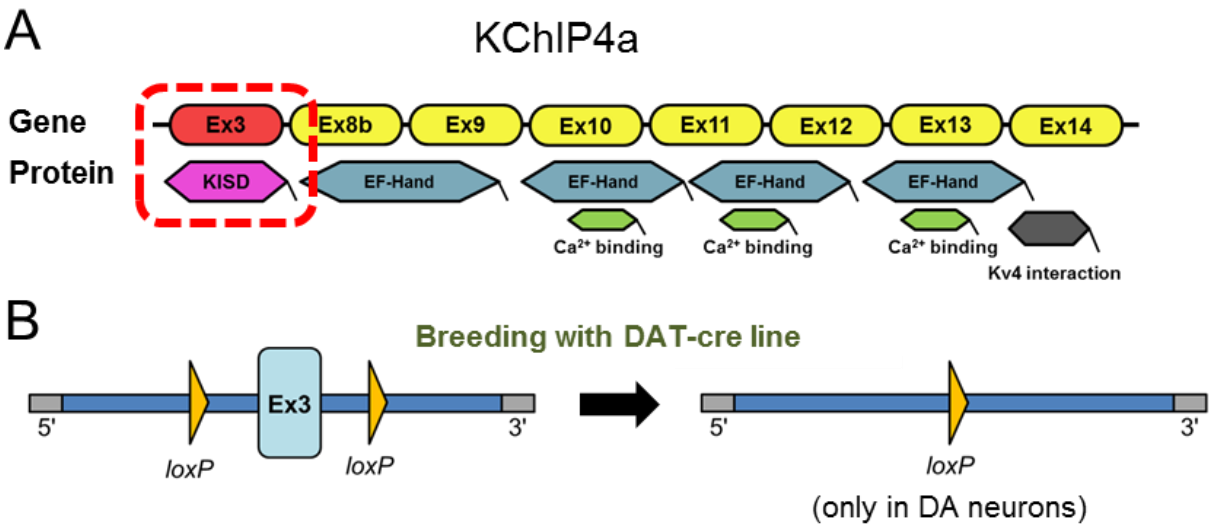

Figure 2.7. Generation of KChIP4-Ex3d mice.
A: Structure of the KChIP4a subunit in relation to the coding regions of the KChIP4 gene. Note that the KISD (magenta) is coded by exon 3 (red), which defines this subunit. B: Selective KChIP4 exon 3 deletion was accomplished by breeding mice with *loxP* sites flanking this exon with a DAT-cre line, where cre-recombinase is expressed under the DAT promoter (in DA neurons).

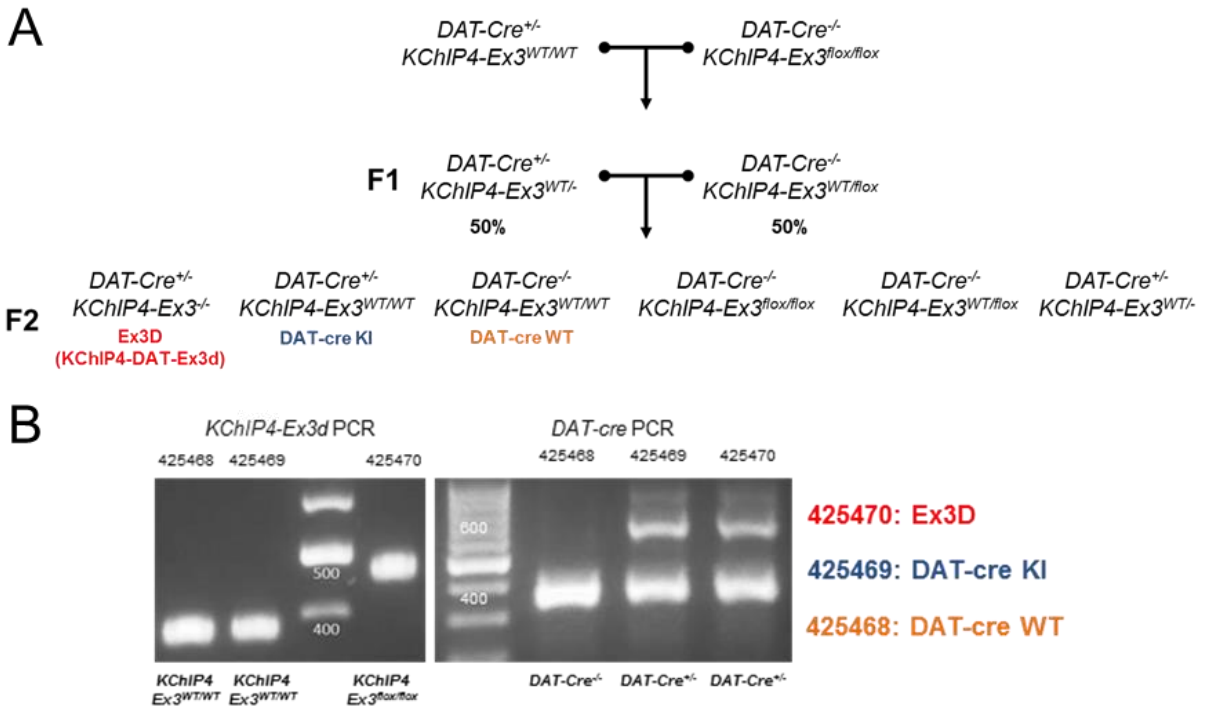

Figure 2.8. Genotypes used for analyzing the function of KChIP4a.
A: breeding of the transgenic mice. Ex3d mice lack KChIP4 exon 3 only in DA neurons. DA-cre KI mice are controls for Ex3d, as they express cre in DA neurons, but do not have the floxed exon 3. DAT-cre WT mice have WT alleles for KChIP4-Ex3d and DAT-cre. B: Example of PCR identification of used genotypes. The PCR gels demonstrate the bands for WT and transgenic alleles for KChIP4-Ex3d and DAT-cre protocols. Examples for three mice (one for each genotype and identified by individual numbers) are shown.

2.6. Procedures for behavioral analysis in transgenic mouse lines

Animals from all four genotypes of the F2 generation of the KChIP4-Ex3-flox and DAT-cre KI crossing (DAT-cre KI, DAT-cre WT, KChIP4-Ex3d and HET) were used for behavioral experiments. Male and female mice over 8 weeks old were genotyped, selected and individually identified by the implantation of a subcutaneous transponder microchip (1.4 mm x 9 mm ISO FDX-B glass transponder, Planet ID, Germany). These procedures were performed by Prof. Jochen Roeper (thesis supervisor), Beatrice Kern (lab manager) and Jasmine Salmen (lab technician). The experimenter (me) was blind during the conditioning experiments, and the inclusion of all genotypes was performed in order to improve blinding. Behavioral comparisons were performed between KChIP4-Ex3d (N = 10) and DAT-cre KI mice (N = 20), as well as between DAT-cre KI (N = 20) and DAT-cre WT mice (N = 17). A total of 60 mice were tested in three runs with 20 animals each. One KChIP4-Ex3d mouse showed erratic behavior during extinction and was excluded from the data analysis.

2.6.1. Water restriction protocol

In order to get animals to perform an appetitive associative learning task, it is essential to restrict their access to either food or water, so that they will be motivated and attentive. This increases the reward value of the US and permits the learning of CS and operant associations (Bodyak and Slotnick, 1999; Parker et al., 2011; Cohen et al., 2012; Steinberg et al., 2013; Guo et al., 2014; Stopper et al., 2014; Eshel et al., 2015). Previous studies have shown that rodents, including mice, have a healthier physiological reaction to water restriction than food restriction, with significant less adverse effects on behavior, tissue integrity and stress responses (Treichler and Hall, 1962; Guo et al., 2014). Furthermore, liquid rewards are more easily apportioned and the same amount of time on water restriction will motivate a mouse more than food restriction (3-4 days compared to 1-2 weeks, respectively), which makes the water restriction protocol easier to perform and reduces the time over which animals are subjected to resource regulation. For this reason, mice were motivated in the following experiments by having their daily access to water restricted (Guo et al., 2014).

Mice underwent a protocol adapted from the study of Guo et al (2014), where mice received around 1 mL of water per day and stayed at approximately 70% of their initial body weight during experimental sessions (Guo et al., 2014). In my study, WT C57BL/6N mice were first tested on different variations of this protocol, with daily water rations varying between 1 and 1.5 mL of water per day, and weight targets between 70 and 85% of their initial body weight. Except during experimental sessions, water was always delivered in a cup placed in their home cage (Guo et al., 2014). Mice were also closely monitored in order to ensure that the water supply was consumed and not spilt over or contaminated. The health of the water restricted mice was evaluated daily (Guo et al., 2014). Animals were checked for weight loss, physiological indicators of hydration (signs of urine and feces; tenting of skin when scruffed), movement patterns (gait; frequency of spontaneous movement), ruffled fur and posture (both signs of stress in rodents). If animals lost more than 30% of their initial body weight, the status of these indicators was scored according to the published protocol by Guo et al. (2014; Figure 2.9), and mice that achieved high scores (signs of health deterioration) were given extra water rations (scores 3 to 5) or removed from the study and received water *ad libitum* (scores of 6 or more).

Preliminary experiments with WT C57BL/6N mice indicated that fixed rations of 1 mL per day led to quick weight loss, sometimes with health scores over two. Based on these preliminary results, mutant mice were given daily rations that varied between 1 and ~1.5 mL depending on the animal's weight on that day, with set a target of 85% of the initial body weight. Animals received 1 mL until they hit the 85% mark, after which they received an additional 0.1 mL for each percentage point below that threshold. For example, a mouse that was at 82% of its initial weight would be given 1.3 mL for that day. This protocol was very successful in maintaining stable body weights around the desired target (Figure 2.10.), and never resulted in health scores going above two.

Cage #:		**Animal ID #:**			**30% Weight Loss (g):**			**Restriction #:**	
Date									
Time Observed									
Body Weight (g)									
Activity									
Moves around the cage (0)									
Moves slowly around the cage or has an abnormal gait (1)									
Moves only when touched (2)									
Does not move (3)									
Posture & Grooming									
Normal posture & smooth fur (0)									
Hunched posture or ruffled fur (1)									
Hunched posture & slightly ruffled fur (2)									
Hunched posture & all fur ruffled (3)									
Signs of Eating/Drinking (Reduce the score by 50% if within 3 days of the cage change)									
Feces & urine observed (0)									
Minimal fecal and/or urine output (1)									
No signs of feces and/or urine (2)									
Signs of Dehydration									
Skin does not tent when scruffed (0)									
Skin tents briefly, but returns to normal (1)									
Skin tents & takes more than a few seconds to return to normal (2)									
Skin tents & stays tented (3)									
Total Score									

Figure 2.9. Health assessment sheet used for evaluating the impact of water restriction. Animals went through the entire checkup if they lost more than 30% of their initial body weight. This sheet was taken from the study by Guo et al. (2014).

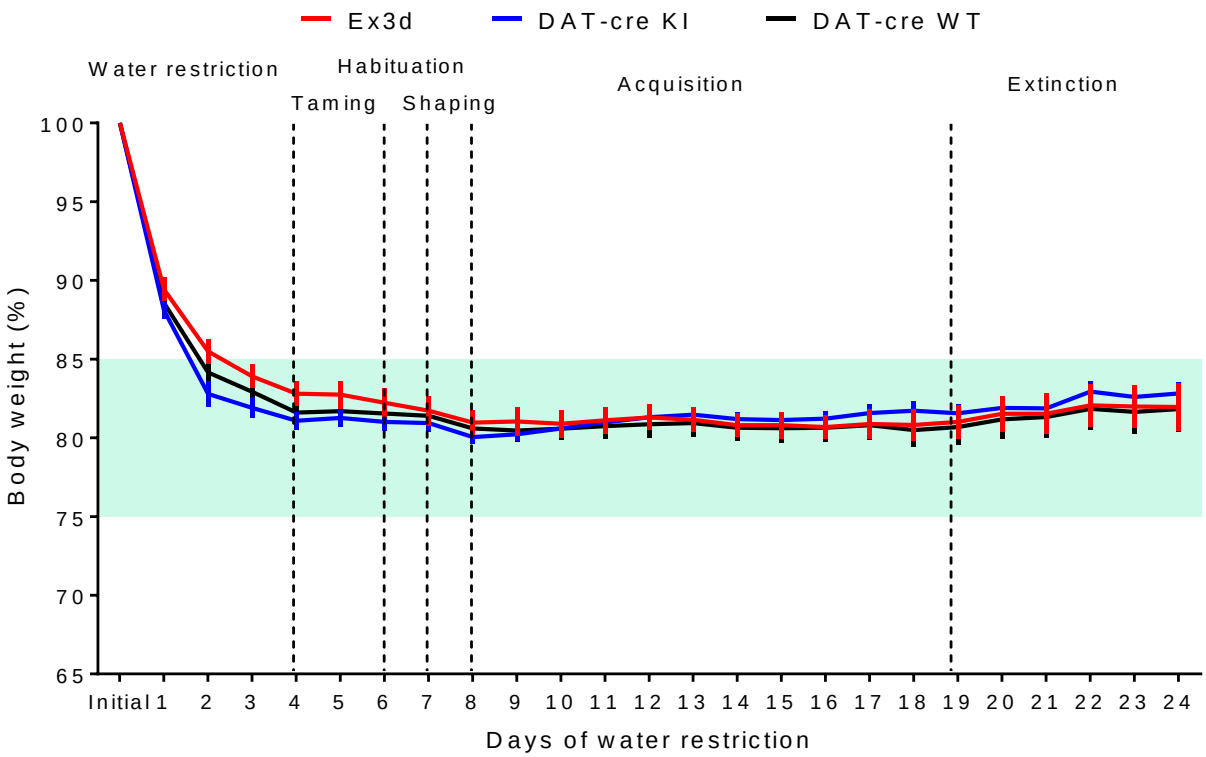

Figure 2.10. Comparisons of weight variations of mutant mice under water restriction.
Lines express the means of each group and error bars represent SEM. Mice lost weight progressively (effect of time, $F_{24, 1032}$ = 148.6, P < 0.0001) and stabilized their weight loss during the acquisition and extinction stages. No significant difference was observed between the genotypes (no effect across genotypes or interaction with time, $F < 1$, $P > 0.05$).

2.6.2. Conditioning: acquisition and extinction

The full experimental paradigm spanned 24 days (Figure 2.11). On the first four days, mice were submitted only to water restriction. In the following two days, they were tamed, i.e. gently handled (held up above their home cage on a spread palm, with no constriction or entrapment by the experimenter) until they no longer tried to escape from the experimenters hand, showed no signs of overt stress and anxiety (hunched posture, ruffled fur and tachypnea) and readily drank a liquid reward (0.2 ml) given by the experimenter via a syringe while being held. Liquid rewards throughout this study were a solution of 10% sucrose in tap water, and drinking the hand-given reward during handling accomplished the double goal of exposing the animal to the rewards he would encounter in the operant chamber and guaranteeing that the animal feels safe and is not under stress (rodents will typically only consume food and water when they do not feel threatened). The following day, the animals were acclimated to the operant chamber (Table 2.5.), as is standard practice in

conditioning studies of freely moving animals (Steinberg et al., 2013; Guo et al., 2014). Mice were placed inside the operant chamber but with the reward port removed. They remained in the chamber for 50 minutes under monitoring with a video camera connected to computer. After this time they were returned to their home cage and given their daily ration of water. The following day, mice were placed in the operant chamber for another 50 minutes, now with the reward port present. At semi-random time intervals (mean of 60 seconds, varying between 30 and 90 seconds), a reward (16.66 µL) was delivered at the port, with no cue to its delivery. Animals had to seek and check the port to find the reward and consume it. The mice learned this immediately, in part due to the fact that the reward port is for them a novel stimulus which they would already normally explore.

The conditioning task used in this study is based on the study by Steinberg et al. (2013). It was initially developed for rats, and was adjusted it in order to be suitable to mice. This task was chosen for its simplicity and for having been specifically designed to demonstrate the role of dopamine neuron activity in conditioning. In this paradigm, animals learned to associate a CS (sound tone pulsed at 3Hz – 0.1s on/0.2 s off – at 70 db) to the availability of reward in the reward port. In a 45 minute session, there were ten trials (mean ITI of 4 minutes, varying between 1.5 minutes and 6.5 minutes) in which the auditory cue was on for 30 seconds. Animals could trigger reward delivery to the port by entering it during CS presentation. Rewards were delivered in a cycle of 2 s reward delivery (16.66 µL) followed by a 3 s consumption interval. Delivery was continuous for as long as the animal kept its head in the port during CS presentation. This allowed for a maximum of 6 rewards per trial and a maximum of 60 rewards per session (a total of ~1 mL or reward in the task per day). This acquisition phase lasted for 11 daily sessions. Extinction of the conditioned response was tested by consistently omitting the reward during CS presentation for six daily sessions. After extinction, animals were returned to their home cage and received water ad libitum for at least three days before being submitted to other behavioral tasks. All animals recovered their initial body weight in this period of time and showed no adverse health effects from water restriction.

Table 2.5. Med-Associates operant chamber components.

Component	Description	Ref. number
Sound attenuating cubicle	Sound attenuating ventilated wooden box	ENV-022MD
Modular mouse cage	Cage with exchangeable walls	ENV-307W
Liquid cup receptacle delivery port	Reward dispenser port	ENV-303LP
Multiple tone generator	Circuit for generating tones from 1-20 kHz	ENV-223
Audio speaker	Plays the inputs from the tone generator	ENV-324W
Syringe pump	Pump for delivering reward to the port	PHM-100
House lamp	Lamp that lights up the cage	ENV-315W
PCI operating package	interface between software and hardware	MED-SYST-8
SmartCtrl 8 Input/16 Output Package	Controls devices in chamber	DIG-716P2

Performance in this task was quantified by the total time the animals spent in the port during the cued trials and the latency to enter the port after cue onset. Time in port was normalized both as a percentage of total reward availability time and also by subtracting the amount of time the animal spend in the port 30 s before cue onset. This means that CS-US associations were quantified by the animal responding both quickly and selectively to the cue. In addition, the time stamps of every head entry and head retraction into the port were recorded, which allowed the quantification of the dynamics of head entries during cue presentation and during the ITI. The dynamics of head entries during extinction were used to infer how the animal adapts it's behavioral response in the absence of an expected reinforce, i.e. whether it perform less head entries (indicating an update of sample-by-sample expectation), head entries that are just shorter in length (indicating a faster disengagement when confronted with unmatched expectations) or a combination of both. Finally, the average number of trials with responses per session and the probability of responding during a trial were also quantified. These variables indicated the likelihood that an animal would respond at all the CS and involves motivational state, strength of associative learning and cost-benefit decision making.

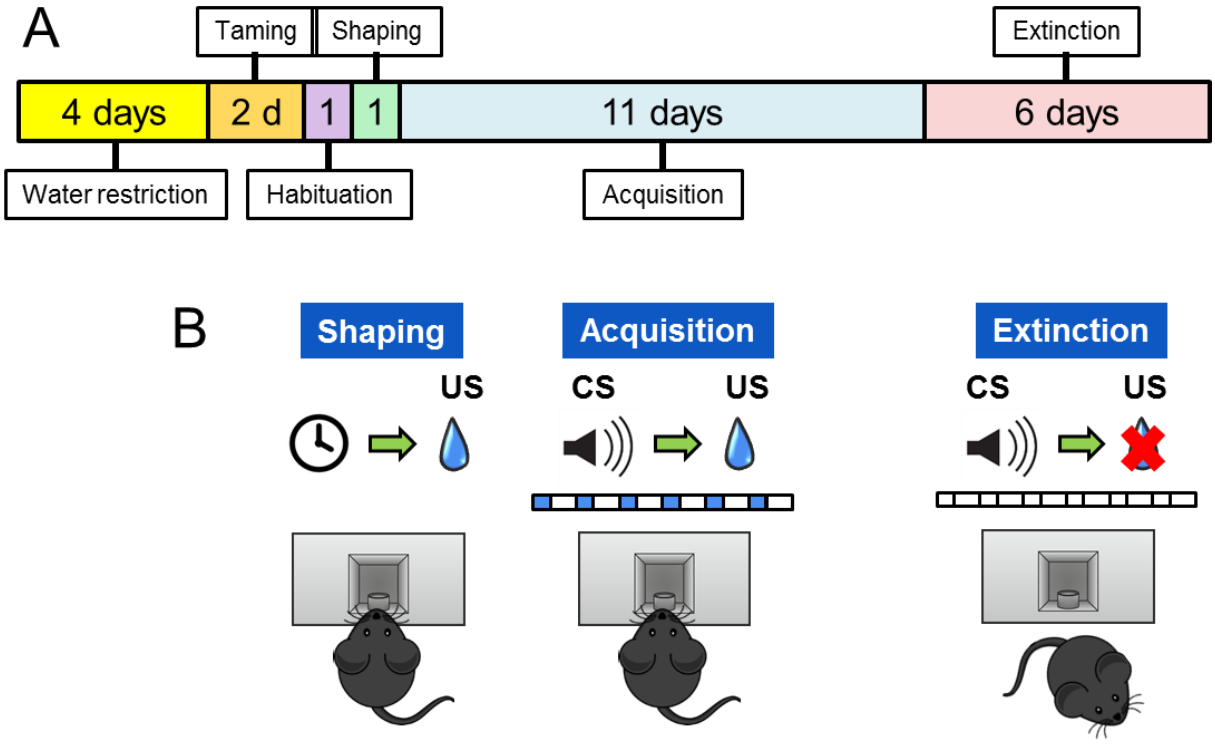

Figure 2.11. Experimental structure of the conditioning task.
A: Experimental timeline, spanning four days of water restriction (1-1.5 mL per day, ~80-85% of the initial body weight), two days of taming, one day of habituation in the chamber, one day of shaping reward seeking to the reward port, eleven days of conditioning acquisition and six days of extinction. B: Contingency of reward delivery for shaping, acquisition and extinction procedures. In shaping, the reward is delivered after a variable interval, with no predictive CS; this shapes the animal to seek reward in the port. In acquisition, an auditory CS signals the availability of the US; this conditions the animal to only seek reward when the cue is presented. In extinction, the CS is presented like in acquisition, but there is no longer reward delivery; this lead to a progressive reduction of CS responding and of reward seeking.

2.6.3. Open field

Spontaneous locomotor and exploratory activity (track length, wall distance, time in center and number of rearings) were evaluated in an open field arena (a lidless box measuring 52 × 52 cm, under red illumination at 3 lux; Figure 2.12) using a video tracking system (Viewer II, Biobserve, Germany) as described in a previous study from our group (Schiemann et al., 2012). This simple, but highly informative task allows the simultaneous evaluation of locomotion, exploration, anxiety and stress (Hall and S., 1934; Walsh and Cummins, 1976; Crawley, 1985; Bronikowski et al., 2001; Montiglio et al., 2010), and is a standard test for transgenic mouse phenotyping (Crawley, 2007; Wahlsten, 2010). Locomotor patterns can be extracted

from the patterns of velocity and movement tracks. Exploratory drive can be inferred from the temporal dynamics of movement tracks (mice tend to explore a novel environment more vigorously in the beginning of a session) and by the number and duration of spontaneous rearings (a stereotypical behavior in which the animal stands on its hind legs). Anxiety-related phenotypes are evaluated based on the proportion of time that an animal spends in the center of the arena, as mice with higher levels of anxiety tend to avoid this area more.

For a comprehensive phenotyping of mutant mice, the total track length, the proportion of bouts of activity (periods in which the velocity of the mouse exceeded 5 cm/s), the time spent and track length within the center area of the arena (defined as a 30x30 cm square zone with all sides equidistant from the walls), as well as the number and duration of rearings (recorded via infra-red beam breaks at a height of 4.5 cm, and defined by being at least 200 ms long and two subsequent rearings had to be at least 80 ms apart). After ten minutes, the animals were returned to their home cages for at least two minutes, and then subjected to the novel object recognition test.

2.6.4. Novel object recognition

A novel object exploration and preference task was used to assess the mice's preference recognition and preference for novel stimuli (Ennaceur and Delacour, 1988; Antunes and Biala, 2012). In this task, animals were placed in the same open field arena described in the previous section, after the open field test (which also served as a habituation for the novel object recognition test), but within the arena are two identical objects (stainless steel cylinders; 3 cm diameter x 6 cm height) placed at equal lengths from each other and at 15 cm from the upper left and right corners (Figure 2.12). The animals were allowed to freely explore the arena and the objects for 10 minutes, after which they were removed from the arena. Subsequently, one of the objects was replaced by a different, novel object (plastic coated rectangular prism; 3x3 cm base x 6 cm height), and the animals were again allowed to explore the arena and the objects. Object recognition was analyzed using a dedicated Biobserve plugin, and object interaction events were defined as periods in which a mouse was directly facing the object (snout directed to the object within a 180° angle)

at a distance shorter than 3 cm. Both the number and duration of these interaction events were quantified for both trials of the task.

Differences between exploration of two similar objects in trial 1and between an already explored (old) and novel (new) object in trial 2, were analyzed. For the quantification of novel object discrimination, I calculated a discrimination index (DI; Equation 2.5) by dividing the difference between the time spent exploring the novel object and the time spent exploring the familiar object by the sum of these two measures (Ennaceur and Delacour, 1988; Antunes and Biala, 2012). This test evaluates how much the mice prefer to explore a new object in relation to one that is already familiar, a critical, dopamine dependent behavioral phenomenon which can be related to memory, sensory recognition, foraging and exploration strategies (Besheer et al., 1999; Belcher et al., 2008; Rossato et al., 2013).

Equation 2.5. Discrimination index for novel object recognition.

$$DI = \frac{T_{New} - T_{Old}}{T_{New} + T_{Old}}$$

where

DI = discrimination index

T_{New} = time spent exploring the novel object

T_{Old} = time spent exploring the familiar object

2.6.5. Hole-board

Exploration of holes, a naturalistic behavior for mice, was evaluated with the hole board task (Nolan and Parkes, 1973; Crawley, 2007). In this task, mice were put in an open field arena similar to the one used for the open field test, but with 4 to 16 circular holes (2 cm in diameter) on its floor (Actimot2, TSE systems; Figure 2.12). When confronted with such an arena, mice tend to spontaneously check the holes by dipping their heads in them. The performance of head dips was recorded with infra-red beam breaks placed immediately under the inferior surface of the floor board. The latency to the first head dip, as well as the total number and duration of head dips, were quantified. The percentage of repeated head dips (two dips performed

sequentially into the same hole) as well as the percentage of dips into the preferred hole (the hole that was most explored during the session) were also quantified and compared between genotypes. In addition to capturing the dynamics of unreinforced hole exploration, this behavior is used as a measure of anxiety, exploratory drive and neophilia (Nolan and Parkes, 1973; File and Wardill, 1975; Crawley, 1985, 2007; Takeda et al., 1998).

2.6.6. Spontaneous alternation in the plus maze

Working memory is the capacity of an animal to temporarily store recently acquired information in order to guide ongoing behavior. Working memory performance was quantified between genotypes using the spontaneous alternation in the plus maze (Figure 2.12), where the animals explore a maze with four walled arms (Ragozzino et al., 1996). In this setting, animals with normal working memory tend to explore each arm in an interleaved fashion (in alternation), avoiding exploration of an arm that has already been explored recently. This strategy requires keeping track of the recently explored arms in working memory (Ragozzino et al., 1996; Lennartz, 2008). Mice were placed in a plastic plus maze (four equidistant 35 x 4.5 cm arms radiating at 90° angles from a circular central arena with 10 cm diameter; walls are 15 cm in height) and allowed free exploration for 12 minutes (Lennartz, 2008). An arm entry was defined as when the animal enters an arm with all its four paws. Each session was recorded with a video camera and quantification of arm entries was made through visual analysis of the videos. A spontaneous alternation was marked when the animal explored four different arms in five consecutive arm entries, and the proportion of spontaneous alternations was quantified as the number of real alternations divided by the total possible number of alternations (sum of all arm entries minus four); chance performance in this task is calculated to be 44% (Ragozzino et al., 1996; Lennartz, 2008).

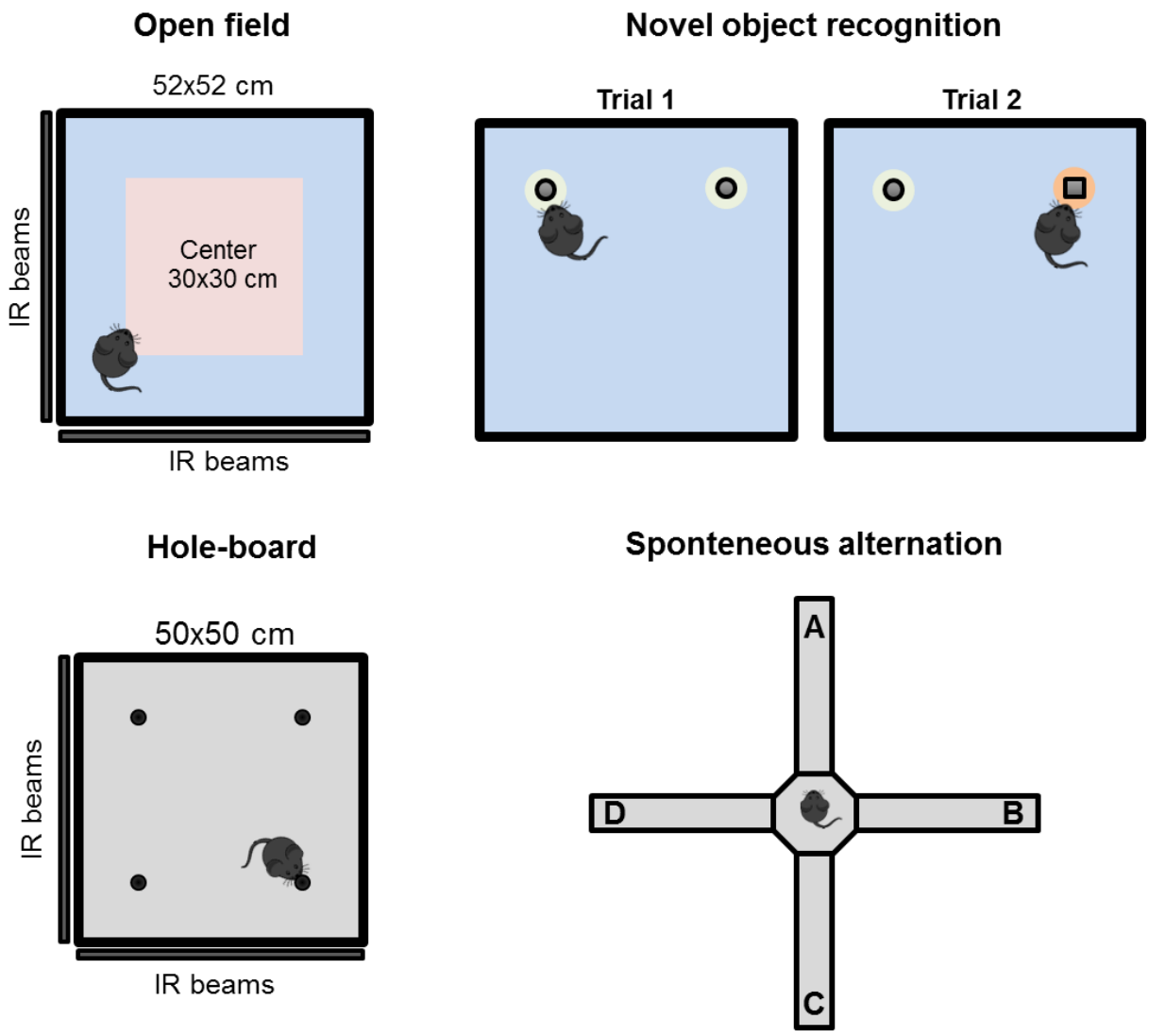

Figure 2.12. Behavioral tests used to assess untrained behaviors in transgenic and WT mice. In order from left to right: the open field arena, trial structure of the novel object recognition, hole-board arena, plus maze for the spontaneous alternation test. Note the novel object recognition test was performed in the same arena as the open field.

2.7. Fitting behavioral data with a modified Rescorla-Wagner model

A modified Rescorla-Wagner model (Equation 2.6) was used in order to formally quantify differences in learning from negative prediction errors during the conditioning task in KChIP4-Exd and DAT-cre KI genotype groups. Similar methods have been previously used in the literature for quantifying the consequences of LHb lesions on mouse appetitive learning and the effects of DAT variants in human fear conditioning (Raczka et al., 2011; Tian and Uchida, 2015). The Rescorla-Wagner model also has the advantages of being trial-based, thus matching my task structure, and not assuming that DA prediction errors are necessarily coding for differences in

subjective value, which is the most general interpretation of DA function (Rescorla and Wagner, 1972; Sharpe et al., 2017).

All modelling and fitting was done with custom MatLab® code. In the conventional Rescorla-Wagner model, a single learning rate is assumed for both positive and negative prediction error updates of the associative strength *V* (Rescorla and Wagner, 1972). In the modified version applied in this study, two learning rates are used, α_P and α_N, representing learning from positive and negative prediction errors, respectively, and a conditional statement is applied that makes α_P be used when there is positive prediction error-based learning and α_N when there is negative prediction error-based learning. Of note, in the original version of the model there is also a secondary learning rate variable β that reflects the salience and intensity of the CS (Rescorla and Wagner, 1972), but as only a single CS with constant intensity was used, this variable was not incorporated into the model in this study, as has been common practice in previous studies (Raczka et al., 2011; Tian and Uchida, 2015).

In the task used in this study, mice underwent 110 trials of acquisition on a fixed rate schedule (only positive prediction errors) and 60 trials of extinction (only negative prediction errors). The percentage of time in port metric was assumed to be a linear read-out of t *V*. The limits of *V* in relation to the empirical data are the initial value of *V* before the task (V_0) the lower and upper limits of associative strength readout (V_{min} and V_{max}, respectively). These parameters were derived empirically from each animal, with V_0 being set as the average response in the first three trials of acquisition, and V_{min} and V_{max} being set as the average responses in the last two sessions of acquisition and extinction, respectively. Modelling was performed by running the prediction error contingencies of the task with different combinations of α_P and α_N (each varying independently from 1 to 0.001). Once all possible learning curves were generated, the models were fitted to the experimental data of each individual mouse with the least absolute residuals method (Narula and Wellington, 1982), i.e. by identifying which combination of α_P and α_N produced the learning curve that had the lowest mean difference in relation to the experimental data. Searching of optimal parameters was performed using the *fminsearch* MatLab® function, i.e. the Nelder-Mead simplex algorithm, which iteratively improves upon an initial guess of function variables until it achieves the lowest possible target output (Lagarias et al., 1998; Tian and Uchida, 2015). In the case of this study, the algorithm optimized the

values of α_P and α_N (the initial guess was set at 0.3 for both variables) and target was to achieve the lowest possible absolute residuals in relation to the experimental data. Goodness of fit is inferred from the residual values of the optimal fit for each animal, and as a proof of principle, experimental data was fitted using the same method but using only one learning rate across acquisition and extinction (conventional Rescorla-Wagner model) and the results of each form of fitting were compared for both genotype groups.

Equation 2.6. Modified Rescorla-Wagner model.

$$if\ (R - V_n)\ \geq 0\ [positive\ RPE]$$

$$V_{n+1} = V_n + \boldsymbol{\alpha_P}(R - V_n)$$

$$if\ (R - V_n) < 0\ [negative\ RPE]$$

$$V_{n+1} = V_n + \boldsymbol{\alpha_N}(R - V_n)$$

where

V = associative strength between CS and US

α_P and α_N = learning rates from positive and negative prediction errors, respectively

R = maximal associative strength of the US (reward value)

n = trial index

2.8. Semi-quantitative IHC of Kv4.3 channels

In order to visualize how KChIP4-DAT-Ex3d affects the expression patterns of Kv4.3 pore-forming sub-units, I performed semi-quantitative IHC to detect and quantify immunolabeling signals of these proteins in the dopaminergic midbrain (Subramaniam et al., 2014a). Both CTRL (N = 3) and Ex3d (N = 3) mice which underwent behavioral characterization experiments were used. They were perfused and their brains fixed as described for the histological identification of neurobiotin labeled cells (section 2.5.3.). For immunolabeling of Kv4.3, slices were washed in

PBS, incubated with blocking solution, and then incubated overnight with carrier solution with anti-Kv4.3 rabbit (1:1000) and anti-TH mouse (1:1000) primary antibodies. After this stage, slices were washed with PBS, then incubated overnight again in carrier solution with anti-rabbit 568 (1:750) and anti-mouse 488 (1:750) secondary antibodies. Slices were then washed and mounted on slides as previously described in section 2.5.3.

For acquisition of immunolabeling signals, slices were imaged under a confocal microscope with the 568 and 488 laser/filter settings. One representative slice, roughly corresponding to the position of -3.08 mm from bregma, was chosen for each immunolabeling group per animal and five images were acquired per slice using the 60x objective. Signals for each channel were averaged 4 times to reduce background noise. Two images were acquired of the VTA and three were acquired of the SN (Figure 2.13 A), with relative positions chosen to cover the approximate extent of both regions. Images were acquired with a 1.1 airy unit (AU) pinhole setting, no offset was applied and laser intensity and gain was fixed for each signal channel (Table 2.6.). Digital images were saved as multi-channel 32-bit RGB tagged image files (tiff).

Acquired images underwent processing with an algorithm (Figure 2.13 B) defined with custom macro scripts written for ImageJ (https://imagej.nih.gov/ij/). The algorithm was: 1) each image was converted to an 8-bit format; 2) The TH channel image was then thresholded using the isodata algorithm (Ridler and Calvard, 1978), which applies an iterative procedure that finds a threshold that is immediately above the composite average of the image's signal intensity; 3) the thresholded TH channel was used to create a mask, defining each region of contiguous TH as a region of interest (ROI); 4) the TH mask was overlaid on the Kv4.3 or KChIP4 signal image, and the average bit intensity (ranging from 0 to 255) was measured for each co-localized TH ROIs. Signal intensity values in ROIs were pooled across anatomical regions and genotypes for statistical comparison.

Table 2.6. Confocal laser intensity settings used for semi-quantitative IHC.

Signal channel	Laser wavelength (nm)	Intensity (%)	Detector gain
TH	488	3.2	60
Kv4.3	568	12.6	80

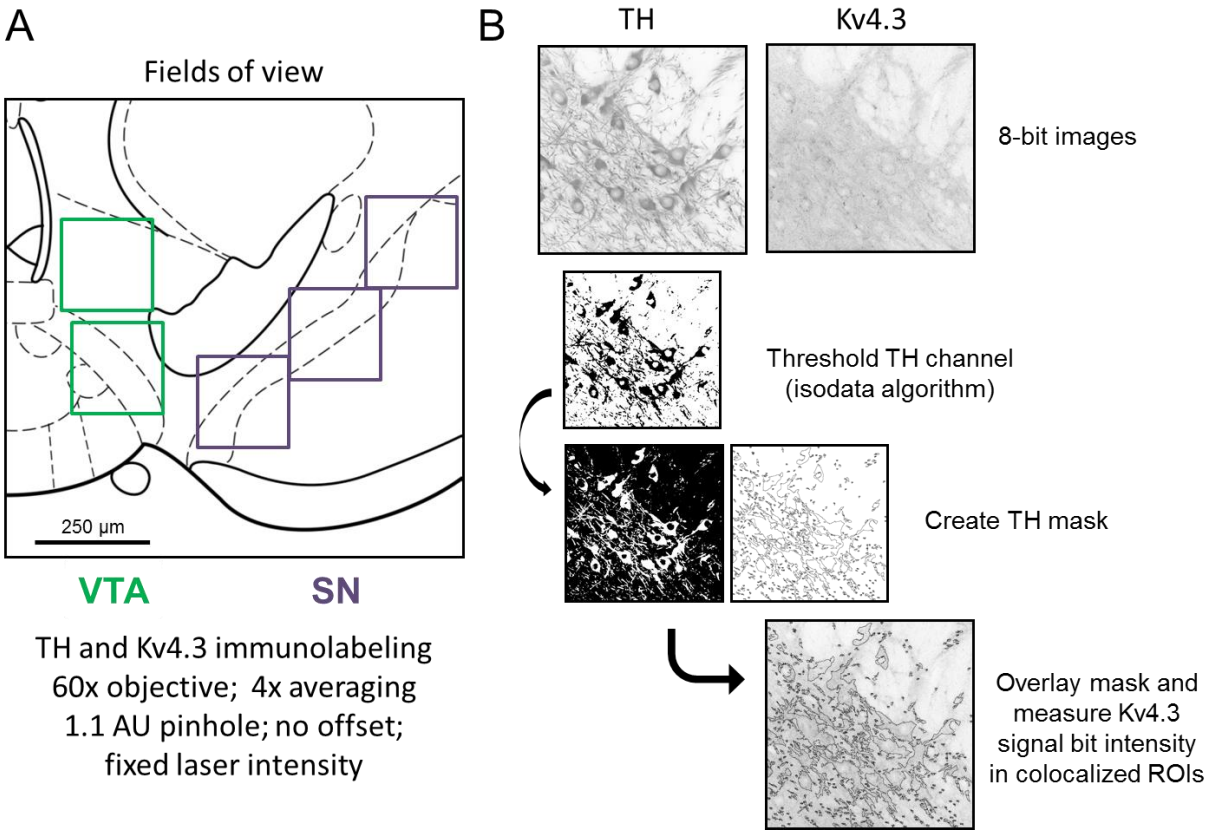

Figure 2.13. Semi-quantitative IHC: image acquisition and analysis.
This process exemplifies the method used for extracting channel immunolabeling intensities in co-localized TH ROIs, as was also applied to the KChIP4 immunolabeling group. A: approximate locations of the acquired fields of view for all slices (Franklin and Paxinos, 2012). B: algorithm used for extracting Kv4.3 signal intensities in co-localized TH ROIs.

2.9. Statistical analyses

For all two-group comparisons, data were tested for normality with the Kolmogorov-Smirnov test. If all distributions were Gaussian, differences were analyzed using two-tailed T-tests. In case where one or both of the distributions were non-Gaussian, differences were tested using the non-parametric two-tailed Mann-Whitney tests. Differences in categorical variables between two groups were evaluated with the Chi-square test. Paired T-tests or Mann Whitney tests were used in the cases were the same groups were analyzed in different conditions. Comparisons between groups over multiple trials or sessions were evaluated with two-way repeated measures ANOVA and Sisak's multiple comparisons *post-hoc* tests. Statistical significance was set at $P < 0.05$ for all comparisons.

3. Results

3.1. Effects of KChIP4 KO on in vivo dopamine neuron activity

3.1.1. Anatomical distribution of recorded cells

I recorded and successfully reconstructed a total of 86 immunohistochemically identified DA neurons (Figure 3.1 and 3.2). They were recorded both in the SN of WT mice (n = 26 cells, N = 15 mice) and KChIP4 KO mice (n = 24 cells, N = 8 mice) and the VTA of WT (n = 18 cells, N = 13 mice) and KChIP4 KO (n = 18 cells, N = 8 mice) animals. The cells were distributed across nearly the entire extent of each region, with the exception of the most medial sections (up to 250 µm from midline) of the VTA (Figure 3.2). On the rostro-caudal axis, cells were located in a range between -2.9 to -3.6 mm from bregma. For visual representations, I displayed the rostral-caudal axis to the one where most cells were located (- 3.16 mm from bregma).

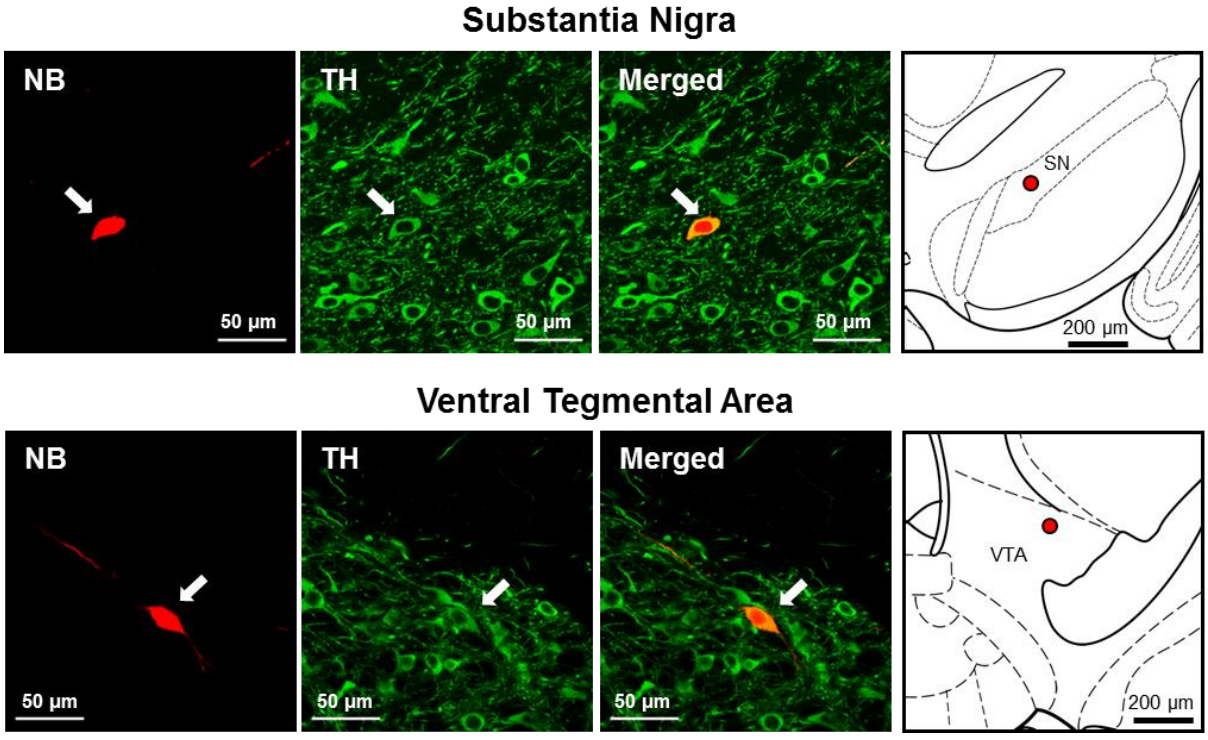

Figure 3.1. Example of a histological identification and anatomical positioning of recorded DA neurons in the SN and VTA.
Neurobiotin (red) identified cells co-localized with TH immunolabeling (green) in the SN and VTA and their mapping onto the anatomical coordinates of the mouse brain atlas (Franklin and Paxinos, 2012).

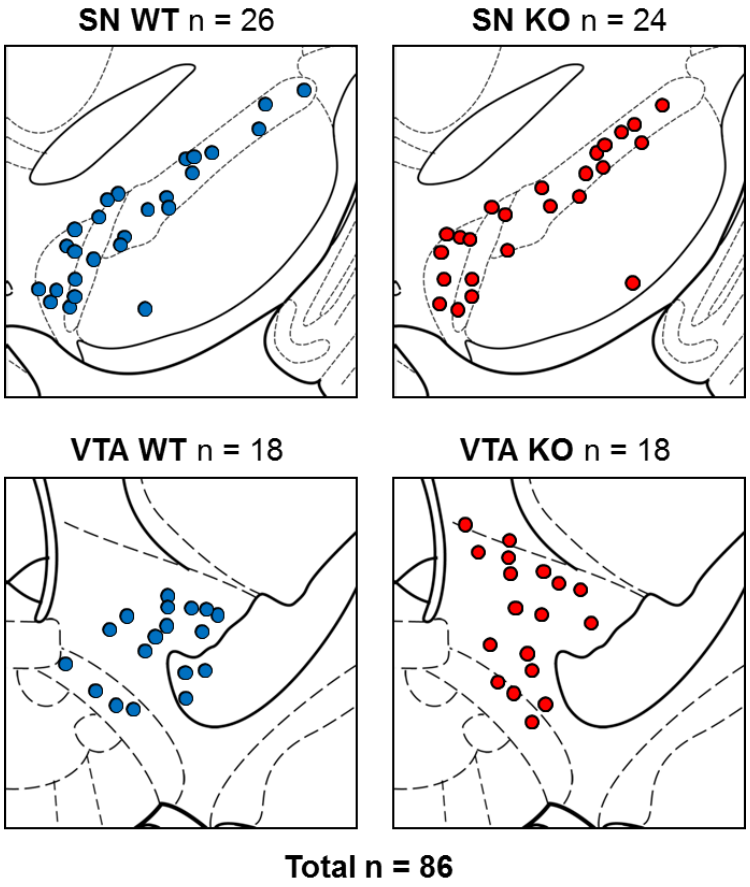

Figure 3.2. Anatomical localization of *in vivo* recorded DA neurons.
All *in vivo* recorded and histologically identified DA neurons in the SN and VTA of KChIP4 KO and WT mice collected in this study.

3.1.2. Firing frequency, ISI variability, bursting and ACH patterns of midbrain dopamine neurons are not changed in KChIP4 KO mice

I found that the average firing frequency (Figure 3.3 A), CV (Figure 3.3 B) and SFB (Figure 3.4) were not significantly different between KChIP4 KO and WT mice, neither in SN nor in VTA. Similarly, the statistics of bursting activity, analyzed within neurons that had at least 5% of their spikes fired within bursts, was not different in SN and VTA DA neurons between KChIP4 KO and WT mice. The number of neurons that felt within this criterion was 12 for the SN WT group, 14 for the SN KO group, 8 for the VTA WT group and 8 for the VTA KO group. This was true for the mean, minimum and maximum intra-burst frequencies and durations of bursts (Figure 3.5). I also found no significant differences in the average number of spikes within each burst and the proportion of bursts with two (doublets), three (triplets) or more than three spikes (Figure 3.6). The proportion of ACH-based firing patterns (Figure 3.7) was also not significantly different between KChIP4 KO and WT mice. All groups displayed at least one of each firing pattern.

Interestingly, VTA DA neurons in KChIP4 KO mice had longer AP widths than WT VTA DA neurons by approximately 10% (Figure 3.8 A, Mann Whitney test; P < 0.05). This difference was due, on average, to a prolonging of the repolarization phase (Figure 3.8 B), indicating that this effect is consistent with changes in repolarizing K^+ currents. No difference was observed in SN DA neuron AP width between the two genotypes.

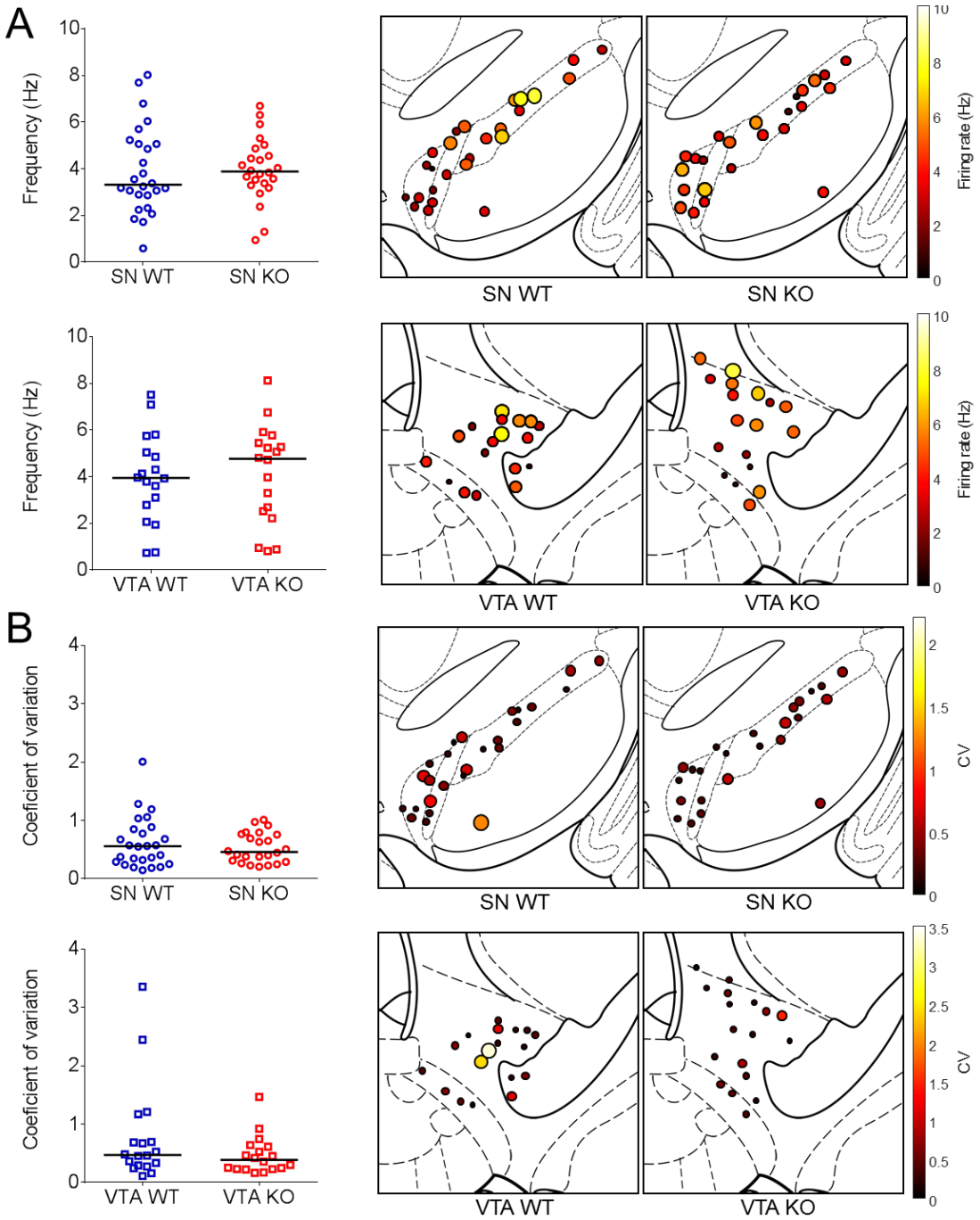

Figure 3.3. KChIP4 KO does not affect firing frequency and CV of DA neurons.
Data from SN and VTA DA neurons in WT and KO mice. Note that there was no significant difference observed between any of the groups (Mann Whitney tests, *P* > 0.05). A: Mean firing frequency. B: CV.

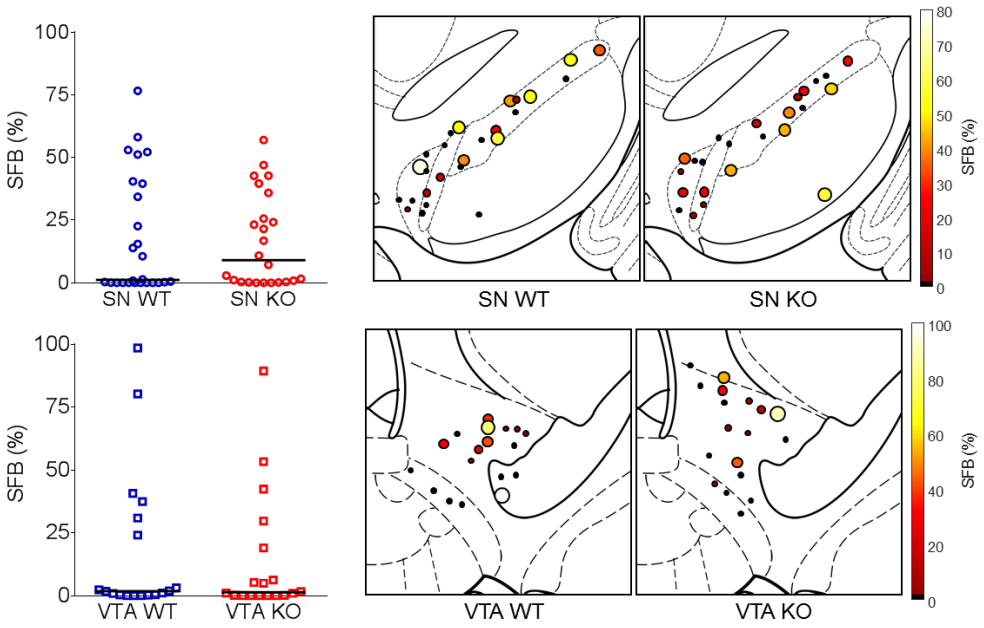

Figure 3.4. KChIP4 KO does not change the percentage of SFB in DA neurons. Percentage of Spikes fired in bursts in SN and VTA DA neurons in WT and KO mice. No significant difference was observed between the groups (Mann Whitney tests, $P > 0.05$).

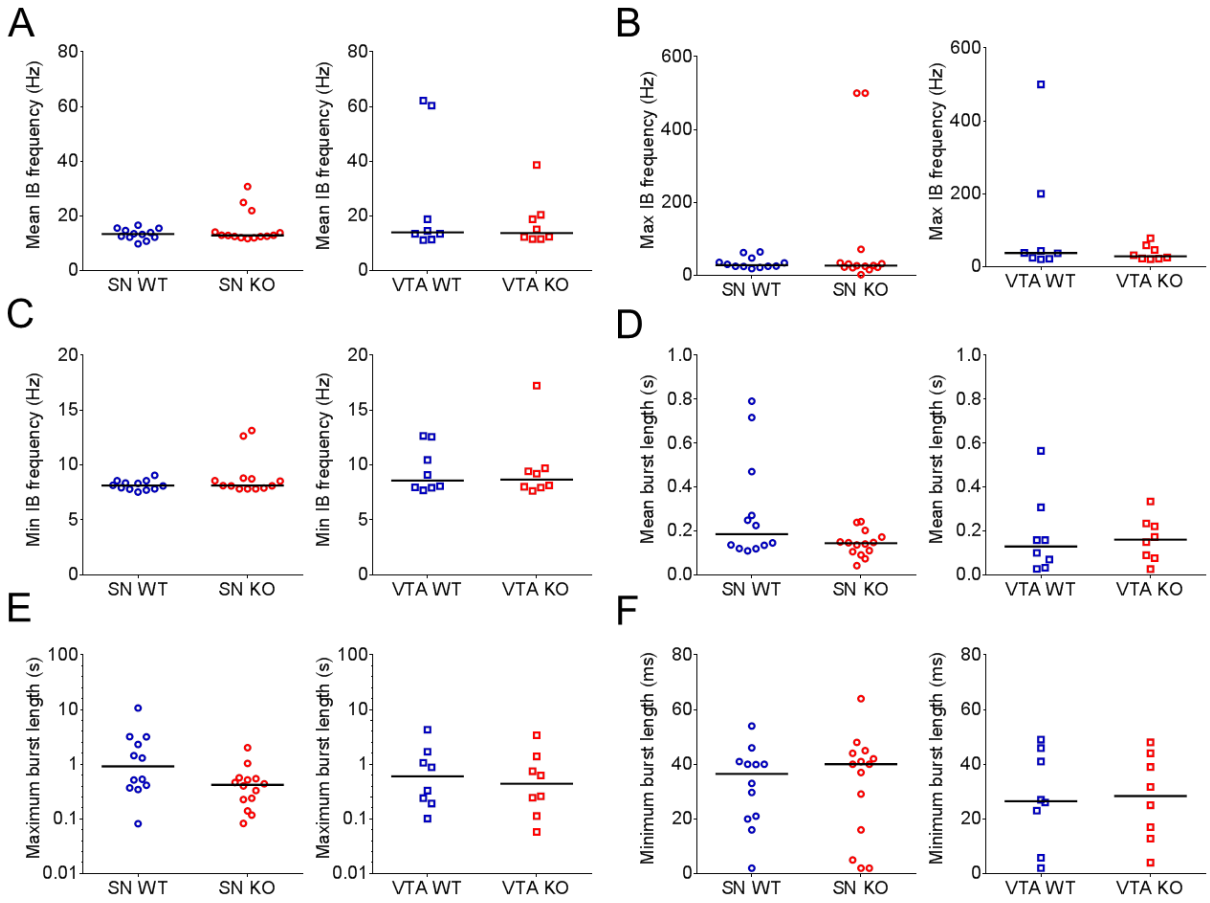

Figure 3.5. KChIP4 KO does not affect intra-burst frequency of *in vivo* recorded DA neurons. Only neurons with >5% SFB were analyzed. No significant difference was observed between any of the groups (Mann Whitney tests, $P > 0.05$). A: Mean intraburst frequency. B: maximum intraburst frequency. C: minimum intraburst frequency. D: mean burst length. E: maximum burst length. F: minimum burst length.

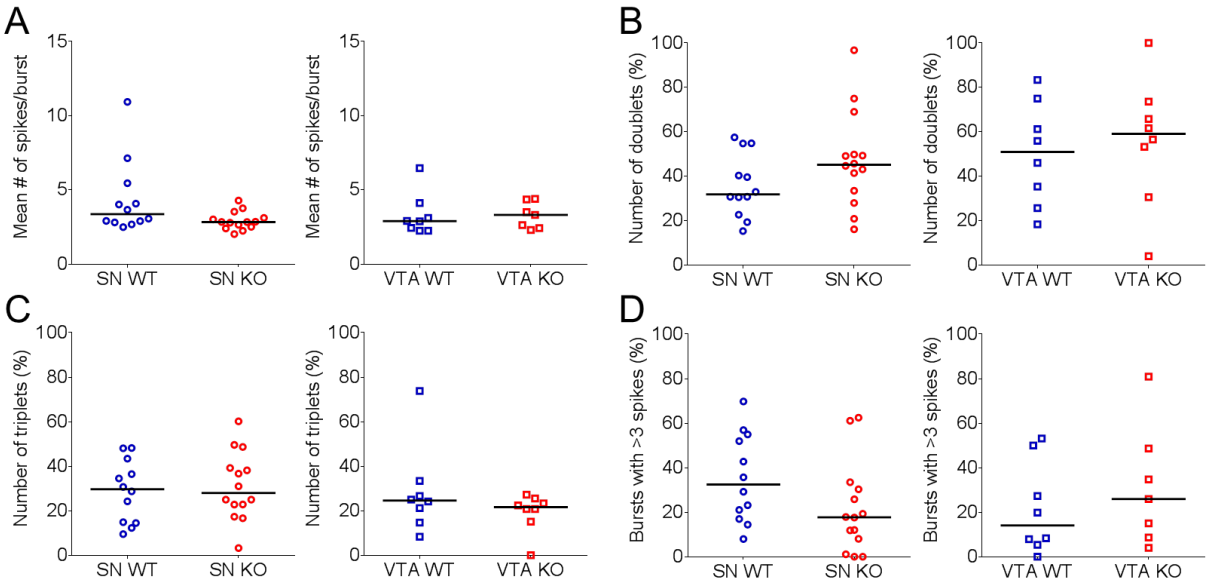

Figure 3.6. KChIP4 KO does not affect intra-burst spikes of *in vivo* recorded DA neurons. Data from SN and VTA DA neurons in WT and KO mice that had >5% of SFB. Note that there was no significant difference observed between any of the groups (Mann Whitney tests, $P > 0.05$). A: Mean number of spikes per burst. B: Proportion of bursts with two spikes (doublets). C: Proportion of bursts with three spikes (triplets). D: Proportion of bursts with more than three spikes.

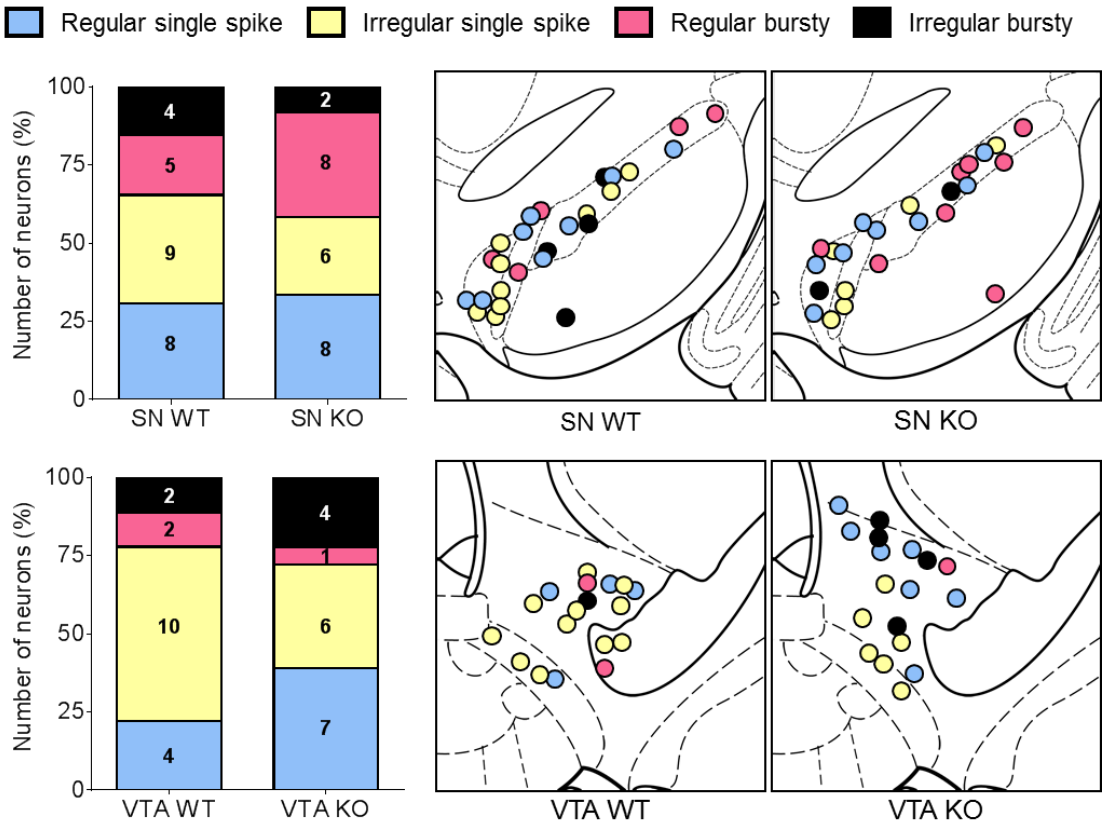

Figure 3.7. KChIP4 KO does not affect ACH-based spike pattern distributions. Proportion and number (graph overlay) of regular single spike, irregular single spike, regular bursty and irregular bursty firing patterns in SN and VTA DA neurons in WT and KO mice, as well as their approximate anatomical mapping in the midbrain.

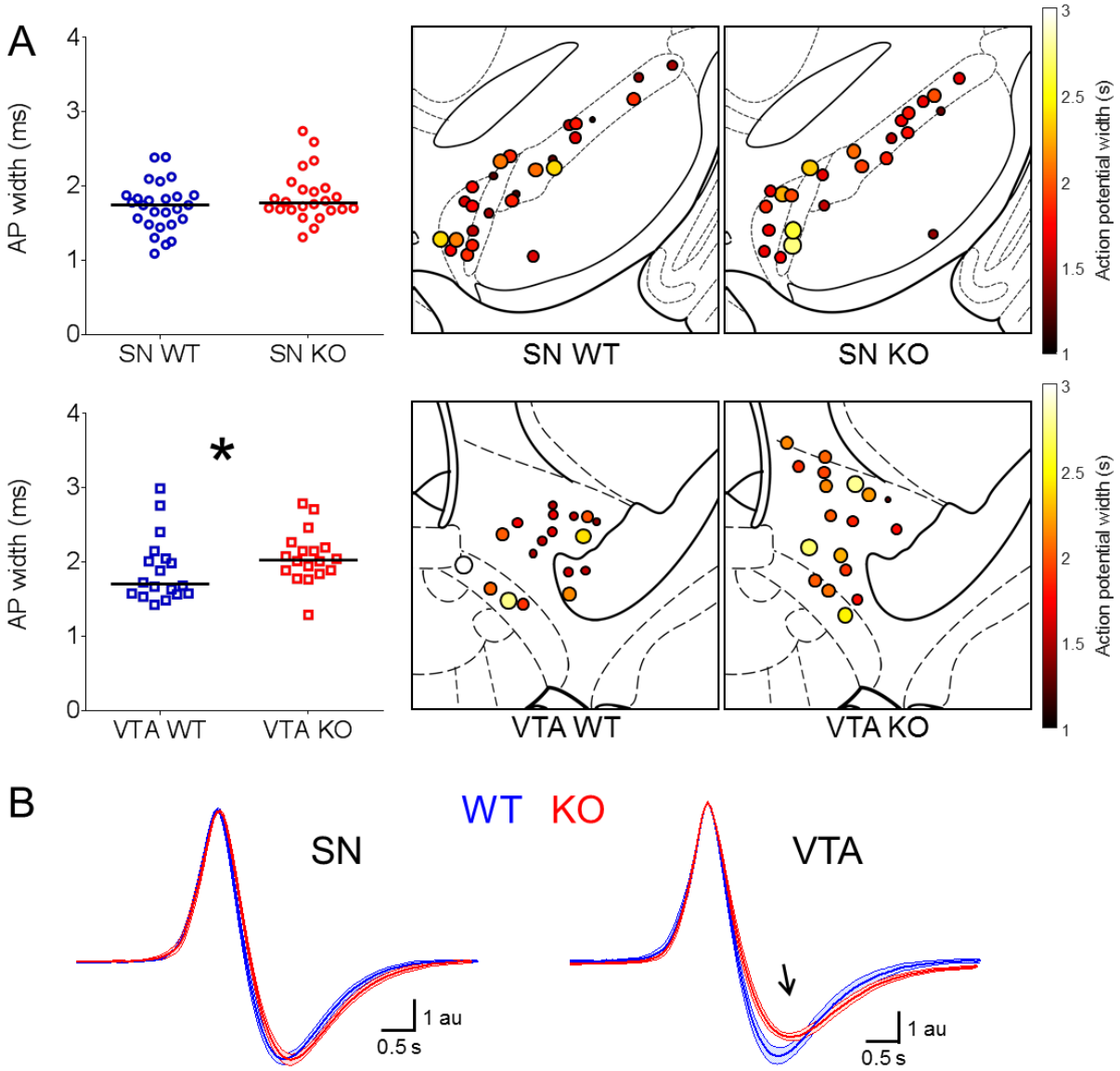

Figure 3.8. KChIP4 KO increases AP width in VTA DA neurons.
A: AP width of DA neurons in the SN and VTA of KChIP4 KO and WT mice. Note the significant genotype difference between VTA, but not SN, DA neurons. B: Averaged AP waveforms from DA neurons in the SN and VTA of KChIP4 KO and WT mice. Overlaid areas indicate SEM. Note that KChIP4 KO VTA DA neurons are similar to WT neurons during depolarization, but display longer repolarization phases. *$P < 0.05$

3.1.3. KChIP4 KO selectively changes the ISI distribution and decreases the number and duration of spontaneous firing pauses in VTA DA neurons

When analyzing the recordings, it was already visually noticeable that spontaneous pauses in firing where either smaller or absent in VTA DA neurons of KChIP4 KO mice, in comparison to the other groups (Figure 3.9). In order to quantify this phenomenon, I first compared the maximum ISI for each cell between groups

(Figure 3.10). I found that the maximum ISI in VTA DA neurons of KChIP4 KO mice were approximately 75% shorter than in VTA DA neurons of WT mice (Figure 3.10 A; Mann Whitney test, $P < 0.05$). This was not a secondary effect of a change in firing rate, as the genotype difference of the maximum/mean ISI ratio in VTA DA neurons was also significantly different, with this measure being approximately 50% shorter in KO VTA DA neurons (Figure 3.10 B; Mann Whitney test; $P < 0.01$). Importantly, I found no difference in these measures in SN DA neurons between the tested genotypes. In addition, the minimum ISIs of VTA and SN DA neurons were similar for both genotypes (Figure 3.11, Mann Whitney test; $P > 0.05$), suggesting that KChIP4 KO created a one-sided change in the ISI range of VTA DA neurons.

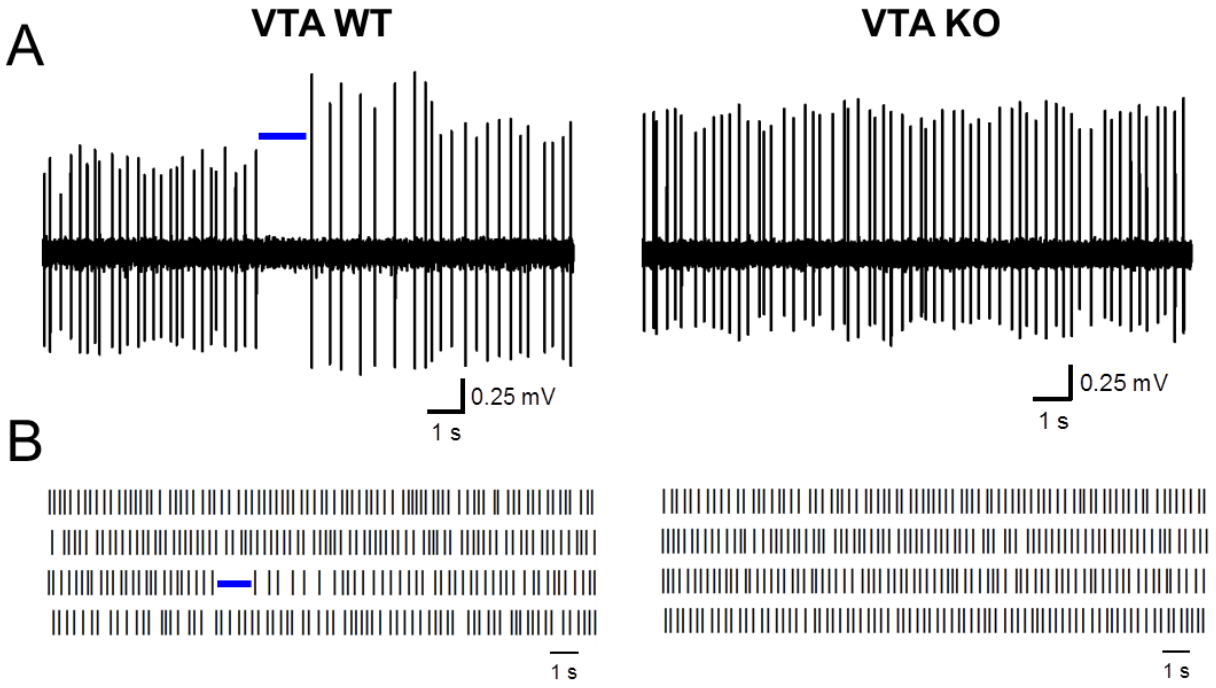

Figure 3.9. KChIP4 KO affects visually identified pauses in VTA DA neuron spike trains.
A: example recording traces showing a spontaneous pause in a WT VTA DA neuron, and continuous pacemaker firing in the KO VTA DA neuron. These are representations of the pauses that are observed in WT spike trains, and that seemed absent or greatly reduced in the KO. B: raster plots showing the pause and the pacemaker firing exemplified in panel A within the context of the neuronal spike train.

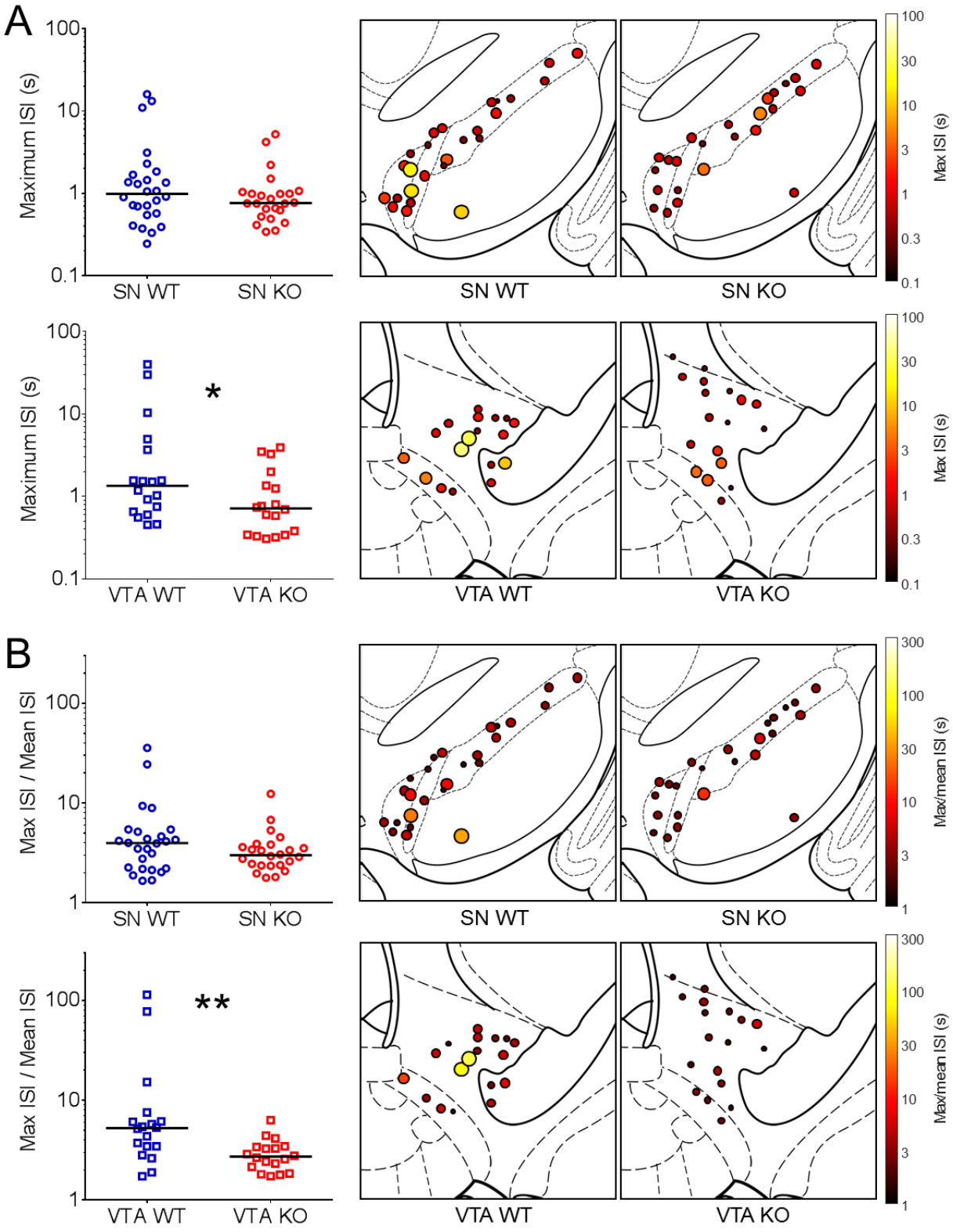

Figure 3.10. KChIP4 KO selectively reduces the maximum ISI range in VTA DA neurons. Data from SN and VTA DA neurons in WT and KO mice. A: Maximum ISI. B: Maximum/mean ISI ratio. Note the significant genotype difference in VTA, but not SN, DA neurons for both variables. *$P < 0.05$; **$P < 0.01$.

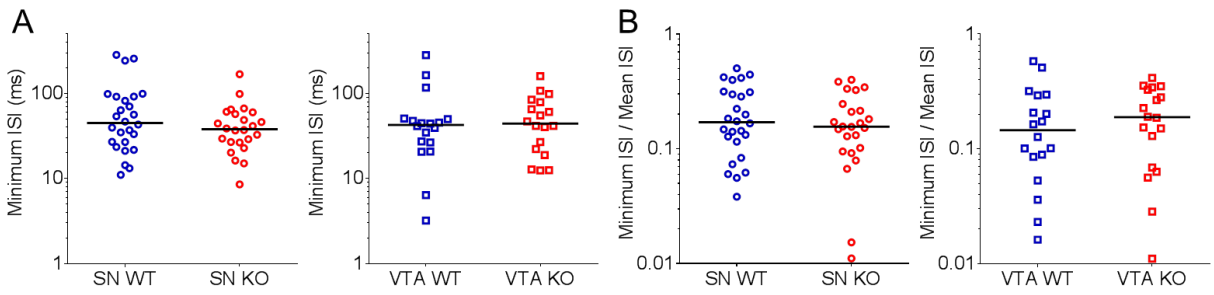

Figure 3.11. KChIP4 KO does not affect the minimum ISI range of DA neurons.
Data from SN and VTA DA neurons in WT and KO mice. Note that there was no significant difference observed between any of the groups for both variables (Mann Whitney tests, $P > 0.05$). A: Minimum ISI. B: Minimum/mean ISI ratio.

In order to quantify these changes in ISI distribution, I analyzed the skewness and kurtosis of the ISI distributions from the recorded neurons. In VTA DA neurons of KChIP4 KO mice, the skewness of the ISI distribution was reduced by approximately 50% in comparison to WT mice (Figure 3.12 A; Mann Whitney test; $P < 0.01$), i.e. their ISI distributions were more symmetrical compared to controls. An interesting observation was that out of all recorded SN and VTA DA neurons, only 3 out of 86 (≈3.5%; 1 neuron each in the SN KO, VTA KO and VTA WT groups) had negative skewness, which implies that the ISI distributions of midbrain DA neurons are predominantly skewed towards positive values, i.e. that longer ISIs have a wider range of variation than shorter ISIs. The distribution of ISIs in VTA DA neurons of KChIP4 KO mice had dramatically lower values of kurtosis in relation to WT mice. Not only were the median values of kurtosis in these neurons nearly 60% lower in KChIP4 KO mice (Figure 3.12 B; Mann Whitney test; $P < 0.001$), but the maximum range of this measure was in KChIP4 KO mice was less than 1% than the maximum range in WT controls (832.3 in WT versus 6.25 in KChIP KO). These differences were visible in the ISI distributions of the recorded neurons, with smaller shifts to the right, higher symmetry and lower frequencies of outliers (shorter “tails”) in the ISI distributions in KO VTA DA neurons in relation to WT (Figure 3.13). This demonstrates that KChIP4 KO severely restricts the number of extreme deviations in ISI values (long pauses) in VTA DA neurons. Importantly, these genotype differences were not observed in SN VTA neurons, confirming the selective nature of the changes induced by KChIP4 KO.

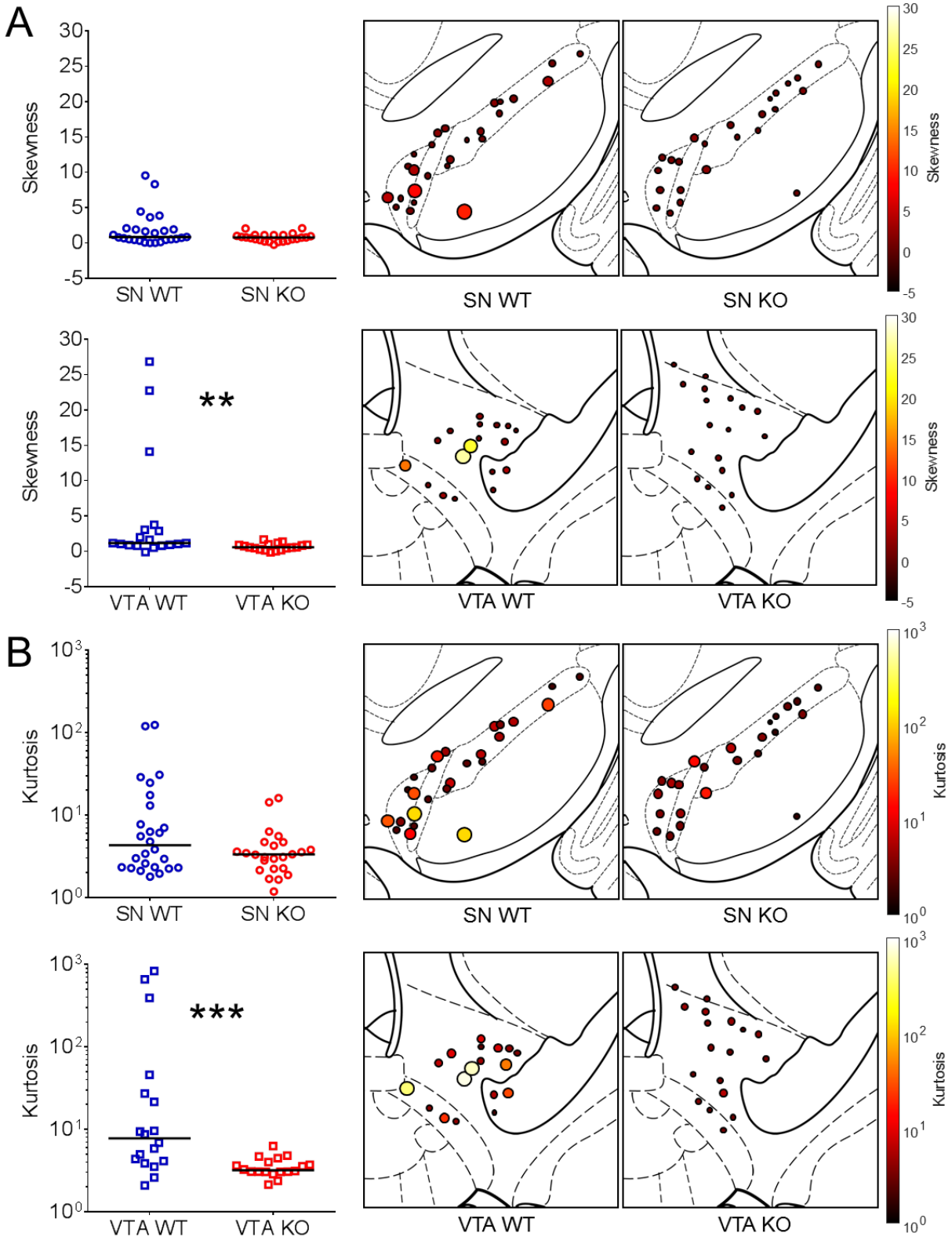

Figure 3.12. KChIP4 KO selectively reduces the skewness and kurtosis of VTA DA neuron ISI distributions.

Data from SN and VTA DA neurons in WT and KO mice. A: Skewness. B: Kurtosis. Note the significant genotype difference in VTA, but not SN, DA neurons for both variables. $^{**}P < 0.01$; $^{***}P < 0.001$.

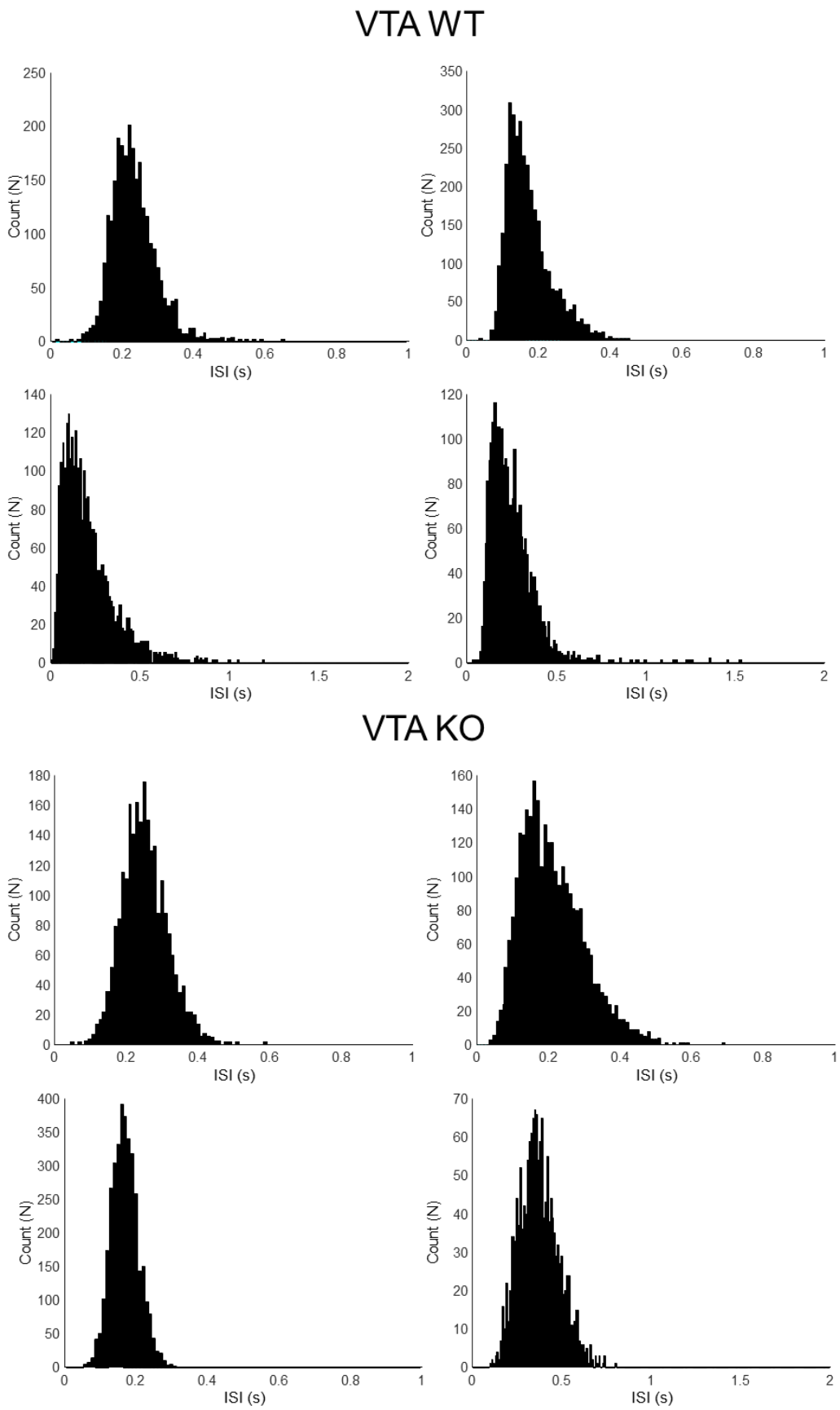

Figure 3.13. Example ISI histograms of SN and VTA DA neurons in WT and KO mice.
Note the smaller shift to the right, higher symmetry and lower frequency of outliers (shorter "tails") in ISI distributions in KO VTA DA neurons in relation to WT. Also note the different axes scales, adjusted to allow the visualization of the long tails in WT VTA neurons.

Building upon these results, I analyzed pauses identified with the RGS method in the recorded spike trains (Figures 3.14 and 3.15). I found that the proportion of neurons without any RGS-identified pauses was almost five-fold higher in VTA DA neurons of KChIP4 KO mice in relation to WT controls (Figure 3.15; Chi-square test, $P < 0.05$). The number (Figure 3.16 A; Mann Whitney test, $P < 0.05$) and duration (Figure 3.16 B; Mann Whitney test, $P < 0.05$) of RGS-identified pauses were also approximately 95% (from a median of 1.25 to 0.05 pauses/minute) and 65% (from a median to 1.2 to 0.35 seconds) lower in VTA DA neurons in KChIP4 KO mice in relation to WT, respectively. It is noticeable, however, that the number of RGS-identified pauses varied widely between cells. In addition, I found no difference in any measure of RGS-identified pauses in SN DA neurons between the tested genotypes.

Finally, I used an outlier detection algorithm to quantify pauses in spike trains. Pauses that were preceded by bursts were not included in the analysis, in order to select for putative inhibitory pauses (Figures 3.17 and 3.18). I found that the proportion of VTA DA neurons without any outlier pause was also higher in the KChIP4 KO genotype, by approximately four-fold (Chi-square test, $P < 0.05$; Figure 3.18). The number (Mann Whitney test, $P < 0.05$) and duration (Mann Whitney test, $P < 0.05$) of these pauses were also significantly lower in VTA DA neurons of KChIP4 KO (Figure 3.19), with the median number of pauses per minute being reduced from ≈0.65 (WT) to 0 (KO) and the duration of pauses being reduced from ≈0.7 (WT) seconds to 0 (KO). I found no difference in any measure of outlier-identified pauses in SN DA neurons between the tested genotypes. As an important control, there was no difference in post-burst pauses between the genotypes (Figure 3.20), confirming that the KChIP4 KO effect was selective for putative inhibitory pauses.

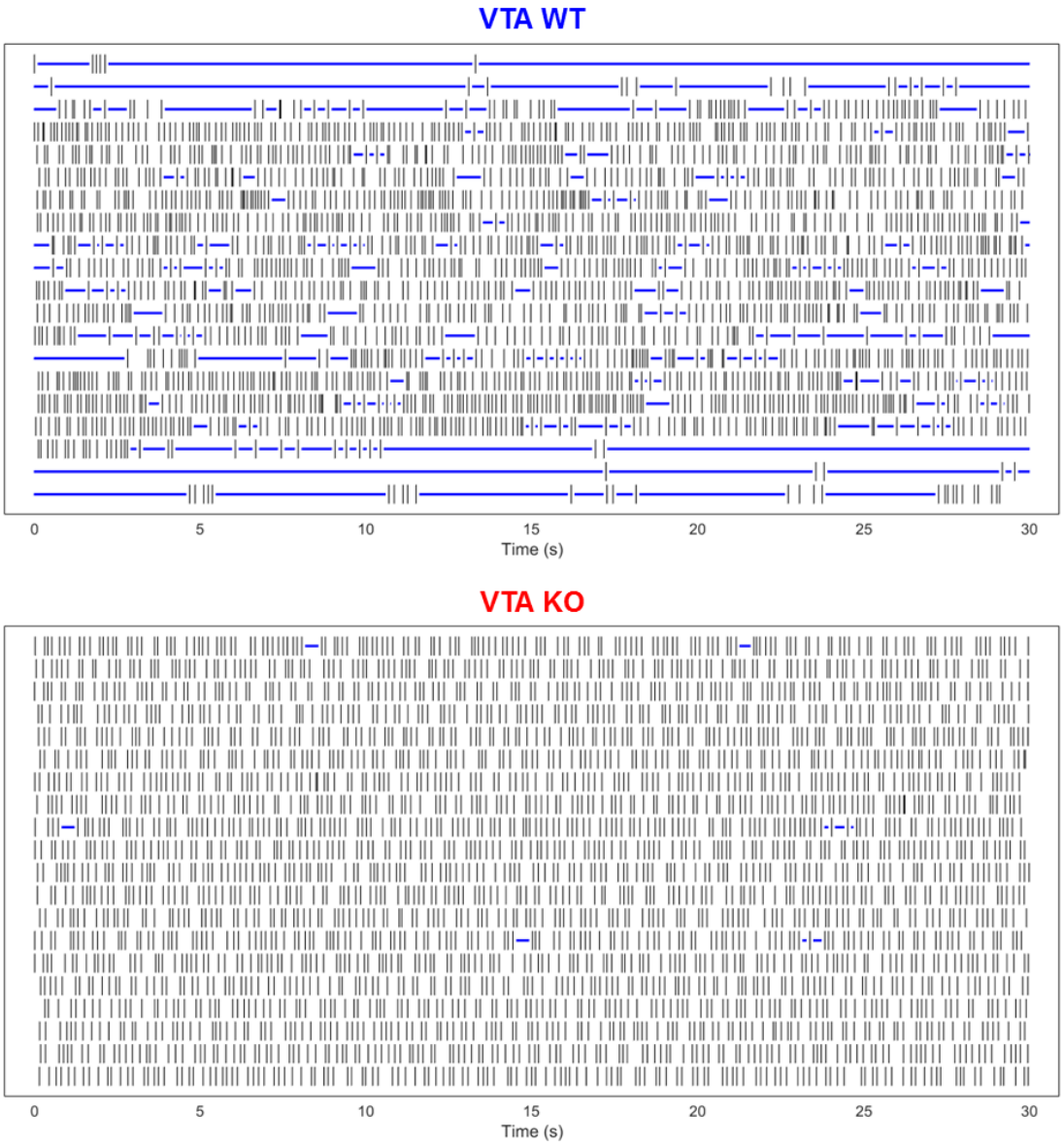

Figure 3.14. Examples of RGS-identified pauses in KChIP4 KO and WT VTA DA neurons. RGS-identified pauses (blue traces) in representative neurons of both genotypes.

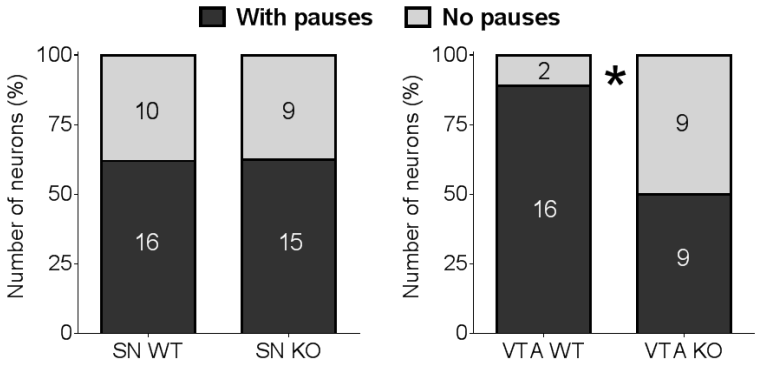

Figure 3.15. KChIP4 KO reduces the proportion of VTA DA neurons with RGS-identified pauses.

Proportion of neurons with and without any RGS-identified pauses. Note the significant genotype difference between VTA, but not SN, DA neurons. *$P < 0.05$.

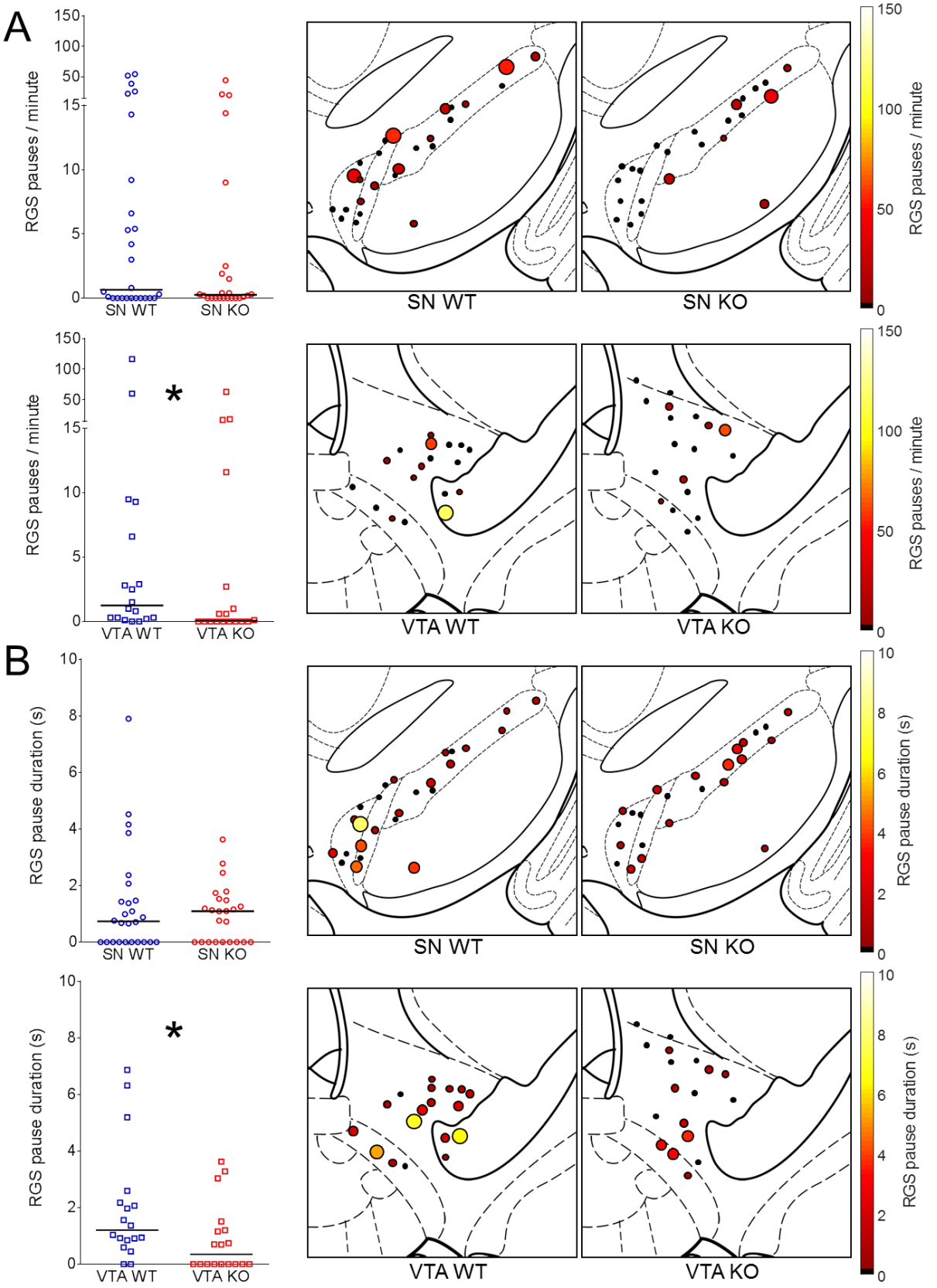

Figure 3.16. KChIP4 KO selectively reduces the number and duration of RGS-identified pauses in VTA DA neurons.

Data from SN and VTA DA neurons in WT and KO mice. A: Number of RGS-identified pauses per minute. B: Mean duration of RGS-identified pauses. Note the significant genotype difference in VTA, but not SN, DA neurons for both variables. *$P < 0.05$.

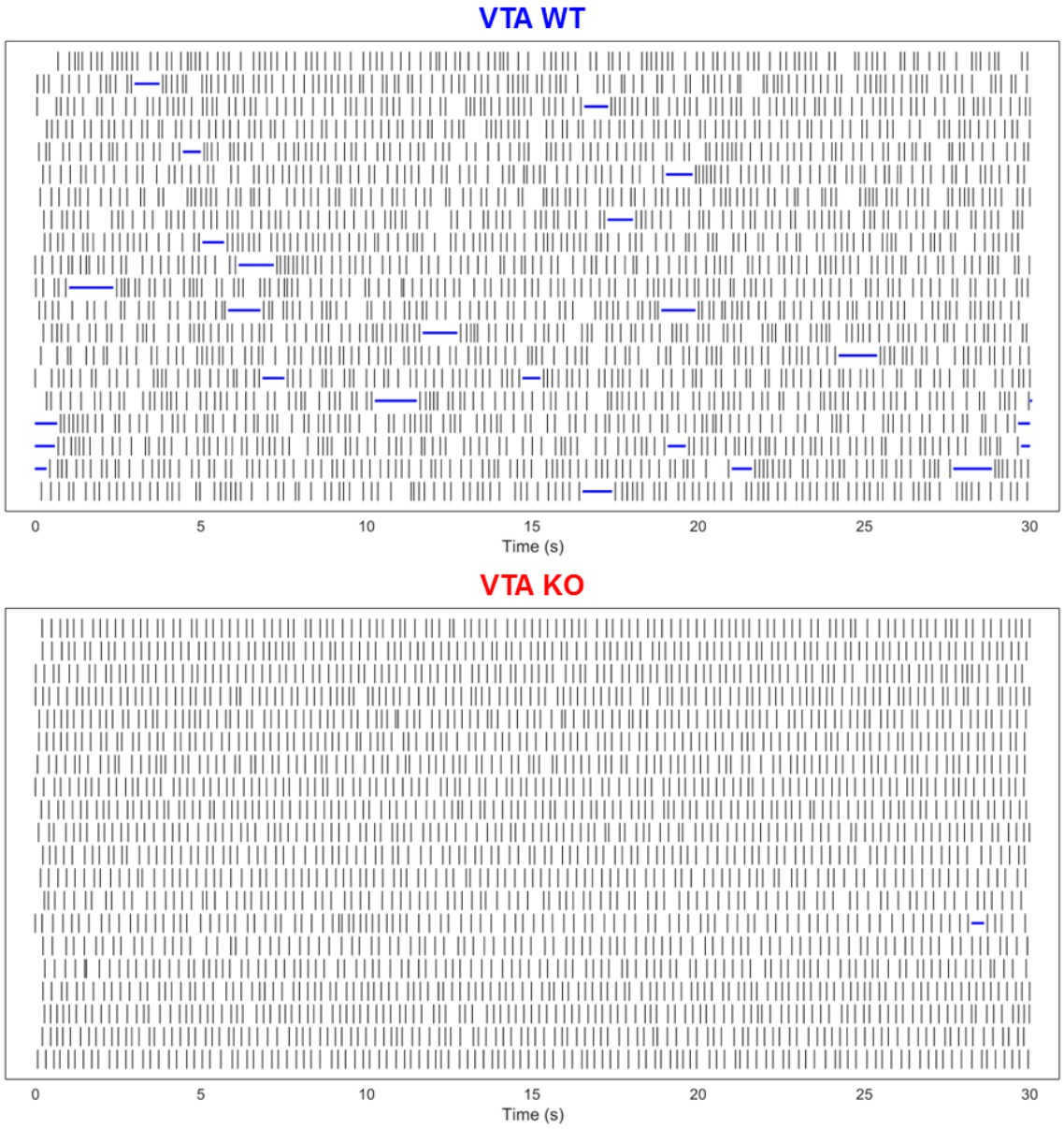

Figure 3.17. Examples of outlier pauses in KChIP4 KO and WT VTA DA neurons.
Outlier-identified pauses (blue traces) in representative neurons of both genotypes.

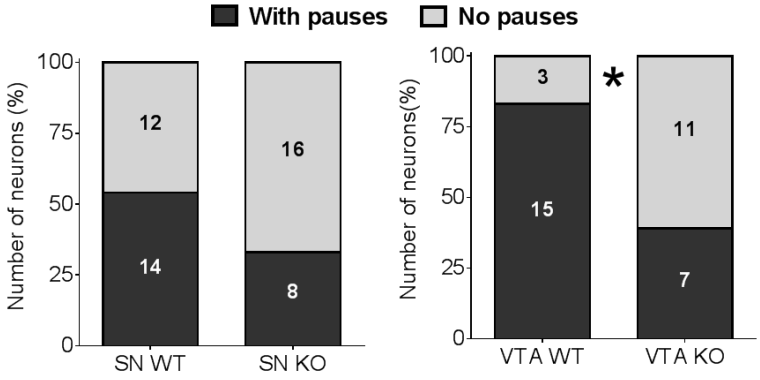

Figure 3.18. KChIP4 KO selectively reduces the proportion of VTA DA neurons that show outlier pauses.
Proportion of neurons with and without any outlier pauses. Note the significant genotype difference between VTA, but not SN, DA neurons. *$P < 0.05$.

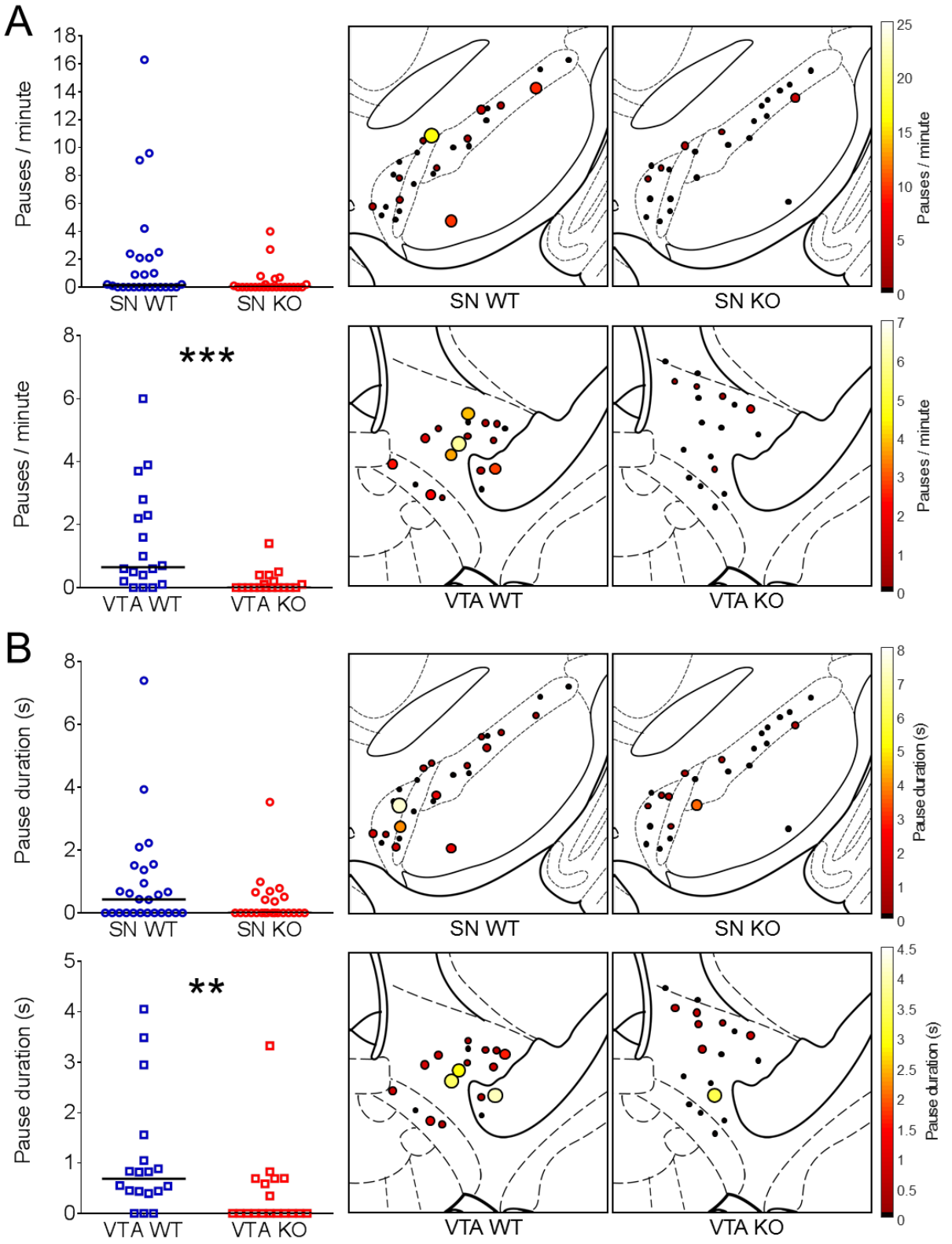

Figure 3.19. KChIP4 KO selectively reduces the number and duration of outlier pauses in VTA DA neurons.

Data from SN and VTA DA neurons in WT and KO mice, as well as their anatomical mapping in the midbrain. A: Number of outlier pauses per minute. Note the significant genotype difference in VTA, but not SN, DA neurons. B: Mean duration of outlier pauses. Note the significant genotype difference in VTA, but not SN, DA neurons. $^{**}P < 0.01$; $^{***}P < 0.001$

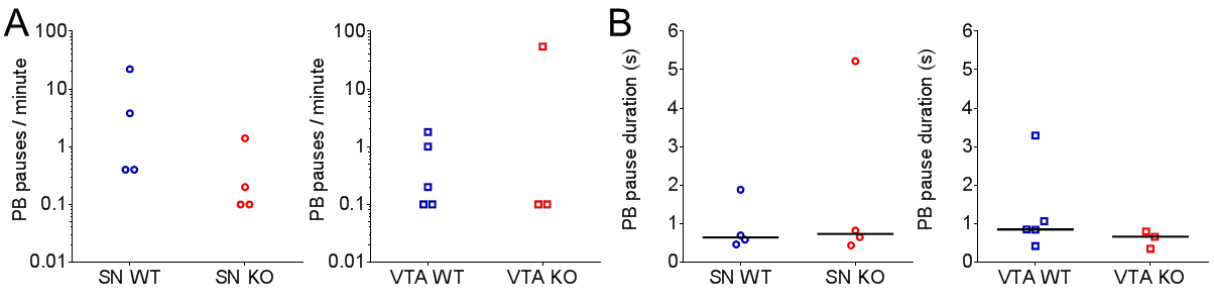

Figure 3.20. KChIP4 KO does not affect post-burst pauses in DA neurons.
A: Number of post-burst pauses per minute (data from DA neurons in WT and KO mice that displayed post-burst pauses). B: Mean duration of post-burst pauses. Note the absence of a genotype effect on these variables (Mann Whitney tests, $P > 0.05$).

3.2. Behavioral differences between KChIP4-DAT-Ex3d and DAT-cre KI mice

3.2.1. KChIP4-Ex3d selectively accelerates extinction learning

Comparing the performance of KChIP4-DAT-Ex3d and DAT-cre KI mice across daily sessions during the conditioning task (Figure 3.21), I found that the acquisition of the appetitive response was similar for both genotypes for both time in port (no effect across genotypes or interaction with sessions, $F < 0.5$, $P > 0.05$), and response latency (no effect across genotypes or interaction with sessions, $F < 2.5$, $P > 0.05$). During this phase of the task, time in port gradually increased over sessions (effect across sessions, $F_{10, 270} = 73.85$, $P < 0.0001$) and response latency progressively decreased over the same period (effect across sessions, $F_{10, 270} = 18.3$, $P < 0.0001$), but with no difference between genotypes. During extinction, there was a gradual session-wise decrease in time in port (effect across sessions, $F_{5, 135} = 47.87$, $P < 0.0001$) and increase in response latency (effect across sessions, $F_{5, 135} = 42.8$, $P < 0.0001$). However, KChIP4-DAT-Ex3d mice had a significantly accelerated reduction in time in port during cue (interaction of genotype and session effect, $F_{5, 135} = 3.2$, $P < 0.01$) and were faster to increase their response latency across sessions (interaction of genotype and session effect, $F_{5, 135} = 2.615$, $P < 0.05$).

In order to differentiate if the effect of KChIP4-DAT-Ex3d was due to a progressive decrease in checking frequency of a faster disengagement during each sequential check, I quantified the number and duration of head entries during CS presentation (Figure 3.22). Only head entries that were initiated after CS presentation were analyzed. During acquisition, the number of head entries remained within a 1-2

range, with a slight decrease over sessions (effect across sessions, $F_{10, 270} = 1.9$, $P < 0.05$), which was expected given that reinforcement was nearly constantly available throughout CS presentation. Duration of directed head entries gradually increased over time during acquisition (effect across sessions, $F_{10, 270} = 22.23$, $P < 0.0001$), matching the fact that the response latency gradually decreased with time as well. As in the effects on time in port and latency, there was no difference between genotypes in the number (no effect across genotypes or interaction with sessions, $F < 1.5$, $P > 0.05$) and duration (no effect across genotypes or interaction with sessions, $F < 1.5$, $P > 0.05$) of directed head entries during acquisition. During extinction, both the number (effect across sessions, $F_{5, 135} = 26.55$, $P < 0.0001$) and duration (effect across sessions, $F_{5, 135} = 6.8$, $P < 0.0001$) of head entries decreased over sessions. There was no significant genotype effect on the duration of head entries (no effect across genotypes or interaction with sessions, $F < 0.6$, $P > 0.05$), but KChIP4-Ex3d mice had significantly reduced head entry numbers in comparison to DAT-cre KI controls (interaction of genotype and session effect, $F_{5, 135} = 3.45$, $P < 0.01$; genotype effect, DAT-cre KI > Ex3d, $F_{1, 27} = 4.82$, $P < 0.05$).

Analyzing behavioral performance trial by trial during the first extinction session (Figure 3.23), I found that both genotype groups responded similarly in the first extinction trial, but had a strong trend for a gradual divergence starting on the second trial for time in port (genotype effect, DAT-cre KI > Ex3d, $F_{1, 27} = 3.51$, $P = 0.07$; across trial effect, $F_{9, 243} = 16.53$, $P < 0.0001$) a significant divergence in response latency starting on the third trial (interaction of genotype and session effect, $F_{9, 243} = 2.01$, $P < 0.05$; genotype effect, Ex3d > DAT-cre KI, $F_{1, 27} = 7.51$, $P < 0.05$; across trial effect, $F_{9, 243} = 5.6$, $P < 0.0001$) and a highly significant difference for head entry number starting on the second trial (genotype effect, $F_{1, 27} = 5.98$, $P < 0.05$; across trial effect, $F_{9, 243} = 4.91$, $P < 0.0001$). These effects were also reflected as statistically significant differences in the session averages for response latency and head entry numbers (unpaired T-tests, $P < 0.05$ and $P < 0.01$, respectively) No difference was observed between genotypes in head entry duration during the first extinction session (no effect across genotypes or interaction with sessions, $F < 0.7$, $P > 0.05$; across trial effect, $F_{9, 243} = 2.21$, $P < 0.05$). Taken together, these measures confirm that the effect of KChIP4-Ex3d was not due to a general decrease in response, but gradually developed as the animals learned that the CS no longer predicted US availability.

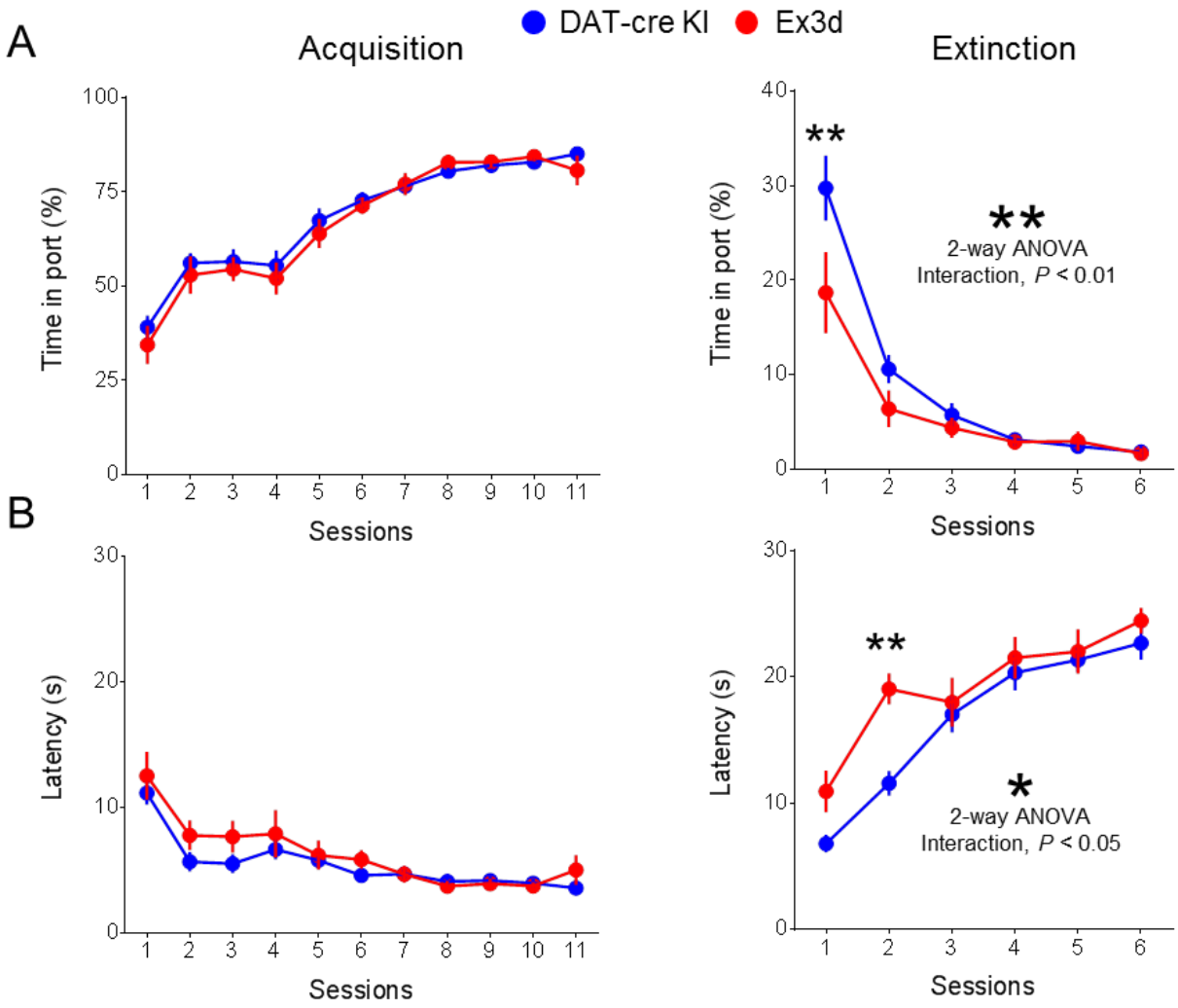

Figure 3.21. KChIP4-Ex3d selectively accelerates extinction learning.
A: Performance in the time in port metric during CS presentation. Note the faster response extinction for KChIP4-Ex3d mice in relation to DAT-cre KI controls, including the significant pair-wise difference during the first extinction session (Sidak's multiple comparisons test). B: Latency to response during CS presentation. Note the faster increase in this measure during extinction in KChIP4-Ex3d mice, including the significant pair-wise difference during the second extinction session (Sidak's multiple comparisons test). *$P < 0.05$; **$P < 0.01$.

There was also a slight phenotype difference between KChIP4 Ex3d and DAT-cre KI mice in the number of trials with responses (Figure 3.24). During acquisition, both genotypes progressively increased the number of trials per session at the same pace (no effect across genotypes or interaction with sessions, $F < 1.3$, $P > 0.05$; across session effect, $F_{27, 270} = 12.86$, P < 0.0001). During extinction sessions, both groups decreased the number of trials with responses at a statistically similar rate (no effect across genotypes or interaction with sessions, $F < 2.5$, $P > 0.05$; across session effect, $F_{5, 135} = 34.17$, $P < 0.0001$). However, in the first session of extinction, KChIP4 Ex3d mice showed a reduced response probability in comparison to DAT-cre

KI mice, especially after the second trial (interaction of genotype and session effect, $F_{9, 243}$ = 2.31, P < 0.05; genotype effect, DAT-cre KI > Ex3d, $F_{1, 27}$ = 6.6, P < 0.05; across trial effect, $F_{9, 243}$ = 1.9, P = 0.052), which was also visible as a significantly lower average number of trial responses in the group (Mann Whitney test, P < 0.05).

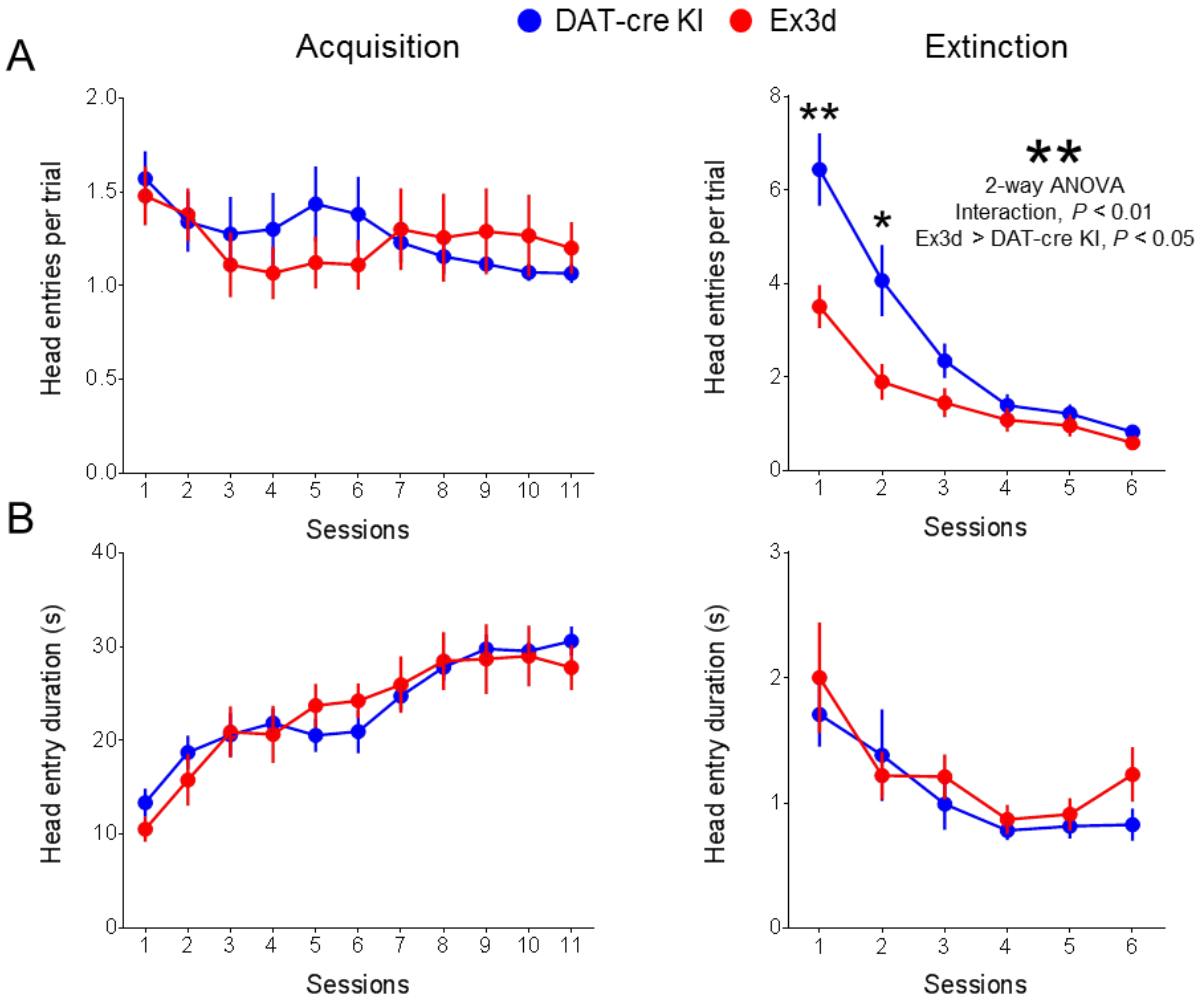

Figure 3.22. KChIP4-Ex3d affects head entry number, but not duration, during extinction.
A: Number of directed head entries into the reward port during CS presentation. Note the faster response extinction for KChIP4-Ex3d mice in relation to DAT-cre KI controls, including the significant pair-wise difference during the first and second extinction sessions (Sidak's multiple comparisons test). B: Duration of directed head entries into the reward port during CS presentation. Note the lack of a genotype effect during acquisition and extinction. *P < 0.05; **P < 0.01.

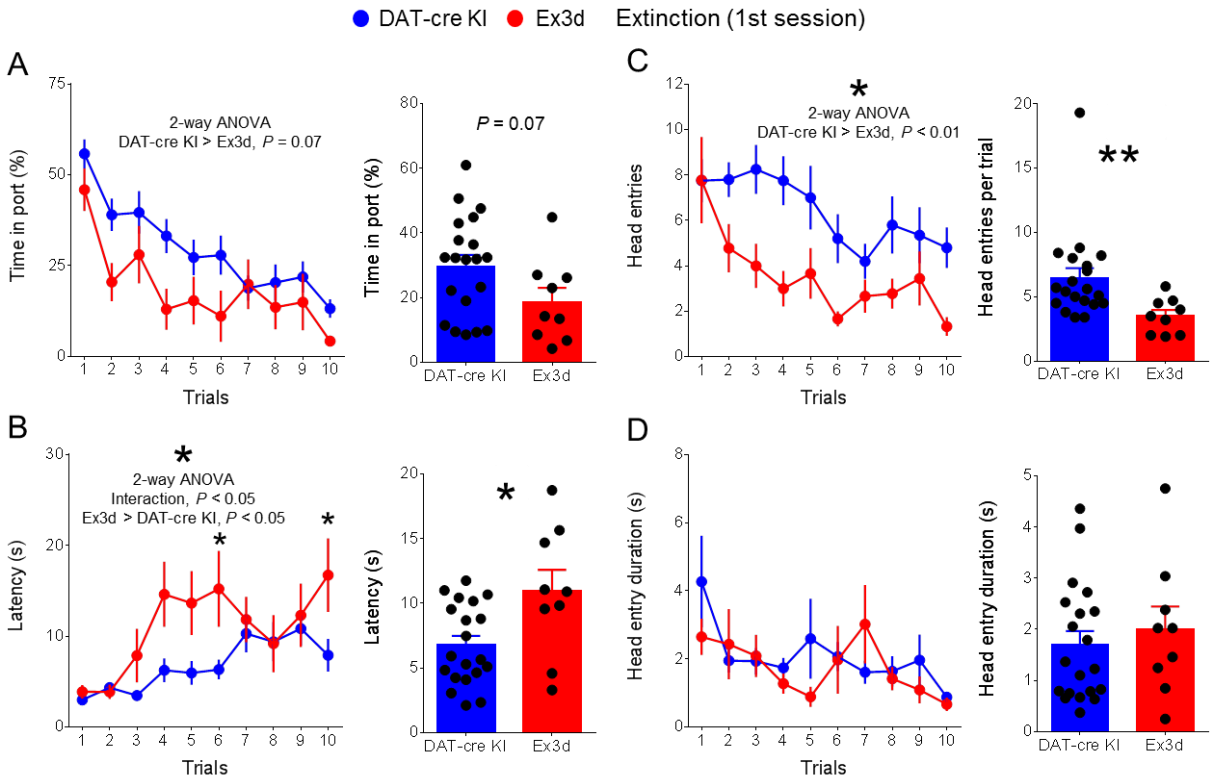

Figure 3.23. Performance of KChIP4-Ex3d and DAT-cre KI mice over trials in the first extinction session in a conditioning task.

Behavioral performance during CS presentation across trials in the first extinction session. Bar graphs show the mean values of all trials. A: Time in port. Note that both genotypes start with similar performances in the first trial, but KChIP4-Ex3d mice show a trend of a progressively faster decrease in subsequent trials. B: Latency to response. Note that both genotypes start with similar performances in the first and second trials, but KChIP4-Ex3d mice show a progressively faster increase in subsequent trials, including significant pair-wise differences on trials 6 and 10 (Sidak's multiple comparisons test). The average latency per trial in this session was also longer for KChIP4-Ex3d mice. C: Number of directed head entries. Note that both genotypes start with similar performances in the first trial, but KChIP4-Ex3d mice show a faster decrease in subsequent trials. The average number of head entries per trial in this session was also longer for KChIP4-Ex3d mice. D: Duration of directed head entries into the reward port during CS presentation. Note the absence of a genotype effect during the extent of the entire session and in the average per trial.*$P < 0.05$; **$P < 0.01$.

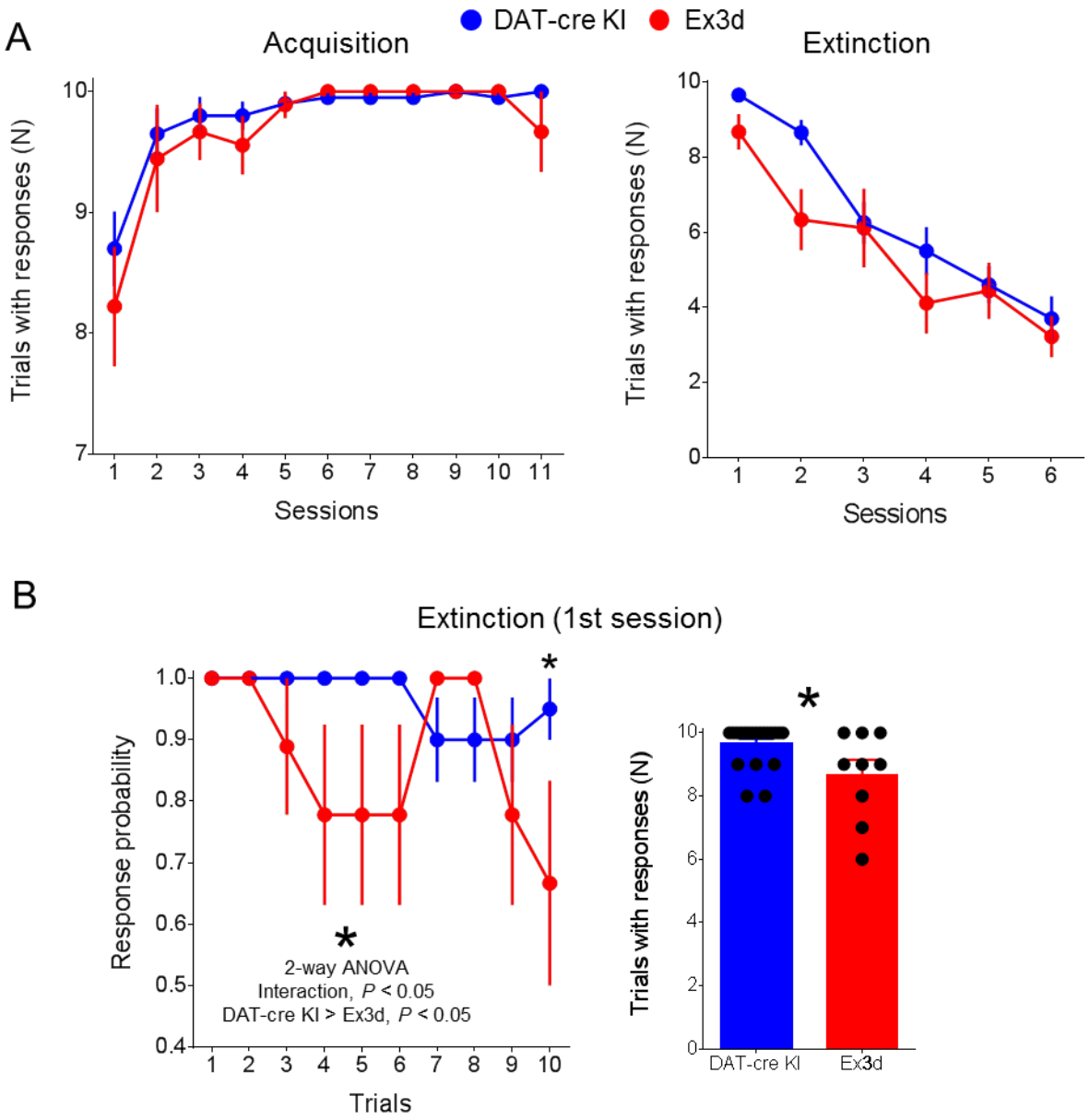

Figure 3.24. Response probability of KChIP4-Ex3d and DAT-cre KI mice over acquisition and extinction sessions and over trials in the first extinction session in a conditioning task.
A: Number of trials with responses during CS presentation across sessions during acquisition and extinction. Note that both genotypes show no significant differences during acquisition, or extinction. B: Response probability during CS presentation in the first session of extinction. Bar graph shows the mean values of all trials. Note that both genotypes start with similar performances in the first two trials, but KChIP4-Ex3d mice show a faster decrease in subsequent trials, including a significant difference on trial 10 (Sidak's multiple comparisons test). The total number of trials with responses in this first session is also lower in KChIP4-Ex3d mice.*$P < 0.05$.

3.2.2. KChIP4-Ex3d effect is consistent with a decrease in learning from negative prediction errors

In order to formally test the hypothesis that only negative prediction errors were affected by KChIp4 Exd, I fitted the trial by trial time in port values for both KChIP4 Ex3d and DAT-cre KI groups with a modified Rescorla-Wagner model (Figures 3.25 and 3.26). The model was able to successfully fit the behavioral data, including the different learning kinetics during extinction (Figure 3.26). The quality of the fitting, as measured by the values of the residuals between the experimental data and the model output, was similar for both genotypes (Figures 3.27 and 3.29 A). Plotting of the residuals for each combination of α_P and α_N in a two dimensional plot showed that the range of most accurate learning rate combinations was shifted towards the right (higher values of α_N) for KChIP4 Ex3d mice in relation to the DAT-cre KI group (Figures 3.28).

Comparisons of the values of α_P and α_N for the best (lowest residual) fit (Figure 3.28) showed that indeed the KChIP4 Ex3d group had significantly higher α_N values, i.e. faster learning from negative prediction errors (Mann Whitney test, $P < 0.05$), without any change in α_P (Mann Whitney test, $P > 0.05$). Importantly, empirically derived model parameters (V_0, V_{max} and V_{min}) were similar for both genotypes (Figure 3.29 B-D; Mann Whitney test, $P > 0.05$), indicating that the effect of KChIP4 Ex3d was selective to learning from negative prediction errors.

As a control, I fitted the experimental data using a classical Rescorla Wagner model, i.e. with only one learning rate α parameter (Figure 3.30). Assuming a single learning rate for both positive and negative prediction errors resulted in a markedly worse quality of fitting, with the residual values for the best fit being nearly two-fold larger in relation to fitting with separate learning rates for both the KChIP4 Ex3d and DAT-cre KI groups (Figure 3.30 C; paired t-tests, $P < 0.001$ for both comparisons). Additionally, the classical model did not capture the differences between KChIP4 Ex3d and DAT-cre KI groups during extinction (Figure 3.30 D; Mann Whitney test, $P > 0.05$).

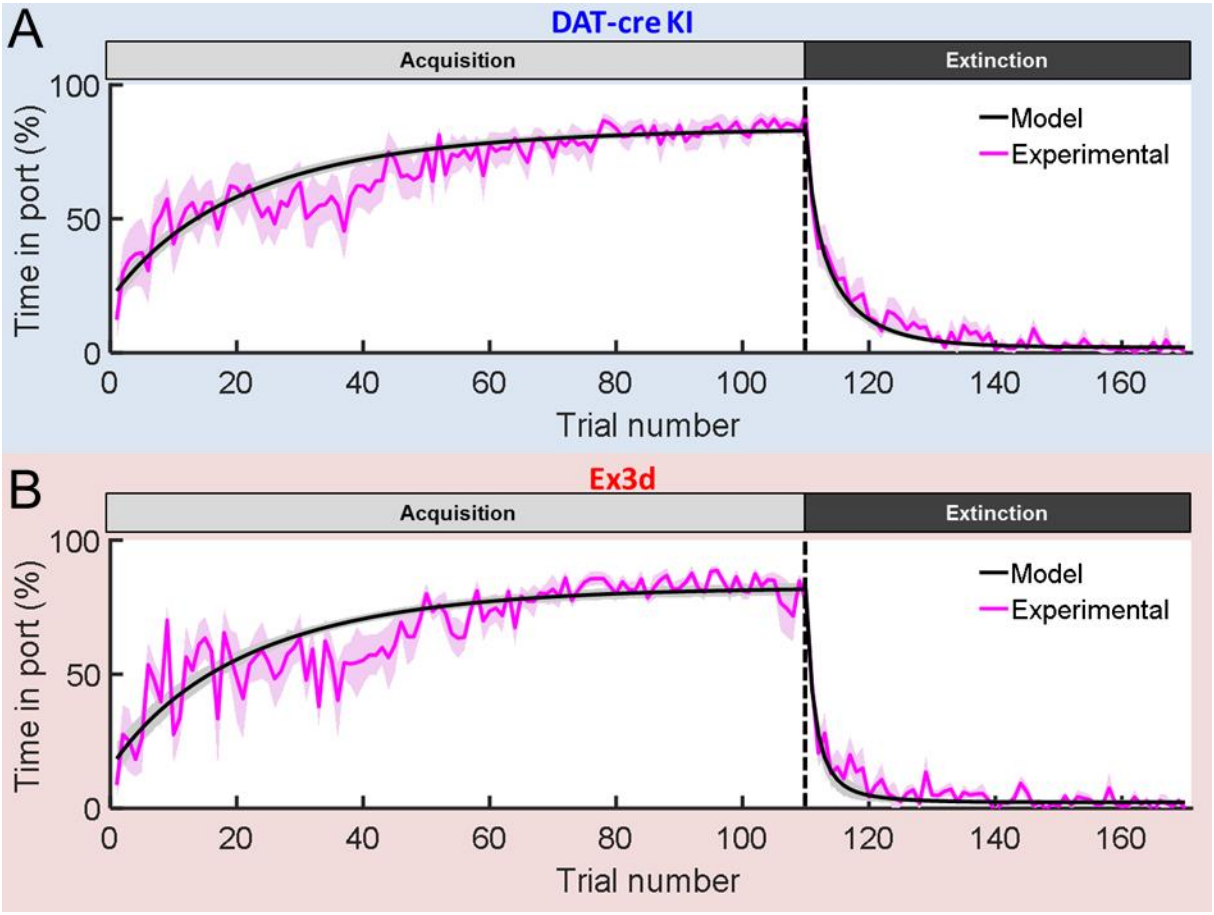

Figure 3.25. Experimental results are accurately fitted with a modified Rescorla-Wagner model.
A: Trial by trial time in port (black and grey; mean ± SEM) and model fit (magenta and pink; mean ± SEM) in both acquisition and extinction for the DAT-cre KI group. B: Trial by trial time in port (black and grey; mean ± SEM) and model fit (magenta and pink; mean ± SEM) in both acquisition and extinction for the KChIP4 Ex3d group. Note that the model fit follows the learning kinetics with a high degree of accuracy for both genotypes.

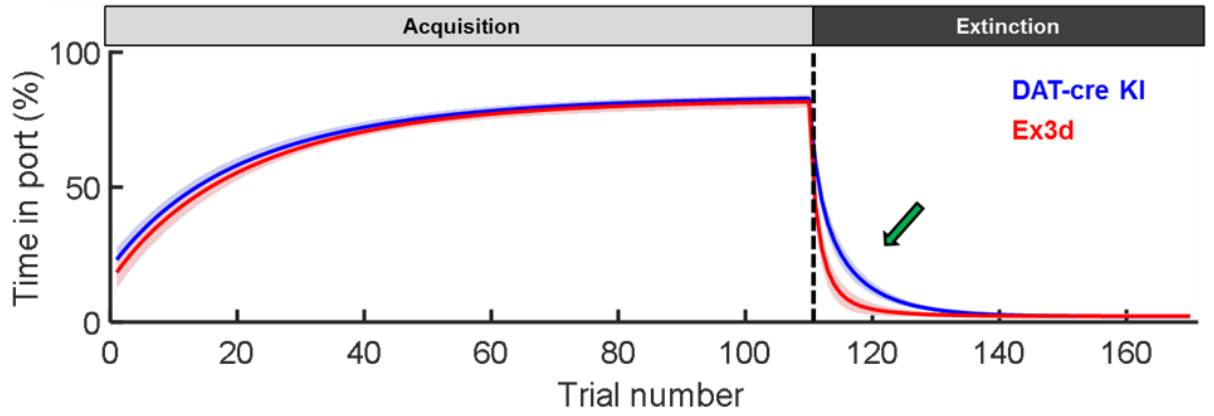

Figure 3.26. Overlay of model fits for KChIP4 Ex3d and DAT-cre KI learning curves.
Note that the model fits overlap almost completely during acquisition, but diverge in extinction, reflecting the faster extinction learning kinetics of the KChIP4 Ex3d mice in relation to DAT-cre KI control (green arrow).

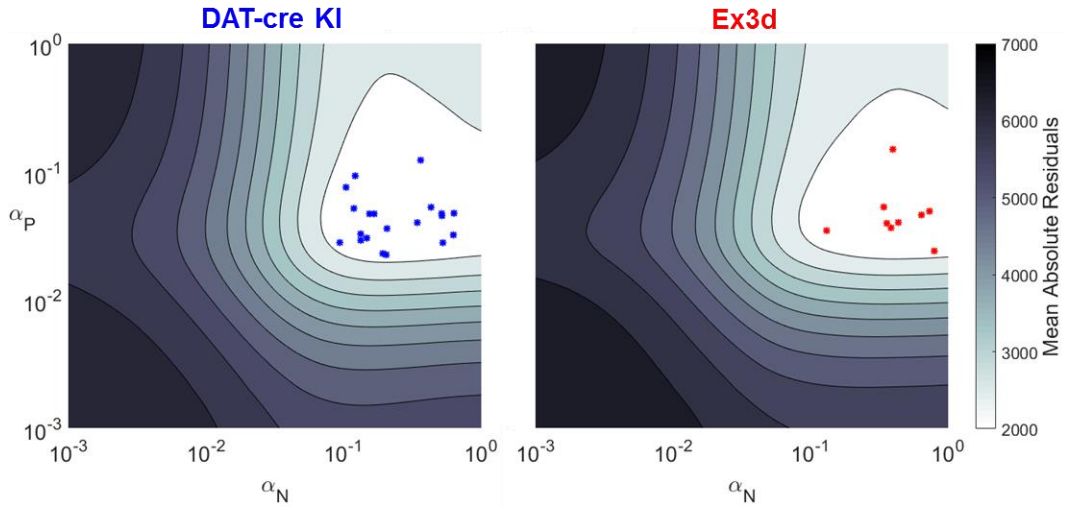

Figure 3.27. Residual values for different combinations of α_P and α_N parameters.
The contour plot shows the mean absolute residuals (all mice per group) for models fitted to KChIP4-Ex3d and DAT-cre KI data with different combinations of α_P and α_N (each varying from 1 to 0.001). Red and blue symbols indicate the optimal (least residual values) combination of α_P and α_N for each individual animal. Note that the shape of the close to optimal contour is shifted towards higher α_N values in the Ex3d group.

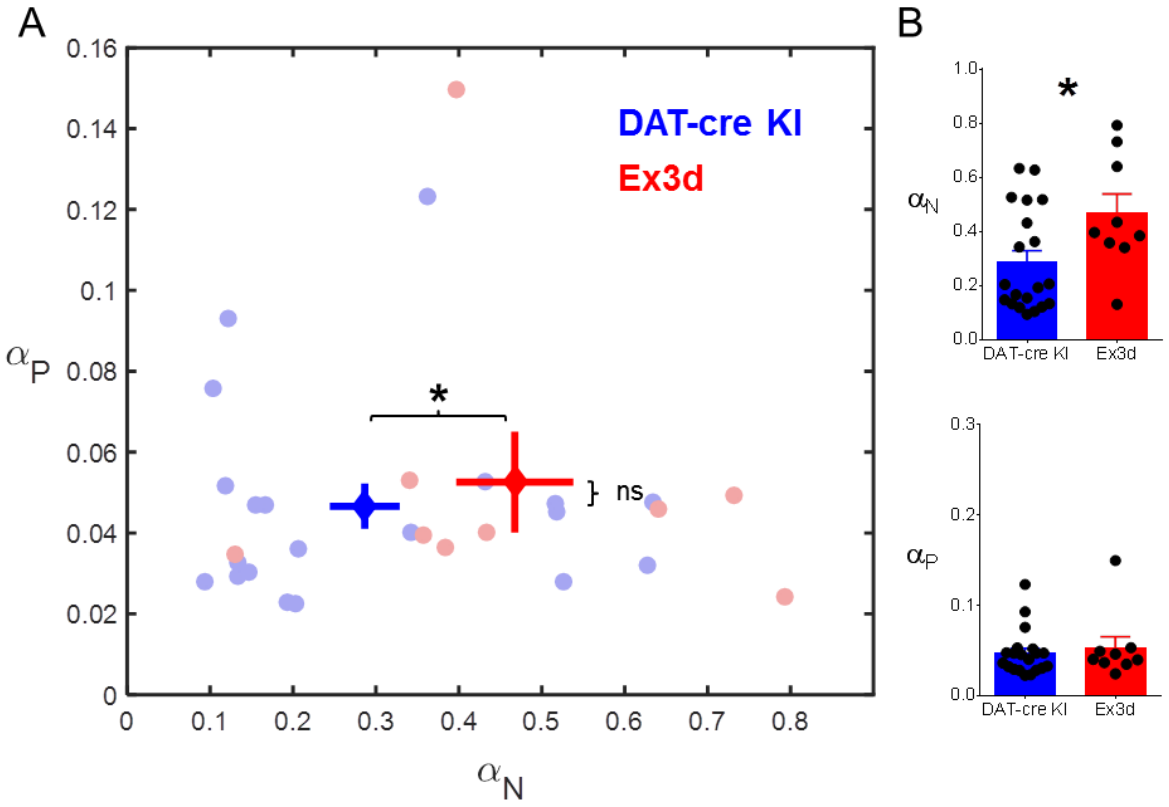

Figure 3.28. KChP4 Ex3d mice show a selective increase in learning from negative prediction errors.
A: Combination of best fit α_P and α_N values for KChIP4 Ex3d (red) and DAT-cre KI (blue) groups. Faded circles represent individual values. Large solid crosses indicate the mean ± SEM of each group. B: Comparison of α_P and α_N values for each genotype. Note the selective increase in α_N (learning from negative prediction errors) in KChIP4 Ex3d in relation to DAT-cre KI controls. *P < 0.05.

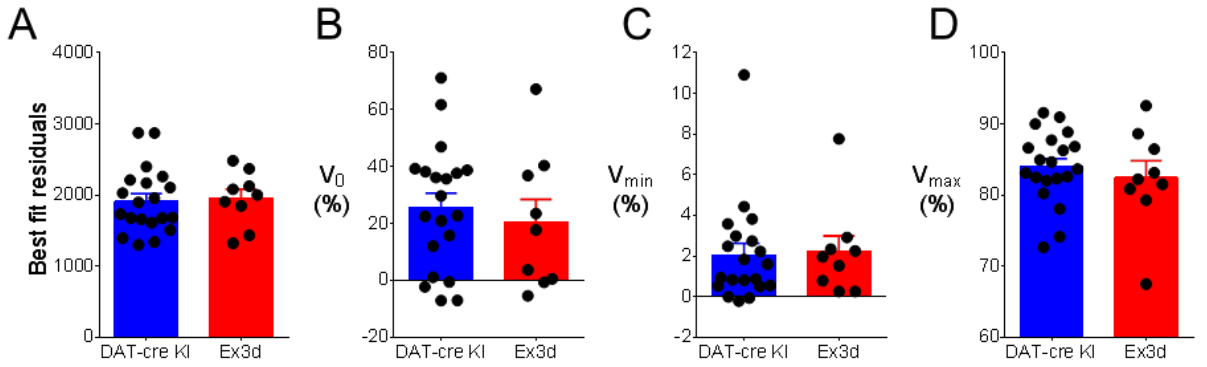

Figure 3.29. Model goodness of fit and empirically derived parameters are similar across genotypes.
A: Residuals of the best model fit for KChIP4 Ex3d and DAT-cre KI groups. B: V_0 (initial assumed associative strength). C: V_{min} (minimal associative strength). D: V_{max} (maximal associative strength). Note that there was no significant difference observed between the compared groups (Mann Whitney tests, $P > 0.05$).

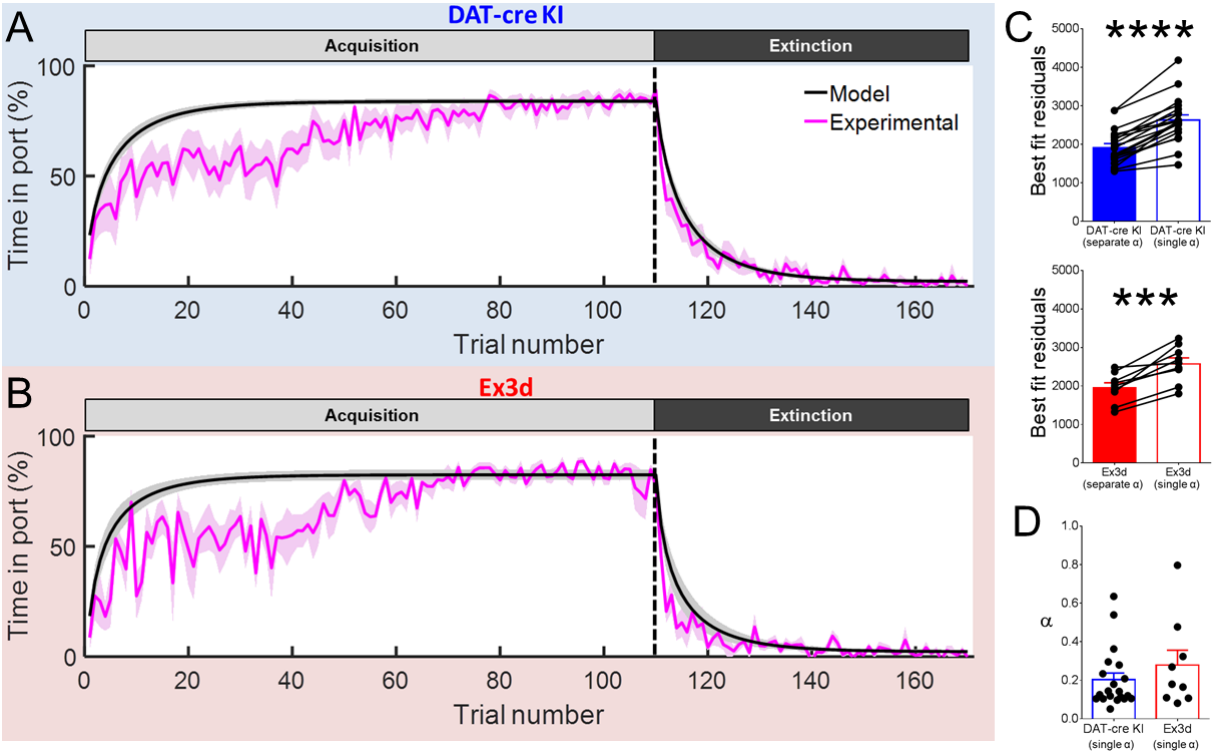

Figure 3.30. Fitting with a classical RW model.
A: Trial by trial time in port (black and grey; mean ± SEM) and model fit (magenta and pink; mean ± SEM) in both acquisition and extinction for the DAT-cre KI group. B: Trial by trial time in port (black and grey; mean ± SEM) and model fit (magenta and pink; mean ± SEM) in both acquisition and extinction for the KChIP4 Ex3d group. Note that the model fit does not follow the learning kinetics accurately in both genotypes. C: Comparison of best fit residuals with single and separate α fitting for both genotypes. Note that the fit residuals are markedly larger with single α fitting, indicating that the goodness of fit is worse than with separate α fitting. D: Values of α learning rate parameters for the classical Rescorla-Wagner model fit. Note the absence of a genotype effect on these measures (paired Mann Whitney tests, $P > 0.05$). ***$P < 0.001$. ***$P < 0.001$.

3.2.3. KChIP4-DAT-Ex3d does not affect spontaneous behaviors

I subjected KChIP4 Ex3d and DAT-cre KI control mice to a series of spontaneous behavior tasks in order to test the selectivity of the KChIP4 Ex3d phenotype. In the open field, there was no difference between the genotypes between any of the major measures of activity in this task (Figure 3.31). Measures of total track length, proportion of activity (periods where movement velocity where velocity exceeded 5 cm/s), time spent in the center area, proportion of track length in center, number and duration of rearings, were statistically similar for both groups (unpaired T tests, $P > 0.05$). I also tracked these variables on a minute by minute basis over the duration of the task (Figure 3.32) and did not detect any difference between the genotypes for any of the analyzed indices of locomotion and exploration (no effect across genotypes or interaction with sessions, $F < 1.7$, $P > 0.05$ for all comparisons). These results indicate that KChIP4 Ex3d does not affect baseline locomotion patterns, open field exploration or general anxiety.

In the novel object preference task, in trial 1, mice from both groups explored the novel objects (same shape) with statistically similar total numbers of object visits and exploration time (Figure 3.33 B and C; unpaired T-test, $P > 0.05$ for both comparisons). In trial 2, where animals had to choose to explore a familiar or novel object, mice from both genotypes showed a marked preference for visiting the novel object, but there was no difference in that preference between the genotypes, both for the proportional number and duration of object exploration visits (Figure 3.34 D and E; unpaired T-test, $P > 0.05$). This finding was confirmed by calculating the object preference discrimination index, which was also similar across genotypes (Figure 3.34 F; unpaired T-test, $P > 0.05$). I also found no genotype effect on the total number of object visits and object exploration time in trial 2 (Figure 3.34 B and C; unpaired T-test, $P > 0.05$). These results indicate that KChIP4 Ex3d does not affect novel object preference.

In the hole board exploration task, I also found no genotype effect for all tested variables: number of head-dips, total head-dip duration, proportion of head-dips made in the preferred hole, proportion of repeated head-dips, latency to first head-dip and mean head-dip duration (Figure 3.35, Mann Whitney tests, $P > 0.05$). These results indicate that KChIP4 Ex3d does not affect exploration in the hole board arena.

Finally, in the spontaneous alternation task, I also did not observe any significant difference between KChIP4 Ex3d mice and DAT-cre KI controls in the number of spontaneous alternations or in the total number of arm entries during plus maze exploration (Figure 3.36, unpaired T-tests, $P > 0.05$), indicating that there was no genotype effect on working memory.

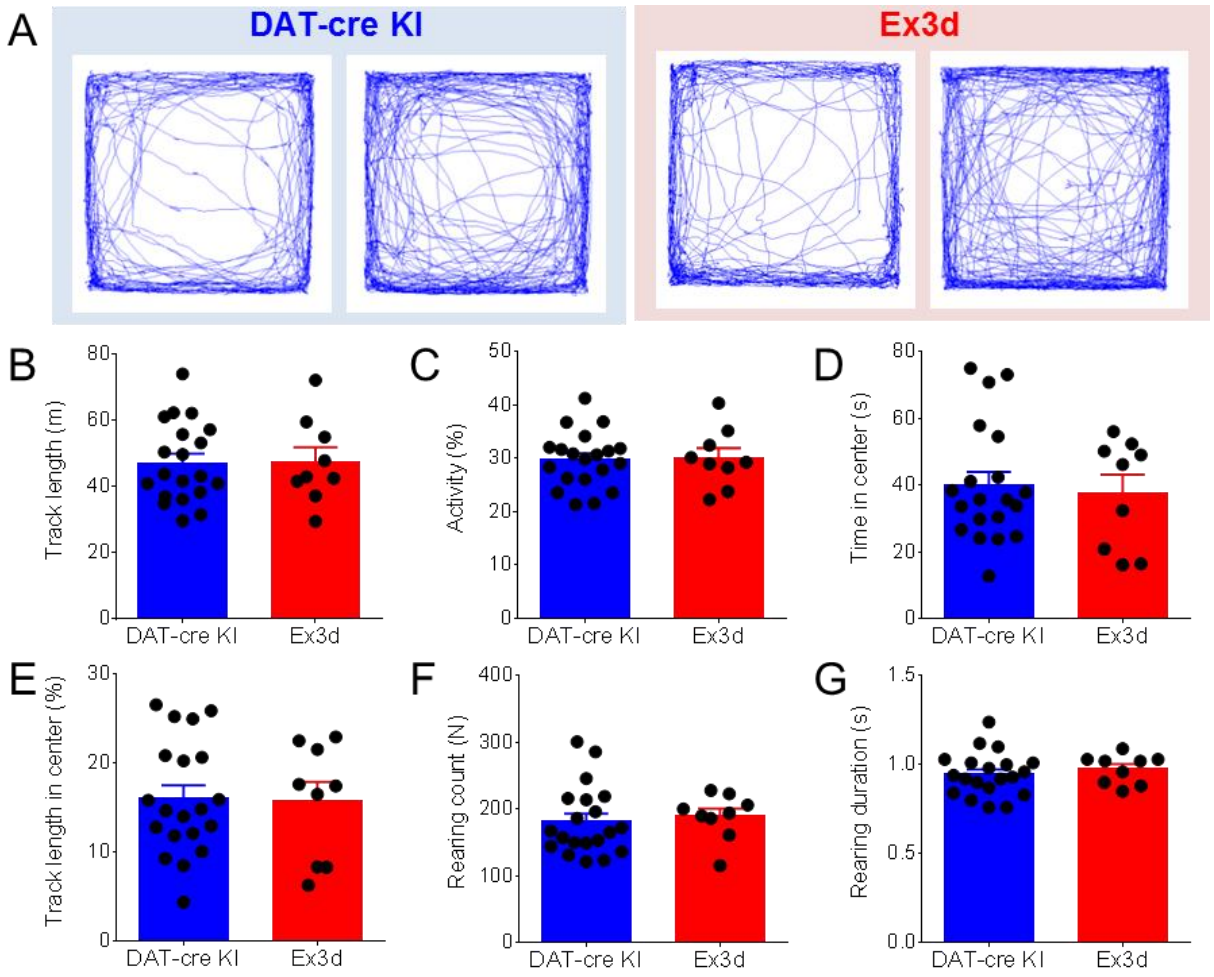

Figure 3.31. Behavioral performance of DAT-cre KI and Ex3d mice in the open field.
A: representative tracks from mice of both genotypes. B: track length. C: proportion of activity (periods where movement velocity > 5 cm/s). D: time in center. E: proportion of track length in center. F: number of rearings. G: duration of rearings. Note the absence of a genotype effect on these variables (unpaired T tests, $P > 0.05$).

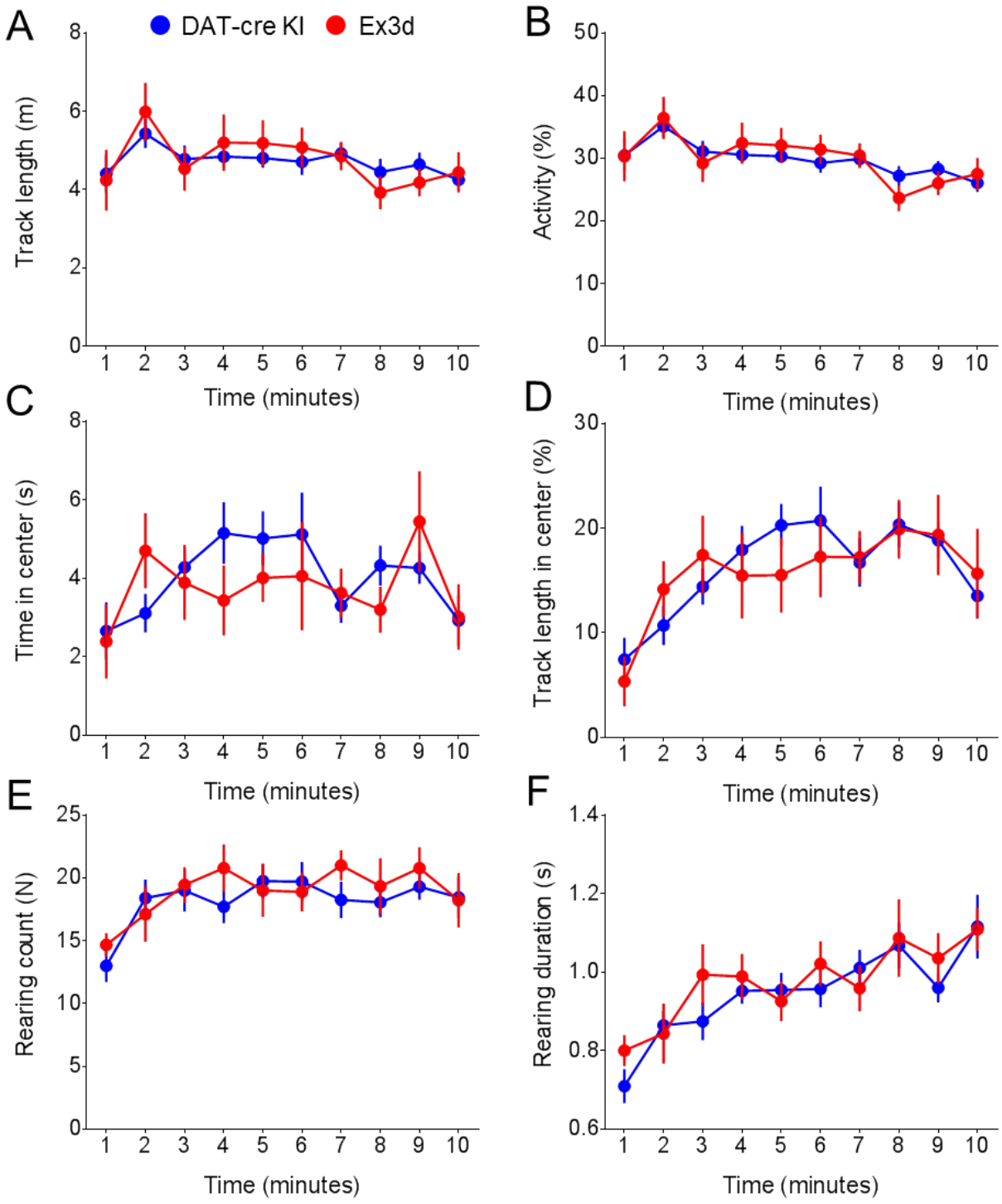

Figure 3.32. Behavioral performance of DAT-cre KI and Ex3d mice in the open field across the duration of the test.

A: track length. B: proportion of activity (periods where movement velocity > 5 cm/s). C: time in center. D: proportion of track length in center. E: number of rearings. F: duration of rearings. Note the absence of a genotype effect on these variables (two-way repeated measures ANOVA, no effect across genotypes or interaction with sessions, $F < 1.7$, $P > 0.05$ for all comparisons).

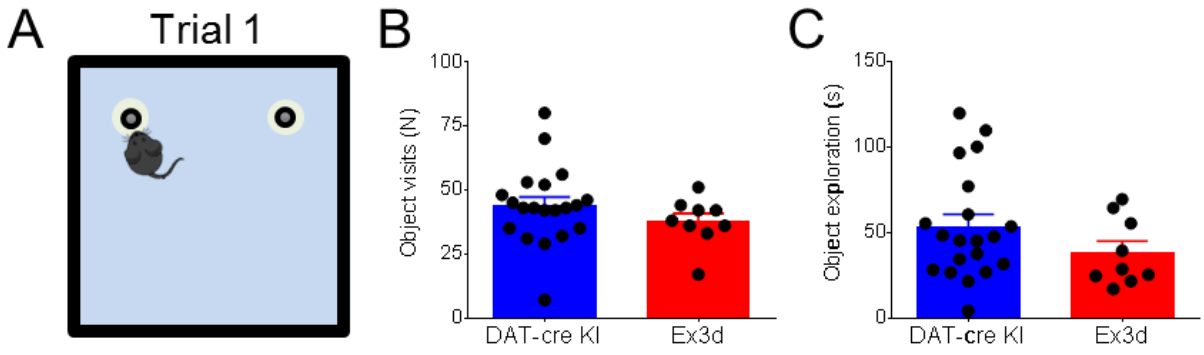

Figure 3.33. Behavioral performance of DAT-cre KI and Ex3d mice in trial 1 of the novel object recognition task.
A: Cartoon representation of object disposition during trial 1 of the task. Note that both objects are similar in shape. B: number of total object visits. C: total object exploration time. Note the absence of a genotype effect on these variables (unpaired T tests, $P > 0.05$)

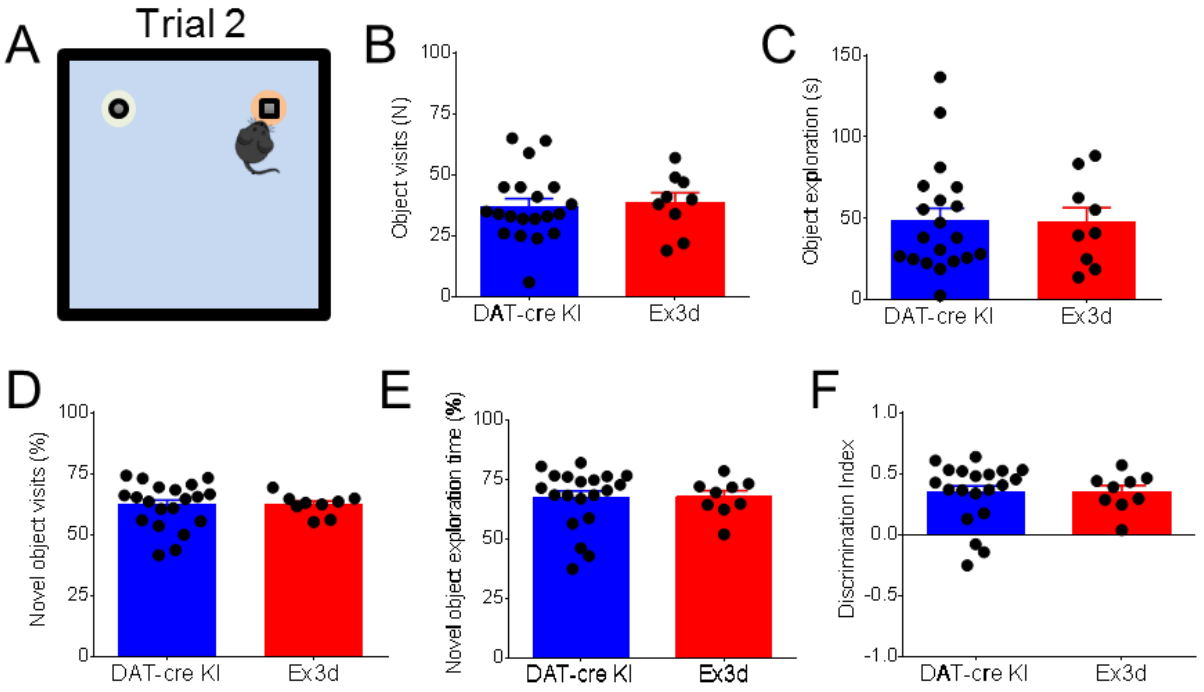

Figure 3.34. Behavioral performance of DAT-cre KI and Ex3d mice in trial 2 of the novel object recognition task.
A: Cartoon representation of object disposition during trial 2 of the task. Note that one of the objects has been replaced by another object with different shape. B: number of total object visits. C: total object exploration time. D: proportion of novel object exploration visits. E: proportion of novel object exploration time. F: discrimination index in trial 2 of the task. Note the absence of a genotype effect on these variables (unpaired T tests, $P > 0.05$). Note that mice from both genotypes displayed a marked preference for exploring the novel object.

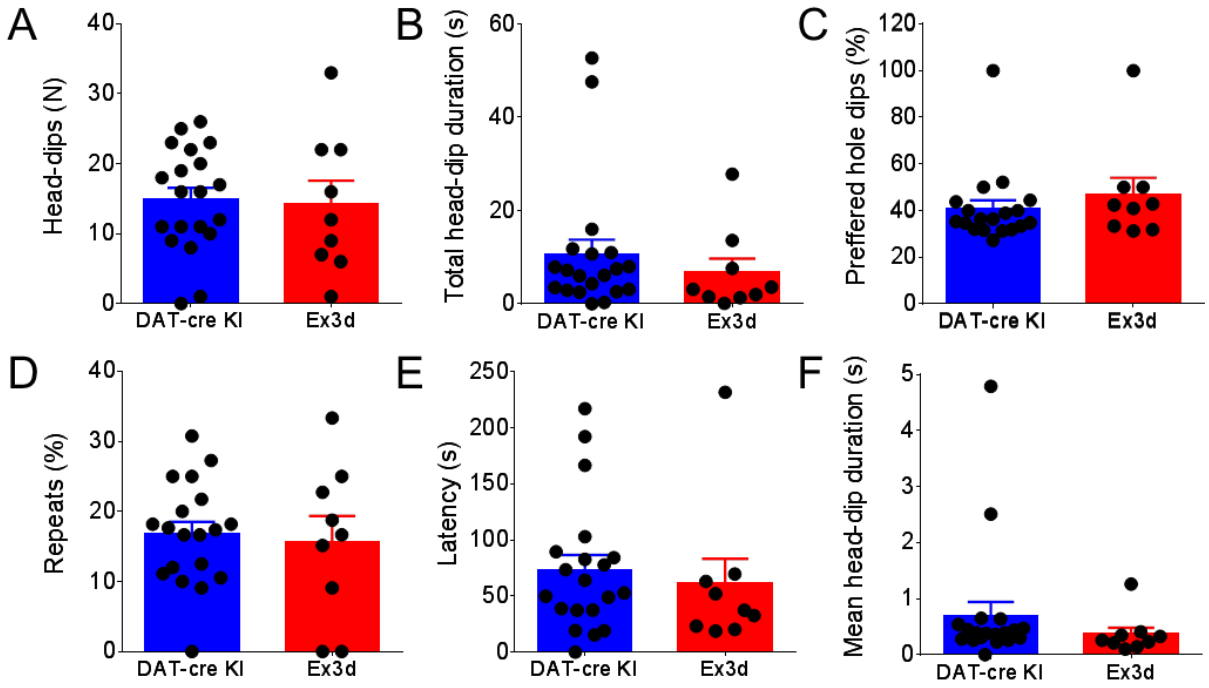

Figure 3.35. Behavioral performance of DAT-cre KI and Ex3d mice in the hole board.
A: Total number of head dips. B: total head-dip duration. C: proportion of head dips into the preferred hole. D: proportion of repeat head-dips. E: latency to first dip. F: mean head-dip duration. Note the absence of a genotype effect on these variables (Mann Whitney tests, $P > 0.05$).

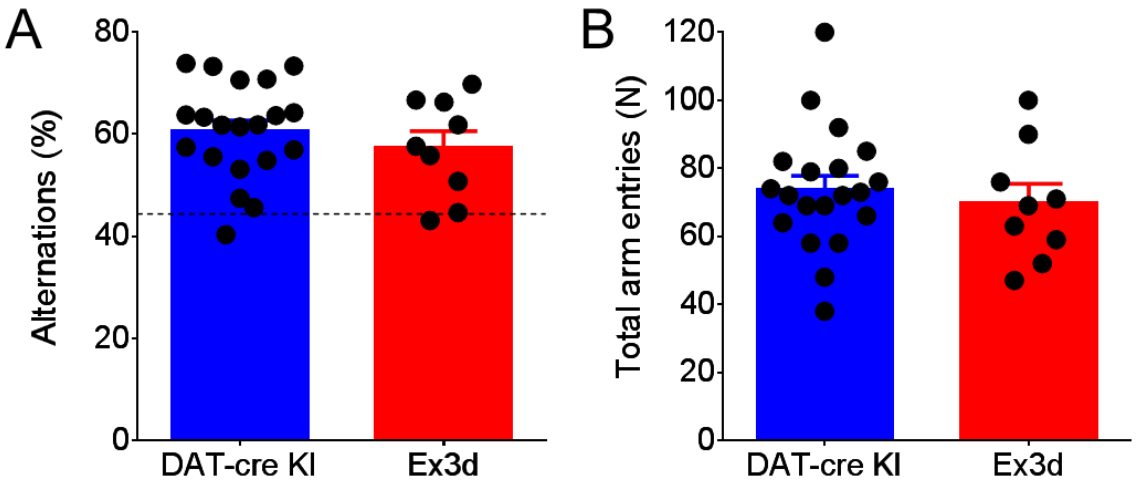

Figure 3.36. Behavioral performance of DAT-cre KI and Ex3d mice in the spontaneous alternation task.
A: proportion of spontaneous alternations (in relation to the total possible alternations). Dotted line indicates chance performance level. B: Total arm entries performed during the task. Note the absence of a genotype effect on these variables (unpaired T tests, $P > 0.05$).

3.3. Effects of KChIP4-DAT-Ex3d on Kv4.3 channel expression

3.3.1. KChIP4-DAT-Ex3d increases Kv4.3 signals in VTA and SN DA neurons

The analysis of Kv4.3 channel IHC revealed a highly significant difference between genotypes, with KChIP4 Ex3d mice exhibiting an increase in Kv4.3 immunolabeling fluorescent signals in TH-colocalized ROIs, both in the VTA and the SN (Figure 3.37; Mann Whitney test, $P < 0.0001$). This result indicates that removing exon 3 from the KChIP4 gene, and thus impeding the expression of the KChIP4a isoform, increases the expression of Kv4.3 subunits in midbrain DA neurons. Importantly, the effect was higher in the VTA (≈60% increase) in relation to the SN (≈40% increase).

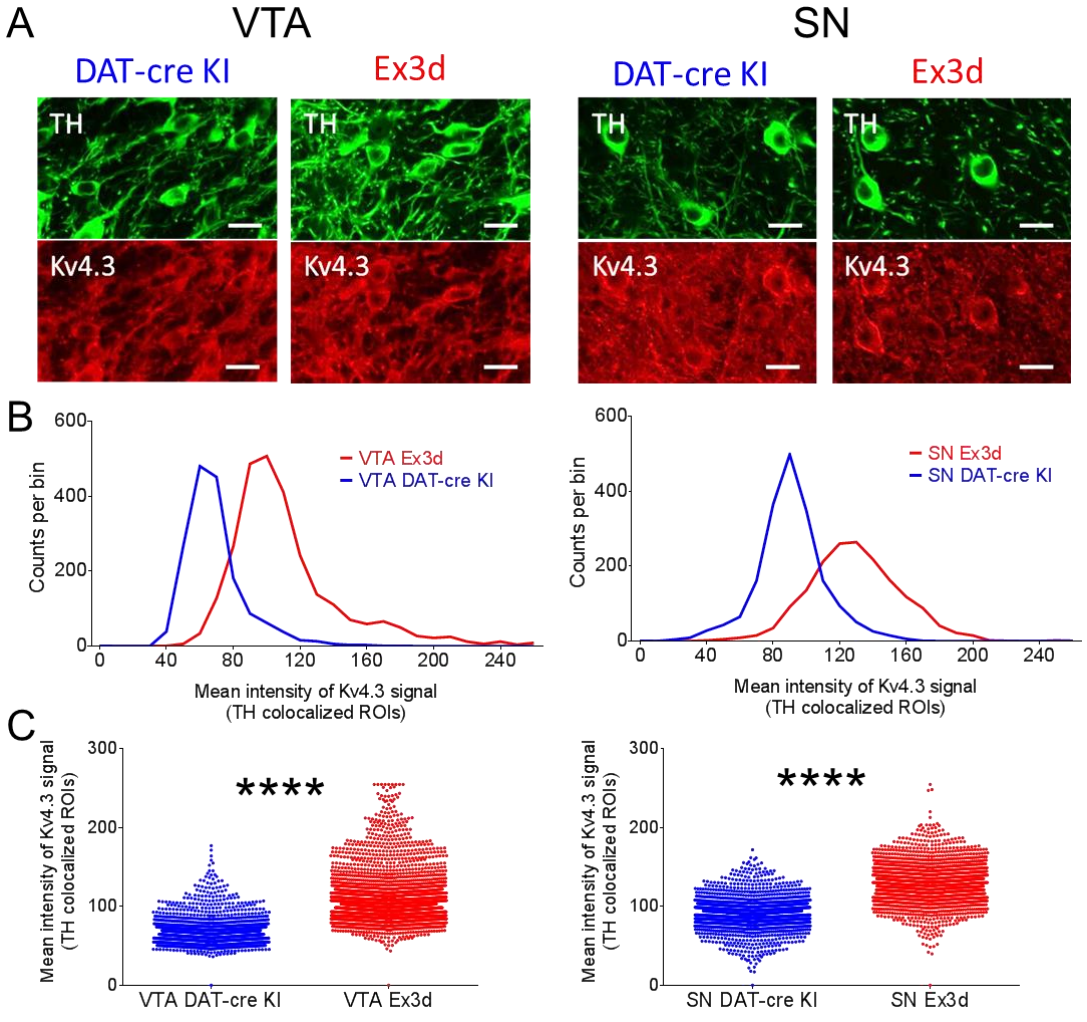

Figure 3.37. Kv4.3 immunolabeling signals in KChIP4-Ex3d and DAT-cre KI mice.
A: Representative immunolabeling figures of the VTA and SN in both genotypes. Contrast has been enhanced to improve visualization on paper. B: Frequency histogram of Kv4.3 signals for TH-colocalized ROIs in the VTA and SN. C: Comparison of Kv4.3 signals for TH-colocalized ROIs in the VTA and SN. Note the highly significant effect between genotypes, which is more pronounced in the VTA. ****$P > 0.0001$.

3.4. Behavioral differences between DAT-cre KI controls and WT mice

3.4.1. DAT-cre KI and WT mice differ in reward conditioning and extinction

When I compared the performance of DAT-cre KI and DAT-cre WT littermate mice in the conditioning task I found significant differences between these groups, in domains that were categorically different than the differences I observed between KChIP4 Ex3d and DAT-cre KI mice. First, DAT-cre KI and DAT-cre WT mice differed in the degree to which they decreased their response latency during acquisition (Figure 3.38, with the DAT-cre KI mice showing a faster learning rate (interaction of genotype and session effect, $F_{10, 350} = 2.3$, $P < 0.05$; genotype effect, DAT-cre WT > DAT-cre KI, $F_{1, 35} = 6.49$, $P < 0.05$; across sessions effect, $F_{10, 350} = 15.6$, P < 0.0001). There was also a statistically non-significant trend for a genotype effect on the time in port during acquisition, also in the direction of faster appetitive learning in the DAT-cre KI mice in relation to DAT-cre WT (trend for genotype effect, DAT-cre KI > DAT-cre WT, $F_{1, 35} = 2.95$, $P = 0.092$; across sessions effect, $F_{10, 350} = 102.4$, $P < 0.0001$).

I also observed a significant divergence between the groups during extinction in both time in port (interaction of genotype and session effect, $F_{5, 175} = 3.18$, $P < 0.01$; across sessions effect, $F_{5, 175} = 78.46$, P < 0.0001) and latency (interaction of genotype and session effect, $F_{5, 175} = 2.8$, $P < 0.05$; across sessions effect, $F_{5, 175} = 60.56$, P < 0.0001). Interestingly, during extinction the DAT-cre KI mice showed slower learning rates for latency, but ultimately achieving the same levels of response than the DAT-cre WT group. For the time in port metric they displayed a steeper learning curve, responding more that DAT-cre WT mice in the first extinction session, but quickly achieving similar response patterns in late extinction sessions (Figure 3.38 A).

I also found a significant difference between genotypes in the number of trials per session during acquisition (interaction of genotype and session effect, $F_{10, 350} = 2.4$, $P < 0.01$; across sessions effect, $F_{10, 350} = 25.86$, P < 0.0001). In the head entry analysis, however, I found that that there was no genotype effect in the number or duration of head entries (Figure 3.39), both during acquisition (no effect across genotypes or interaction with sessions, $F < 1.8$, $P > 0.05$) and extinction (no effect across genotypes or interaction with sessions, $F < 1.4$, $P > 0.05$).

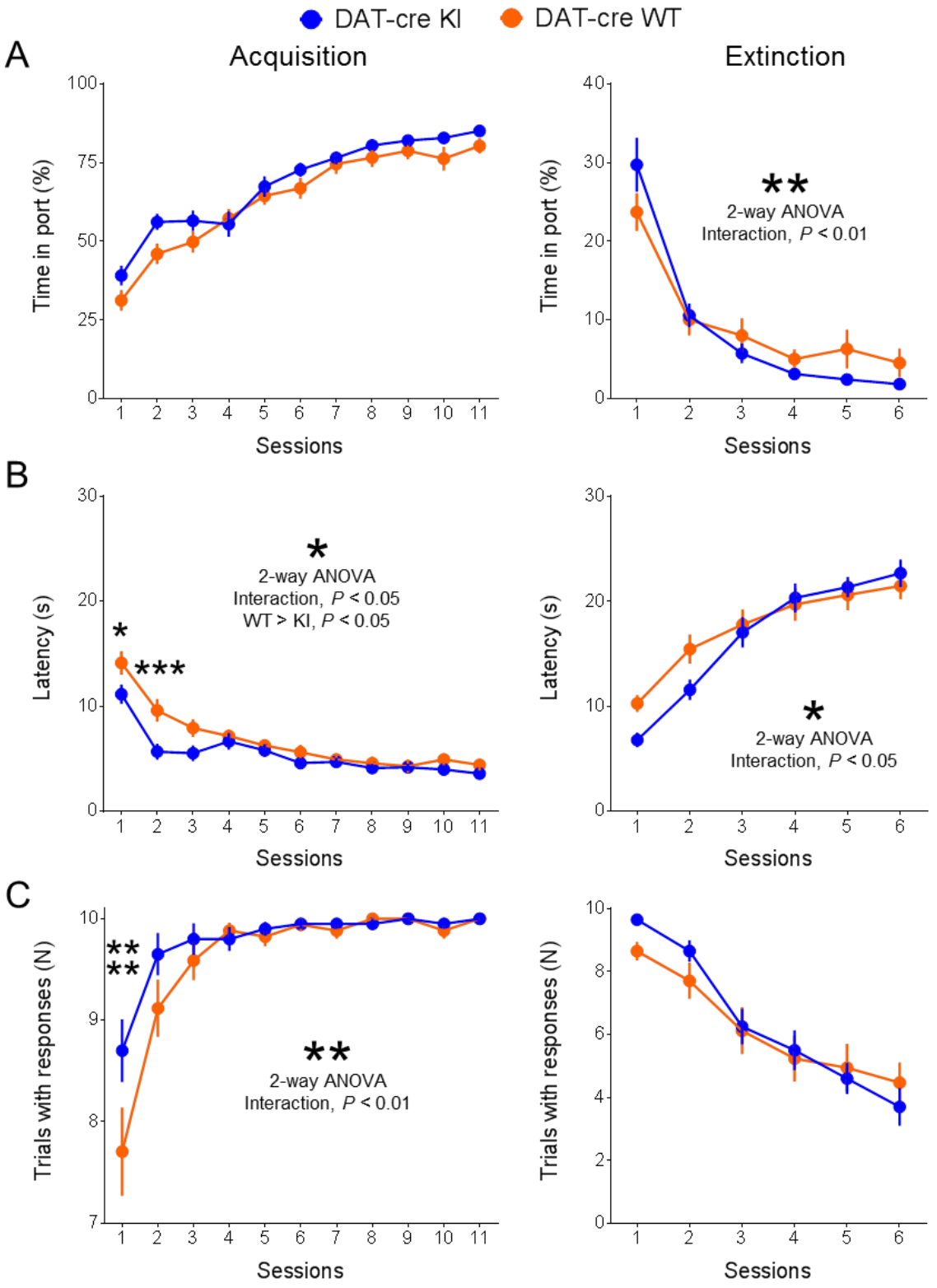

Figure 3.38. DAT-cre KI mice have faster acquisition and slower extinction than DAT-cre WT mice.

A: Performance in the time in port metric during CS presentation in acquisition and extinction. Note the faster response extinction for DAT-cre WT mice in relation to DAT-cre KI controls. B: Latency to response during CS presentation in acquisition and extinction. Note that DAT-cre KI mice showed a faster decrease in latency during acquisition, including the significant pair-wise difference during the first and second acquisition session (Sidak's multiple comparisons test), and a slower increase in latency during extinction. *$P < 0.05$; **$P < 0.01$.

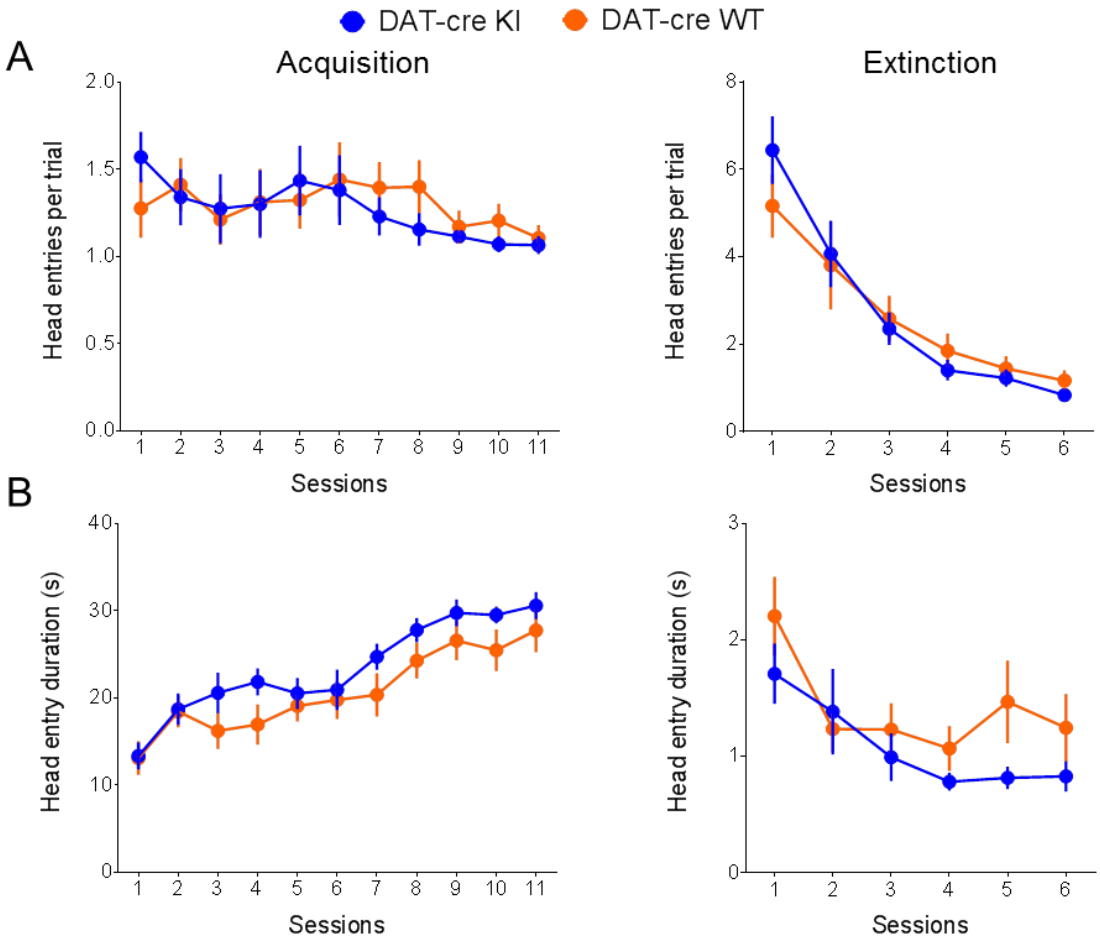

Figure 3.39. DAT-cre KI and DAT-cre WT mice have similar head entry dynamics during acquisition and extinction.
A: Number of directed head entries into the reward port during CS presentation for both genotypes. B: Duration of directed head entries into the reward port during CS presentation. Note the lack of a genotype in both measures effect during acquisition and extinction (two way repeated measures ANOVA).

3.4.2. Fitting DAT-cre KI and DAT-cre WT mice with a modified Rescorla-Wagner model

I also fitted and compared the trial by trial time in port values for DAT-cre KI and DAT-cre WT groups with a modified Rescorla-Wagner model (Figures 3.40, 3.41 and 3.42). Interestingly, the model fits between these two genotypes only differed significantly in the empirically derived parameter V_0 (Mann Whitney test, $P < 0.05$), i.e. the average response of the first three trials of acquisition, but not in best fit residuals, learning rates for positive and negative prediction errors (α_P and α_N, respectively), V_{min} or V_{max} (Mann Whitney test, $P > 0.05$). This means that the model only identified a significant difference in initial performance, likely indicating a difference in motivation.

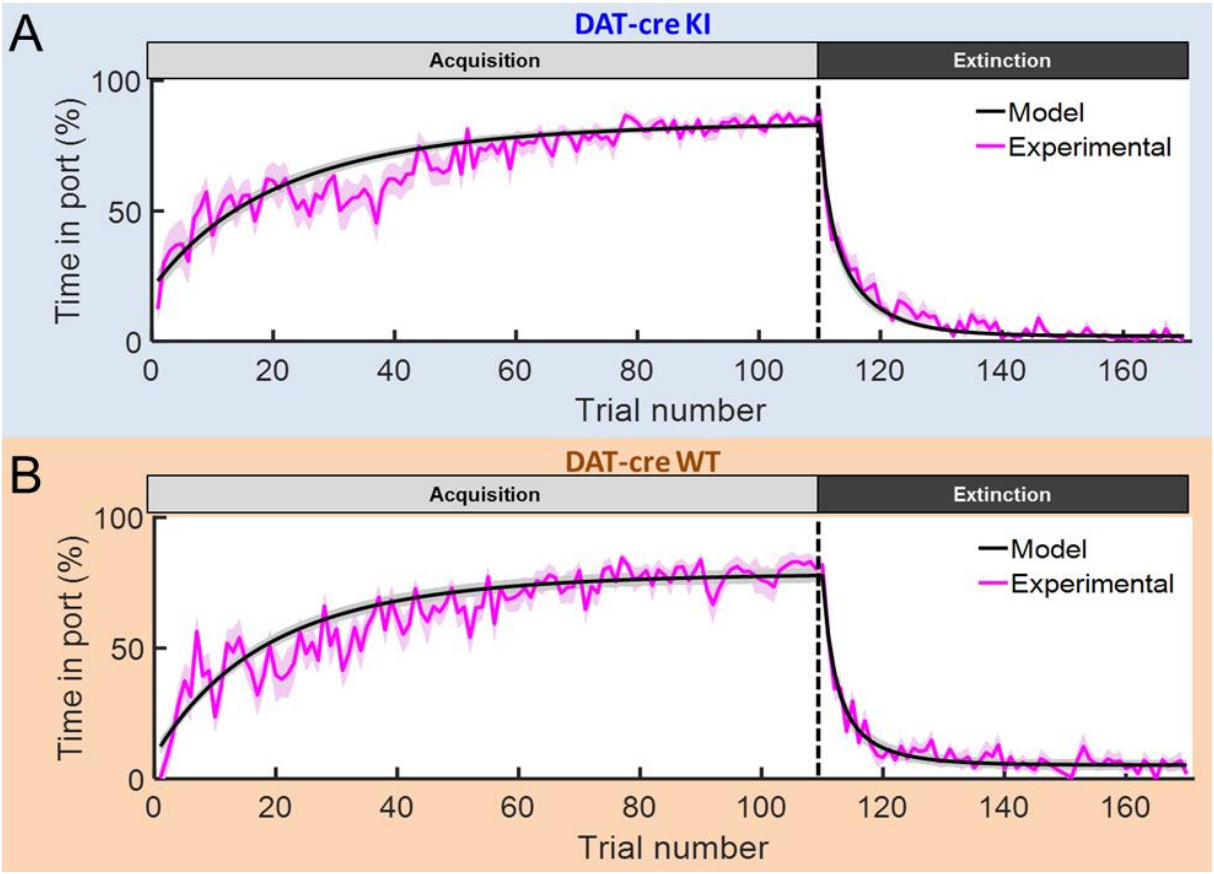

Figure 3.40. Fitted behavior from DAT-cre KI and DAT-cre WT mice with a modified Rescorla-Wagner model.
A: Trial by trial time in port (black and grey; mean ± SEM) and model fit (magenta and pink; mean ± SEM) in both acquisition and extinction for the DAT-cre KI group. B: Trial by trial time in port (black and grey; mean ± SEM) and model fit (magenta and pink; mean ± SEM) in both acquisition and extinction for the DAT-cre WT group.

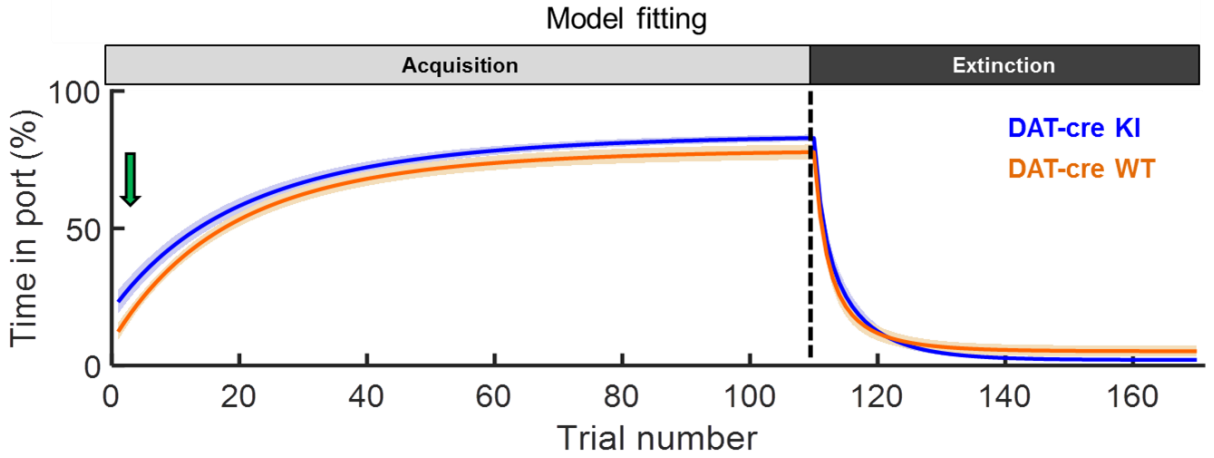

Figure 3.41. Overlay of model fits for DAT-cre KI and DAT-cre WT learning curves.
Note the model fits have different initial starting points, indicating different V_0 parameters (green arrow).

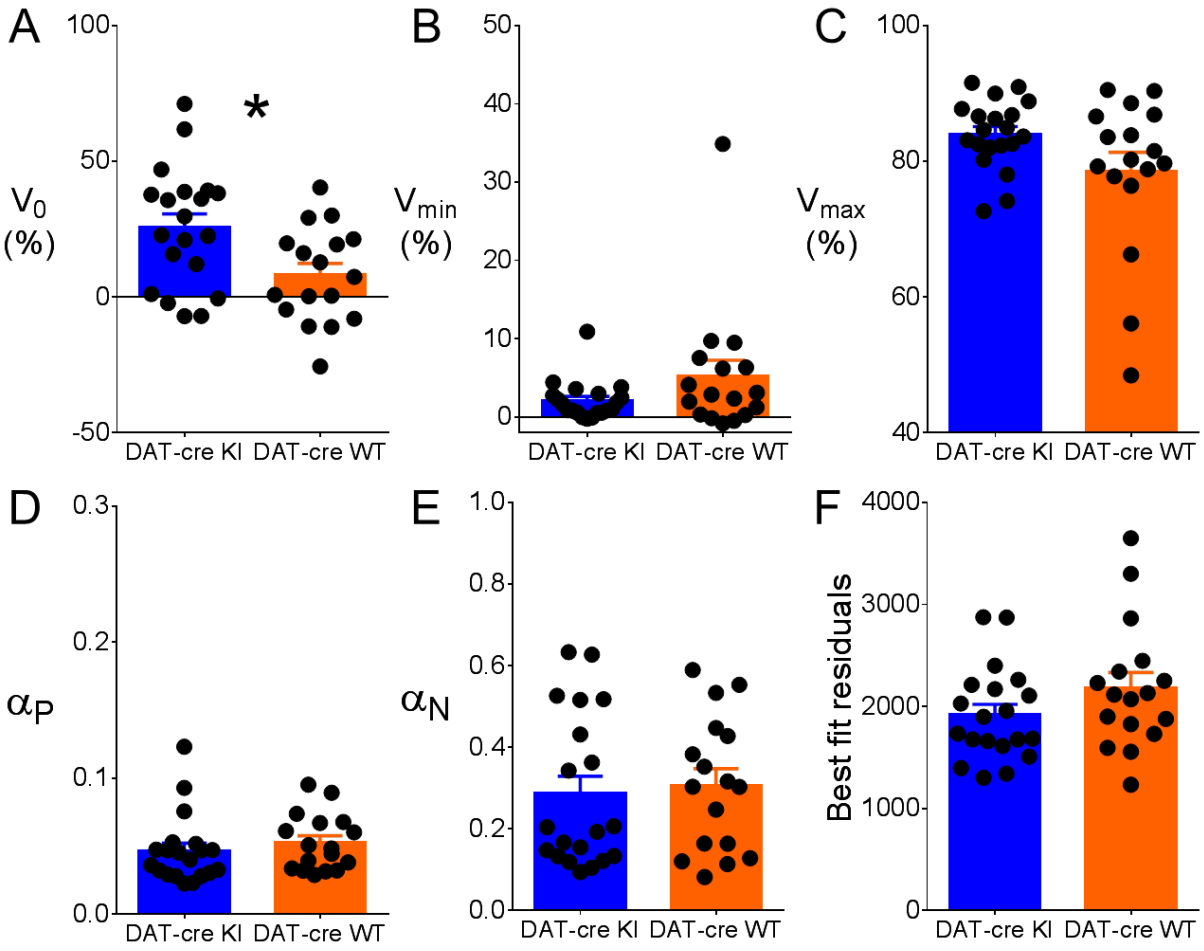

Figure 3.42. DAT-cre KI and DAT-cre WT model fits differ only in the V_0 parameter.
A: V_0 (initial assumed associative strength). B: V_{min} (minimal associative strength). C: V_{max} (maximal associative strength). D: F: Residuals of the best model fit for KChIP4 Ex3d and DAT-cre KI groups. Note that there was no significant difference observed between the compared groups except in the V_0 parameter (Mann Whitney tests, $P > 0.05$). *$P < 0.05$

3.4.3. DAT-cre KI and DAT-cre WT mice have similar spontaneous behaviors

In the open field task, there was no difference between DAT-cre KI and DAT-cre WT mice in any of the measured variables (Figures 3.43). Measures of total track length, proportion of activity (periods where movement velocity where velocity exceeded 5 cm/s), time spent in the center area, proportion of track length in center, number and duration of rearings, were statistically similar for both groups (unpaired T tests, P > 0.05). I also tracked these variables on a minute by minute basis over the duration of the task (Figures 3.44) and did not detect any difference between the genotypes for any of the analyzed indices of locomotion and exploration (no effect across genotypes or interaction with sessions, $F < 1.5$, $P > 0.05$ for all comparisons).

In the novel object preference task, in trial 1, mice from both the DAT-cre KI and DAT-cre WT groups explored the novel objects (same shape) with statistically similar total numbers of object visits and exploration time (Figure 3.45 B and C; unpaired T-test, $P > 0.05$ for both comparisons). In trial 2, where animals had to choose to explore a familiar or novel object, mice from both genotypes showed a marked preference for visiting the novel object, but there was no difference in that preference between the genotypes, both for the proportional number and duration of object exploration visits (Figure 3.46 D and E; unpaired T-test, $P > 0.05$). This finding was confirmed by calculating the object preference discrimination index, which was also similar across genotypes (Figure 3.46 F; unpaired T-test, $P > 0.05$). I also found no genotype effect on the total number of object visits and object exploration time in trial 2 (Figure 3.46 B and C; unpaired T-test, $P > 0.05$).

In the hole board exploration task, I also found no genotype effect for all tested variables: number of head-dips, total head-dip duration, proportion of head-dips made in the preferred hole, proportion of repeated head-dips, latency to first head-dip and mean head-dip duration (Figure 3.47, Mann Whitney tests, $P > 0.05$).

Finally, in the spontaneous alternation task, I also did not observe any significant difference between DAT-cre WT and DAT-cre KI controls in the number of spontaneous alternations or in the total number of arm entries during plus maze exploration (Figure 3.48, unpaired T-tests, $P > 0.05$), indicating that there was no genotype effect on working memory.

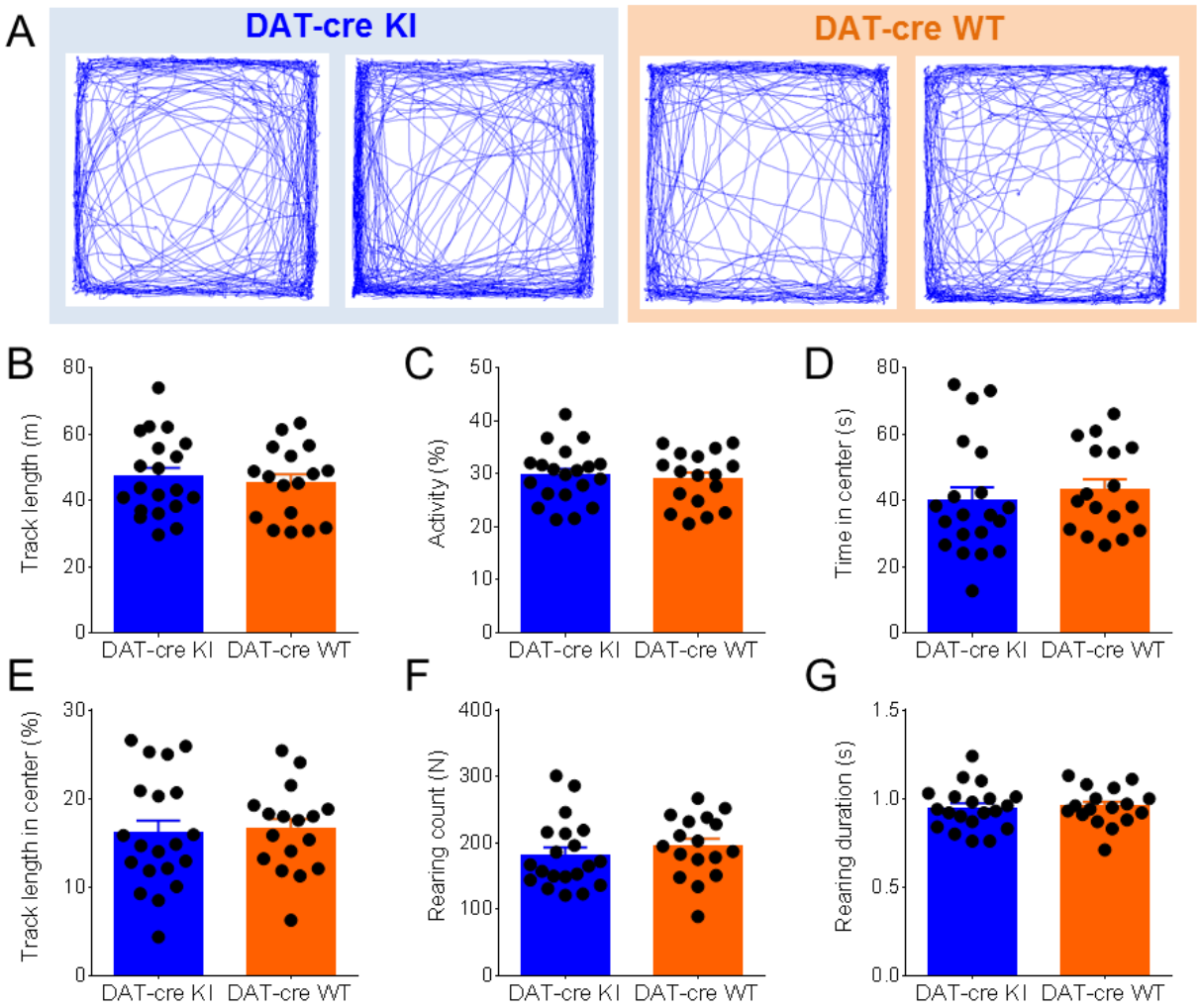

Figure 3.43. Behavioral performance of DAT-cre KI and DAT-cre WT mice in the open field. A: representative tracks from mice of both genotypes. B: track length. C: proportion of activity (periods where movement velocity > 5 cm/s). D: time in center. E: proportion of track length in center. F: number of rearings. G: duration of rearings. Note the absence of a genotype effect on these variables (unpaired T tests, $P > 0.05$).

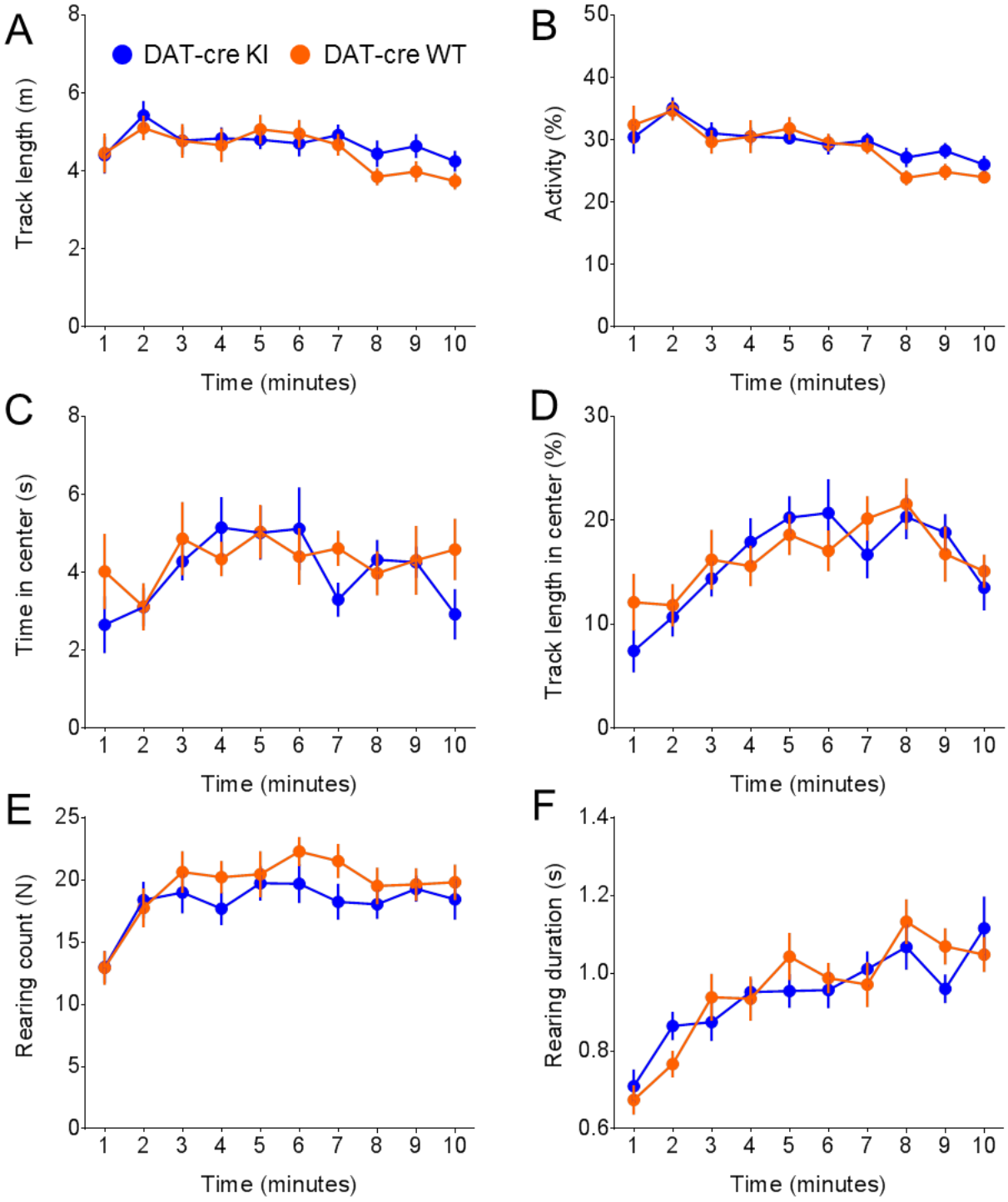

Figure 3.44. Behavioral performance of DAT-cre KI and DAT-cre WT mice in the open field across the duration of the test.

A: track length. B: proportion of activity (periods where movement velocity > 5 cm/s). C: time in center. D: proportion of track length in center. E: number of rearings. F: duration of rearings. Note the absence of a genotype effect on these variables (two-way repeated measures ANOVA, no effect across genotypes or interaction with sessions, $F < 1.5$, $P > 0.05$ for all comparisons).

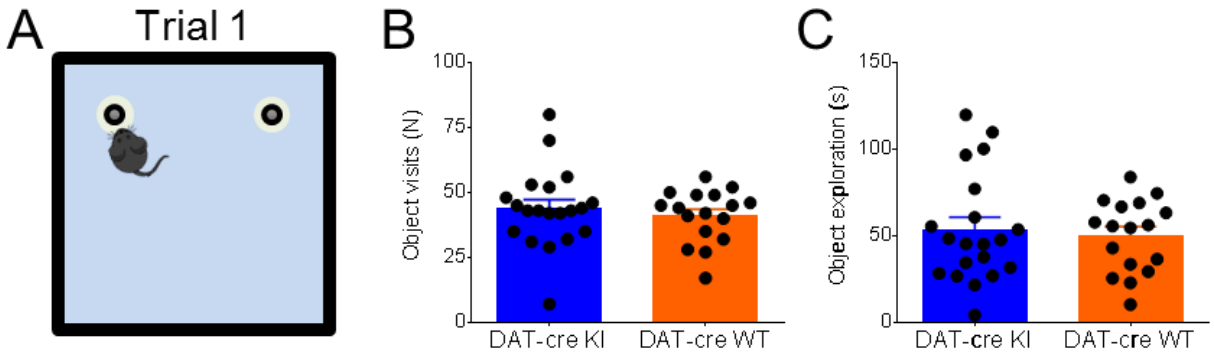

Figure 3.45. Behavioral performance of DAT-cre KI and DAT-cre WT mice in trial 1 of the novel object recognition task.
A: Cartoon representation of object disposition during trial 1 of the task. Note that both objects are similar in shape. B: number of total object visits. C: total object exploration time. Note the absence of a genotype effect on these variables (unpaired T tests, $P > 0.05$)

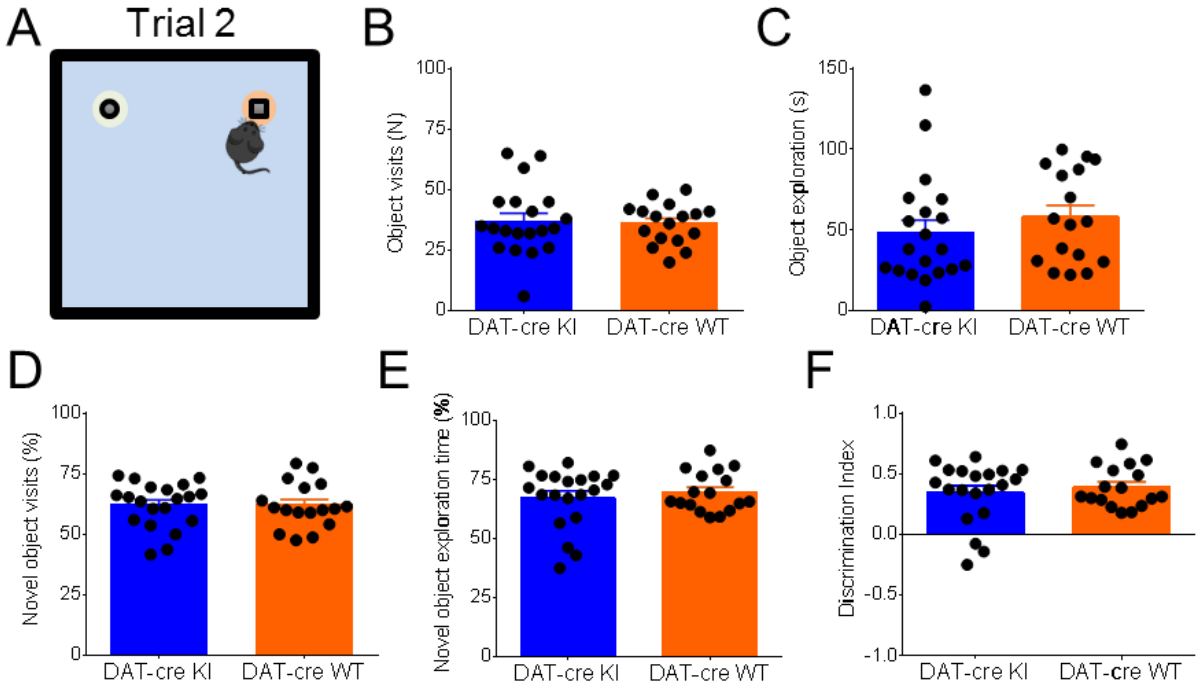

Figure 3.46. Behavioral performance of DAT-cre KI and DAT-cre WT mice in trial 2 of the novel object recognition task.
A: Cartoon representation of object disposition during trial 2 of the task. Note that one of the objects has been replaced by another object with different shape. B: number of total object visits. C: total object exploration time. D: proportion of novel object exploration visits. E: proportion of novel object exploration time. F: discrimination index in trial 2 of the task. Note the absence of a genotype effect on these variables (unpaired T tests, $P > 0.05$). Note that mice from both genotypes displayed a marked preference for exploring the novel object.

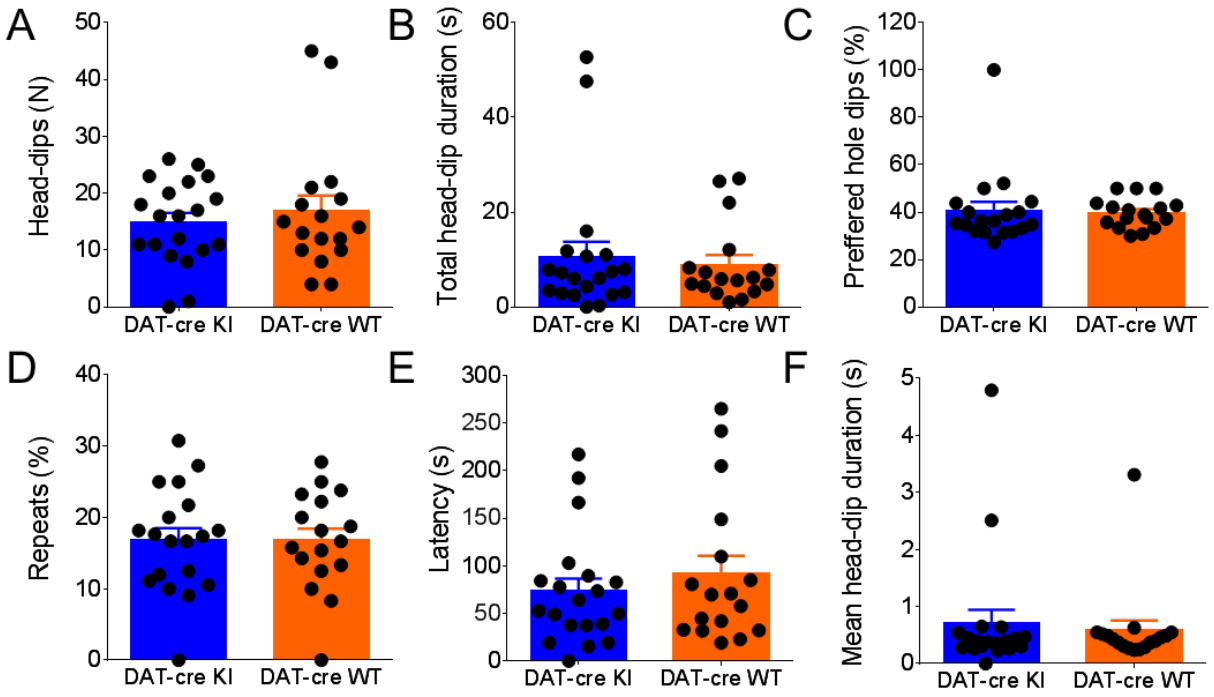

Figure 3.47. Behavioral performance of DAT-cre KI and DAT-cre WT mice in the hole board. A: Total number of head dips. B: total head-dip duration. C: proportion of head dips into the preferred hole. D: proportion of repeat head-dips. E: latency to first dip. F: mean head-dip duration. Note the absence of a genotype effect on these variables (Mann Whitney tests, $P > 0.05$).

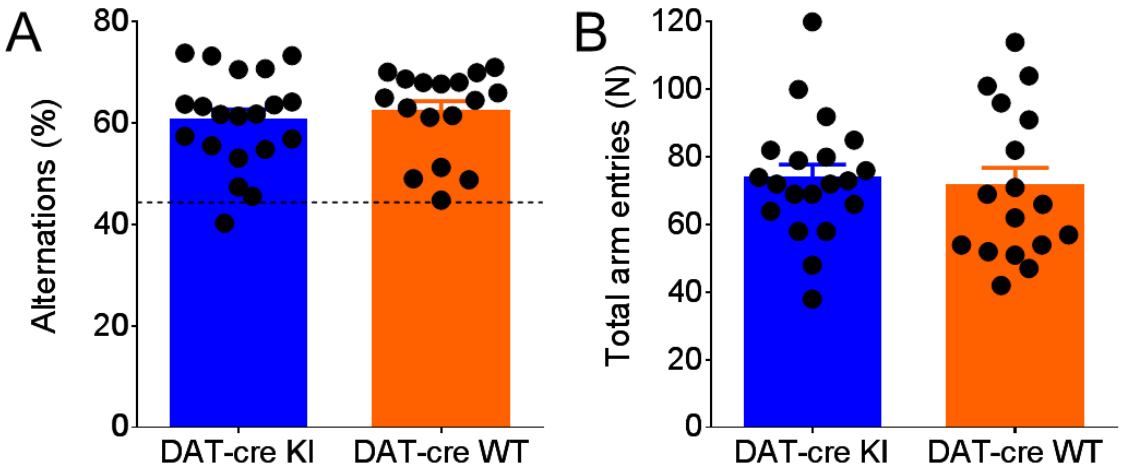

Figure 3.48. Behavioral performance of DAT-cre KI and DAT-cre WT mice in the spontaneous alternation task.
A: proportion of spontaneous alternations (in relation to the total possible alternations). Dotted line indicates chance performance level. B: Total arm entries performed during the task. Note the absence of a genotype effect on these variables (unpaired T tests, $P > 0.05$).

4. Discussion

4.1. Full KChIP4 KO reduces spontaneous pausing of VTA DA neuron activity

I found that the full KO of the KChIP4 gene had a surprisingly selective effective on the spontaneous firing pattern of VTA, but not SN, DA neurons in relation to WT controls. KChIP4 KO specifically reduced the frequency and duration of spontaneous firing pauses, as defined with two different detection algorithms, the maximum ISI range of VTA DA neurons and the measures of skewness and kurtosis of the ISI distribution, without affecting any other firing parameter, including mean frequency, bursting and CV (Figures 3.3 to 3.7). These results are congruent with the previous *ex vivo* findings from our lab that KChIP4 KO slowed down the inactivation of I_A and decreased firing pauses generated by inhibition via hyperpolarizing current injections in VTA DA neurons (Kashiotis, 2013). Indeed, my results indicate that the biophysical phenotype of KChIP4 KO observed *ex vivo*, namely the removal of an intrinsic amplifier of hyperpolarizing inhibition, is related to reduced spontaneous pausing *in vivo*.

Importantly, this phenotype was confirmed using two statistical methods for detecting pauses in non-stationary spike trains with very different assumptions. Both the RGS method, which takes into account local statistical structures for detecting unexpectedly long ISIs, and my novel outlier-based algorithm, which established a non-parametric threshold for identifying ISIs that far exceed the interquartile range of the total ISI distribution of a given spike train, confirmed that KChIP4 KO VTA DA neurons displayed fewer and shorter pauses in relation to WT controls within similar effect size ranges (Figures 3.10 to 3.19). Importantly, the outlier-based pause detection algorithm ignored pauses that were preceded by bursts, which could potentially be generated by depolarization block and SK channels (Paladini and Roeper, 2014). Likewise, the ISI distribution had drastically reduced skewness, kurtosis and maximum range. Finally, this phenotype was entirely selective for VTA DA neurons, as I did not observe changes in pause number and duration in SN DA neurons. These results strongly suggest that the observed change in firing pauses is not a false positive result, but a feature of KChIP4-dependent modulation of inhibition in VTA DA neuron.

Why did KChIP4 KO not affect mean firing frequency and CV? It would stand to reason that the removal of long ISIs by KChIP4 KO would decrease the CV of the ISI distribution, as well as increase the mean firing frequency. However, due to the relative low number of pauses in relation to the total number of ISIs, this did not happen. Pauses are, almost by definition, relatively rare events in ISI distributions. In WT VTA DA neurons, the maximum incidence of outlier-detected pauses observed in a single spike train was 6/minute, and the median number was 0.6/minute, while the median number of ISIs in a spike train was around 2400 (from a median firing frequency of ≈4 Hz over 10 minutes) and the minimal number of ISIs was ≈425 (from a median firing frequency of 0.7 Hz over 10 minutes). This would mean that at most pauses comprise 14% of all ISIs in a distribution, but usually this was less than 1%. Due to this reason, the number of pauses had little influence on the mean frequency and CV of VTA DA neurons within the ranges observed in this study. Similarly, ACH-based classification of VTA DA neurons was not affected (Figure 3.7), as a large proportion of ISIs would have to be affected in order to change autocorrelation patterns.

These results suggest that Kv4.3-mediated I_A in some VTA DA neurons is likely not active in steady-state conditions, only being revealed during pronounced hyperpolarization (Khaliq and Bean, 2008). As VTA DA neurons express less SK channels in relation to SN DA neurons, and therefore do not show prominent AHPs, the maximal hyperpolarization amplitudes and depolarization slopes during the ISIs in normal pacemaker firing are likely not enough to promote the activation of I_A after each AP, precluding a role for this current in tuning ISI duration (Liss et al., 2001; Wolfart et al., 2001; Khaliq and Bean, 2008). Likewise, all aspects of bursting activity were also not affected by KChIP4 KO, including SFB and intraburst statistics (Figure 3.4 to 3.6). Post-burst pauses were also not affected by KChIP4 KO (Figure 3.20). This suggests that potential SK-mediated post-burst AHPs are not enough to significantly activate I_A in VTA DA neurons. This would imply that *in vivo* post-burst pauses in these neurons are due primarily to depolarization block, or perhaps that bursting may drive Kv4.3 channels into inactivation.

One unexpected phenotype I identified was that AP width in VTA DA neurons of KChIP4 KO was modestly (10%) but significantly ($P < 0.05$) longer than in WT controls, due to an increase in repolarization time (Figure 3.8). A similar trend was

also observed in previous *ex vivo* recordings of these neurons conducted in our laboratory, but it did not reach statistical significance (Kashiotis, 2013). Because they are activated by subthreshold voltage ranges, Kv4 channels are usually not heavily implicated in neuronal AP repolarization (Kimm et al., 2015). However, Kv4.3 channels are known contributors to AP repolarization in cardiac myocytes, and Kv4.2 channels have been reported to regulate AP width and repolarization time in cultured hippocampal pyramidal cells (Dixon et al., 1996; Kim et al., 2005). My results suggest that Kv4.3 channels may modestly contribute to AP repolarization in VTA DA neurons. However, it is also possible that KChIP4 KO might indirectly lead to reductions in the expression of other K^+ channels which are involved in AP repolarization, such as Kv2 and big conductance Ca^{++}-activated K^+ (BK) channels (Kimm et al., 2015). The mechanism of KChIP4 KO effects on AP width therefore still needs to be explored more rigorously, specifically with the recording of VTA DA neuron APs after Kv4.3 pharmacological or genetic manipulation.

4.2. KChIP4a as a selective modulator of learning from negative feedback

I found that the deletion of KChIP4 exon 3 in DA neurons selectively enhanced extinction of a conditioned response, without changing acquisition learning, in relation to littermate controls (Figures 3.21 to 3.24). KChIP4 Ex3d mice had a faster response reduction during extinction as measured by the time spent in port and number of head entries during cue presentation, response latency and probability of responding to cue presentation. Importantly, during the very first extinction trial the performance between the groups was not distinct, with significant differences in performance parameters only occurring from the second or third trial onwards. Over multiple sessions, the performance of KChIP4 Ex3d and DAT-cre KI controls eventually converged, with the groups showing similar performances in all behavioral metrics in the fourth, fifth and sixth extinction sessions. This confirms that the effect during extinction is not due to a generalized decrease in responding in the absence of a reward, but is rather a learning phenotype, which requires the updating of expected value over multiple trials.

Importantly, head entry dynamics revealed that the decrease in time in port during the cue observed in KChIP4 Ex3d mice was due only to a decrease in the number, not the duration, of directed head entries. This is a crucial piece of information as it implies that KChIP4 Ex3d does not affect immediate decision making in the face of the omission of an expected reward, i.e. the decision to remove the head from the reward port (stop the reward-seeking action mid-execution; see section 4.3).

Another important finding was that KChIP4 Ex3d did not affect performance in spontaneous behaviors. These animals were similar to controls in open field exploration, novel object preference, hole board exploration or spontaneous alternation in the plus maze (Figures 3.31 to 3.36). The open field results demonstrate that there is no baseline difference in locomotor activity (as indicated by the track length and activity measures), anxiety (measured by the time and track length in the center of the arena) and exploratory drive (measured by the rearing activity and track length dynamics over time) between this group and the controls (Walsh and Cummins, 1976; Crawley, 1985, 2007).

The novel object preference test showed that KCHIP4 Ex3d does not affect novelty-induced exploration, object recognition memory and novelty preference (Ennaceur and Delacour, 1988; Antunes and Biala, 2012). The hole board test confirmed that disrupting KChIP4a expression in DA neurons does not affect exploratory drive, anxiety and novelty preference, while also showing that head-dipping behavior itself was not affected by KChIP4 Ex3d (Nolan and Parkes, 1973; File and Wardill, 1975; Crawley, 1985, 2007; Takeda et al., 1998). Finally, the spontaneous alternation test suggested that KChIP4 Ex3d did not affect working memory (Ragozzino et al., 1996; Lennartz, 2008).

These combined results suggest that KChIP4 Ex3d does not affect any baseline behavior, and – in the context of conditioning – it does not affect motivation, acute decision making during reward omission, reward valuation or acquisition learning rate. Indeed, the effect of KChIP4 Ex3d was highly selective for extinction learning rates. In order to formally test if these effects were attributable to a deficit in learning from negative prediction errors, I fitted the time in port metric of KChIP4 Ex3d and DAT-cre KI controls during the two phases of conditioning with a modified Rescorla-Wagner, fitting different α learning parameters to learning from positive and negative

prediction errors (Figures 3.25 to 3.30). This analysis revealed that KChIP4 Ex3d mice only differed from controls by displaying higher α_N values, supporting the idea that they learn faster from negative prediction errors. All other fitted model parameters, namely α_P $V_{0,}$ V_{min} and V_{max} were similar between KChIP4 Ex3d and controls, demonstrating that the behavioral differences between these groups were not likely to be cause by changes in learning from positive prediction errors, initial responding before conditioning or both maximal and minimal response levels. Based on this finding, I propose that KChIP4a is a selective modulator of formal negative prediction error-based learning.

Semi-quantitative IHC for Kv4.3 channels in TH colocalized ROIs demonstrated that KChIP4 Ex3d mice had a significantly elevated expression of these subunits in DA neurons located in both the SN and VTA (Figure 3.37). This increase was, however, larger in the VTA (≈60% increase) in relation to the SN (≈40% increase), suggesting that disruption of KChIP4a expression affects VTA DA neurons more than SN DA neurons. The increased expression of Kv4.3 in KChIP4 Ex3d mice provide a mechanistic explanation for the accelerated extinction observed in this mouse line, as an a larger density of Kv4.3 channels would results in an increased I_A density in DA, which would thus potentiate the endogenous amplification of hyperpolarizing inhibition, enhance the pause-duration coding of negative prediction errors by DA neuron firing, increase the time in which ventral striatal indirect pathway MSNs are released from D2R-dependent inhibition, and speed up learning from negative prediction errors, as validated by computational fitting to a Rescorla-Wagner model. In order to fully test this causal mechanistic chain, additional experiments would need to be conducted. In the following sections, I will discuss the details of each mechanistic stage of this hypothesis and which experiments would be necessary to test them.

4.3. Circuit mechanisms of the behavioral effects of KChIP4 Ex3d

How could the removal of KChIP4a from DA neurons selectively affect only one aspect of learning? Assuming that the molecular phenotype of KChIP4 Ex3d is indeed an increase in negative prediction error-related hyperpolarizing inhibition, the behavioral effects can be explained by assuming that this effect is restricted to

specific DA pathways. Previous studies have demonstrated that individual components of cue-outcome and action-outcome learning are mediated by separate, parallel DA -modulated circuits in the basal ganglia. Part of this functional subdivision has been introduced in section 1 of this thesis, in particular the proposed functional division between dorsal striatum (more involved in movement control) and ventral striatum (more involved in learning and motivation), as well as the differences between the direct ("go") and indirect ("no go") pathways. However, there is also evidence that highly specific components of value-based behaviors (including value-dependency, speed, accuracy and probability) are regulated by separate basal ganglia networks (Hikosaka et al., 2014, 2017; Dudman and Krakauer, 2016; Schmidt and Berke, 2017). For example, MSNs located in the rostral (a.k.a. the head) and caudal ends (a.k.a. the tail) of the primate dorsal striatum seem to be respectively involved in goal-oriented (value-guided) and "automatic" (non-value guided) gaze orientation (Hikosaka et al., 2014; Kim and Hikosaka, 2015).

In this context, a recent study by Tecuapetla et al (2016) found that, in mice trained to press a lever to obtain rewards, optogenetic manipulation (both inhibitory and excitatory) of D1R- and D2R expressing MSNs lead to a reduced number of reward-seeking behavior (bouts of lever pressing). However, the behavioral effects that lead to this decreased performance were very different according to the cell-type that was being controlled. Manipulation of D2R-expressing MSNs in the dorsal striatum made the animals abort the initiation of reward-seeking behaviors, without impairing their execution once they were initiated; mice instead engaged in other behaviors, including the exploration of the Skinner-box, thus reducing the probability of lever pressing. Conversely, manipulation of D1R-expressing MSNs slowed down the initiation of reward-seeking behavior, but did not affect the animals' engagement in the task (mice remained close to the lever, but were slower to perform the lever presses). The authors' conclusion was that specific patterns of activity in indirect pathway MSNs in the dorsal striatum are responsible for coding the probability of performing a reward-seeking behavior, while the activity of direct pathway MSNs regulates the vigor or speed with which a behavior is executed.

In light of this study (keeping in mind the functional differences between DA signaling in different regions of the striatum), as well as other literature on the control of reward-seeking behavior by separate basal ganglia circuits, the faster decrease in

response probability and the number of head entries in KChIP4 Ex3d mice, without an accompanying effect on the duration of head entries, may be due to a relatively higher increase in the activation of D2R-expressing MSNs over the extinction learning period (thereby leading to less action initiation).

The behavioral differences between KChIP4-Ex3d mice and DAT-cre KI controls also suggest that the effects of this manipulation are relatively restricted to certain striatal regions. Previous studies have shown that closed-loop stimulation of direct or indirect pathway MSNs in the dorsal striatum during action performance lead to immediate changes in movement kinematics (Tecuapetla et al., 2016; Yttri and Dudman, 2016). Given that I did not observe an effect in the duration of head entries (a cue-triggered reward seeking behavior) it is likely that DA signaling in the dorsal striatum is relatively unaffected in KChIP4 Ex3d mice. This is, of course, corroborated by the fact that both genotypes had similar locomotor performance in the open field (Révy et al., 2014; Barbera et al., 2016).

In addition, the fact that the differences in behavioral performance in KChIP4 Ex3d mice were only expressed over multiple trials and sessions also suggests that KChIP4a may have a more prominent role in controlling the integration of inhibition in neurons that project to the ventral striatum, as the activity of MSNs in this region codes and is essential for progressive reward-based learning, but not for action performance (Atallah et al., 2007, 2014). Furthermore, studies that have quantified DA release in different regions of the ventral striatum during conditioning learning or value-based decision making have consistently shown that decreases in DA concentrations in response to negative prediction errors are more prominent in the NAcc core than in the NAcc shell (Sugam et al., 2012; Sunsay and Rebec, 2014; Biesdorf et al., 2015; Saddoris et al., 2015).

Therefore, the most likely explanation for my behavioral results, from a circuit perspective, is that KChIP4 Ex3d promotes a selective amplification of negative prediction error-related hyperpolarizing inhibition primarily in DA neurons that project to the NAcc core, leading to increased activity and plasticity in indirect pathway MSNs in that region. It is still possible however, that other DA neuron populations, and therefore other DA-modulated circuits, are affected in KChIP4 Ex3d mice, but that the behavioral experiments applied in this thesis were not able to reveal these effects, either because they were too subtle to be detected or because they are

involved in behaviors that were not explicitly tested. In order to test this conclusion, it would be necessary to track DA signals or record the activity of identified D1R and D2R MSNs in different regions of the striatum of KChIP4 Ex3d mice. One potential experimental approach would be to use fiber photometry methods to record bulk Ca^{++} signals from the axons of DA neurons or the soma of specific populations of MSNs in these mice while they execute a reward prediction error-based task (Cui et al., 2014a; Gunaydin et al., 2014; Lerner et al., 2015; Kim et al., 2016; Tecuapetla et al., 2016; Menegas et al., 2017). A more sophisticated version of these experiments would involve recording Ca^{++} transients from individual DA axons or MSNs using *in vivo* deep tissue two-photon or (for recording from MSNs) fluorescence microscopy (Howe and Dombeck, 2016; Klaus et al., 2017). In addition, it would be interesting to perform single-unit electrophysiological from genetically identified MSNs in different striatal regions, given that Ca^{++} imaging does not yet have the resolution to dissect firing patterns at single AP in many cell types (Kravitz et al., 2013; Klaus et al., 2017).

Other approaches to this question could involve the direct recording of sub-second DA release in the NAcc core and other striatal regions using cyclic voltammetry during behavior (Sugam et al., 2012; Sunsay and Rebec, 2014; Biesdorf et al., 2015; Saddoris et al., 2015). Aside from methods which involve recording mesolimbic core signals in a behavioral context, the circuit basis of this hypothesis could also be answered by transiently inducing hyperpolarizing inhibition of DA neurons (either optogenetically or by exciting inhibitory afferents) and recording the effects in the striatum with electrophysiological, Ca^{++} imaging or electrochemical methods. If my hypothesis is correct, a transient inhibition of DA neurons should be amplified in KChIP4 Ex3d mice, and therefore lead to enhanced post synaptic effects, preferentially in the NAcc core, in relation to controls. Relatively simple behavioral correlates, such as real time place-preference, could be used to monitor the behavioral correlates of these manipulations (Lammel et al., 2012; Stamatakis and Stuber, 2012b).

4.4. Physiological effects of KChIP4 KO versus KChIP4 Ex3d on DA neurons

The results from the two main sections of this thesis display an apparent contradiction. If a full knockout of the KChIP4 gene reduces pauses in VTA DA neuron activity, one would predict that removing KChIP4a modulation of Kv4.3 channels selectively in DA neurons would impair learning from disappointment. However, I observed an increased acceleration of extinction in the KChIP Ex3d mice. I believe the answer to this conjectural conundrum lies in the different effects of the splice-variant selectivity of the KChIP4 Ex3d experimental construct versus the complete KChIP4 gene knockout. In KChIP4 Ex3d mice, only the KChIP4a splice variant is deleted, but the cell is expected to be capable of expressing all other splice variants of the KChIP4 gene, i.e. KChIP4b, KChIP4bL, KChIP4c, KChIP4d and KChIP4e (Jerng and Pfaffinger, 2014). These other alternative splice variants lack the N-terminal KISD, and therefore are expected to affect Kv4.3 subunits mainly by blocking its ER-retention motif, thereby increasing channel surface expression and increasing I_A amplitudes, as has been confirmed for the KChIP4bL and KChIP4e variants (Shibata et al., 2003; Jerng and Pfaffinger, 2008; Zhou et al., 2015).

It is also important to remember that KChIP4a dramatically increases inactivation time constant and closed state inactivation, while most other variants of KChIP1-3 have the opposite effect on closed state inactivation and have a much more mild effect on inactivation kinetics (Holmqvist et al., 2002; Patel et al., 2002; Bähring and Covarrubias, 2011) and that the ultimate effect of any given KChIP variant is stoichiometric and dependent on its relative expression level in relation to all other KChIP variants in the cell (Kitazawa et al., 2014; Zhou et al., 2015), with the ultimate effect on current density being an integration of the effects of each KChIP splice variant on Kv4 surface expression and inactivation properties.

In order to test this, it would be necessary to record A-type currents from DA neurons in KChIP4 Ex3d mice using voltage clamp techniques (thus resolving its biophysical properties) and to use cell-specific methods (such as single cell real-time reverse transcriptase PCR (RT-qPCR) for quantifying the expression levels of each KChIP variant in these cells (Liss et al., 2001; Liss and Roeper, 2004; Lammel et al., 2008). In addition, one could use freeze-fracture electron microscopy combined with IHC (immuno-EM) to quantitatively determine if KChIP4 Ex3d really increases the membrane expression of Kv4.3 subunits (Subramaniam et al., 2014a).

Our results suggest that in the KChIP4 KO mice the complete deletion of all KChIP4 splice variants, including the ones that promote increased surface expression (e.g. KChIP4BL), which ultimately leads to observed faster inactivation time constant, but without a large effect on current amplitude (Kashiotis, 2013). This leads to a decreased K^+ charge transfer, less effective hyperpolarizing inhibition and ultimately in fewer observable pauses in VTA DA neuron activity *in vivo*. On the other hand, when I selectively removed the KChIP4a splice variant in the KChIP4 Ex3d mice, I allowed for the other KChIP4 variants (such as KChIP4bL and KChIP4e) to continue to exert their effects. Ultimately, this is expected to increase in I_A peak amplitude and charge density despite potentially faster inactivation kinetics. This manipulation then triggers a chain of mechanistic steps by which the increased I_A amplitude presumably potentiates hyperpolarizing inhibition, increasing negative prediction error-dependent pauses in DA neuron activity and ultimately resulting in an observable acceleration of extinction learning.

This hypothesis could be tested by recording these neurons in current clamp and testing whether hyperpolarization –by direct current injection, simulation of GABAergic synaptic input with dynamic clamp, puffs of inhibitory neurotransmitters onto the cell body or even direct stimulation of inhibitory afferents – is extended in time in DA neurons of KChIP4 Ex3d mice in relation to controls (Nugent et al., 2007; Khaliq and Bean, 2008; Deister et al., 2009; Tarfa et al., 2017). It is also likely that this proposed amplification of inhibition is more relevant for the control of the temporal summation of inhibitory inputs, i.e. the effectiveness with which multiple trains of inhibitory synaptic potentials are able to pause DA neuron firing (Paladini and Roeper, 2014). To test this, an experimenter would have to examine how different frequencies and durations of hyperpolarizing events are integrated by DA neurons in KChIP4 Ex3d and DAT-cre KI controls.

A comparison of the results from the KChIP4 KO and KChIP4 Ex3d is a powerful indicator that DA neurons may use relative alternative splicing mechanisms to bidirectionally tune hyperpolarizing inhibition, assuming that the differences in pausing in the KChIP4 KO VTA DA neurons is primarily due to post-synaptic effects. This would mean that a given DA cell could either increase or decrease the gain of phasic synaptic inhibition by changing the ratio of KChIP4a expression in relation to other KChIP4 and KChIP1-3 isoforms. In the subsequent sections I will discuss the

implications of this interpretation for the understanding of DA neuron physiology in health and disease, as well as potential experimental approaches to address them.

4.5. Potential implications for synaptic integration and plasticity

4.5.1. Integration of phasic hyperpolarizing inhibition and tuning of specific GABAergic synapses

Neurons adjust the strength of individual synapses depending on homeostatic load and computational necessity (Turrigiano, 2012; Keck et al., 2017). Current theories postulate that this is underlined by local molecular processes, including synapse-specific activity-dependent mRNA trafficking, protein synthesis and membrane insertion of synaptic receptors (Sutton and Schuman, 2006). Part of the utility of synapse-specific tuning is enabling the cell to respond differently to inputs from different upstream regions. Recent studies have demonstrated that GABAergic synapses on VTA DA neurons from different afferent nuclei have distinct subunit composition and plasticity responses to repeated synaptic stimulation, as well as different roles in behavior (Edwards et al., 2017; Simmons et al., 2017). The results presented in this thesis highlight the potential of Kv4.3-mediated amplification or dampening of inhibitory input due to differential expression of different KChIP subunits. Our lab has previously reported that somatodendritic Kv4.3 channels in SN DA neurons are not homogeneously distributed within the membrane or across synapses, but rather cluster around certain individual putative GABAergic post-synaptic regions (Subramaniam et al., 2014a). This opens the possibility that KChIP-modulated Kv4.3 channels selectively control the strength of synapses from one or more individual input regions, and that the cell may dynamically change the properties of Kv4.3 currents in a synapse-specific manner through local expression of different KChIP subunits. Specifically, increasing the amplitude or duration of GABAergic IPSPs can potentially not only increase the inhibitory effects of individual IPSPs but also extend the window for their temporal summation.

Future studies could directly test the first part of this hypothesis by selectively stimulating GABAergic inputs from different regions (likely using optogenetics) in the presence of Kv4.3 channel blockers, such as the scorpion toxins AmmTX3 or phrixotoxins, and activators, such as NS5806, and/or in KChIP4 Ex3d mice versus

DAT-cre KI controls (Calloe et al., 2008, 2010; Lundby et al., 2010; Kimm and Bean, 2014; Tarfa et al., 2017). The experimenter would then determine if the intensity and duration of IPSCs and IPSPs, as well as the effect of terminal stimulation on DA cell firing, triggered by the stimulation of individual upstream inputs are differentially affected by the pharmacological or genetic modulation of Kv4.3 channels.

Another important issue is the potential effect of KChIP4a and Kv4.3 on spatial integration in dendrites. Neurons perform compute information through integration of synaptic input, which is largely shaped by the morphological and biophysical properties of their dendrites (London and Häusser, 2005; Stuart and Spruston, 2015). In general, the propagation of post-synaptic potentials along dendrites can be amplified, dampened either linearly or non-linearly by the passive and active membrane properties of the dendrites, with the ultimate effect on post-synaptic firing rate being determined by the geometrical organization of dendritic branching and synaptic connectivity (London and Häusser, 2005; Bui et al., 2008). In this context, the effectiveness of a GABAergic synapse in reducing neuronal firing rates depends on its relative location to the soma and how post-synaptic inhibitory potentials are amplified or dampened by membrane properties along the dendrites (London and Häusser, 2005). For example, active amplification of synaptic inputs, similar to what I propose for the KChIP4a-Kv4.3-GABA interaction, can increase the effectiveness of GABAergic synapses that are located distal to the AIS, both by amplifying individual IPSPs (which would propagate farther down the dendritic tree) and by increasing temporal summation (Kuo et al., 2003; Hyngstrom et al., 2008). Therefore, it could be that in physiological conditions the local dendritic expression or trafficking of KChIP4a regulates the integration of distal versus local GABAergic inputs by modulating the amplitude and time constants of propagating IPSPs.

GABAergic synapses also play an important role in filtering excitatory input along dendritic arbors, as local inhibition downstream of excitatory synapses can shunt or override depolarizing inputs (Koch et al., 1983; Marlin and Carter, 2014). In DA neurons, it has been proposed that back-propagating dendritic spikes can adjust the gain of excitatory synaptic inputs, as has also been proposed in other cell types (Häusser et al., 1995; Holthoff et al., 2006; Hage and Khaliq, 2015). This would mean that GABAergic synapses on DA neuron dendritic branches could potentially serve as both downstream and upstream filter nodes, by shunting or overriding both distal

EPSPs and back-propagating spikes in specific contexts or for specific inputs. In this hypothetical framework, a single GABAergic IPSP could “shut off” entire sections of a cell’s dendritic arbor for extended periods of time (>500 ms) through amplification by KChIP4a, and this property could be dynamically regulated by local variations in KChIP4a expression. This would have interesting functional consequences for dendritic processing in DA cells. For example, this could be a mechanism by which individual dendrites could be tuned to veto specific categories of excitatory inputs in a contextual manner, or define dendrites that would be less likely to have synapses that will undergo LTP. These speculative propositions beckon future experimental investigation given their potential implications for dendritic processing in DA neurons.

4.5.2. Effects on DA neuron synaptic plasticity

Can the KChIP4-Ex3d phenotype be related to altered synaptic plasticity onto VTA DA neurons? It could be that the accelerated extinction in these mice is related an enhanced reversal of NMDAR-LTP, given that this process involves the de-potentiation of synapses that have already undergone a LTP, which is a clear candidate for a cellular mechanism for extinction learning (Harnett et al., 2009). Within the framework of this hypothesis, increasing the effectiveness of VTA DA neuron inhibition synchronously with CS-related glutamatergic synaptic input could result in faster and more effective reversal of NMDAR-LTP by increasing the duration of pauses in AP firing during, thus accelerating the reduction of subsequent VTA DA neuron responses to CS-related input and promoting the faster extinction of CS-paired behaviors (Harnett et al., 2009; Degoulet et al., 2016). If KChIP4 Ex3d and the consequent Kv4.3 channel modulation do indeed enhance hyperpolarizing inhibition, a faster reversal of NMDAR-LTP could be one of the mechanistic links that tie KChIP4 Ex3d to accelerated extinction. This hypothesis could potentially be tested is by applying the following protocol to VTA DA neurons in KChIP4-Ex3d and control mice: first induce NMDAR-LTP and then apply, in current clamp, a short train of hyperpolarizing pulses (preferentially simulated GABAergic currents in dynamic clamp) to the post-synaptic cell and a train of glutamatergic afferent stimulation that extends beyond the offset of hyperpolarizing current injection. According to the current data on NMDAR-LTP, keeping the post-synaptic cell silent during the stimulation time period reverses NMDAR-LTP, while a single AP during the stimulation time period impedes this reversal (Harnett et al., 2009). If hyperpolarizing

inhibition is indeed potentiated in VTA DA neurons of KChIP4-Ex3d mice, one would expect that a hyperpolarizing pulse would be more effective in blocking the induction of APs by afferent stimulation, and therefore the reversal of NMDAR-LTP would be more likely or more intense in this genotype compared to littermate controls. Of course, it would first have to be validated that this current clamp protocol is as effective as the voltage clamp protocols used in previous studies in reversing NMDAR-LTP, and different stimulation periods and intensity of hyperpolarizing inhibition may need to be tested in combination.

While it is not yet clear how the duration and timing of periods of inactivity in relation to input stimulation affects NMDAR-LTP reversal, nor how this relates to post-synaptic mechanisms, this interpretation does allow for some experimental predictions. For example Ex3d mice could present faster extinction of drug seeking behavior and faster reversal of depressive symptoms after social defeat (Degoulet et al., 2016; Stelly et al., 2016). It is harder to formulate specific predictions of potential effects of pharmacological blockade of NMDAR, mGluR1 and L-type Ca^{++} channels in KChIP4 Ex3d animals, but it would seem logical that the expected increase in VAT DA neuron Kv4.3 currents in these mice might potentiate the effects of blocking the NMDAR-LTP pathway only during extinction, but not during acquisition, of a conditioned response. In other words, KChIP4 Ex3d should not affect the post-synaptic intracellular cascade of NMDAR-LTP during acquisition, but only during extinction, when pauses are mechanistically relevant for this process (Harnett et al., 2009).

It is also possible that the KChIP4-Ex3d phenotype may involve the facilitation of AMPAR-LTD and GABA-LTP in VTA DA neurons. Although it is not immediately clear how these forms of synaptic plasticity would be involved specifically in extinction learning, they could be mechanisms by which DA neurons reduce the responses to action- or cue- related inputs that are no longer valid predictors of rewards (Bellone and Lüscher, 2005, 2006; Mameli et al., 2007; Nugent et al., 2007; Nugent and Kauer, 2008). Similarly to what was proposed previously for NMDAR-LTP reversal, enhanced inhibition in KChIP4-Ex3d VTA DA neurons would result in longer pauses in AP firing could increase the induction probability or intensity of AMPAR-LTD. Testing this would involve a similar approach to what was described previously for NMDAR-LTP reversal: while applying the induction protocols for

AMPAR-LTD in VTA DA neurons, instead of keeping the cells from firing by clamping their voltage, the experimenter could apply trains of hyperpolarizing pulses in current clamp and observe the effectiveness of LTD induction in KChIP4-Ex3d mice and controls. It is much harder to speculate on a potential link for GABA-LTP, as this form of induction requires both the activation of GABARs and NMDARs, but perhaps just testing whether this form of plasticity is affected in KChIP4-Ex3d mice with previously established protocols could reveal if it is a plausible contributing mechanism for the KChIP4-Ex3d behavioral phenotype,

It is not immediately clear whether the induction of any form of glutamatergic LTP is affected in KChIP4-Ex3d mice, but the behavioral results would indicate that these processes are untouched, given that acquisition of a conditioned response was not affected in these animals. It is important to point out, however, that Kv4 channels have already been strongly implicated in the control of spike-time dependent AMPAR-LTP in hippocampal pyramidal cells, albeit by affecting a different mechanism. In hippocampal neurons, currents mediated by Kv4 channels, specifically Kv4.2, attenuate backpropagating APs, reducing EPSP amplification and reducing the efficacy of LTP induction by pre-synaptic inputs (Watanabe et al., 2002; Frick et al., 2004; Chen et al., 2006). This process is dynamically regulated and relevant for behavior (Lugo et al., 2012; Truchet et al., 2012; Vernon et al., 2016). It is possible that a similar, Kv4.3 dependent, process occurs in VTA DA neurons. It would need to be tested whether backpropagating APs are affected in VTA DA neurons of KChIP4-Ex3d mice in relation to controls, and if the efficacy of LTP-induction is changed in this genotype compared to controls.

4.5.3. Effects on MSN synaptic plasticity

One of the potential effects of enhanced inhibition in KChIP4 Ex3d mice is a more pronounced reduction of DA release during negative prediction error signaling, ultimately leading to more D2R neurons not being activated. This may lead to enhanced reduction of LTD in D2R-expressing MSNs and reduced induction of LTP in D1R-expressing MSNs, which would facilitate negative prediction error-based learning (Shen et al., 2008). Experimental testing of this hypothesis is complicated, given that currently used rodent *ex vivo* striatal preparations (brain slices) do not

include DA neuron cell bodies (where the biophysical effect of the KChIP4-Ex3d mutation would be relevant).

Aside from the development of an *ex vivo* preparation with intact meso-accumbal circuitry, a potential approach would be to simulate tonic levels of DA release, as well as pauses and bursts, with controlled stimulation of DA afferents in *ex vivo* striatal preparations (Dodson et al., 2016). With this method, the experimenter can test whether combining plasticity-inducing protocols with decreases in tonic DA fiber stimulation indeed lead to different levels of induction for LTD in indirect pathway MSNs and LTP in direct pathway accumbal MSNs. Another approach would be to subject KChIP4-Ex3d and DAT-cre KI controls to a behavioral paradigm where they must learn from negative prediction errors (such as the extinction learning protocol used in this thesis) and then record *a posteriori* from D1R- and D2R-expressing accumbal MSNs of these animals *ex vivo* (Yin et al., 2009; Hawes et al., 2015). Plasticity that occurred in vivo can be inferred in these preparations by measuring the slope of evoked EPSPs (a measure of synaptic strength), the AMPA/NMDA ratio of glutamatergic currents and by applying LTD and LTP induction protocols (when a particular form of plasticity has occurred *in vivo*, it's effective induction *ex vivo* is reduced, which is interpreted as a sign of plasticity saturation). KChIP4-Ex3d mice subjected to such a protocol should display reduced signs of LTD on D2R-expressing MSNs and LTP on D1R-expressing MSNs in relation to littermate controls.

Another, more direct approach would be to record from MSNs in the NAcc of mice *in vivo* using whole-cell patch clamp. While technically challenging, this method has already been successfully implemented in the dorsal striatum of anesthetized and awake behaving head-fixed mice (Reig and Silberberg, 2014; Sippy et al., 2015; Ketzef et al., 2017). In this preparation, it could be tested whether direct or indirect pathway MSNs in KChIP4-Ex3d have different changes in synaptic strength during short bouts of learning, or following the exposure to a few trials of reward omission.

4.5.4. Control of DA population activity

Another potential effect of inhibition amplification in DA neurons could be to promote constant silencing of DA neurons, as proposed by multiple studies from the laboratory of Tony Grace (Floresco et al., 2003; Grace et al., 2007; Valenti et al.,

2012; Chang and Grace, 2014; Grace, 2016). According to this hypothesis, around half of VTA DA neurons are silent in normal physiological conditions, and are kept in this state by constant inhibitory input from the VP (Grace and Bunney, 1984a; Floresco et al., 2003). In pathophysiological conditions, the population of silent DA neurons can increase (such as in depression) or decrease (such as in schizophrenia), thus regulating the tonic levels of DA release and the amplitude of phasic DA signals (Grace, 2012, 2016).

While this is a compelling hypothesis, with high explanatory power, I did not find any evidence that this population level control of DA neuron activity was affected by disrupting KChIP4a expression. In KChIP4 KO mice I did not systematically check for the number of neurons/track in each animal, but in the KChIP4 Ex3d mice there was no indication of altered DA signaling-dependent behaviors outside of extinction learning. If the number of active DA neurons would have been smaller in KChIP4 Ex3d mice, as would have been expected from an increased amplification of VP inhibitory input, I would have expected to see decreased motivation during acquisition, as well as altered locomotor patterns and anxiety-related phenotypes in the spontaneous behavior tests (Chang and Grace, 2014; Grace, 2016).

This suggests that KChIP4-dependent modulation of I_A in midbrain DA neurons does not regulate the number of tonically active DA neurons. This could relate to VP inhibition of VTA DA neurons having a stronger $GABA_B$ component than $GABA_A$, which would mean that it would result in slower, less intense hyperpolarizations, which would be relatively insensitive to Kv4.3 amplification (Häusser and Yung, 1994; Panagis and Kastellakis, 2002; Tepper and Lee, 2007; Khaliq and Bean, 2008). It could also be, as I discussed in the previous sub-section, that Kv4.3 channels, and consequently I_A modulation of inhibitory input, affect specific subsets of inhibitory inputs, which perhaps do not include the VP.

In addition to the method of systematic sampling recording tracks popularized by the Grace lab, another approach that could be used in future experiment is the recording of individual DA neurons in the midbrain using Ca^{++} imaging and implantable fluorescence microscopes (Akerboom et al., 2012; Goltstein et al., 2013; Klaus et al., 2017). While recording from deep structures with this technique may be challenging, perhaps in the future it could offer a more direct measurement of the

ratio of active to inactive DA cells in specific behavioral contexts, and how this may be affected by KChIP4 Ex3d.

4.5.5. Excitation-inhibition balance

In a state of high conductance due to constant synaptic input, transitions in DA neuron activity patterns are expected to be dependent on shifting the excitation-inhibition balance. This means that a burst can be generated both by an increase in excitation or a decrease in inhibition, and a pause can be generated by an increase in inhibition or a decrease in excitation (Lobb et al., 2010, 2011; Morikawa and Paladini, 2011; Paladini and Roeper, 2014). This means that manipulations that constitutively affect tonic inhibitory input will necessarily influence the processing of phasic excitatory inputs.

One elegant experimental demonstration of this phenomenon can be seen in the study by Parker et al. (2011), where the authors demonstrated that constitutively attenuating GABAergic transmission to DA neurons by selectively knocking out the $GABA_A$ β3 subunit in these cells led to amplified excitatory responses to PPTg stimulation and accelerated acquisition in an operant task (without affecting extinction) and increased risk-preference. Therefore, "attenuating GABAergic transmission in DA neurons enhances their excitability", presumably by decreasing the relative inhibition/excitation ratio in these cells (Parker et al., 2011).

Given my *in vivo* electrophysiological results in KChIP4 KO mice, which clearly demonstrated that neither pacemaker nor burst firing were affect, and the fact that the behavioral differences observed in KChIP4 Ex3d mice were highly selective to extinction learning (without affecting acquisition), suggest that KChIP4-dependent modulation of I_A does not affect DA neurons excitability. Kashiotis (2013) also found that VTA DA neurons in KChIP4 KO mice did not have altered input resistance or responses to g depolarizing current injection. This is congruent with the previously established voltage dependency of activation and recovery from inactivation of Kv4.3 channels (Patel et al., 2002, 2004; Jerng and Pfaffinger, 2008; Khaliq and Bean, 2008; Tang et al., 2013). These channels require hyperpolarization to be recovered from inactivation and are then activated by fast depolarization slopes, which would mean Kv4.3-mediated I_A in VTA DA neurons only contributes to membrane

conductance after hyperpolarizing inhibition (Khaliq and Bean, 2008; Tarfa et al., 2017). The opposition of my electrophysiological and behavioral results with those reported by Parker et al. (2011) is a further indication that the effects of Kv4.3 modulation of inhibition is selective for phasic, negative prediction error-related inhibitory input, with no effect on tonic inhibition or phasic excitatory input.

4.6. Neuronal subtype specificity of KChIP4a function

An issue that remains to be fully addressed is which DA neuron subpopulations display a high KChIP4a/other KChIPs ratio and, therefore, are most affected by KChIP4 Ex3d. Based on my electrophysiological results with the full KO, including the *in vivo* data reported in this thesis and the *ex vivo* study of Kashiotis (2013), and the semi-quantitative IHC profile of Kv4.3 channels in KChIP4 Ex3d mice, it is likely that that VTA DA neurons are more controlled by endogenous KChIP4a than SN DA neurons. However, as previously discussed, this interpretation must be confirmed using more sensitive techniques, such as cell type-specific RT-qPCR and proteomic quantification for measuring the endogenous levels of KChIP4a expression in non-transgenic mice, and freeze-fracture electron microscopy for confirming the effects of KChIP4 Ex3d on the membrane expression of Kv4.3 subunits (Lammel et al., 2008; Schwenk et al., 2008, 2014; Subramaniam et al., 2014a).

But which subtypes within the VTA would be most affected? Lammel et al. (2008) demonstrated that VTA DA neurons that project to the lateral shell of the NAcc have similar functional properties to mesostriatal DA neurons, including a short rebound delay after transient inhibition, while VTA DA neurons that project to the medial shell and core of the NAcc, the amygdala and the PFC (the atypical DA neurons) have long rebound delays. These results have been replicated and extended, with new evidence suggesting that differences in rebound delay in DA neurons are determined by Kv4.3 currents and KChIP4 expression, although it is not known how well this generalizes beyond the comparison of NAcc- and dorsal striatal-projecting DA neurons (Kashiotis, 2013; Tarfa et al., 2017). This would indicate that KChIP4a Ex3d should preferentially affect the function of atypical VTA DA neurons (mesocortical, mesoamygdaloid, mesolimbic medial shell and core), with a relatively smaller effect on nigrostriatal and mesolimbic lateral shell neurons. While a more

detailed electrophysiological characterization is still necessary, the behavioral phenotype I observed in KChIP4a mice falls in line with this hypothesis, as KChIP4 Ex3d mice did not display any overt deficits in locomotion or exploration, as would have been expected from a disruption in the activity of nigrostriatal DA neurons (Schiemann et al., 2012; Menegas et al., 2017).

Given my semi-quantitative IHC results, where there was also an increase in Kv4.3 immunolabeling signal intensity in SN TH^+ ROIs of KChIP4-Exd mice in relation to DAT-cre KI controls (albeit with a smaller effect size in comparison to the VTA), it could have been expected that there would also have been a nigrostriatal-related behavioral phenotype. One potential reason as too why this did not occur is classical nigrostriatal and mesolimbic lateral shell DA neurons express a strong I_h current, while atypical VTA DA neurons show little to no I_h (Neuhoff et al., 2002; Lammel et al., 2008; Tarfa et al., 2017). In a previous study from our lab, Neuhoff et al. (2002) found that the rebound delay from hyperpolarization in midbrain DA neurons was very strongly anti-correlated ($r = -0.95$) with the amplitude of I_h-mediated voltage sags and I_h charge densities, indicating that expression of HCN channels, indicating that HCN expression can also shape the integration of post-synaptic inhibition in these cells. This relationship between I_h and rebound delay followed an anatomical gradient, with neurons in the medial VTA displaying the lowest I_h amplitudes and the longest rebound delays, and neurons in the lateral SN having the largest I_h and shortest rebound delays. Recently, Tarfa et al. (2017) confirmed these results and showed that DA neuron I_A and I_h amplitudes are positively correlated and that the properties of both current shape their responses to inhibition, especially within nigrostriatal SN DA neurons. In SN (but not atypical VTA) DA neurons, I_A and I_h also have opposing effects on the control of pacemaker firing, with I_A decreasing and I_h increasing tonic AP frequency (Liss et al., 2001; Neuhoff et al., 2002; Kuznetsova et al., 2010; Subramaniam et al., 2014a). It could be that in KChIP4-Ex3d SN DA neurons, the cellular effects of increased I_A amplitude are effectively compensated by a proportional increase in I_h. Atypical VTA DA neurons, however, perhaps cannot compensate the increase in I_A as effectively (due to the relative lack of HCN expression), and therefore are more vulnerable to the KChIP4-Ex3d mutation.

As discussed in section 4.3 of this thesis, one consistent finding from multiple cyclic voltammetry and microdialysis studies on the post-synaptic DA release signaling of reward prediction errors is that phasic decreases in DA release in response to less than expected rewards is preferentially observed in the NAcc core, in relation to the shell or dorsal striatum (Sugam et al., 2012; Hart et al., 2014a, 2015; Sunsay and Rebec, 2014; Biesdorf et al., 2015; Saddoris et al., 2015). It is therefore likely that phasic inhibition of mesolimbic core neurons has a greater functional contribution to learning from disappointment. In addition, the observed behavioral phenotype of KChIP4 Ex3d mice is consistent with a selective effect on indirect pathway signaling in this region. This would suggest that KChIP4a expression might be linked specifically to the effects of Kv4.3-mediated amplification of negative prediction error-related phasic inhibitory input to mesolimbic core neurons.

However, there remains the question of why there was no effect of KChIP4 Ex3d on working memory, given that mesocortical DA signaling has been extensively linked to this cognitive function (Watanabe et al., 1997; Durstewitz et al., 1999; Wang et al., 2004; Fujisawa and Buzsáki, 2011; Murty et al., 2011). The clearest explanation would be that KChIP4 Ex3d would have, like the full KChIP4 KO, a highly selective effect on modulating responses to phasic inhibition, but not bursting or tonic pacemaker firing. To my knowledge, there is no evidence that phasic inhibition of mesocortical neurons are involved in working memory, but rather that working memory performance is correlated with increases in PFC DA concentrations (Watanabe et al., 1997; Floresco, 2013).

In relation to potential locomotor effects, only one study has found that pauses in SN DA neurons correlate with locomotion initiation, while the vast majority of published work found that bursts in SN DA neurons, when associated with behavior, code for action initiation (York, 1973; Vaccarino and Franklin, 1982; Gratton and Wise, 1985; Jin and Costa, 2010; Dodson et al., 2016; Howe and Dombeck, 2016).

Therefore in order to elucidate the role of KChIP4a in different DA neuron subtypes, it is necessary to investigate what is the behavioral outcome or information content of phasic inhibition in each subpopulation and to apply behavioral paradigms that would reveal the effect of inhibition enhancement in each subtype. It would also be of extreme advantage to develop DA neuron-selective retrograde viral strategies

that would allow the selective excision of KChIP4a in projection target-defined DA neuron populations in KChIP4-Ex3$^{lox/lox}$ mice (Cardozo Pinto and Lammel, 2017).

4.7. Potential implications for disease

4.7.1. KChIP4 alternative splicing in mental illness

As previously mentioned, KChIP4 gene variants have been associated with a variety of mental illnesses, in particular ADHD, depression and drug abuse in multiple GWAS (see section 1.4.4; Tables 1.2 to 1.4). Most of these diseases share the fact that they are characterized by dysfunctions of the midbrain DA system and that their symptoms include changes in learning from negative outcomes (see sections 1.2 and 1.3.5). Specifically, depression is associated with hypodopaminergia and an overvaluation of disappointment; ADHD is believed to be associated with a dysregulation of DA transmission and decreased learning from disappointment; and drug abuse is associated with markedly increased levels of DA concentrations during drug consumption and decreased learning from negative feedback. I propose that there may be a potential link between KChIP4a expression and the control of inhibition in DA neurons with the susceptibility to mental illness.

In the case of depression, animal model results strongly suggest that that the control of DA neuron inhibition affects the progression of the disease (Tye and Deisseroth, 2012; Tye et al., 2012; Valenti et al., 2012; Chang and Grace, 2014; Grace, 2016). While I found no evidence of increased persistent DA neuron silencing, which has been proposed as a neural substrate of depressive symptoms, an increase in phasic inhibition could also lead to increased susceptibility to depression-related stressors. In a very exciting study, Tye et al. (2012) found that relatively short-term (minute-long) optogenetic inhibition of DA neurons induces a rapid depressive phenotype in mice, suggesting that mechanism that extend DA neuron pauses from the millisecond to the second range could promote depressive behaviors as well. Another promising study found that increased activity in the LHb, which mediates phasic inhibition to DA neurons, correlates with and determines the expression of depressive symptoms (Li et al., 2013).

It would be of great value to test whether KChIP4 Ex3d mice are more sensitive to stressors that are known to induce depressive symptoms, such as early maternal separation and chronic social defeat stress (CSDS), given the observed amplification of learning from negative events (Krishnan et al., 2007; Vetulani, 2013). CSDS is particularly promising, as it only induces depressive symptoms, namely anhedonia and social avoidance, in 50-60% of exposed mice; this allows the parallel investigation of mechanisms that promote susceptibility to depression and resilience to stress (Krishnan et al., 2007). Depressive-like symptoms in this model have also been linked to long term increases in DA neuron firing due to enhanced I_h, specifically increased pacemaker and burst firing, and resilience to CSDS has been linked to homeostatic increases in K^+ channel expression, specifically of I_M-mediating KCNQ channels (Cao et al., 2010; Lobo et al., 2010; Friedman et al., 2016; Isingrini et al., 2016).

While it is not entirely clear how and increase in DA activity leads to depressive symptoms in this model, it has been suggested that stress-related increases in DA activity is transient and ultimately leads to increased inhibition of DA neurons due to an opponent process-like allostatic adaptation, which could be affected by Kv4.3-dependent modulation of inhibitory input (Grace, 2016). It would therefore be extremely interesting to investigate whether KChIP4a and Kv4.3 expression is also affected in CSDS, how KChIP4 Ex3d mice respond to this protocol, and how changes in Kv4.3 alfa and beta subunits expression and modulation relate to the proposed alterations in HCN and KCNQ channels.

Interestingly, one study reported that susceptible (anhedonic) Long-Evans rats exposed to CSDS and then trained on a sucrose-rewarded operant conditioning paradigm displayed a pronounced slowdown of extinction learning in relation to controls without any deficits in acquisition learning (Riga et al., 2015). To my knowledge, it has not been tested whether CSDS in mice leads to the same type of selective extinction deficits, but the results of Riga et al. (2015) point in the direction that CSDS might also induce changes in the KChIP4-Kv4.3 dependent modulation of extinction learning described in this dissertation.

Perhaps the mental disorder that has been most conclusively linked to KChIP4 variants in ADHD (Lasky-Su et al., 2008; Neale et al., 2008; Weißflog et al., 2013). While extinction deficits and other forms of learning from negative outcomes have not

been extensively explored in animal models of ADHD, the strong association of ADHD with resistance to extinction suggests a mechanistic relation between less learning from disappointment and the impulsivity and hyperactivity that characterize the disorder (Johansen et al., 2002; Russell et al., 2005; Sagvolden et al., 2005a). Specifically, impulsivity and hyperactivity in ADHD has been proposed to result, in part, from reduced learning when behavior leads to no reward (or even social punishments), which would increase general activity as the patients fail to learn and eliminate motor patterns that do not lead to rewarding outcomes (Sagvolden et al., 2005a). Considering that KChIP4 Ex3d mice have enhanced extinction learning but have normal baseline activity, it would indicate that these two aspects of behavior are not necessarily linked. It would be interesting to test whether KChIP4 Ex3d mice also display other opposite phenotypes relevant to ADHD pathology, such as decreased impulsivity or increased attention (Russell et al., 2005). However, perhaps a more promising approach would be to test if specific animal models of ADHD, such as the spontaneously hyperactive rat and acallosal mice, display increased KChIP4a expression and/or impaired Kv4.3 channel function (Sagvolden et al., 2005b). It might also be very informative to develop an animal model that reconstitutes specific ADHD-associated SNPs in KCNIP4, in order to observe what is the functional relevance of these SNPs for KChIP4 expression and if they have a causal role in the development of ADHD-like symptoms (Blendy, 2011).

Another pathological behavior potentially modulates by KChIP4a expression is drug abuse and addiction, particularly extinction and relapse of drug use behavior, which is a crucial aspect of treating addicted patients (Kaplan et al., 2011; Torregrossa and Taylor, 2013). It is thought the relative deficit in learning from negative outcomes contributes to the pathophysiology of addiction by making patients refractory to negative outcomes that might otherwise motivate them to give up drug use (Parvaz et al., 2015). Interestingly, in what was perhaps the most behaviorally specific test of KChIP4 gene variants on drug use behaviors, Uhl et al. (2008) found clusters of SNPs in the KChIP4 gene (KCNIP4) that were associated with different outcomes in attempts to quit smoking.

Mice also display population variability in the effectiveness of extinction of drug use behaviors and susceptibility to relapse, which depends on the drug and the structure of drug delivery paradigms (Yan and Nabeshima, 2009; Lynch et al., 2010).

Future studies should examine whether KChIP4a expression is lower and/or Kv4.3 currents are smaller in animals that are more prone to relapse and show deficient drug use extinction, and whether KChIP4 Ex3d mice are more efficient, as a population, in extinguishing drug use behaviors.

Given the results of GWASs presented in this dissertation, an interesting approach that could maximize the translational potential of investigating KChIP4a function would be to a determine which disease-associated SNPs are located in the KISD-coding exon 3 using bioinformatic methods (Holmqvist et al., 2002; Jerng and Pfaffinger, 2008; Johnson, 2009). Another region of interest would be intron 1, which codes for the 38A ncRNA that controls the relative expression of KChIP4a, as variations in the expression of this RNA could also regulate cellular KChIP4a levels (Massone et al., 2011). Identification of these SNPs could provide a number of candidate KChIP4 gene variants that could be subsequently investigated in animal models (Blendy, 2011). Such an approach could be used to determine if specific KChIP4 SNPs are involved in negative prediction error processing and the development of mental disease-symptoms.

4.7.2. Response to inflammation

A known mechanism for direct alternative splicing control of the KChIP4 gene is the RNA polymerase III-mediated transcription of the ncRNA 38A (Massone et al., 2011). This regulatory process is highly sensible to the pro-inflammatory cytokine IL1- α, which would suggest that inflammatory processes could potentially affect KChIP4 alternative splicing in DA neurons. Indeed, inflammation is known to acutely and rapidly bias behavior, promoting lethargy, anorexia and selectively enhancing sensitivity to punishment and reward omission (Hart, 1988; Dantzer et al., 2008; Harrison et al., 2016). This has a clear adaptive function for sick animals, as it promotes energy conservation and diverts all bodily resources towards combating the infective pathogen. However, allostatic inflammatory processes are also thought to be involved in the pathophysiological development of mental illnesses, particularly depression (Dantzer et al., 2008).

Our behavioral findings suggest the hypothesis that one of the mechanisms by which inflammation biases behavior towards negative affect might be the regulation of alternative KChIP4 splicing in DA neurons. This would mean that IL1- α, which is

released in response to infective pathogens and involved in the promotion of fever (Gabay et al., 2010; Sims and Smith, 2010), would in parallel promote the expression of KChIP4a in VTA DA neurons by increasing the levels of 38A ncRNA, thereby increasing the biophysical amplification of GABAergic pauses and enhancing the neural representation and behavioral consequences of negative prediction errors (and potentially primary punishments). This would also occur in diseases characterized by chronic inflammation, such as rheumatoid arthritis (Gabay et al., 2010). This could be tested by quantifying KChIP4a mRNA and protein expression, as well as the expression levels of 38A ncRNA and DA neuron electrophysiological properties, following the experimental induction of inflammation in non-transgenic mice. Likewise, KChIP4 Ex3d mice should be resistant to these potential molecular, cellular and behavioral effects of experimental inflammation. If this is true, this could have dramatic consequences on our understanding of neuro-immune interactions, how inflammation can affect behavioral control and decision making, and how chronic inflammatory processes such can lead to depression beyond pain and metabolic control (Dantzer et al., 2008).

4.8. Alternative splicing and behavior

Alternative splicing occurs when a cell combines the pre-mRNA translated from exons of a single gene in different configurations, producing different proteins. It is a widespread phenomenon in vertebrates; in humans approximately 95% of genes with multiple exons undergo alternative splicing, with an average rate of seven splice variants for each multiexon gene (Pan et al., 2008a). This feature increases the combinatorial power of genomic encoding of protein transcripts by two to seven fold (Modrek and Lee, 2002; Carrillo Oesterreich et al., 2016). In the wake of the initial results of the Human Genome Project, where the discovery that the full human genome contained only around an estimated 32 thousand protein-coding genes (with current estimates being as low as 19 thousand genes) dramatically undercut the expectations of the general scientific community, alternative splicing was proposed as one fundamental mechanism by which a relatively limited amount of genes could encode a multifold number of proteins (Lander et al., 2001; Venter et al., 2001; Roberts and Smith, 2002; Ezkurdia et al., 2014; Mukherjee, 2016). Concordantly, alternative splicing events have since been implicated in processes that are essential

for survival and reproduction, such as apoptosis and sex determination (Boise et al., 1993; Lopez, 1998).

Despite the critical theoretical importance of alternative splicing for genomic encoding and the recognized importance of splice variants in regulating vital signaling pathways, very little is known about how this process regulates neuronal activity and behavior in mammalian species. Only a handful of studies in mammals have investigated how alternative splicing within specific neuronal subtypes controls specific cellular processes, such as ion channel and receptor expression, and mapped how this influences neuronal information processing and behavior (Naughton et al., 2012; Zhou et al., 2013; Mandela et al., 2014; Nguyen et al., 2016; Marron Fernandez de Velasco et al., 2017).

In the DA system, it has been shown that two splice variants of D2R, D2L (long) and D2S (short), are differentially localized post-synaptically in MSN and pre-synaptically in DA neurons, respectively (Borrelli et al., 2000; Colelli et al., 2010; Naughton et al., 2012; Neve et al., 2013). The two isoforms differ in the presence (D2L) or absence (D2S) of an alternatively spliced exon (D2 exon 6) that encodes a 29-amino acid insert in the third intracellular loop of the D2R protein (Dal Toso et al., 1989; Borrelli et al., 2000). This process of alternative splicing confers distinct properties to post-synaptic and pre-synaptic (i.e. autoreceptor) D2Rs, with the notable property that the D2S isoform is functionally insensitive to haloperidol (Borrelli et al., 2000). Because of these differential properties and cellular expression profiles, mice that lack the D2L isoform show blunted behavioral responses to haloperidol and a characteristic manifestation of stereotypical climbing under D1R and D2R pharmacological co-stimulation (Borrelli et al., 2000; Fetsko et al., 2003). Interestingly, one study suggested that the enhanced expression of the D2L isoform in the striatum in relation to the midbrain is strain-specific, only being observed in C57BL/6J mice (Colelli et al., 2010). Specifically, the ratio of D2L/D2S mRNA expression was similar in the striata and midbrains of DBA/2J mice (2:1 ratio for D2L/D2S, respectively, in both regions), despite differing dramatically in C57BL/6J mice (5:1 ratio for D2L/D2S in the striatum and 2:1 ratio in the midbrain). This change in expression patterns had an associated behavioral phenotype, with DBA/2J mice not showing stereotyped climbing under D1R and D2R co-stimulation, which is congruent with a more pronounced relative post-synaptic expression of the D2S

isoform. Furthermore, viral-mediated knockdown of the D2L variant selectively in the NAcc reduced locomotor activity and cocaine-induced conditioned place preference (Naughton et al., 2012). This would suggest that the control of alternative splicing in striatal MSN could dynamically influence behavior. However, it is not clear whether a similar process occurs, or can occur, in midbrain DA neurons, and what would be its consequence for the expression of natural behaviors.

To the best of my knowledge, my thesis is the first to show a causal link between alternative splicing processes within DA neurons and the control of behavior. This finding outlines a novel avenue of research for understanding DA neuron regulation. Moreover, I propose a mechanistic chain of events between alternative splicing, KChIP4 isoform expression, structural modulation of Kv4.3 subunits, I_A properties, synaptic integration and learning from negative prediction errors. The illumination of the causal chain between alternative splicing and a behavioral phenotype is a powerful approach for the understanding of post-translational genetic determination of behavioral variance.

Importantly, the form of alternative splicing I investigated already has a known intronic ncRNA-dependent regulatory mechanism, which invites future research on the transcriptional and post-transcriptional regulatory processes that might affect this physiological chain of events, and involves a gene that has been linked to multiple diseases that involve similar behavioral phenotypes as those observed in my transgenic mice, beckoning the investigation of how the mechanism I identified can be involved in the etiology of mental disorders.

4.9. Behavioral differences between DAT-cre KI and DAT-cre WT mice

As a serendipitous consequence of my experimental design, I were able to identify that DAT-cre KI mice have a different behavioral phenotype during appetitive conditioning and extinction in relation to DAT-cre WT mice (Figures 3.38 and 3.39). DAT-cre KI mice displayed shorter response latencies and higher response probability during the initial session of conditioning training. During extinction, they also showed an initial resistance to extinction in both response latency and time in port, but in later extinction sessions they responded with similar latencies and time in port when compared to DAT-cre WT mice. Computational fitting of the time in port

metric revealed a difference between the two groups only in the initial response during the first three acquisition trials (the V_0 parameter of the modified Rescorla-Wagner model), with DAT-cre KI mice having higher initial responding than controls (Figure 3.42). I did not observe a significant difference in learning rates during acquisition or extinction (positive or negative prediction error-bases learning, respectively), confirming that the effects of DAT-cre KI during acquisition were restricted to the first session and that the effects seen during acquisition are not likely to be due to learning deficits (Figures 3.40 to 3.42).

The most likely explanation, in my interpretation, for the behavioral differences between DAT-cre KI and DAT-cre WT mice would be that DAT-cre KI promotes an increase in motivation, particularly incentive salience, i.e. a cue-triggered drive to pursue rewards independently of learned associative value (Berridge and Robinson, 2003; Berridge, 2012). As the mice had already been shaped to pursue sucrose water in the reward port, a higher motivational state in the presence of a cue can explain the higher responding probabilities and shorter latencies in the first session and the increased time in port in the first three acquisition trials, before a CS-US association has been established. By the third acquisition session, however, both DAT-cre KI and DAT-cre WT mice had the same behavioral performance, and fitting the time in port metric to a Rescorla-Wagner model confirmed only a difference in initial responding with no effect on learning rates or maximal response performances in the last sessions of acquisition, indicating that DAT-cre KI does not affect associative learning or reward valuation *per se*. Enhanced incentive salience also explains the initial differences in responding during early extinction, as animals would be motivated to pursue rewards in the presence of a salient cue even in the absence of reward (Berridge, 2012).

Importantly, there were no differences between DAT-cre KI and DAT-cre WT controls in open field exploration (including time in center, which is a measure of anxiety), novel object preference, hole board exploration or spontaneous alternation in the plus maze (a test of working memory), suggesting that the behavioral phenotype of DAT-cre KI mice is subtle and restricted to specific behavioral domains (Figures 3.43 to 3.48).

DAT-cre KI mice have a heterozygous insertion of the cre-recombinase gene preceded by an internal ribosomal entry site (IRES; allows for translation initiation) in

the 3' untranslated region (3'UTR) of the DAT locus, which results in the expression of cre under the DAT promoter (Bäckman et al., 2006). The reason why only heterozygous mice are used for research is that in the original description of this line it was reported that homozygous DAT-cre mice have an approximately 50% decrease in DAT expression in the striatum, which was known to cause a state of allostatic hyperdopaminergia (Giros et al., 1996; Li et al., 2010b; Deng et al., 2015). DAT-cre KI induced an ~20% decrease in DAT expression in the striatum, although this results did not reach significance ($P > 0.05$); nevertheless the authors concluded that "insertion of an IRES-Cre sequence in the 3'UTR interferes with the function of the DAT gene" (Bäckman et al., 2006). The authors even acknowledged that "the possibility remains that under certain behavioral or pharmacological challenges, which may be applied to these mice in future studies, the difference between wild-type animals and heterozygous mutants may become more apparent". One could therefore interpret that the DAT-cre KI line is likely also a partial DAT knockdown line. Despite these results, little attention has been given to the potential behavioral effects of this genetic manipulation and how this could potentially affect the interpretation and design of experiments concerning DA neurotransmission.

The most direct comparison of the DAT-cre KI mice would be the $DAT^{+/-}$ line, the heterozygous littermates of DAT KO mice, which have a 50% reduction in striatal DA clearance efficacy and have been used as a model of constitutive hyperdopaminergia (Giros et al., 1996; Morice et al., 2007; Li et al., 2010b; Deng et al., 2015). $DAT^{+/-}$ animals display normal open field exploration, novel object recognition and anxiety; this is very similar to my results in DAT-cre KI mice, which also show no changes in these behavioral tests and measures. Interestingly, I found that DA-cre KI mice did not display working memory deficits, in contrast to what was observed in the $DAT^{+/-}$ line (Deng et al., 2015). It should be stated that other tests for working memory, including the eight-arm radial arm maze and forced alternation on a T-maze (which was used to reveal working memory deficits in $DAT^{+/-}$ mice), might be more sensitive in revealing subtle deficits potentially present in DAT-cre KI mice. Future studies should investigate this possibility. However, another interpretation is that the behavioral phenotype of DAT-cre KI is less severe than that of $DAT^{+/-}$ mice, which is also plausible, given that the estimated decrease in DAT function in DAT-cre mice, inferred from protein expression levels, is only 20% (Giros et al., 1996; Bäckman et al., 2006).

Crucially, my hypothesis that the behavioral alterations in DAT-cre KI during conditioning and extinction may be due to increased motivation is entirely congruent with the consistent findings that DAT KO and DAT KD mice have increased motivation, but not necessarily increased learning, over a variety of reward-conditioned tasks (Cagniard et al., 2006a; Yin et al., 2006; Thomsen et al., 2009; Balci et al., 2010; Beeler et al., 2010). Cagniard et al. (2006b) tested the specificity of DAT's effect on motivation by inducing DAT knockdown after mice had already learned to press a lever to obtain food rewards. They found that after DAT expression decrease, which was interestingly paralleled by an increase in pacemaker activity and a reduction of bursting in DA neurons, mice would work significantly more in order to obtain a reward in a progressive ratio schedule task. Inducing DAT knockdown before learning, however, did not change the speed of acquisition of the lever press response. This study strongly suggests that DAT is a major regulator of motivation to obtain rewards, but not of learning action-outcome associations over time, which falls in line directly with my results.

Two studies have analyzed the how animals with lower DAT expression respond during the extinction of an appetitive response, with diametrically opposite conclusions. Hironaka et al. (2004) found that food-restricted DAT KO and $DAT^{+/-}$ mice trained to nosepoke in order to obtain a food pellet reward learned to perform the task with the same speed and performance levels as WT controls; however, the DAT KO mice showed dramatically slower extinction learning, with persistently higher nosepoking even after five extinction sessions. Interestingly, $DAT^{+/-}$ mice did not differ from controls in any phase of this task. On the other hand, Rossi and Yin (2015), comparing only the behavior water-restricted DAT KO and WT mice during 30 minutes of free access to a sucrose water bottle, found DAT KO mice had altered patterns of licking behavior, displaying longer and more frequent licks in relation to controls. During extinction, when no water was available in the bottle, DAT KO mice had the same licking patterns as control, but surprisingly showed dramatically accelerated extinction learning. In my experiments, I observed a subtle, but significant resistance to extinction during the initial sessions, which was more pronounced in the changes in response latency than in the actual time spent in port during the cue. In that regard, my results more closely approximate the findings of Hironaka et al. (2004). However, if could be that these differences in extinction response may be due to the different structures of the task. While Hironaka et al.

(2004) and I used operant conditioning paradigms, in which the animal must perform a specific action in order to obtain reward (head entry into a port or lever pressing), Rossi and Yin (2015) only tested *ad libitum* innate consummatory behaviors. Furthermore, in my task the animals had to respond to a specific CS, while CS-US associations were not directly tested in the other two studies. These different forms of learning and behaviors (instrumental vs. innate; cued vs. self-paced) have different neural substrates and therefore may be affected in highly different ways by any experimental procedure (Flagel et al., 2011; Hart et al., 2014b; Averbeck and Costa, 2017; McCutcheon and Roitman, 2017; Rothenhoefer et al., 2017). For example, there is evidence that learning the value of cues (Pavlovian learning), but not of actions (instrumental learning), that predict reward delivery is selectively disrupted by ventral striatum lesions, but also that cues that predict action-dependent reward delivery (collection of a sucrose pellet; a combination of both forms of learning) evoke more dopamine release in the ventral striatum than cues that predict rewards that were directly presented to animals without requiring a behavioral response (direct oral infusion of a sucrose solution) (McCutcheon and Roitman, 2017; Rothenhoefer et al., 2017).How task structure might affect the effect of DAT knockdown and what are the neural substrates of these differences is a subject that merits further investigation.

My comparison of DAT-cre KI and DAT-cre WT mice during conditioning shines light on a potential minor confound of using the DAT-cre KI line for experimental research on the effects of DA in learning. Physiological and behavioral differences between mouse strains are known feature of neuroscience research, and are increasingly being exploited as a research tool to understand the consequences of specific genes (Crawley, 2007; Colelli et al., 2010; Matsuo et al., 2010). Understanding the behavioral profiles of individual strains, especially those engineered for cell-type specific interventions, is also crucial for the design and execution of experimental protocols. Based on my discovery, I can strongly recommend that all investigations with the DAT-cre KI must be done using littermate controls with the same DAT-cre genotype. Furthermore, DAT-cre KI mice have a behavioral phenotype that is consistent with reduced DAT expression, a feature that must be noted when using this line to study the physiology of post-synaptic DA effects in the striatum or the relative expression patterns of DAT in any cell type.

Another interesting feature is that $DAT^{+/-}$ mice displayed compensatory reductions in D1R and D2R mRNA expression (Giros et al., 1996). They also displayed decreased prodynorphin and increased preproenkephalin A mRNA expression, two endogenous opioids that are positively modulated, respectively, by D1R and D2R activation (Giros et al., 1996; Wang and McGinty, 1996). In the initial characterization of the DAT-cre KI line, a significant increase in prodynorphin expression in homozygous DAT-cre animals was reported, but there were also a non-significant trend towards higher prodynorphin and lower preproenkephalin expression in DAT-cre KI mice (Bäckman et al., 2006). These previous results, in combination with my behavioral findings, suggest that perhaps DAT-cre KI mice display changes in gene expression relevant for the post-synaptic readout of DA concentrations that were not fully detected in previous studies.

Further studies will be needed to characterize the extent of DAT loss of function in this line, which behavioral processes might be affected and if there are compensatory changes in the expression or function of DA receptors or in the firing patterns of DA neurons. Importantly, my proposition that DAT-cre KI have increased motivation should be confirmed using progressive ratio schedules (Cagniard et al., 2006a). These mice should also be specifically tested for attention deficits, as decreases in DAT function has been proposed to be a contributing factor to ADHD pathology (Faraone et al., 2005; Vaughan and Foster, 2013). Another important aspect that must be investigated is whether DAT-cre mice are also relativity insensitive to cocaine, like the DAT KO, DAT KD and $DAT^{+/-}$ lines (Giros et al., 1996; Jones et al., 1998; Mead et al., 2002). If so, this could have significant impact on the use of DAT-cre mice in the study of drug consumption and abuse.

4.10. Perspectives

The results presented in this thesis inspire a number of promising new avenues of research. A priority issue is too perform a comprehensive electrophysiological characterization of the biophysical effects of KChIP4 Ex3d in projection identified DA neurons, and confirm my semi-quantitative IHC results with proteomic analyses and freeze-fracture EM.

From a neurophysiological point of view, the discovery of a biophysical amplifier of hyperpolarizing inhibition in VTA DA neurons reveals a new independent modulator of information processing within cortico-BG-limbic circuits, opening up a number of questions that need to be addressed. How does this mechanism relate to DA release and post-synaptic readout and clearance in specific target regions? Is this a plastic process that changes in response to environmental or physiological challenges? How does KChIP4a expression and Kv4.3 regulation interact with the expression of other ion channels in specific subpopulations of VTA neurons?

Another open question is how KChIP4a expression affects other behaviors, especially those involved in negative learning. Future studies should address if KChIP4 Ex3d mice display differences in fear conditioning learning, conditioned inhibition learning paradigms and inhibitory avoidance. It could be that these animals have altered performance in other measures of baseline negative emotionality, such as behavioral despair thresholds, which can be measured in tail suspension and forced swim tests. Importantly, an overvaluation of negative feedback would mean these animals would tend to be risk-averse and cost-avoiding; these features must be tested with specific learning paradigms in follow up studies.

It is also important to determine whether altered KChIP4 expression regulation affects behavior and physiological markers in disease models. It would be interesting to test whether increases in relative KChIP4a expression might be found following treatments that induce depression-like states (such as CSDS), compulsive drug addiction, inflammation, stress and other physiological challenges. It could be that changes in KChIP4a regulation might be observed in these models both at a molecular level (by quantifying mRNA and protein expression) and in the biophysics of DA neurons. It would also be interesting to test whether KChIP4 Ex3d mice are relatively resistant to the molecular, cellular and behavioral changes induced by these disease models, and to which extent other cellular processes (such as drug-induced synaptic plasticity or stress-related biophysical changes) are affected by precluding KChIP4a expression.

Finally, one approach to better explore the translational potential of my findings would be to identify disease-relevant regions within the KChIP4 gene that could affect the structure of KChIP4a or that control its expression levels. A good start would be to see which disease-associated KChIP4 gene SNPs (see section 1.4.4) are located

in the exon 3 (which codes for the KISD) and intron 1 (which codes for the 38A ncRNA that controls the relative expression of KChIP4a). This could provide a number of candidate KChIP4 gene variants that could be causally linked to negative prediction error processing and the development of mental illnesses. It would also be interesting to investigate in animal models whether changes in the expression and post-translational modulation of KChIP4a, other KChIP variants and Kv4.3 correlate with and are causally affected in protocols and genetic lines that recapitulate symptoms of depression, ADHD, drug abuse, schizophrenia and other disorders.

In addition to my findings on KChIP4a function, my discovery that DAT-cre KI mice show a moderate but significant behavioral phenotype in conditioning learning should prompt an effort to characterize the physiology of this line in detail. Specifically, it would be important to test how these animals respond to DAT-blocker stimulants such as cocaine, as well as quantify the expression patterns of DAT and DA receptors in the striatal subcompartments of these mice. These findings should guide future research based on this line, which must take its baseline behavior into account, as is done for other major lines of laboratory mice (Crawley, 2007; Wahlsten, 2010).

4.11. Conclusion

I have identified that KChP4 gene products act as a modulator of putative hyperpolarizing pauses in VTA DA neurons, and that selectively disrupting the expression of one splice variant of this gene, KChIP4a, only in DA neurons, increases the expression of Kv4.3 subunits in these cells and selectively biases behavior in the direction of overvaluing negative prediction errors. Combining these findings with previous results from our group (Kashiotis, 2013), I propose a working model of how KChIP4a deletion can lead to the observed behavioral phenotype (Figure 4.1).

In my proposal, the disruption of KChIP4a expression in DA neurons by a selective deletion of exon 3 of the KChIP4 gene leads to an increase in binding of other KChIP variants (especially other KChIP4 variants, such as KChIP4bL) to Kv4.3 subunits. This increases the surface expression of Kv4.3 and, consequently, I_A current density, enhancing firing pauses in response to hyperpolarizing inhibition. In behaving animals, phasic synaptic inhibition of DA neurons code for negative prediction errors, which promote learning from less than expected outcomes. Therefore, mice with a selective deletion of KChIP4a in DA neurons display longer firing pauses in response to disappoint outcomes, and consequently learn faster from these events. In brief, KChIP4a in DA neurons acts as a biophysical amplifier of negative prediction error-based learning.

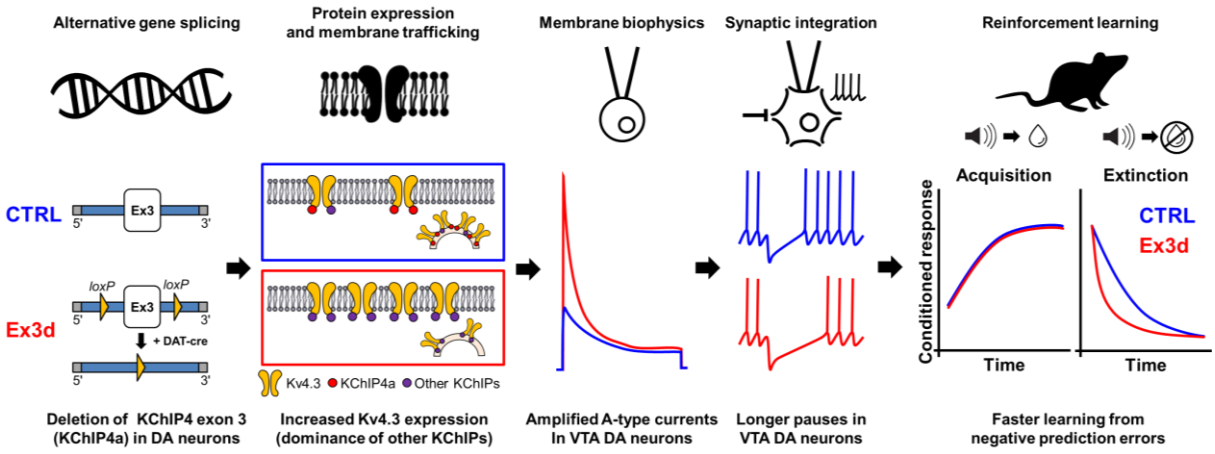

Figure 4.1. Graphical summary of the proposed mechanistic connections between KChIP4 Ex3d in DA neurons and accelerated extinction learning.

References

Abizaid A (2009) Ghrelin and Dopamine: New Insights on the Peripheral Regulation of Appetite. J Neuroendocrinol 21:787–793.

Akerboom J et al. (2012) Optimization of a GCaMP Calcium Indicator for Neural Activity Imaging. J Neurosci 32:13819–13840.

Albin RL, Young AB, Penney JB (1989) The functional anatomy of basal ganglia disorders. Trends Neurosci 12:366–375.

Alexander BK (2000) The Globalization of Addiction. Addict Res 8:501–526.

Alexander BK, Beyerstein BL, Hadaway PF, Coambs RB (1981) Effect of early and later colony housing on oral ingestion of morphine in rats. Pharmacol Biochem Behav 15:571–576.

Alladi PA, Mahadevan A, Yasha TC, Raju TR, Shankar SK, Muthane U (2009) Absence of age-related changes in nigral dopaminergic neurons of Asian Indians: Relevance to lower incidence of Parkinson's disease. Neuroscience 159:236–245.

Ambroggi F, Ghazizadeh A, Nicola SM, Fields HL (2011) Roles of Nucleus Accumbens Core and Shell in Incentive-Cue Responding and Behavioral Inhibition. J Neurosci 31:6820–6830.

An WF, Bowlby MR, Betty M, Cao J, Ling H-PP, Mendoza G, Hinson JW, Mattsson KI, Strassle BW, Trimmer JS, Rhodes KJ (2000) Modulation of A-type potassium channels by a family of calcium sensors. Nature 403:553–556.

Angstman KB, Rasmussen NH (2011) Personality disorders: review and clinical application in daily practice. Am Fam Physician 84:1253–1260.

Antunes M, Biala G (2012) The novel object recognition memory: Neurobiology, test procedure, and its modifications. Cogn Process 13:93–110.

Aransay A, Rodrí-guez-López C, Garcí-a-Amado M, Clascá¡ F, Prensa L (2015) Long-range projection neurons of the mouse ventral tegmental area: a single-cell axon tracing analysis. Front Neuroanat 9:59.

Ascherio A, Schwarzschild MA (2016) The epidemiology of Parkinson's disease: risk factors and prevention. Lancet Neurol 15:1257–1272.

Ashok AH, Marques TR, Jauhar S, Nour MM, Goodwin GM, Young AH, Howes OD (2017) The dopamine hypothesis of bipolar affective disorder: the state of the art and implications for treatment. Mol Psychiatry 22:666–679.

Atallah HE, Lopez-Paniagua D, Rudy JW, O'Reilly RC (2007) Separate neural substrates for skill learning and performance in the ventral and dorsal striatum. Nat Neurosci 10:126–131.

Atallah HE, McCool AD, Howe MW, Graybiel AM (2014) Neurons in the Ventral Striatum Exhibit Cell-Type-Specific Representations of Outcome during Learning. Neuron 82:1145–1156.

Averbeck BB, Costa VD (2017) Motivational neural circuits underlying reinforcement learning. Nat Neurosci 20:505–512.

Bäckman CM, Malik N, Zhang Y, Shan L, Grinberg A, Hoffer BJ, Westphal H, Tomac AC (2006) Characterization of a mouse strain expressing Cre recombinase from the 3′ untranslated region of the dopamine transporter locus. genesis 44:383–390.

Badrinarayan a., Wescott SA, Vander Weele CM, Saunders BT, Couturier BE, Maren S, Aragona BJ (2012) Aversive Stimuli Differentially Modulate Real-Time Dopamine Transmission Dynamics within the Nucleus Accumbens Core and Shell. J Neurosci 32:15779–15790.

Bähring R, Covarrubias M (2011) Mechanisms of closed-state inactivation in voltage-gated ion channels). For many years, Drs Bähring and Covarrubias have shared an interest in the intriguing mechanisms of inactivation of Kv4.x channels and their modulation by accessory β-subunits. J Physiol J Physiol J Physiol 5893:461–4793.

Balci F, Ludvig EA, Abner R, Zhuang X, Poon P, Brunner D (2010) Motivational effects on interval timing in dopamine transporter (DAT) knockdown mice. Brain Res 1325:89–99.

Balcita-Pedicino JJ, Omelchenko N, Bell R, Sesack SR (2011) The inhibitory influence of the lateral habenula on midbrain dopamine cells: Ultrastructural evidence for indirect mediation via the rostromedial mesopontine tegmental nucleus. J Comp Neurol 519:1143–1164.

Baldwin TJ, Tsaur ML, Lopez GA, Jan YN, Jan LY (1991) Characterization of a mammalian cDNA for an inactivating voltage-sensitive K+ channel. Neuron 7:471–483.

Baranauskas G (2004) Cell-type-specific splicing of KChIP4 mRNA correlates with slower kinetics of A-type current. Eur J Neurosci 20:385–391.

Barbeau A (1984) Etiology of Parkinson's Disease: A Research Strategy. Can J Neurol Sci / J Can des Sci Neurol 11:24–28.

Barbera G, Liang B, Zhang L, Gerfen CR, Culurciello E, Chen R, Li Y, Lin D-T (2016) Spatially Compact Neural Clusters in the Dorsal Striatum Encode Locomotion Relevant Information. Neuron 92:202–213.

Barger G, Dale HH (1910) Chemical structure and sympathomimetic action of amines. J Physiol 41:19–59.

Barron AB, Søvik E, Cornish JL (2010) The Roles of Dopamine and Related Compounds in Reward-Seeking Behavior Across Animal Phyla. Front Behav Neurosci 4:163.

Barter JW, Li S, Lu D, Bartholomew RA, Rossi MA, Shoemaker CT, Salas-Meza D, Gaidis E, Yin HH (2015) Beyond reward prediction errors: the role of dopamine in movement kinematics. Front Integr Neurosci 9:39.

Bauer CK, Schwarz JR (2001) Physiology of EAG K+ channels. J Membr Biol 182:1–15.

Bayer HM, Glimcher PW, Schultz W, Kimura M, Sahakian BJ, Carter CS (2005) Midbrain dopamine neurons encode a quantitative reward prediction error signal. Neuron 47:129–141.

Bayer HM, Lau B, Glimcher PW (2007) Statistics of midbrain dopamine neuron spike trains in the awake primate. J Neurophysiol 98:1428–1439.

Beard C, Donahue RJ, Dillon DG, Van't Veer A, Webber C, Lee J, Barrick E, Hsu KJ, Foti D, Carroll FI, Carlezon Jr WA, Björgvinsson T, Pizzagalli DA (2015) Abnormal error processing in depressive states: a translational examination in humans and rats. Transl Psychiatry 5:e564.

Beats BC, Sahakian BJ, Levy R (1996) Cognitive performance in tests sensitive to frontal lobe dysfunction in the elderly depressed. Psychol Med 26:591.

Beaulieu J-M, Gainetdinov RR (2011) The Physiology, Signaling, and Pharmacology of Dopamine Receptors. Pharmacol Rev 63.

Beckstead MJ, Grandy DK, Wickman K, Williams JT (2004) Vesicular Dopamine Release Elicits an Inhibitory Postsynaptic Current in Midbrain Dopamine Neurons. Neuron 42:939–946.

Beeler JA, Daw N, Frazier CRM, Zhuang X (2010) Tonic Dopamine Modulates Exploitation of Reward Learning. Front Behav Neurosci 4:170.

Beier KT, Steinberg EE, DeLoach KE, Xie S, Miyamichi K, Schwarz L, Gao XJ, Kremer EJ, Malenka RC, Luo L (2015) Circuit Architecture of VTA Dopamine Neurons Revealed by Systematic Input-Output Mapping. Cell 162:622–634.

Belcher AM, Feinstein EM, O'Dell SJ, Marshall JF (2008) Methamphetamine Influences on Recognition Memory: Comparison of Escalating and Single-Day Dosing Regimens. Neuropsychopharmacology 33:1453–1463.

Belin D, Everitt BJ (2008) Cocaine Seeking Habits Depend upon Dopamine-Dependent Serial Connectivity Linking the Ventral with the Dorsal Striatum. Neuron 57:432–441.

Bello EP, Mateo Y, Gelman DM, Noaín D, Shin JH, Low MJ, Alvarez VA, Lovinger DM, Rubinstein M (2011) Cocaine supersensitivity and enhanced motivation for reward in mice lacking dopamine D2 autoreceptors. Nat Neurosci 14:1033–1038.

Bellone C, Lüscher C (2005) mGluRs induce a long-term depression in the ventral tegmental area that involves a switch of the subunit composition of AMPA receptors. Eur J Neurosci 21:1280–1288.

Bellone C, Lüscher C (2006) Cocaine triggered AMPA receptor redistribution is reversed in vivo by mGluR-dependent long-term depression. Nat Neurosci 9:636–641.

Benes FM (2001) Carlsson and the discovery of dopamine. Trends Pharmacol Sci 22:46–47.

Benoit-Marand M, Borrelli E, Gonon F (2001) Inhibition of dopamine release via presynaptic D2 receptors: time course and functional characteristics in vivo. J Neurosci 21:9134–9141.

Berger B, Gaspar P, Verney C (1991) Dopaminergic innervation of the cerebral cortex: unexpected differences between rodents and primates. Trends Neurosci 14:21–27.

Berridge KC (2007) The debate over dopamine's role in reward: the case for incentive salience. Psychopharmacology (Berl) 191:391–431.

Berridge KC (2012) From prediction error to incentive salience: mesolimbic computation of reward motivation. Eur J Neurosci 35:1124–1143.

Berridge KC, Robinson TE (2003) Parsing reward. Trends Neurosci 26:507–513.

Besheer J, Jensen HC, Bevins RA (1999) Dopamine antagonism in a novel-object recognition and a novel-object place conditioning preparation with rats. Behav Brain Res 103:35–44.

Bethesda (MD): National Library of Medicine (US); National Center for Biotechnology Information (2017) National Center for Biotechnology Information (NCBI)[Internet]. Available at:

https://www.ncbi.nlm.nih.gov/ [Accessed May 8, 2017].

Biesdorf C, Wang A-L, Topic B, Petri D, Milani H, Huston JP, de Souza Silva MA (2015) Dopamine in the nucleus accumbens core, but not shell, increases during signaled food reward and decreases during delayed extinction. Neurobiol Learn Mem 123:125–139.

Bingmer M, Schiemann J, Roeper J, Schneider G (2011) Measuring burstiness and regularity in oscillatory spike trains. J Neurosci Methods 201:426–437.

Birkmayer W, Hornykiewicz O (1961) [The L-3,4-dioxyphenylalanine (DOPA)-effect in Parkinson-akinesia]. Wien Klin Wochenschr 73:787–788.

Birkmayer W, Hornykiewicz O (1962) [The L-dihydroxyphenylalanine (L-DOPA) effect in Parkinson's syndrome in man: On the pathogenesis and treatment of Parkinson akinesis]. Arch Psychiatr Nervenkr Z Gesamte Neurol Psychiatr 203:560–574.

Birnbaum SG, Varga AW, Yuan L-L, Anderson AE, Sweatt JD, Schrader LA (2004) Structure and function of Kv4-family transient potassium channels. Physiol Rev 84:803–833.

Björklund A, Dunnett SB (2007) Dopamine neuron systems in the brain: an update. Trends Neurosci 30:194–202.

Blendy JA (2011) Modeling neuropsychiatric disease-relevant human SNPs in mice. Neuropsychopharmacology 36:364–365.

Bliss T V, Lomo T (1973) Long-lasting potentiation of synaptic transmission in the dentate area of the anaesthetized rabbit following stimulation of the perforant path. J Physiol 232:331–356.

Bodyak N, Slotnick B (1999) Performance of Mice in an Automated Olfactometer: Odor Detection, Discrimination and Odor Memory. 24.

Boise LH, González-García M, Postema CE, Ding L, Lindsten T, Turka LA, Mao X, Nuñez G, Thompson CB (1993) bcl-x, a bcl-2-related gene that functions as a dominant regulator of apoptotic cell death. Cell 74:597–608.

Bolam JP, Pissadaki EK (2012) Living on the edge with too many mouths to feed: Why dopamine neurons die. Mov Disord 27:1478–1483.

Bonci A, Malenka RC (1999) Properties and Plasticity of Excitatory Synapses on Dopaminergic and GABAergic Cells in the Ventral Tegmental Area. J Neurosci 19.

Bonci A, Williams JT (1997) Increased probability of GABA release during withdrawal from morphine. J Neurosci 17:796–803.

Borrelli E, Usiello A, Baik J-H, Rougé-Pont F, Picetti R, Dierich A, LeMeur M, Piazza PV (2000) Distinct functions of the two isoforms of dopamine D2 receptors. Nature 408:199–203.

Bossé R, Fumagalli F, Jaber M, Giros B, Gainetdinov RR, Wetsel WC, Missale C, Caron MG (1997) Anterior Pituitary Hypoplasia and Dwarfism in Mice Lacking the Dopamine Transporter. Neuron 19:127–138.

Bowden C, Theodorou AE, Cheetham SC, Lowther S, Katona CL, Crompton MR, Horton RW (1997) Dopamine D1 and D2 receptor binding sites in brain samples from depressed suicides and controls. Brain Res 752:227–233.

Branch SY, Sharma R, Beckstead MJ (2014) Aging Decreases L-Type Calcium Channel Currents and Pacemaker Firing Fidelity in Substantia Nigra Dopamine Neurons. J Neurosci 34:9310–9318.

Brennan MD, Phillips DK (2009) Genetic markers of schizophrenia.

Brinschwitz K, Dittgen A, Madai VI, Lommel R, Geisler S, Veh RW (2010) Glutamatergic axons from the lateral habenula mainly terminate on GABAergic neurons of the ventral midbrain. Neuroscience 168:463–476.

Brischoux F, Chakraborty S, Brierley DI, Ungless MA (2009) Phasic excitation of dopamine neurons in ventral VTA by noxious stimuli. Proc Natl Acad Sci U S A 106:4894–4899.

Bromberg-Martin ES, Hikosaka O (2011) Lateral habenula neurons signal errors in the prediction of reward information. Nat Neurosci 14:1209–1216.

Bromberg-Martin ES, Matsumoto M, Hikosaka O (2010a) Dopamine in motivational control: rewarding, aversive, and alerting. Neuron 68:815–834.

Bromberg-Martin ES, Matsumoto M, Hikosaka O (2010b) Distinct Tonic and Phasic Anticipatory Activity in Lateral Habenula and Dopamine Neurons. Neuron 67:144–155.

Bromberg-Martin ES, Matsumoto M, Hong S, Hikosaka O (2010c) A Pallidus-Habenula-Dopamine Pathway Signals Inferred Stimulus Values. J Neurophysiol 104:1068–1076.

Bronikowski AM, Carter PA, Swallow JG, Girard IA, Rhodes JS, Garland T (2001) Open-field behavior of house mice selectively bred for high voluntary wheel-running. Behav Genet 31:309–316.

Brown DA, Passmore GM (2009) Neural KCNQ (Kv7) channels. Br J Pharmacol 156:1185–1195.

Brown MTC, Henny P, Bolam JP, Magill PJ (2009) Activity of Neurochemically Heterogeneous Dopaminergic Neurons in the Substantia Nigra during Spontaneous and Driven Changes in Brain State. J Neurosci 29:2915–2925.

Buckholtz JW, Treadway MT, Cowan RL, Woodward ND, Benning SD, Li R, Ansari MS, Baldwin RM, Schwartzman AN, Shelby ES, Smith CE, Cole D, Kessler RM, Zald DH (2010) Mesolimbic dopamine reward system hypersensitivity in individuals with psychopathic traits. Nat Neurosci 13:419–421.

Bui T V., Grande G, Rose PK (2008) Relative Location of Inhibitory Synapses and Persistent Inward Currents Determines the Magnitude and Mode of Synaptic Amplification in Motoneurons. J Neurophysiol 99:583–594.

Buse J, Schoenefeld K, Münchau A, Roessner V (2013) Neuromodulation in Tourette syndrome: Dopamine and beyond. Neurosci Biobehav Rev 37:1069–1084.

Butler A, Wei AG, Baker K, Salkoff L (1989) A family of putative potassium channel genes in Drosophila. Science 243:943–947.

Byrd AL, Loeber R, Pardini DA (2014) Antisocial Behavior, Psychopathic Features and Abnormalities in Reward and Punishment Processing in Youth. Clin Child Fam Psychol Rev 17:125–156.

Cagniard B, Balsam PD, Brunner D, Zhuang X (2006a) Mice with Chronically Elevated Dopamine Exhibit Enhanced Motivation, but not Learning, for a Food Reward. Neuropsychopharmacology 31:1362–1370.

Cagniard B, Beeler JA, Britt JP, McGehee DS, Marinelli M, Zhuang X (2006b) Dopamine Scales Performance in the Absence of New Learning.

Calabresi P, Pisani A, Mercuri NB, Bernardi G (1992) Long-term Potentiation in the Striatum is Unmasked by Removing the Voltage-dependent Magnesium Block of NMDA Receptor Channels. Eur J Neurosci 4:929–935.

Calloe K, Cordeiro JM, Di Diego JM, Hansen RS, Grunnet M, Olesen SP, Antzelevitch C (2008) A transient outward potassium current activator recapitulates the electrocardiographic manifestations of Brugada syndrome. Cardiovasc Res 81:686–694.

Calloe K, Soltysinska E, Jespersen T, Lundby A, Antzelevitch C, Olesen S-P, Cordeiro JM (2010) Differential effects of the transient outward K+ current activator NS5806 in the canine left ventricle. J Mol Cell Cardiol 48:191–200.

Cao J-L, Covington HE, Friedman AK, Wilkinson MB, Walsh JJ, Cooper DC, Nestler EJ, Han M-H, Han M-H (2010) Mesolimbic dopamine neurons in the brain reward circuit mediate susceptibility to social defeat and antidepressant action. J Neurosci 30:16453–16458.

Carboni E, Tanda GL, Frau R, Di Chiara G (1990) Blockade of the noradrenaline carrier increases extracellular dopamine concentrations in the prefrontal cortex: evidence that dopamine is taken up in vivo by noradrenergic terminals. J Neurochem 55:1067–1070.

Cardozo Pinto DF, Lammel S (2017) Viral vector strategies for investigating midbrain dopamine circuits underlying motivated behaviors. Pharmacol Biochem Behav.

Carlsson A (1988) The current status of the dopamine hypothesis of schizophrenia. Neuropsychopharmacology 1:179–186.

Carlsson A, Lindqvist M (1963) Effect of chlorpromazine or haloperidol on formation of 3methoxytyramine and normetanephrine in mouse brain. Acta Pharmacol Toxicol (Copenh) 20:140–144.

Carlsson A, Lindqvist M, Magnusson T (1957) 3,4-Dihydroxyphenylalanine and 5-Hydroxytryptophan as Reserpine Antagonists. Nature 180:1200–1200.

Carlsson A, Lindqvist M, Magnusson T, Waldeck B (1958) On the presence of 3-hydroxytyramine in brain. Science 127:471.

Carpenter AC, Saborido TP, Stanwood GD (2012) Development of Hyperactivity and Anxiety Responses in Dopamine Transporter-Deficient Mice. Dev Neurosci 34:250–257.

Carr DB, Sesack SR (2000) Projections from the rat prefrontal cortex to the ventral tegmental area: target specificity in the synaptic associations with mesoaccumbens and mesocortical neurons. J Neurosci 20:3864–3873.

Carrillo Oesterreich F, Bowne-Anderson H, Howard J (2016) The contribution of alternative splicing probability to the coding expansion of the genome. bioRxiv.

Castellanos FX, Lee PP, Sharp W, Jeffries NO, Greenstein DK, Clasen LS, Blumenthal JD, James RS, Ebens CL, Walter JM, Zijdenbos A, Evans AC, Giedd JN, Rapoport JL (2002) Developmental trajectories of brain volume abnormalities in children and adolescents with

attention-deficit/hyperactivity disorder. JAMA 288:1740–1748.
Cerruti C, Walther DM, Kuhar MJ, Uhl GR (1993) Dopamine transporter mRNA expression is intense in rat midbrain neurons and modest outside midbrain. Mol Brain Res 18:181–186.
Chabala LD, Bakry N, Covarrubias M (1993) Low molecular weight poly(A)+ mRNA species encode factors that modulate gating of a non-Shaker A-type K+ channel. J Gen Physiol 102:713–728.
Chan CS, Guzman JN, Ilijic E, Mercer JN, Rick C, Tkatch T, Meredith GE, Surmeier DJ (2007) "Rejuvenation" protects neurons in mouse models of Parkinson's disease. Nature 447:1081–1086.
Chang C, Grace AA (2014) Amygdala-Ventral Pallidum Pathway Decreases Dopamine Activity After Chronic Mild Stress in Rats. Biol Psychiatry 76:223–230.
Chang CY, Esber GR, Marrero-Garcia Y, Yau H-J, Bonci A, Schoenbaum G (2015) Brief optogenetic inhibition of dopamine neurons mimics endogenous negative reward prediction errors. Nat Neurosci 19:1–8.
Chen X, Ruan M-Y, Cai S-Q (2015) KChIP-Like Auxiliary Subunits of Kv4 Channels Regulate Excitability of Muscle Cells and Control Male Turning Behavior during Mating in Caenorhabditis elegans. J Neurosci 35.
Chen X, Yuan L-L, Zhao C, Birnbaum SG, Frick A, Jung WE, Schwarz TL, Sweatt JD, Johnston D (2006) Deletion of Kv4.2 gene eliminates dendritic A-type K+ current and enhances induction of long-term potentiation in hippocampal CA1 pyramidal neurons. J Neurosci 26:12143–12151.
Cheramy A, Leviel V, Glowinski J (1981) Dendritic release of dopamine in the substantia nigra. Nature 289:537–543.
Chesney E, Goodwin GM, Fazel S (2014) Risks of all-cause and suicide mortality in mental disorders: a meta-review. World Psychiatry 13:153–160.
Chevalier G, Deniau JM (1990) Disinhibition as a basic process in the expression of striatal functions. Trends Neurosci 13:277–280.
Chivers CE, Koner AL, Lowe ED, Howarth M (2011) How the biotin-streptavidin interaction was made even stronger: investigation via crystallography and a chimaeric tetramer. Biochem J 435:55–63.
Choi KL, Aldrich RW, Yellen G (1991) Tetraethylammonium blockade distinguishes two inactivation mechanisms in voltage-activated K+ channels. Proc Natl Acad Sci U S A 88:5092–5095.
Christoph GR, Leonzio RJ, Wilcox KS (1986) Stimulation of the lateral habenula inhibits dopamine-containing neurons in the substantia nigra and ventral tegmental area of the rat. J Neurosci 6:613–619.
Ciliax BJ, Drash GW, Staley JK, Haber S, Mobley CJ, Miller GW, Mufson EJ, Mash DC, Levey AI (1999) Immunocytochemical localization of the dopamine transporter in human brain. J Comp Neurol 409:38–56.
Ciliax BJ, Heilman C, Demchyshyn LL, Pristupa ZB, Ince E, Hersch SM, Niznik HB, Levey AI (1995) The dopamine transporter: immunochemical characterization and localization in brain. J Neurosci 15:1714–1723.
Cohen JY, Haesler S, Vong L, Lowell BB, Uchida N (2012) Neuron-type-specific signals for reward and punishment in the ventral tegmental area. Nature 482:85–88.
Cohen MX, Frank MJ (2009) Neurocomputational models of basal ganglia function in learning, memory and choice. Behav Brain Res 199:141–156.
Colelli V, Fiorenza MT, Conversi D, Orsini C, Cabib S (2010) Strain-specific proportion of the two isoforms of the dopamine D2 receptor in the mouse striatum: associated neural and behavioral phenotypes. Genes, Brain Behav 9:703–711.
Collier TJ, Kanaan NM, Kordower JH (2011) Ageing as a primary risk factor for Parkinson's disease: evidence from studies of non-human primates. Nat Rev Neurosci 12:359–366.
Cone JJ, McCutcheon JE, Roitman MF (2014) Ghrelin Acts as an Interface between Physiological State and Phasic Dopamine Signaling. J Neurosci 34.
Cools R, Altamirano L, D'Esposito M (2006) Reversal learning in Parkinson's disease depends on medication status and outcome valence. Neuropsychologia 44:1663–1673.
Corbett D, Wise RA (1980) Intracranial self-stimulation in relation to the ascending dopaminergic systems of the midbrain: A moveable electrode mapping study. Brain Res 185:1–15.
Costa KM (2014) The Effects of Aging on Substantia Nigra Dopamine Neurons. J Neurosci 34:15133–15134.
Costa RM, Gutierrez R, de Araujo IE, Coelho MRP, Kloth AD, Gainetdinov RR, Caron MG, Nicolelis MAL, Simon SA (2007) Dopamine levels modulate the updating of tastant values. Genes, Brain

Behav 6:314–320.

Costa RP, Padamsey Z, D'Amour JA, Emptage NJ, Froemke RC, Vogels TP (2017) Synaptic Transmission Optimization Predicts Expression Loci of Long-Term Plasticity. Neuron 96:177–189.e7.

Covarrubias M, Bhattacharji A, De Santiago-Castillo JA, Dougherty K, Kaulin YA, Na-Phuket TR, Wang G (2008) The neuronal Kv4 channel complex. Neurochem Res 33:1558–1567.

Cragg SJ, Rice ME (2004) DAncing past the DAT at a DA synapse. Trends Neurosci 27:270–277.

Cramér H (1946) Mathematical methods of statistics. Princeton University Press.

Crawley JN (1985) Exploratory behavior models of anxiety in mice. Neurosci Biobehav Rev 9:37–44.

Crawley JN (2007) What's Wrong With My Mouse? Behavioural Phenotyping of Transgenic and Knockout Mice. Wiley-Interscience.

Creed M, Ntamati NR, Chandra R, Lobo MK, Lüscher C, Schlyer DJ, Dewey SL, Wolf AP, Martina M, Surmeier DJ, Mameli M (2016) Convergence of Reinforcing and Anhedonic Cocaine Effects in the Ventral Pallidum. Neuron 92:214–226.

Crick F, Koch C (1990) Towards a Neurobiological Theory of Consciousness. Semin Neurosci 2.

Crow TJ (1972) A map of the rat mesencephalon for electrical self-stimulation. Brain Res 36:265–273.

Cui G, Bernier BE, Harnett MT, Morikawa H (2007) Differential Regulation of Action Potential- and Metabotropic Glutamate Receptor-Induced Ca2+ Signals by Inositol 1,4,5-Trisphosphate in Dopaminergic Neurons. J Neurosci 27.

Cui G, Jun SB, Jin X, Luo G, Pham MD, Lovinger DM, Vogel SS, Costa RM (2014a) Deep brain optical measurements of cell type-specific neural activity in behaving mice. Nat Protoc 9:1213–1228.

Cui G, Jun SB, Jin X, Pham MD, Vogel SS, Lovinger DM, Costa RM (2014b) Concurrent activation of striatal direct and indirect pathways during action initiation. Nature 494:238–242.

Dahlstroem A, Fuxe K (1964) Evidence for the existence of monoamine-containing neurons in the central nervous system. I. Demonstration of monoamines in cell bodies of brain stem neurons. Acta Physiol Scand Suppl:SUPPL 232:1-55.

Dal Toso R, Sommer B, Ewert M, Herb A, Pritchett DB, Bach A, Shivers BD, Seeburg PH (1989) The dopamine D2 receptor: two molecular forms generated by alternative splicing. EMBO J 8:4025–4034.

Danjo T, Yoshimi K, Funabiki K, Yawata S, Nakanishi S (2014) Aversive behavior induced by optogenetic inactivation of ventral tegmental area dopamine neurons is mediated by dopamine D2 receptors in the nucleus accumbens. Proc Natl Acad Sci U S A 111:6455–6460.

Dantzer R, O'Connor JC, Freund GG, Johnson RW, Kelley KW (2008) From inflammation to sickness and depression: when the immune system subjugates the brain. Nat Rev Neurosci 9:46–56.

Dautan D, Souza AS, Huerta-Ocampo I, Valencia M, Assous M, Witten IB, Deisseroth K, Tepper JM, Bolam JP, Gerdjikov T V, Mena-Segovia J (2016) Segregated cholinergic transmission modulates dopamine neurons integrated in distinct functional circuits. Nat Neurosci 19:1025–1033.

Daw ND, Kakade S, Dayan P (2002) Opponent interactions between serotonin and dopamine. Neural Netw 15:603–616.

Dayan P, Niv Y (2008) Reinforcement learning: The Good, The Bad and The Ugly. Curr Opin Neurobiol 18:185–196.

Degoulet M, Stelly CE, Ahn K-C, Morikawa H (2016) L-type Ca2+ channel blockade with antihypertensive medication disrupts VTA synaptic plasticity and drug-associated contextual memory. Mol Psychiatry 21:394–402.

Deister CA, Teagarden MA, Wilson CJ, Paladini CA (2009) An Intrinsic Neuronal Oscillator Underlies Dopaminergic Neuron Bursting. J Neurosci 29:15888–15897.

del Campo N, Chamberlain SR, Sahakian BJ, Robbins TW (2011) The Roles of Dopamine and Noradrenaline in the Pathophysiology and Treatment of Attention-Deficit/Hyperactivity Disorder. Biol Psychiatry 69:e145–e157.

Deng S, Zhang L, Zhu T, Liu Y-M, Zhang H, Shen Y, Li W-G, Li F (2015) A behavioral defect of temporal association memory in mice that partly lack dopamine reuptake transporter. Sci Rep 5:17461.

Deng X-Y, Cai F, Xia K, Pan Q, Long Z-G, Wu L-Q, Liang D-S, Dai H-P, Zhang Z-H, XIA J-H (2005) Identification of the Alternative Promoters of the KChIP4 Subfamily. Acta Biochim Biophys Sin (Shanghai) 37:241–247.

Denys D, Zohar J, Westenberg HGM (2004) The role of dopamine in obsessive-compulsive disorder: preclinical and clinical evidence. J Clin Psychiatry 65 Suppl 14:11–17.

Di Chiara G (2002) Nucleus accumbens shell and core dopamine: differential role in behavior and addiction. Behav Brain Res 137:75–114.

Di Chiara G, Tanda GL, Frau R, Carboni E (1992) Heterologous monoamine reuptake: lack of transmitter specificity of neuron-specific carriers. Neurochem Int 20 Suppl:231S–235S.

Ding S, Wei W, Zhou F-M (2011) Molecular and functional differences in voltage-activated sodium currents between GABA projection neurons and dopamine neurons in the substantia nigra. J Neurophysiol 106:3019–3034.

Dixon JE, Shi W, Wang HS, McDonald C, Yu H, Wymore RS, Cohen IS, McKinnon D (1996) Role of the Kv4.3 K+ channel in ventricular muscle. A molecular correlate for the transient outward current. Circ Res 79:659–668.

Dodson PD, Dreyer JK, Jennings KA, Syed ECJ, Wade-Martins R, Cragg SJ, Bolam JP, Magill PJ (2016) Representation of spontaneous movement by dopaminergic neurons is cell-type selective and disrupted in parkinsonism. Proc Natl Acad Sci U S A 113:E2180-8.

Domingues-Montanari S, Fernández-Cadenas I, del Río-Espinola A, Mendioroz M, Fernandez-Morales J, Corbeto N, Delgado P, Ribó M, Rubiera M, Obach V, Martí-Fàbregas J, Freijo M, Serena J, Montaner J (2010) KCNK17 genetic variants in ischemic stroke. Atherosclerosis 208:203–209.

Dong Y, Saal D, Thomas M, Faust R, Bonci A, Robinson T, Malenka RC (2004) Cocaine-induced potentiation of synaptic strength in dopamine neurons: behavioral correlates in GluRA(-/-) mice. Proc Natl Acad Sci U S A 101:14282–14287.

Douglas RJ, Martin KAC (2004) Neuronal Circuits of the Neocortex. Annu Rev Neurosci 27:419–451.

Douglas VI, Parry PA (1994) Effects of reward and nonreward on frustration and attention in attention deficit disorder. J Abnorm Child Psychol 22:281–302.

Doyle DA, Morais Cabral J, Pfuetzner RA, Kuo A, Gulbis JM, Cohen SL, Chait BT, MacKinnon R (1998) The structure of the potassium channel: molecular basis of K+ conduction and selectivity. Science 280:69–77.

Dragicevic E, Poetschke C, Duda J, Schlaudraff F, Lammel S, Schiemann J, Fauler M, Hetzel A, Watanabe M, Lujan R, Malenka RC, Striessnig J, Liss B (2014) Ca<inf>v</inf>1.3 channels control D2-autoreceptor responses via NCS-1 in substantia nigra dopamine neurons. Brain 137:2287–2302.

Dreyer JK, Herrik KF, Berg RW, Hounsgaard JD (2010) Influence of phasic and tonic dopamine release on receptor activation. J Neurosci 30:14273–14283.

Dudman JT, Krakauer JW (2016) The basal ganglia: from motor commands to the control of vigor. Curr Opin Neurobiol 37:158–166.

Dufour MA, Woodhouse A, Goaillard J-M (2014) Somatodendritic ion channel expression in substantia nigra pars compacta dopaminergic neurons across postnatal development. J Neurosci Res 92:981–999.

Dunlop BW, Nemeroff CB, E E, E E, JH K, GR H, DS C, BJ S, A B, M A, GB C, JP S, RB I, DS C (2007) The Role of Dopamine in the Pathophysiology of Depression. Arch Gen Psychiatry 64:327.

Durstewitz D, Kelc M, Gu O (1999) A Neurocomputational Theory of the Dopaminergic Modulation of Working Memory Functions. 19:2807–2822.

Dzirasa K, Ramsey AJ, Takahashi DY, Stapleton J, Potes JM, Williams JK, Gainetdinov RR, Sameshima K, Caron MG, Nicolelis MAL (2009a) Hyperdopaminergia and NMDA receptor hypofunction disrupt neural phase signaling. J Neurosci 29:8215–8224.

Dzirasa K, Santos LM, Ribeiro S, Stapleton J, Gainetdinov RR, Caron MG, Nicolelis MAL (2009b) Persistent hyperdopaminergia decreases the peak frequency of hippocampal theta oscillations during quiet waking and REM sleep. PLoS One 4.

Edwards NJ, Tejeda HA, Pignatelli M, Zhang S, McDevitt RA, Wu J, Bass CE, Bettler B, Morales M, Bonci A (2017) Circuit specificity in the inhibitory architecture of the VTA regulates cocaine-induced behavior. Nat Neurosci 20:438–448.

Efimova E V, Gainetdinov RR, Budygin EA, Sotnikova TD (2016) Dopamine transporter mutant animals: a translational perspective. J Neurogenet 30:5–15.

Elliott R, Sahakian BJ, Herrod JJ, Robbins TW, Paykel ES (1997) Abnormal response to negative feedback in unipolar depression: evidence for a diagnosis specific impairment. J Neurol

Neurosurg Psychiatry 63:74–82.

Elliott R, Sahakian BJ, McKay AP, Herrod JJ, Robbins TW, Paykel ES (1996) Neuropsychological impairments in unipolar depression: the influence of perceived failure on subsequent performance. Psychol Med 26:975.

Ellwood IT, Patel T, Wadia V, Lee AT, Liptak AT, Bender KJ, Sohal VS (2017) Tonic or phasic stimulation of dopaminergic projections to prefrontal cortex causes mice to maintain or deviate from previously learned behavioral strategies. J Neurosci.

Engström G, Alling C, Blennow K, Regnéll G, Träskman-Bendz L (1999) Reduced cerebrospinal HVA concentrations and HVA/5-HIAA ratios in suicide attempters. Eur Neuropsychopharmacol 9:399–405.

Ennaceur A, Delacour J (1988) A new one-trial test for neurobiological studies of memory in rats. 1: Behavioral data. Behav Brain Res 31:47–59.

Ericsson J, Stephenson-Jones M, Kardamakis A, Robertson B, Silberberg G, Grillner S (2013) Evolutionarily conserved differences in pallial and thalamic short-term synaptic plasticity in striatum. J Physiol 591:859–874.

Ersche KD, Gillan CM, Jones PS, Williams GB, Ward LHE, Luijten M, de Wit S, Sahakian BJ, Bullmore ET, Robbins TW (2016) Carrots and sticks fail to change behavior in cocaine addiction. Science (80-) 352:1468–1471.

Eshel N, Bukwich M, Rao V, Hemmelder V, Tian J, Uchida N (2015) Arithmetic and local circuitry underlying dopamine prediction errors. Nature 525:243–246.

Ezkurdia I, Juan D, Rodriguez JM, Frankish A, Diekhans M, Harrow J, Vazquez J, Valencia A, Tress ML (2014) Multiple evidence strands suggest that there may be as few as 19 000 human protein-coding genes. Hum Mol Genet 23:5866–5878.

Faraone S V., Perlis RH, Doyle AE, Smoller JW, Goralnick JJ, Holmgren MA, Sklar P (2005) Molecular Genetics of Attention-Deficit/Hyperactivity Disorder. Biol Psychiatry 57:1313–1323.

Fearnley JM, Lees AJ (1991) Ageing and Parkinson's disease: substantia nigra regional selectivity. Brain 114 (Pt 5):2283–2301.

Fetsko LA, Xu R, Wang Y (2003) Alterations in D1/D2 synergism may account for enhanced stereotypy and reduced climbing in mice lacking dopamine D2L receptor. Brain Res 967:191–200.

Fibiger HC, LePiane FG, Jakubovic A, Phillips AG (1987) The role of dopamine in intracranial self-stimulation of the ventral tegmental area. J Neurosci 7:3888–3896.

File SE, Wardill AG (1975) The reliability of the hole-board apparatus. Psychopharmacologia 44:47–51.

Fiorillo CD (2013) Two Dimensions of Value : Dopamine Neurons Represent Reward But Not Aversiveness. Science (80-) 341:546–549.

Fiorillo CD, Song MR, Yun SR (2013a) Multiphasic Temporal Dynamics in Responses of Midbrain Dopamine Neurons to Appetitive and Aversive Stimuli. J Neurosci 33.

Fiorillo CD, Yun SR, Song MR (2013b) Diversity and Homogeneity in Responses of Midbrain Dopamine Neurons. J Neurosci 33.

Fisher RA (1930) The Moments of the Distribution for Normal Samples of Measures of Departure from Normality. Proc R Soc A Math Phys Eng Sci 130:16–28.

Flagel SB, Clark JJ, Robinson TE, Mayo L, Czuj A, Willuhn I, Akers CA, Clinton SM, Phillips PEM, Akil H (2011) A selective role for dopamine in stimulus–reward learning. Nature 469:53–57.

Floresco SB (2013) Prefrontal dopamine and behavioral flexibility: Shifting from an "inverted-U" toward a family of functions. Front Neurosci 7:1–12.

Floresco SB, West AR, Ash B, Moore H, Grace AA (2003) Afferent modulation of dopamine neuron firing differentially regulates tonic and phasic dopamine transmission. Nat Neurosci 6:968–973.

Florian R V. (2007) Reinforcement Learning Through Modulation of Spike-Timing-Dependent Synaptic Plasticity. Neural Comput 19:1468–1502.

Ford CP (2014) The role of D2-autoreceptors in regulating dopamine neuron activity and transmission. Neuroscience 282:13–22.

Fournier F, Müller CM, Laurent G (2015) Looking for the roots of cortical sensory computation in three-layered cortices. Curr Opin Neurobiol 31:119–126.

Fox MA, Panessiti MG, Hall FS, Uhl GR, Murphy DL (2013) An evaluation of the serotonin system and perseverative, compulsive, stereotypical, and hyperactive behaviors in dopamine transporter (DAT) knockout mice. Psychopharmacology (Berl) 227:685–695.

Frank MJ (2005) Dynamic Dopamine Modulation in the Basal Ganglia: A Neurocomputational Account of Cognitive Deficits in Medicated and Nonmedicated Parkinsonism. J Cogn Neurosci 17:51–72.

Frank MJ, Samanta J, Moustafa AA, Sherman SJ (2007) Hold Your Horses: Impulsivity, Deep Brain Stimulation, and Medication in Parkinsonism. Science (80-) 318.

Frank MJ, Seeberger LC, O'Reilly RC (2004) By Carrot or by Stick: Cognitive Reinforcement Learning in Parkinsonism. Science (80-) 306.

Franklin KBJ, Paxinos G (2012) Paxinos and Franklin's The mouse brain in stereotaxic coordinates.

Freed C, Revay R, Vaughan RA, Kriek E, Grant S, Uhl GR, Kuhar MJ (1995) Dopamine transporter immunoreactivity in rat brain. J Comp Neurol 359:340–349.

Frick A, Magee J, Johnston D (2004) LTP is accompanied by an enhanced local excitability of pyramidal neuron dendrites. Nat Neurosci 7:126–135.

Friedel RO (2004) Dopamine Dysfunction in Borderline Personality Disorder: A Hypothesis. Neuropsychopharmacology 29:1029–1039.

Friedman A, Lax E, Dikshtein Y, Abraham L, Flaumenhaft Y, Sudai E, Ben-Tzion M, Ami-Ad L, Yaka R, Yadid G (2010) Electrical stimulation of the lateral habenula produces enduring inhibitory effect on cocaine seeking behavior. Neuropharmacology 59:452–459.

Friedman A, Lax E, Dikshtein Y, Abraham L, Flaumenhaft Y, Sudai E, Ben-Tzion M, Yadid G (2011) Electrical stimulation of the lateral habenula produces an inhibitory effect on sucrose self-administration. Neuropharmacology 60:381–387.

Friedman AK, Juarez B, Ku SM, Zhang H, Calizo RC, Walsh JJ, Chaudhury D, Zhang S, Hawkins A, Dietz DM, Murrough JW, Ribadeneira M, Wong EH, Neve RL, Han M-H (2016) KCNQ channel openers reverse depressive symptoms via an active resilience mechanism. Nat Commun 7:11671.

Fujisawa S, Buzsáki G (2011) A 4 Hz Oscillation Adaptively Synchronizes Prefrontal, VTA, and Hippocampal Activities. Neuron 72:153–165.

Gabay C, Lamacchia C, Palmer G (2010) IL-1 pathways in inflammation and human diseases. Nat Rev Rheumatol 6:232–241.

Gainetdinov RR, Jones SR, Caron MG (1999) Functional hyperdopaminergia in dopamine transporter knock-out mice. Biol Psychiatry 46:303–311.

García-García I, Zeighami Y, Dagher A (2017) Reward Prediction Errors in Drug Addiction and Parkinson's Disease: from Neurophysiology to Neuroimaging. Curr Neurol Neurosci Rep 17:46.

Garris PA, Wightman RM (1994) Different kinetics govern dopaminergic transmission in the amygdala, prefrontal cortex, and striatum: an in vivo voltammetric study. J Neurosci 14:442–450.

Gebauer M, Isbrandt D, Sauter K, Callsen B, Nolting A, Pongs O, Bähring R (2004) N-type inactivation features of Kv4.2 channel gating. Biophys J 86:210–223.

Geffen LB, Jessel TM, Cuello AC, Iversen LL (1976) Release of dopamine from dendrites in rat substantia nigra. Nature 260:258–260.

Gelernter J, Kranzler H, Coccaro E, Siever L, New A, Mulgrew CL (1997) D4 Dopamine-Receptor (DRD4) Alleles and Novelty Seeking in Substance-Dependent, Personality-Disorder, and Control Subjects. Am J Hum Genet 61:1144–1152.

Genro JP, Kieling C, Rohde LA, Hutz MH (2010) Attention-deficit/hyperactivity disorder and the dopaminergic hypotheses. Expert Rev Neurother 10:587–601.

Gentry RN, Lee B, Roesch MR (2016) Phasic dopamine release in the rat nucleus accumbens predicts approach and avoidance performance. Nat Commun 7:13154.

Georges F, Aston-Jones G (2002) Activation of ventral tegmental area cells by the bed nucleus of the stria terminalis: a novel excitatory amino acid input to midbrain dopamine neurons. J Neurosci 22:5173–5187.

Gerfen CR, Staines WA, Fibiger HC, Arbuthnott GW (1982) Crossed connections of the substantia nigra in the rat. J Comp Neurol 207:283–303.

German DC, Manaye KF (1993) Midbrain dopaminergic neurons (nuclei A8, A9, and A10): Three-dimensional reconstruction in the rat. J Comp Neurol 331:297–309.

Gibb WR, Lees AJ (1991) Anatomy, pigmentation, ventral and dorsal subpopulations of the substantia nigra, and differential cell death in Parkinson's disease. J Neurol Neurosurg Psychiatry 54:388–396.

Giros B, Jaber M, Jones SR, Wightman RM, Caron MG (1996) Hyperlocomotion and indifference to cocaine and amphetamine in mice lacking the dopamine transporter. Nature 379:606–612.

Gizer IR, Bizon C, Gilder DA, Ehlers CL, Wilhelmsen KC (2017) Whole genome sequence study of

cannabis dependence in two independent cohorts. Addict Biol.

Glimcher PW (2011) Understanding dopamine and reinforcement learning: the dopamine reward prediction error hypothesis. Proc Natl Acad Sci U S A 108 Suppl 3:15647–15654.

Goetz CG et al. (2008) Movement Disorder Society-sponsored revision of the Unified Parkinson's Disease Rating Scale (MDS-UPDRS): Scale presentation and clinimetric testing results. Mov Disord 23:2129–2170.

Goltstein PM, Coffey EBJ, Roelfsema PR, Pennartz CM a. (2013) In vivo two-photon Ca2+ imaging reveals selective reward effects on stimulus-specific assemblies in mouse visual cortex. J Neurosci 33:11540–11555.

Gonon F, Al. et (2009) The dopaminergic hypothesis of attention-deficit/hyperactivity disorder needs re-examining. Trends Neurosci 32:2–8.

González M, Argaraña CE, Fidelio GD (1999) Extremely high thermal stability of streptavidin and avidin upon biotin binding. Biomol Eng 16:67–72.

Goodman DW (2007) The Consequences of Attention-Deficit/Hyperactivity Disorder in Adults. J Psychiatr Pract 13:318–327.

Gouaux E, Mackinnon R (2005) Principles of selective ion transport in channels and pumps. Science 310:1461–1465.

Grace AA (1992) The depolarization block hypothesis of neuroleptic action: implications for the etiology and treatment of schizophrenia. :91–131.

Grace AA (2012) Dopamine system dysregulation by the hippocampus: Implications for the pathophysiology and treatment of schizophrenia. Neuropharmacology 62:1342–1348.

Grace AA (2016) Dysregulation of the dopamine system in the pathophysiology of schizophrenia and depression. Nat Rev Neurosci 17:524–532.

Grace AA, Bunney BS (1983a) Intracellular and extracellular electrophysiology of nigral dopaminergic neurons - 1. Identification and characterization. Neuroscience 10:301–315.

Grace AA, Bunney BS (1983b) Intracellular and extracellular electrophysiology of nigral dopaminergic neurons-3. Evidence for electrotonic coupling. Neuroscience 10.

Grace AA, Bunney BS (1983c) Intracellular and extracellular electrophysiology of nigral dopaminergic neurons-2. Action potential generating mechanisms and morphological correlates. Neuroscience 10.

Grace AA, Bunney BS (1984a) The control of firing pattern in nigral dopamine neurons: single spike firing. J Neurosci 4:2866–2876.

Grace AA, Bunney BS (1984b) The control of firing pattern in nigral dopamine neurons: burst firing. J Neurosci 4:2877–2890.

Grace AA, Bunney BS (1986) Induction of depolarizing block in midbrain dopamine neurons by repeated administration of haloperidol: analysis using in vivo intracellular recording. J Pharmacol Exp Ther 238:1092–1100.

Grace AA, Floresco SB, Goto Y, Lodge DJ (2007) Regulation of firing of dopaminergic neurons and control of goal-directed behaviors. Trends Neurosci 30:220–227.

Grace A, Bunney B (1980) Nigral dopamine neurons: intracellular recording and identification with L-dopa injection and histofluorescence. Science (80-) 210:654–656.

Gradin VB, Kumar P, Waiter G, Ahearn T, Stickle C, Milders M, Reid I, Hall J, Steele JD (2011) Expected value and prediction error abnormalities in depression and schizophrenia. Brain 134:1751–1764.

Gratton A, Wise RA (1985) Mapping of contraversive and ipsiversive circling responses to ventral tegmental and substantia nigra electrical stimulation. Physiol Behav 35:61–65.

Greenberg PE, Fournier A-A, Sisitsky T, Pike CT, Kessler RC (2015) The Economic Burden of Adults With Major Depressive Disorder in the United States (2005 and 2010). J Clin Psychiatry 76:155–162.

Grueter BA, Rothwell PE, Malenka RC (2012) Integrating synaptic plasticity and striatal circuit function in addiction. Curr Opin Neurobiol 22:545–551.

Gunaydin LA, Grosenick L, Finkelstein JC, Kauvar IV, Fenno LE, Adhikari A, Lammel S, Mirzabekov JJ, Airan RD, Zalocusky KA, Tye KM, Anikeeva P, Malenka RC, Deisseroth K (2014) Natural Neural Projection Dynamics Underlying Social Behavior. Cell 157:1535–1551.

Guo ZVZ et al. (2014) Procedures for Behavioral Experiments in Head-Fixed Mice Simon SA, ed. PLoS One 9:e88678.

Gutlerner JL, Penick EC, Snyder EM, Kauer JA (2002) Novel protein kinase A-dependent long-term

depression of excitatory synapses. Neuron 36:921–931.
Guzman JN, Sanchez-Padilla J, Chan CS, Surmeier DJ (2009) Robust Pacemaking in Substantia Nigra Dopaminergic Neurons. J Neurosci 29:11011–11019.
Haber SN (2014) The place of dopamine in the cortico-basal ganglia circuit. Neuroscience 282:248–257.
Haber SN, Fudge JL, McFarland NR (2000) Striatonigrostriatal pathways in primates form an ascending spiral from the shell to the dorsolateral striatum. J Neurosci 20:2369–2382.
Hage TA, Khaliq ZM (2015) Tonic Firing Rate Controls Dendritic Ca2+ Signaling and Synaptic Gain in Substantia Nigra Dopamine Neurons. J Neurosci 35:5823–5836.
Hahn J, Tse TE, Levitan ES (2003) Long-term K+ channel-mediated dampening of dopamine neuron excitability by the antipsychotic drug haloperidol. J Neurosci 23:10859–10866.
Hall CS, S. C (1934) Emotional behavior in the rat. I. Defecation and urination as measures of individual differences in emotionality. J Comp Psychol 18:385–403.
Hamid AA, Pettibone JR, Mabrouk OS, Hetrick VL, Schmidt R, Vander Weele CM, Kennedy RT, Aragona BJ, Berke JD (2015) Mesolimbic dopamine signals the value of work. Nat Neurosci 19:117–126.
Han S, Yang B-Z, Kranzler HR, Liu X, Zhao H, Farrer LA, Boerwinkle E, Potash JB, Gelernter J (2013) Integrating GWASs and Human Protein Interaction Networks Identifies a Gene Subnetwork Underlying Alcohol Dependence. Am J Hum Genet 93:1027–1034.
Harnett MT, Bernier BE, Ahn K-C, Morikawa H (2009) Burst-Timing-Dependent Plasticity of NMDA Receptor-Mediated Transmission in Midbrain Dopamine Neurons. Neuron 62:826–838.
Harrison NA, Voon V, Cercignani M, Cooper EA, Pessiglione M, Critchley HD (2016) A Neurocomputational Account of How Inflammation Enhances Sensitivity to Punishments Versus Rewards. Biol Psychiatry 80:73–81.
Hart AS, Clark JJ, Phillips PEM (2015) Dynamic shaping of dopamine signals during probabilistic Pavlovian conditioning. Neurobiol Learn Mem 117:84–92.
Hart AS, Rutledge RB, Glimcher PW, Phillips PEM (2014a) Phasic dopamine release in the rat nucleus accumbens symmetrically encodes a reward prediction error term. J Neurosci 34:698–704.
Hart BL (1988) Biological basis of the behavior of sick animals. Neurosci Biobehav Rev 12:123–137.
Hart G, Leung BK, Balleine BW (2014b) Dorsal and ventral streams: The distinct role of striatal subregions in the acquisition and performance of goal-directed actions. Neurobiol Learn Mem 108:104–118.
Häusser MA, Yung WH (1994) Inhibitory synaptic potentials in guinea-pig substantia nigra dopamine neurones in vitro. J Physiol 479 (Pt 3):401–422.
Häusser M, Stuart G, Racca C, Sakmann B (1995) Axonal initiation and active dendritic propagation of action potentials in substantia nigra neurons. Neuron 15:637–647.
Hawes SL, Evans RC, Unruh BA, Benkert EE, Gillani F, Dumas TC, Blackwell KT (2015) Multimodal Plasticity in Dorsal Striatum While Learning a Lateralized Navigation Task. J Neurosci 35:10535–10549.
Heckers S (2001) Neuroimaging studies of the hippocampus in schizophrenia. Hippocampus 11:520–528.
Hedegaard H, Chen L-H, Warner M (2015) Drug-poisoning deaths involving heroin: United States, 2000-2013. NCHS Data Brief:1–8.
Heginbotham L, Lu Z, Abramson T, MacKinnon R (1994) Mutations in the K+ channel signature sequence. Biophys J 66:1061–1067.
Heinz A, Schlagenhauf F (2010) Dopaminergic Dysfunction in Schizophrenia: Salience Attribution Revisited. Schizophr Bull 36:472–485.
Hikosaka O, Ghazizadeh A, Griggs W, Amita H (2017) Parallel basal ganglia circuits for decision making. J Neural Transm:1–15.
Hikosaka O, Kim HF, Yasuda M, Yamamoto S (2014) Basal Ganglia Circuits for Reward Value-Guided Behavior. Annu Rev Neurosci 37:289–306.
Hille B (2001) Ion channels of excitable membranes. Sinauer.
Hills TT (2006) Animal foraging and the evolution of goal-directed cognition. Cogn Sci 30:3–41.
Hironaka N, Ikeda K, Sora I, Uhl GR, Niki H (2004) Food-reinforced operant behavior in dopamine transporter knockout mice: Enhanced resistance to extinction. Ann N Y Acad Sci 1025:140–145.

Hirsch E, Graybiel AM, Agid YA (1988) Melanized dopaminergic neurons are differentially susceptible to degeneration in Parkinson's disease. Nature 334:345–348.

Hirtz D, Thurman DJ, Gwinn-Hardy K, Mohamed M, Chaudhuri AR, Zalutsky R (2007) How common are the "common" neurologic disorders? Neurology 68:326–337.

Holmqvist MH, Cao J, Hernandez-Pineda R, Jacobson MD, Carroll KI, Sung MA, Betty M, Ge P, Gilbride KJ, Brown ME, Jurman ME, Lawson D, Silos-Santiago I, Xie Y, Covarrubias M, Rhodes KJ, Distefano PS, An WF (2002) Elimination of fast inactivation in Kv4 A-type potassium channels by an auxiliary subunit domain. Proc Natl Acad Sci U S A 99:1035–1040.

Holthoff K, Kovalchuk Y, Konnerth A (2006) Dendritic spikes and activity-dependent synaptic plasticity. Cell Tissue Res 326:369–377.

Hong S, Hikosaka O (2008) The Globus Pallidus Sends Reward-Related Signals to the Lateral Habenula. Neuron 60:720–729.

Hong S, Hikosaka O (2013) Diverse sources of reward value signals in the basal ganglia nuclei transmitted to the lateral habenula in the monkey. Front Hum Neurosci 7:778.

Hong S, Jhou TC, Smith M, Saleem KS, Hikosaka O (2011) Negative reward signals from the lateral habenula to dopamine neurons are mediated by rostromedial tegmental nucleus in primates. J Neurosci 31:11457–11471.

Hornykiewicz O (1962) Dopamin (3-Hydroxytyramin) im Zentralnervensystem und seine Beziehung zum Parkinson-Syndrom des Menschen. DMW - Dtsch Medizinische Wochenschrift 87:1807–1810.

Hornykiewicz O (1963) [The tropical localization and content of noradrenalin and dopamine (3-hydroxytyramine) in the substantia nigra of normal persons and patients with Parkinson's disease]. Wien Klin Wochenschr 75:309–312.

Hornykiewicz O (2002a) Dopamine miracle: From brain homogenate to dopamine replacement. Mov Disord 17:501–508.

Hornykiewicz O (2002b) L-DOPA: From a biologically inactive amino acid to a successful therapeutic agent. Amino Acids 23:65–70.

Horvitz JC (2000) Mesolimbocortical and nigrostriatal dopamine responses to salient non- reward events. Neuroscience 96:651–656.

Hoshi T, Zagotta W, Aldrich R (1990) Biophysical and molecular mechanisms of Shaker potassium channel inactivation. Science (80-) 250.

Hosp JA, Luft AR (2013) Dopaminergic meso-cortical projections to M1: Role in motor learning and motor cortex plasticity. Front Neurol 4 OCT:1–7.

Howe MW, Dombeck DA (2016) Rapid signalling in distinct dopaminergic axons during locomotion and reward. Nature 535:505–510.

Howes OD, McCutcheon R, Owen MJ, Murray RM (2017) The Role of Genes, Stress, and Dopamine in the Development of Schizophrenia. Biol Psychiatry 81:9–20.

Huang Q, Zhou D, DiFiglia M (1992) Neurobiotin, a useful neuroanatomical tracer for in vivo anterograde, retrograde and transneuronal tract-tracing and for in vitro labeling of neurons. J Neurosci Methods 41:31–43.

Hull CL, Hovland CI, Ross RT, Hall M, Perkins DT, Fitch FB (1940) Mathematico-deductive theory of rote learning: a study in scientific methodology.

Hussman JP, Chung R-H, Griswold AJ, Jaworski JM, Salyakina D, Ma D, Konidari I, Whitehead PL, Vance JM, Martin ER, Cuccaro ML, Gilbert JR, Haines JL, Pericak-Vance MA (2011) A noise-reduction GWAS analysis implicates altered regulation of neurite outgrowth and guidance in autism. Mol Autism 2:1.

Huys QJM, Daw ND, Dayan P (2015) Depression: A Decision-Theoretic Analysis. Annu Rev Neurosci 38:1–23.

Hyngstrom AS, Johnson MD, Heckman CJ (2008) Summation of Excitatory and Inhibitory Synaptic Inputs by Motoneurons With Highly Active Dendrites. J Neurophysiol 99:1643–1652.

Ikai Y, Takada M, Shinonaga Y, Mizuno N (1992) Dopaminergic and non-dopaminergic neurons in the ventral tegmental area of the rat project, respectively, to the cerebellar cortex and deep cerebellar nuclei. Neuroscience 51:719–728.

Ikemoto S, Yang C, Tan A (2015) Basal ganglia circuit loops, dopamine and motivation: A review and enquiry. Behav Brain Res 290:17–31.

Ilango A, Kesner AJ, Keller KL, Stuber GD, Bonci A, Ikemoto S (2014) Similar roles of substantia nigra and ventral tegmental dopamine neurons in reward and aversion. J Neurosci 34:817–822.

Isingrini E, Perret L, Rainer Q, Amilhon B, Guma E, Tanti A, Martin G, Robinson J, Moquin L, Marti F, Mechawar N, Williams S, Gratton A, Giros B (2016) Resilience to chronic stress is mediated by noradrenergic regulation of dopamine neurons. Nat Neurosci 19:560–563.

Ito R, Hayen A (2011) Opposing Roles of Nucleus Accumbens Core and Shell Dopamine in the Modulation of Limbic Information Processing. J Neurosci 31.

Iversen LL, Iversen SD, Dunnett SB, Björklund A (2010) Dopamine handbook. Oxford University Press.

Izhikevich EM (2007) Solving the Distal Reward Problem through Linkage of STDP and Dopamine Signaling. Cereb Cortex 17:2443–2452.

Jackson DM, Westlind-Danielsson A (1994) Dopamine receptors: Molecular biology, biochemistry and behavioural aspects. Pharmacol Ther 64:291–370.

Jensen J, Willeit M, Zipursky RB, Savina I, Smith AJ, Menon M, Crawley AP, Kapur S (2008) The Formation of Abnormal Associations in Schizophrenia: Neural and Behavioral Evidence. Neuropsychopharmacology 33:473–479.

Jerng HH, Pfaffinger PJ (2008) Multiple Kv channel-interacting proteins contain an N-terminal transmembrane domain that regulates Kv4 channel trafficking and gating. J Biol Chem 283:36046–36059.

Jerng HH, Pfaffinger PJ (2014) Modulatory mechanisms and multiple functions of somatodendritic A-type K + channel auxiliary subunits. Front Cell Neurosci 8:1–20.

Jerng HH, Pfaffinger PJ, Blauw H, Franke L, Saris C (2012) Incorporation of DPP6a and DPP6k variants in ternary Kv4 channel complex reconstitutes properties of A-type K current in rat cerebellar granule cells Bondarenko VE, ed. PLoS One 7:e38205.

Jerng HH, Pfaffinger PJ, Covarrubias M (2004) Molecular physiology and modulation of somatodendritic A-type potassium channels. Mol Cell Neurosci 27:343–369.

Ji H, Shepard PD (2007) Lateral Habenula Stimulation Inhibits Rat Midbrain Dopamine Neurons through a GABAA Receptor-Mediated Mechanism. J Neurosci 27:6923–6930.

Jin X, Costa RM (2010) Start/stop signals emerge in nigrostriatal circuits during sequence learning. Nature 466:457–462.

Jin X, Costa RM (2015) Shaping action sequences in basal ganglia circuits. Curr Opin Neurobiol 33:188–196.

Jin X, Tecuapetla F, Costa RM (2014) Basal ganglia subcircuits distinctively encode the parsing and concatenation of action sequences. Nat Neurosci 17:423–430.

Joanes DN, Gill CA (1998) Comparing measures of sample skewness and kurtosis. J R Stat Soc Ser D (The Stat 47:183–189.

Joel D, Niv Y, Ruppin E (2002) Actor-critic models of the basal ganglia: new anatomical and computational perspectives. Neural Netw 15:535–547.

Johansen EB, Aase H, Meyer A, Sagvolden T (2002) Attention-deficit/hyperactivity disorder (ADHD) behaviour explained by dysfunctioning reinforcement and extinction processes. Behav Brain Res 130:37–45.

John Mann J, Malone KM, Goodwin F, Linnoila M, Yates C, Nicolaou N (1997) Cerebrospinal fluid amines and higher-lethality suicide attempts in depressed inpatients. Biol Psychiatry 41:162–171.

Johnson AD (2009) Single-nucleotide polymorphism bioinformatics: a comprehensive review of resources. Circ Cardiovasc Genet 2:530–536.

Johnson C, Drgon T, Walther D, Uhl GR (2011) Genomic regions identified by overlapping clusters of nominally-positive SNPs from Genome-Wide studies of alcohol and illegal substance dependence. PLoS One 6.

Jones S, Kornblum JL, Kauer JA (2000) Amphetamine blocks long-term synaptic depression in the ventral tegmental area. J Neurosci 20:5575–5580.

Jones SR, Gainetdinov RR, Jaber M, Giros B, Wightman RM, Caron MG (1998) Profound neuronal plasticity in response to inactivation of the dopamine transporter. Proc Natl Acad Sci U S A 95:4029–4034.

Käenmäki M, Tammimäki A, Myöhänen T, Pakarinen K, Amberg C, Karayiorgou M, Gogos JA, Männistö PT (2010) Quantitative role of COMT in dopamine clearance in the prefrontal cortex of freely moving mice. J Neurochem 114:1745–1755.

Kamin LJ (1968) “Attention-like” processes in classical conditioning. In: Miami Symposium on the Prediction of Behavior, 1967 (Jones MR, ed), pp 9–31.

Kandel ER, Schwartz JH, Jessell TM (2000) Principles of neural science. McGraw-Hill, Health Professions Division.

Kaplan GB, Heinrichs SC, Carey RJ (2011) Treatment of addiction and anxiety using extinction approaches: Neural mechanisms and their treatment implications. Pharmacol Biochem Behav 97:619–625.

Kapur S, Remington G (2001) Dopamine D2 receptors and their role in atypical antipsychotic action: still necessary and may even be sufficient. Biol Psychiatry 50:873–883.

Kashiotis A-M (2013) Zur funktionellen Rolle von A-Typ Kaliumkanälen und deren β-Untereinheit KChIP4 in dopaminergen Mittelhirnneuronen der Maus.

Keck T, Toyoizumi T, Chen L, Doiron B, Feldman DE, Fox K, Gerstner W, Haydon PG, Hübener M, Lee H-K, Lisman JE, Rose T, Sengpiel F, Stellwagen D, Stryker MP, Turrigiano GG, van Rossum MC (2017) Integrating Hebbian and homeostatic plasticity: the current state of the field and future research directions. Philos Trans R Soc London B Biol Sci 372.

Kempadoo KA, Tourino C, Cho SL, Magnani F, Leinninger G-M, Stuber GD, Zhang F, Myers MG, Deisseroth K, de Lecea L, Bonci A (2013) Hypothalamic neurotensin projections promote reward by enhancing glutamate transmission in the VTA. J Neurosci 33:7618–7626.

Ketzef M, Spigolon G, Johansson Y, Bonito-Oliva A, Fisone G, Silberberg G (2017) Dopamine Depletion Impairs Bilateral Sensory Processing in the Striatum in a Pathway-Dependent Manner. Neuron 94:855–865.e5.

Khaliq ZM, Bean BP (2008) Dynamic, Nonlinear Feedback Regulation of Slow Pacemaking by A-Type Potassium Current in Ventral Tegmental Area Neurons. J Neurosci 28:10905–10917.

Khaliq ZM, Bean BP (2010) Pacemaking in dopaminergic ventral tegmental area neurons: depolarizing drive from background and voltage-dependent sodium conductances. J Neurosci 30:7401–7413.

Kim CK, Yang SJ, Pichamoorthy N, Young NP, Kauvar I, Jennings JH, Lerner TN, Berndt A, Lee SY, Ramakrishnan C, Davidson TJ, Inoue M, Bito H, Deisseroth K (2016) Simultaneous fast measurement of circuit dynamics at multiple sites across the mammalian brain. Nat Methods 13:325–328.

Kim HF, Hikosaka O (2015) Parallel basal ganglia circuits for voluntary and automatic behaviour to reach rewards. Brain 138:1776–1800.

Kim J, Wei D-S, Hoffman DA (2005) Kv4 potassium channel subunits control action potential repolarization and frequency-dependent broadening in rat hippocampal CA1 pyramidal neurones. J Physiol 569:41–57.

Kim KM, Baratta M V., Yang A, Lee D, Boyden ES, Fiorillo CD (2012) Optogenetic Mimicry of the Transient Activation of Dopamine Neurons by Natural Reward Is Sufficient for Operant Reinforcement Zhuang X, ed. PLoS One 7:e33612.

Kimm T, Bean BP (2014) Inhibition of A-type potassium current by the peptide toxin SNX-482. J Neurosci 34:9182–9189.

Kimm T, Khaliq ZM, Bean BP (2015) Differential Regulation of Action Potential Shape and Burst-Frequency Firing by BK and Kv2 Channels in Substantia Nigra Dopaminergic Neurons. J Neurosci 35:16404–16417.

Kita H, Armstrong W (1991) A biotin-containing compound N-(2-aminoethyl)biotinamide for intracellular labeling and neuronal tracing studies: Comparison with biocytin. J Neurosci Methods 37:141–150.

Kitazawa M, Kubo Y, Nakajo K (2014) The stoichiometry and biophysical properties of the Kv4 potassium channel complex with K+ channel-interacting protein (KChIP) subunits are variable, depending on the relative expression level. J Biol Chem 289:17597–17609.

Klaus A, Martins GJ, Paixao VB, Zhou P, Paninski L, Costa RM (2017) The Spatiotemporal Organization of the Striatum Encodes Action Space. Neuron 95:1171–1180.e7.

Knowland D, Lilascharoen V, Pacia CP, Shin S, Wang EH-J, Lim BK, Doi H, Onoe H, Ferguson D, Golden SA, al. et (2017) Distinct Ventral Pallidal Neural Populations Mediate Separate Symptoms of Depression. Cell 170:284–297.e18.

Ko D, Wilson CJ, Lobb CJ, Paladini CA (2012) Detection of bursts and pauses in spike trains. J Neurosci Methods 211:145–158.

Koch C, Poggio T, Torre V (1983) Nonlinear interactions in a dendritic tree: localization, timing, and role in information processing. Proc Natl Acad Sci U S A 80:2799–2802.

Kodangattil JN, Dacher M, Authement ME, Nugent FS (2013) Spike timing-dependent plasticity at GABAergic synapses in the ventral tegmental area. J Physiol 591:4699–4710.

Kopin IJ (1993) Parkinson's Disease: Past, Present, and Future. Neuropsychopharmacology 9:1–12.

Korotkova TM, Sergeeva OA, Eriksson KS, Haas HL, Brown RE (2003) Excitation of ventral tegmental area dopaminergic and nondopaminergic neurons by orexins/hypocretins. J Neurosci 23:7–11.

Krabbe S, Duda J, Schiemann J, Poetschke C, Schneider G, Kandel ER, Liss B, Roeper J, Simpson EH (2015) Increased dopamine D2 receptor activity in the striatum alters the firing pattern of dopamine neurons in the ventral tegmental area. Proc Natl Acad Sci U S A 112:E1498-506.

Krauth C, Stahmeyer JT, Petersen JJ, Freytag A, Gerlach FM, Gensichen J (2014) Resource utilisation and costs of depressive patients in Germany: results from the primary care monitoring for depressive patients trial. Depress Res Treat 2014:730891.

Kravitz A V., Owen SF, Kreitzer AC (2013) Optogenetic identification of striatal projection neuron subtypes during in vivo recordings. Brain Res 1511:21–32.

Kreitzer AC, Malenka RC (2005) Dopamine modulation of state-dependent endocannabinoid release and long-term depression in the striatum. J Neurosci 25:10537–10545.

Kreitzer AC, Malenka RC (2007) Endocannabinoid-mediated rescue of striatal LTD and motor deficits in Parkinson's disease models. Nature 445:643–647.

Kreitzer AC, Malenka RC (2008) Striatal Plasticity and Basal Ganglia Circuit Function. Neuron 60:543–554.

Kremer EF (1978) The Rescorla-Wagner model: losses in associative strength in compound conditioned stimuli. J Exp Psychol Anim Behav Process 4:22–36.

Kring AM, Caponigro JM (2010) Emotion in Schizophrenia: Where Feeling Meets Thinking. Curr Dir Psychol Sci 19:255–259.

Krishnan V et al. (2007) Molecular Adaptations Underlying Susceptibility and Resistance to Social Defeat in Brain Reward Regions. Cell 131:391–404.

Kubis N, Faucheux BA, Ransmayr G, Damier P, Duyckaerts C, Henin D, Forette B, Le Charpentier Y, Hauw JJ, Agid Y, Hirsch EC (2000) Preservation of midbrain catecholaminergic neurons in very old human subjects. Brain 123 (Pt 2):366–373.

Kuo JJ, Lee RH, Johnson MD, Heckman HM, Heckman CJ (2003) Active Dendritic Integration of Inhibitory Synaptic Inputs In Vivo. J Neurophysiol 90:3617–3624.

Kupchik YM, Brown RM, Heinsbroek JA, Lobo MK, Schwartz DJ, Kalivas PW (2015) Coding the direct/indirect pathways by D1 and D2 receptors is not valid for accumbens projections. Nat Neurosci 18:1230–1232.

Kupchik YM, Kalivas PW (2017) The Direct and Indirect Pathways of the Nucleus Accumbens are not What You Think. Neuropsychopharmacology 42:369–370.

Kuznetsova AY, Huertas MA, Kuznetsov AS, Paladini CA, Canavier CC (2010) Regulation of firing frequency in a computational model of a midbrain dopaminergic neuron. J Comput Neurosci 28:389–403.

Lagarias JC, Reeds JA, Wright MH, Wright Siam J Optim PE (1998) Convergence Properties of the Nelder–Mead Simplex Method in Low Dimensions. SIAM J Optim 9:112–147.

Lak A, Stauffer WR, Schultz W (2014) Dopamine prediction error responses integrate subjective value from different reward dimensions. Proc Natl Acad Sci 111:2343–2348.

Lammel S, Hetzel A, Häckel O, Jones I, Liss B, Roeper J (2008) Unique Properties of Mesoprefrontal Neurons within a Dual Mesocorticolimbic Dopamine System. Neuron 57:760–773.

Lammel S, Ion DI, Roeper J, Malenka RC (2011) Projection-Specific Modulation of Dopamine Neuron Synapses by Aversive and Rewarding Stimuli.

Lammel S, Lim BK, Malenka RC (2014) Reward and aversion in a heterogeneous midbrain dopamine system. Neuropharmacology 76:351–359.

Lammel S, Lim BK, Ran C, Huang KW, Betley MJ, Tye KM, Deisseroth K, Malenka RC (2012) Input-specific control of reward and aversion in the ventral tegmental area. Nature 491:212–217.

Lammel S, Steinberg EE, Földy C, Wall NR, Beier K, Luo L, Malenka RC (2015) Diversity of Transgenic Mouse Models for Selective Targeting of Midbrain Dopamine Neurons. Neuron 85:429–438.

Lander ES et al. (2001) Initial sequencing and analysis of the human genome. Nature 409:860–921.

Lasky-Su J et al. (2008) Genome-wide association scan of quantitative traits for attention deficit hyperactivity disorder identifies novel associations and confirms candidate gene associations. Am J Med Genet Part B Neuropsychiatr Genet 147:1345–1354.

Lees AJ, Tolosa E, Olanow CW (2015) Four pioneers of L-dopa treatment: Arvid Carlsson, Oleh Hornykiewicz, George Cotzias, and Melvin Yahr. Mov Disord 30:19–36.

Lennartz RC (2008) The role of extramaze cues in spontaneous alternation in a plus-maze. Learn Behav a Psychon Soc Publ 36:138–144.

Lerner TN, Shilyansky C, Davidson TJ, Evans KE, Beier KT, Zalocusky KA, Crow AK, Malenka RC, Luo L, Tomer R, Deisseroth K (2015) Intact-Brain Analyses Reveal Distinct Information Carried by SNc Dopamine Subcircuits. Cell 162:635–647.

Leshner AI (1997) Addiction is a brain disease, and it matters. Science 278:45–47.

Levy F (1991) The Dopamine Theory of Attention Deficit Hyperactivity Disorder (ADHD). Aust New Zeal J Psychiatry 25:277–283.

Lewis DA, Hashimoto T, Volk DW (2005) Cortical inhibitory neurons and schizophrenia. Nat Rev Neurosci 6:312–324.

Li B, Arime Y, Hall FS, Uhl GR, Sora I (2010a) Impaired spatial working memory and decreased frontal cortex BDNF protein level in dopamine transporter knockout mice. Eur J Pharmacol 628:104–107.

Li F, Wang LP, Shen X, Tsien JZ (2010b) Balanced Dopamine Is Critical for Pattern Completion during Associative Memory Recall Chapouthier G, ed. PLoS One 5:e15401.

Li K, Zhou T, Liao L, Yang Z, Wong C, Henn F, Malinow R, Yates JR, Hu H (2013) βCaMKII in Lateral Habenula Mediates Core Symptoms of Depression. Science (80-) 341:1016–1020.

Li Y, He Y, Chen M, Pu Z, Chen L, Li P, Li B, Li H, Huang Z-L, Li Z, Chen J-F (2016) Optogenetic Activation of Adenosine A2A Receptor Signaling in the Dorsomedial Striatopallidal Neurons Suppresses Goal-Directed Behavior. Neuropsychopharmacology 41:1003–1013.

Liang P, Wang H, Chen H, Cui Y, Gu L, Chai J, Wang KW (2009) Structural insights into KChIP4a modulation of Kv4.3 inactivation. J Biol Chem 284:4960–4967.

Lin L, Sun W, Wikenheiser AM, Kung F, Hoffman DA (2010) KChIP4a regulates Kv4.2 channel trafficking through PKA phosphorylation. Mol Cell Neurosci 43:315–325.

Lindvall O, Björklund A, Moore RY, Stenevi U (1974) Mesencephalic dopamine neurons projecting to neocortex. Brain Res 81:325–331.

Liss B, Franz O, Sewing S, Bruns R, Neuhoff H, Roeper J (2001) Tuning pacemaker frequency of individual dopaminergic neurons by Kv4.3L and KChip3.1 transcription. EMBO J 20:5715–5724.

Liss B, Haeckel O, Wildmann J, Miki T, Seino S, Roeper J (2005) K-ATP channels promote the differential degeneration of dopaminergic midbrain neurons. Nat Neurosci 8:1742–1751.

Liss B, Roeper J (2004) Correlating function and gene expression of individual basal ganglia neurons. Trends Neurosci 27:475–481.

Liu Q, Pu L, Poo M (2005) Repeated cocaine exposure in vivo facilitates LTP induction in midbrain dopamine neurons. Nature 437:1027–1031.

Liu Y, Jurman ME, Yellen G, Jurman M., Shafer J., Pongs O, Stühmer W (1996) Dynamic rearrangement of the outer mouth of a K+ channel during gating. Neuron 16:859–867.

Ljungberg T, Apicella P, Schultz W (1992) Responses of monkey dopamine neurons during learning of behavioral reactions. J Neurophysiol 67:145–163.

Lobb CJ, Troyer TW, Wilson CJ, Paladini C a (2011) Disinhibition bursting of dopaminergic neurons. Front Syst Neurosci 5:25.

Lobb CJ, Wilson CJ, Paladini CA (2010) A dynamic role for GABA receptors on the firing pattern of midbrain dopaminergic neurons. J Neurophysiol 104:403–413.

Lobo MK, Covington HE, Chaudhury D, Friedman AK, Sun H, Damez-Werno D, Dietz DM, Zaman S, Koo JW, Kennedy PJ, Mouzon E, Mogri M, Neve RL, Deisseroth K, Han M-H, Nestler EJ (2010) Cell Type-Specific Loss of BDNF Signaling Mimics Optogenetic Control of Cocaine Reward. Science (80-) 330:385–390.

London M, Häusser M (2005) Dendritic computation. Annu Rev Neurosci 28:503–532.

Lopez AJ (1998) Alternative Splicing of Pre-mRNA: Developmental Consequences and Mechanisms of Regulation. Annu Rev Genet 32:279–305.

Lorang D, Amara SG, Simerly RB (1994) Cell-type-specific expression of catecholamine transporters in the rat brain. J Neurosci 14:4903–4914.

Loughlin SE, Fallon JH (1984) Substantia nigra and ventral tegmental area projections to cortex: Topography and collateralization. Neuroscience 11:425–435.

Lugo JN, Brewster AL, Spencer CM, Anderson AE (2012) Kv4.2 knockout mice have hippocampal-dependent learning and memory deficits. Learn Mem 19:182–189.

Luksys G, Gerstner W, Sandi C (2009) Stress, genotype and norepinephrine in the prediction of mouse behavior using reinforcement learning. Nat Neurosci 12:1180–1186.

Luman M, Tripp G, Scheres A (2010) Identifying the neurobiology of altered reinforcement sensitivity in ADHD: A review and research agenda. Neurosci Biobehav Rev 34:744–754.

Lundby A, Jespersen T, Schmitt N, Grunnet M, Olesen S-P, Cordeiro J, Calloe K (2010) Effect of the Ito activator NS5806 on cloned Kv4 channels depends on the accessory protein KChIP2. Br J Pharmacol 160:2028–2044.

Luu P, Malenka RC (2008) Spike Timing-Dependent Long-Term Potentiation in Ventral Tegmental Area Dopamine Cells Requires PKC. J Neurophysiol 100.

Lynch WJ, Nicholson KL, Dance ME, Morgan RW, Foley PL (2010) Animal models of substance abuse and addiction: implications for science, animal welfare, and society. Comp Med 60:177–188.

Maasz A, Melegh B (2010) Three periods of one and a half decade of ischemic stroke susceptibility gene research: lessons we have learned. Genome Med 2:64.

Madras BK (2013) History of the Discovery of the Antipsychotic Dopamine D2 Receptor: A Basis for the Dopamine Hypothesis of Schizophrenia. J Hist Neurosci 22:62–78.

Maggos CE, Spangler R, Zhou Y, Schlussman SD, Ho A, Kreek MJ (1997) Quantitation of dopamine transporter mRNA in the rat brain: Mapping, effects of “binge” cocaine administration and withdrawal. Synapse 26:55–61.

Maia T. V, Frank MJ (2017) An Integrative Perspective on the Role of Dopamine in Schizophrenia. Biol Psychiatry 81:52–66.

Mameli M, Balland B, Luján R, Lüscher C (2007) Rapid synthesis and synaptic insertion of GluR2 for mGluR-LTD in the ventral tegmental area. Science 317:530–533.

Mandela P, Yan Y, LaRese T, Eipper BA, Mains RE (2014) Elimination of Kalrn expression in POMC cells reduces anxiety-like behavior and contextual fear learning. Horm Behav 66:430–438.

Mann DMA, Yates PO (1982) Pathogenesis of Parkinson’s Disease. Arch Neurol 39:545–549.

Marcott PF, Mamaligas AA, Ford CP (2014) Phasic dopamine release drives rapid activation of striatal D2-receptors. Neuron 84:164–176.

Marder E, Goaillard J-M (2006) Variability, compensation and homeostasis in neuron and network function. Nat Rev Neurosci 7:563–574.

Margolis EB, Mitchell JM, Ishikawa J, Hjelmstad GO, Fields HL (2008) Midbrain Dopamine Neurons: Projection Target Determines Action Potential Duration and Dopamine D2 Receptor Inhibition. J Neurosci 28.

Marlin JJ, Carter AG (2014) GABA-A Receptor Inhibition of Local Calcium Signaling in Spines and Dendrites. J Neurosci 34:15898–15911.

Marron Fernandez de Velasco E, Zhang L, N Vo B, Tipps M, Farris S, Xia Z, Anderson A, Carlblom N, Weaver CD, Dudek SM, Wickman K (2017) GIRK2 splice variants and neuronal G protein-gated K(+) channels: implications for channel function and behavior. Sci Rep 7:1639.

Marwaha S, Johnson S (2004) Schizophrenia and employment. Soc Psychiatry Psychiatr Epidemiol 39:337–349.

Massone S, Vassallo I, Castelnuovo M, Fiorino G, Gatta E, Robello M, Borghi R, Tabaton M, Russo C, Dieci G, Cancedda R, Pagano A (2011) RNA polymerase III drives alternative splicing of the potassium channel-interacting protein contributing to brain complexity and neurodegeneration. J Cell Biol 193:851–866.

Matarin M et al. (2007) A genome-wide genotyping study in patients with ischaemic stroke. Lancet Neurol 6:414–420.

Matsuda W, Furuta T, Nakamura KC, Hioki H, Fujiyama F, Arai R, Kaneko T (2009) Single Nigrostriatal Dopaminergic Neurons Form Widely Spread and Highly Dense Axonal Arborizations in the Neostriatum. J Neurosci 29.

Matsumoto H, Tian J, Uchida N, Watabe-Uchida M (2016) Midbrain dopamine neurons signal aversion in a reward-context-dependent manner. Elife 5.

Matsumoto M, Hikosaka O (2007) Lateral habenula as a source of negative reward signals in dopamine neurons. Nature 447:1111–1115.

Matsumoto M, Hikosaka O (2009a) Representation of negative motivational value in the primate lateral habenula. Nat Neurosci 12:77–84.

Matsumoto M, Hikosaka O (2009b) Two types of dopamine neuron distinctly convey positive and negative motivational signals. Nature 459:837–841.

Matsuo N, Takao K, Nakanishi K, Yamasaki N, Tanda K, Miyakawa T (2010) Behavioral profiles of three C57BL/6 substrains. Front Behav Neurosci 4:29.

McCutcheon J, Roitman MF (2017) Mode Of Sucrose Delivery Alters Reward-Related Phasic Dopamine Signals In Nucleus Accumbens. bioRxiv:132126.

McGeer PL, McGeer EG, Suzuki JS (1977) Aging and extrapyramidal function. Arch Neurol 34:33–35.

Mckinzie DL, Spear NE (1995) Ontogenetic differences in conditioning to context and CS as a function of context saliency and CS-US interval. Anim Learn Behav 23:304–313.

Mead AN, Rocha BA, Donovan DM, Katz JL (2002) Intravenous cocaine induced-activity and behavioural sensitization in norepinephrine-, but not dopamine-transporter knockout mice. Eur J Neurosci 16:514–520.

Meier MH, Caspi A, Reichenberg A, Keefe RSE, Fisher HL, Harrington H, Houts R, Poulton R, Moffitt TE (2014) Neuropsychological decline in schizophrenia from the premorbid to the postonset period: evidence from a population-representative longitudinal study. Am J Psychiatry 171:91–101.

Melis M, Camarini R, Ungless MA, Bonci A (2002) Long-lasting potentiation of GABAergic synapses in dopamine neurons after a single in vivo ethanol exposure. 22:2074–2082.

Menegas W et al. (2017) Opposite initialization to novel cues in dopamine signaling in ventral and posterior striatum in mice. Elife 6:751–767.

Mileykovskiy B, Morales M (2011) Duration of inhibition of ventral tegmental area dopamine neurons encodes a level of conditioned fear. J Neurosci 31:7471–7476.

Milienne-Petiot M, Kesby JP, Graves M, van Enkhuizen J, Semenova S, Minassian A, Markou A, Geyer MA, Young JW (2017) The effects of reduced dopamine transporter function and chronic lithium on motivation, probabilistic learning, and neurochemistry in mice: Modeling bipolar mania. Neuropharmacology 113:260–270.

Miller C (2000) An overview of the potassium channel family. Genome Biol 1:REVIEWS0004.

Mirenowicz J, Schultz W (1994) Importance of unpredictability for reward responses in primate dopamine neurons. J Neurophysiol 72:1024–1027.

Mirenowicz J, Schultz W (1996) Preferential activation of midbrain dopamine neurons by appetitive rather than aversive stimuli. Nature 379:449–451.

Missale C, Nash SR, Robinson SW, Jaber M, Caron MG (1998) Dopamine Receptors: From Structure to Function. Physiol Rev 78.

Miyazaki T, Lacey MG (1998) Presynaptic inhibition by dopamine of a discrete component of GABA release in rat substantia nigra pars reticulata. J Physiol 513:805–817.

Modrek B, Lee C (2002) A genomic view of alternative splicing. Nat Genet 30:13–19.

Montiglio PO, Garant D, Thomas D, Réale D (2010) Individual variation in temporal activity patterns in open-field tests. Anim Behav 80:905–912.

Moorman DE, Aston-Jones G (2010) Orexin/Hypocretin Modulates Response of Ventral Tegmental Dopamine Neurons to Prefrontal Activation: Diurnal Influences. J Neurosci 30:15585–15599.

Moran PM, Owen L, Crookes AE, Al-Uzri MM, Reveley MA (2008) Abnormal prediction error is associated with negative and depressive symptoms in schizophrenia. Prog Neuro-Psychopharmacology Biol Psychiatry 32:116–123.

Moran Y, Barzilai MG, Liebeskind BJ, Zakon HH (2015) Evolution of voltage-gated ion channels at the emergence of Metazoa. J Exp Biol 218:515–525.

Morice E, Billard J-M, Denis C, Mathieu F, Betancur C, Epelbaum J, Giros B, Nosten-Bertrand M (2007) Parallel Loss of Hippocampal LTD and Cognitive Flexibility in a Genetic Model of Hyperdopaminergia. Neuropsychopharmacology 32:2108–2116.

Morice E, Denis C, Giros B, Nosten-Bertrand M (2004) Phenotypic expression of the targeted null-mutation in the dopamine transporter gene varies as a function of the genetic background. Eur J Neurosci 20:120–126.

Morikawa H, Paladini CA (2011) Dynamic regulation of midbrain dopamine neuron activity: Intrinsic, synaptic, and plasticity mechanisms. Neuroscience 198:95–111.

Morohashi Y, Hatano N, Ohya S, Takikawa R, Watabiki T, Takasugi N, Imaizumi Y, Tomita T, Iwatsubo T (2002) Molecular cloning and characterization of CALP/KChIP4, a novel EF-hand protein interacting with presenilin 2 and voltage-gated potassium channel subunit Kv4. J Biol Chem 277:14965–14975.

Mukherjee S (2016) The gene: an intimate history, 1st editio. New York.

Murphy FC, Michael A, Robbins TW, Sahakian BJ (2003) Neuropsychological impairment in patients with major depressive disorder: the effects of feedback on task performance. Psychol Med 33:S0033291702007018.

Murty VP, Sambataro F, Radulescu E, Altamura M, Iudicello J, Zoltick B, Weinberger DR, Goldberg TE, Mattay VS (2011) Selective updating of working memory content modulates meso-cortico-striatal activity. Neuroimage 57:1264–1272.

Muthane U, Yasha TC, Shankar SK (1998) Low numbers and no loss of melanized nigral neurons with increasing age in normal human brains from India. Ann Neurol 43:283–287.

Nakahara H, Itoh H, Kawagoe R, Takikawa Y, Hikosaka O, Dickinson A, Sakagami M, Hikosaka O (2004) Dopamine neurons can represent context-dependent prediction error. Neuron 41:269–280.

Naoi M, Maruyama W (1999) Cell death of dopamine neurons in aging and Parkinson's disease. Mech Ageing Dev 111:175–188.

Narula SC, Wellington JF (1982) The Minimum Sum of Absolute Errors Regression: A State of the Art Survey. Int Stat Rev / Rev Int Stat 50:317.

Nasser HM, Calu DJ, Schoenbaum G, Sharpe MJ (2017) The Dopamine Prediction Error: Contributions to Associative Models of Reward Learning. Front Psychol 8:244.

Naude J et al. (2016) Nicotinic receptors in the ventral tegmental area promote uncertainty-seeking. Nat Neurosci 19:471–478.

Naughton BJ, Thirtamara-Rajamani K, Wang C, During MJ, Gu HH (2012) Specific knockdown of the D2 long dopamine receptor variant. Neuroreport 23:1–5.

Nauta WJH, Smith GP, Faull RLM, Domesick VB (1978) Efferent connections and nigral afferents of the nucleus accumbens septi in the rat. Neuroscience 3:385–401.

Neale BM et al. (2008) Genome-wide association scan of attention deficit hyperactivity disorder. Am J Med Genet Part B Neuropsychiatr Genet 147:1337–1344.

Nelson EL, Liang CL, Sinton CM, German DC (1996) Midbrain dopaminergic neurons in the mouse: computer-assisted mapping. J Comp Neurol 369:361–371.

Neuhoff H, Neu A, Liss B, Roeper J (2002) I(h) channels contribute to the different functional properties of identified dopaminergic subpopulations in the midbrain. J Neurosci 22:1290–1302.

Neve KA, Ford CP, Buck DC, Grandy DK, Neve RL, Phillips TJ (2013) Normalizing dopamine D2 receptor-mediated responses in D2 null mutant mice by virus-mediated receptor restoration: Comparing D2L and D2S. Neuroscience 248:479–487.

Nguyen T-M, Schreiner D, Xiao L, Traunm?ller L, Bornmann C, Scheiffele P (2016) An alternative splicing switch shapes neurexin repertoires in principal neurons versus interneurons in the mouse hippocampus. Elife 5.

NIDA (2016) Understanding Drug Use and Addiction. Available at: https://www.drugabuse.gov/publications/drugfacts/understanding-drug-use-addiction on 2017 [Accessed July 12, 2017].

NIDA (2017) Trends & Statistics. Available at: https://www.drugabuse.gov/related-topics/trends-statistics [Accessed July 21, 2017].

Niehaus JL, Murali M, Kauer JA (2010) Drugs of abuse and stress impair LTP at inhibitory synapses in the ventral tegmental area. Eur J Neurosci 32:108–117.

NIMH (2015) Depression: what you need to know, NIH Public. Bethesda, MD: U.S. Government Printing Office.

Niv Y, Duff MO, Dayan P (2005) Dopamine, uncertainty and TD learning. Behav Brain Funct 1:6.

Nolan NA, Parkes MW (1973) The effects of benzodiazepines on the behaviour of mice on a hole-board. Psychopharmacologia 29:277–288.

Norris AJ, Foeger NC, Nerbonne JM (2010) Interdependent roles for accessory KChIP2, KChIP3, and KChIP4 subunits in the generation of Kv4-encoded IA channels in cortical pyramidal neurons. J Neurosci 30:13644–13655.

Northcutt RG, Kaas JH (1995) The emergence and evolution of mammalian neocortex. Trends Neurosci 18:373–379.

Nugent FS, Kauer JA (2008) LTP of GABAergic synapses in the ventral tegmental area and beyond. J Physiol 586:1487–1493.

Nugent FS, Penick EC, Kauer JA (2007) Opioids block long-term potentiation of inhibitory synapses. Nature 446:1086–1090.

O'Leary T, Williams AH, Caplan JS, Marder E (2013) Correlations in ion channel expression emerge from homeostatic tuning rules. Proc Natl Acad Sci U S A 110:E2645-54.

O'Leary T, Williams AH, Franci A, Marder E (2014) Cell Types, Network Homeostasis, and Pathological Compensation from a Biologically Plausible Ion Channel Expression Model. Neuron

82:809–821.

Oakman SA, Faris PL, Kerr PE, Cozzari C, Hartman BK (1995) Distribution of pontomesencephalic cholinergic neurons projecting to substantia nigra differs significantly from those projecting to ventral tegmental area. J Neurosci 15:5859–5869.

Ogawa SK, Cohen JY, Hwang D, Uchida N, Watabe-Uchida M (2014) Organization of Monosynaptic Inputs to the Serotonin and Dopamine Neuromodulatory Systems. Cell Rep 8:1105–1118.

Ogawa SK, Watabe-Uchida M (2017) Organization of dopamine and serotonin system: Anatomical and functional mapping of monosynaptic inputs using rabies virus. Pharmacol Biochem Behav.

Olds J, Milner P (1954) Positive reinforcement produced by electrical stimulation of septal area and other regions of rat brain. J Comp Physiol Psychol 47:419–427.

Olesen J, Gustavsson A, Svensson M, Wittchen H-U, Jönsson B, CDBE2010 study group, European Brain Council (2012) The economic cost of brain disorders in Europe. Eur J Neurol 19:155–162.

Oleson EB, Gentry RN, Chioma VC, Cheer JF (2012) Subsecond Dopamine Release in the Nucleus Accumbens Predicts Conditioned Punishment and Its Successful Avoidance. J Neurosci 32.

Omelchenko N, Bell R, Sesack SR (2009) Lateral habenula projections to dopamine and GABA neurons in the rat ventral tegmental area. Eur J Neurosci 30:1239–1250.

Overton P, Clark D (1992) Iontophoretically administered drugs acting at the N-methyl-D-aspartate receptor modulate burst firing in A9 dopamine neurons in the rat. Synapse 10:131–140.

Overton PG, Clark D (1997) Burst firing in midbrain dopaminergic neurons. Brain Res Brain Res Rev 25:312–334.

Overton PG, Richards CD, Berry MS, Clark D (1999) Long-term potentiation at excitatory amino acid synapses on midbrain dopamine neurons. Neuroreport 10:221–226.

Overton PG, Vautrelle N, Redgrave P (2014) Sensory regulation of dopaminergic cell activity: Phenomenology, circuitry and function. Neuroscience 282:1–12.

Paddock SW (2000) Principles and Practices of Laser Scanning Confocal Microscopy. Mol Biotechnol 16:127–150.

Pak MD, Baker K, Covarrubias M, Butler A, Ratcliffe A, Salkoff L (1991) mShal, a subfamily of A-type K+ channel cloned from mammalian brain. 88.

Paladini C a, Robinson S, Morikawa H, Williams JT, Palmiter RD (2003) Dopamine controls the firing pattern of dopamine neurons via a network feedback mechanism. Proc Natl Acad Sci U S A 100:2866–2871.

Paladini CA, Roeper J (2014) Generating bursts (and pauses) in the dopamine midbrain neurons. Neuroscience 282:109–121.

Pan Q, Shai O, Lee LJ, Frey BJ, Blencowe BJ (2008a) Deep surveying of alternative splicing complexity in the human transcriptome by high-throughput sequencing. Nat Genet 40:1413–1415.

Pan W-X, Schmidt R, Wickens JR, Hyland BI (2008b) Tripartite mechanism of extinction suggested by dopamine neuron activity and temporal difference model. J Neurosci 28:9619–9631.

Panagis G, Kastellakis A (2002) The effects of ventral tegmental administration of GABAA, GABAB, NMDA and AMPA receptor agonists on ventral pallidum self-stimulation. Behav Brain Res 131:115–123.

Panigrahi B, Martin KA, Li Y, Graves AR, Vollmer A, Olson L, Mensh BD, Karpova AY, Dudman JT (2015) Dopamine Is Required for the Neural Representation and Control of Movement Vigor. Cell 162:1418–1430.

Park H, Popescu A, Poo M (2014) Essential role of presynaptic NMDA receptors in activity-dependent BDNF secretion and corticostriatal LTP. Neuron 84:1009–1022.

Park MR, Kita H, Klee MR, Oomura Y (1983) Bridge balance in intracellular recording; introduction of the phase-sensitive method. J Neurosci Methods 8:105–125.

Parker JG, Wanat MJ, Soden ME, Ahmad K, Zweifel LS, Bamford NS, Palmiter RD (2011) Attenuating GABA(A) receptor signaling in dopamine neurons selectively enhances reward learning and alters risk preference in mice. J Neurosci Off J Soc Neurosci 31:17103–17112.

Parker NF, Cameron CM, Taliaferro JP, Lee J, Choi JY, Davidson TJ, Daw ND, Witten IB (2016) Reward and choice encoding in terminals of midbrain dopamine neurons depends on striatal target. Nat Neurosci 19:845–854.

Parvaz MA, Konova AB, Proudfit GH, Dunning JP, Malaker P, Moeller SJ, Maloney T, Alia-Klein N, Goldstein RZ (2015) Impaired Neural Response to Negative Prediction Errors in Cocaine Addiction. J Neurosci 35:1872–1879.

Patel SP, Campbell DL, Strauss HC (2002) Elucidating KChIP effects on Kv4.3 inactivation and recovery kinetics with a minimal KChIP2 isoform. J Physiol 545:5–11.

Patel SP, Parai R, Parai R, Campbell DL (2004) Regulation of Kv4.3 voltage-dependent gating kinetics by KChIP2 isoforms. J Physiol 557:19–41.

Pearce JM, Hall G (1980) A model for Pavlovian learning: Variations in the effectiveness of conditioned but not of unconditioned stimuli. Psychol Rev 87:532–552.

Pelham WE, Foster EM, Robb JA (2007) The Economic Impact of Attention-Deficit/Hyperactivity Disorder in Children and Adolescents. Ambul Pediatr 7:121–131.

Perona MTG, Waters S, Hall FS, Sora I, Lesch K-P, Murphy DL, Caron M, Uhl GR (2008) Animal models of depression in dopamine, serotonin, and norepinephrine transporter knockout mice: prominent effects of dopamine transporter deletions. Behav Pharmacol 19:566–574.

Perroud N et al. (2012) Genome-wide association study of increasing suicidal ideation during antidepressant treatment in the GENDEP project. Pharmacogenomics J 12:68–77.

Phillips PEM, Hancock PJ, Stamford JA (2002) Time window of autoreceptor-mediated inhibition of limbic and striatal dopamine release. Synapse 44:15–22.

Pignatelli M, Bonci A (2015) Role of Dopamine Neurons in Reward and Aversion: A Synaptic Plasticity Perspective. Neuron 86:1145–1157.

Pinault D (1996) A novel single-cell staining procedure performed in vivo under electrophysiological control: Morpho-functional features of juxtacellularly labeled thalamic cells and other central neurons with biocytin or Neurobiotin. J Neurosci Methods 65:113–136.

Ping HX, Shepard PD (1999) Blockade of SK-type Ca2+-activated K+ channels uncovers a Ca2+-dependent slow afterdepolarization in nigral dopamine neurons. J Neurophysiol 81:977–984.

Pizzagalli DA, Peccoralo LA, Davidson RJ, Cohen JD (2006) Resting anterior cingulate activity and abnormal responses to errors in subjects with elevated depressive symptoms: A 128-channel EEG study. Hum Brain Mapp 27:185–201.

Poetschke C, Dragicevic E, Duda J, Benkert J, Dougalis A, DeZio R, Snutch TP, Striessnig J, Liss B (2015) Compensatory T-type Ca2+ channel activity alters D2-autoreceptor responses of Substantia nigra dopamine neurons from Cav1.3 L-type Ca2+ channel KO mice. Sci Rep 5:13688.

Pongs O, Kecskemethy N, Müller R, Krah-Jentgens I, Baumann A, Kiltz HH, Canal I, Llamazares S, Ferrus A (1988) Shaker encodes a family of putative potassium channel proteins in the nervous system of Drosophila. EMBO J 7:1087–1096.

Popescu AT, Zhou MR, Poo M (2016) Phasic dopamine release in the medial prefrontal cortex enhances stimulus discrimination. Proc Natl Acad Sci 113:E3169–E3176.

Previc FH (1999) Dopamine and the Origins of Human Intelligence. Brain Cogn 41:299–350.

Pruunsild P, Timmusk T (2005) Structure, alternative splicing, and expression of the human and mouse KCNIP gene family. Genomics 86:581–593.

Pruunsild P, Timmusk T (2012) Subcellular localization and transcription regulatory potency of KCNIP/Calsenilin/DREAM/KChIP proteins in cultured primary cortical neurons do not provide support for their role in CRE-dependent gene expression. J Neurochem 123:29–43.

Puopolo M, Raviola E, Bean BP (2007) Roles of Subthreshold Calcium Current and Sodium Current in Spontaneous Firing of Mouse Midbrain Dopamine Neurons. J Neurosci 27:645–656.

Putzier I, Kullmann PH, Horn JP, Levitan ES (2009) Cav1.3 channel voltage dependence, not Ca2+ selectivity, drives pacemaker activity and amplifies bursts in nigral dopamine neurons. J Neurosci 29:15414–15419.

Putzier I, Kullmann PHM, Horn JP, Levitan ES (2008) Dopamine Neuron Responses Depend Exponentially on Pacemaker Interval. J Neurophysiol 101:926–933.

Qi J, Zhang S, Wang H-L, Wang H, de Jesus Aceves Buendia J, Hoffman AF, Lupica CR, Seal RP, Morales M (2014) A glutamatergic reward input from the dorsal raphe to ventral tegmental area dopamine neurons. Nat Commun 5:5390.

Qian K, Yu N, Tucker KR, Levitan ES, Canavier CC (2014) Mathematical analysis of depolarization block mediated by slow inactivation of fast sodium channels in midbrain dopamine neurons. J Neurophysiol 112.

Raczka KA, Mechias M-L, Gartmann N, Reif A, Deckert J, Pessiglione M, Kalisch R (2011) Empirical support for an involvement of the mesostriatal dopamine system in human fear extinction. Transl Psychiatry 1:e12.

Raghanti MA, Stimpson CD, Marcinkiewicz JL, Erwin JM, Hof PR, Sherwood CC (2008) Cortical

dopaminergic innervation among humans, chimpanzees, and macaque monkeys: a comparative study. Neuroscience 155:203–220.

Ragozzino ME, Unick KE, Gold PE (1996) Hippocampal acetylcholine release during memory testing in rats: augmentation by glucose. Proc Natl Acad Sci U S A 93:4693–4698.

Redgrave P, Rodriguez M, Smith Y, Rodriguez-Oroz MC, Lehericy S, Bergman H, Agid Y, DeLong MR, Obeso JA (2010) Goal-directed and habitual control in the basal ganglia: implications for Parkinson's disease. Nat Rev Neurosci 11:760–772.

Regier DA, Farmer ME, Rae DS, Locke BZ, Keith SJ, Judd LL, Goodwin FK (1990) Comorbidity of Mental Disorders With Alcohol and Other Drug Abuse. JAMA 264:2511.

Reig R, Silberberg G (2014) Multisensory Integration in the Mouse Striatum. Neuron 83:1200–1212.

Rescorla RA (1976) Stimulus generalization: Some predictions from a model of Pavlovian conditioning. J Exp Psychol Anim Behav Process 2:88–96.

Rescorla RA (2006) Spontaneous recovery from overexpectation. Learn Behav 34:13–20.

Rescorla RA (2007) Renewal after overexpectation. Anim Learn Behav 35:19–26.

Rescorla, Wagner A (1972) A theory of Pavlovian conditioning: Variations in the effectiveness of reinforcement and nonreinforcement.

Révy D, Jaouen F, Salin P, Melon C, Chabbert D, Tafi E, Concetta L, Langa F, Amalric M, Kerkerian-Le Goff L, Marie H, Beurrier C (2014) Cellular and Behavioral Outcomes of Dorsal Striatonigral Neuron Ablation: New Insights into Striatal Functions. Neuropsychopharmacology 39:2662–2672.

Reynolds JNJ, Hyland BI, Wickens JR (2001) A cellular mechanism of reward-related learning. Nature 413:67–70.

Rice ME, Patel JC (2015) Somatodendritic dopamine release: recent mechanistic insights. Philos Trans R Soc B Biol Sci 370:20140185.

Richfield EK, Penney JB, Young AB (1989) Anatomical and affinity state comparisons between dopamine D1 and D2 receptors in the rat central nervous system. Neuroscience 30:767–777.

Ridler, Calvard S (1978) Picture Thresholding Using an Iterative Selection Method. IEEE Trans Syst Man Cybern 8:630–632.

Riga D, Theijs JT, De Vries TJ, Smit AB, Spijker S (2015) Social defeat-induced anhedonia: effects on operant sucrose-seeking behavior. Front Behav Neurosci 9:195.

Ripke S et al. (2013) A mega-analysis of genome-wide association studies for major depressive disorder. Mol Psychiatry 18:497–511.

Roberts GC, Smith CWJ (2002) Alternative splicing: combinatorial output from the genome. Curr Opin Chem Biol 6:375–383.

Robertson GS, Jian M (1995) D1 and D2 dopamine receptors differentially increase fos-like immunoreactivity in accumbal projections to the ventral pallidum and midbrain. Neuroscience 64:1019–1034.

Rocha BA, Fumagalli F, Gainetdinov RR, Jones SR, Ator R, Giros B, Miller GW, Caron MG (1998) Cocaine self-administration in dopamine-transporter knockout mice. Nat Neurosci 1:132–137.

Roeper J (2013) Dissecting the diversity of midbrain dopamine neurons. Trends Neurosci 36:336–342.

Roesch MR, Calu DJ, Schoenbaum G (2007) Dopamine neurons encode the better option in rats deciding between differently delayed or sized rewards. Nat Neurosci 10:1615–1624.

Romaniuk L, Honey GD, King JRL, Whalley HC, McIntosh AM, Levita L, Hughes M, Johnstone EC, Day M, Lawrie SM, Hall J (2010) Midbrain Activation During Pavlovian Conditioning and Delusional Symptoms in Schizophrenia. Arch Gen Psychiatry 67:1246.

Rossato JI, Radiske A, Kohler CA, Gonzalez C, Bevilaqua LR, Medina JH, Cammarota M (2013) Consolidation of object recognition memory requires simultaneous activation of dopamine D1/D5 receptors in the amygdala and medial prefrontal cortex but not in the hippocampus. Neurobiol Learn Mem 106:66–70.

Rossi MA, Sukharnikova T, Hayrapetyan VY, Yang L, Yin HH (2013) Operant Self-Stimulation of Dopamine Neurons in the Substantia Nigra Zhuang X, ed. PLoS One 8:e65799.

Rossi MA, Yin HH (2015) Elevated dopamine alters consummatory pattern generation and increases behavioral variability during learning. Front Integr Neurosci 9:37.

Rothenhoefer KM, Costa VD, Bartolo R, Vicario-Feliciano R, Murray EA, Averbeck BB (2017) Effects of Ventral Striatum Lesions on Stimulus-Based versus Action-Based Reinforcement Learning. J Neurosci 37:6902–6914.

Rudd RA, Seth P, David F, Scholl L (2016) Increases in Drug and Opioid-Involved Overdose Deaths

— United States, 2010–2015. MMWR Morb Mortal Wkly Rep 65:1445–1452.

Rudy B, Maffie J, Amarillo Y, Clark B, Goldberg EM, Jeong H-Y, Kruglikov I, Kwon E, Nadal M, Zagha E (2009) Voltage Gated Potassium Channels: Structure and Function of Kv1 to Kv9 Subfamilies. In: Encyclopedia of Neuroscience, pp 397–425.

Russell VA, Sagvolden T, Johansen EB (2005) Animal models of attention-deficit hyperactivity disorder. Behav Brain Funct 1:9.

Saal D, Dong Y, Bonci A, Malenka RC (2003) Drugs of abuse and stress trigger a common synaptic adaptation in dopamine neurons. Neuron 37:577–582.

Saddoris MP, Cacciapaglia F, Wightman RM, Carelli RM (2015) Differential Dopamine Release Dynamics in the Nucleus Accumbens Core and Shell Reveal Complementary Signals for Error Prediction and Incentive Motivation. J Neurosci 35.

Sagvolden T, Aase H, Zeiner P, Berger D (1998) Altered reinforcement mechanisms in attention-deficit/hyperactivity disorder. Behav Brain Res 94:61–71.

Sagvolden T, Johansen EB, Aase H, Russell VA (2005a) A dynamic developmental theory of attention-deficit/hyperactivity disorder (ADHD) predominantly hyperactive/impulsive and combined subtypes. Behav Brain Sci 28:397-419-68.

Sagvolden T, Russell VA, Aase H, Johansen EB, Farshbaf M, Nishimura T, al. et, al. et (2005b) Rodent Models of Attention-Deficit/Hyperactivity Disorder. Biol Psychiatry 57:1239–1247.

Salkoff L, Baker K, Butler A, Covarrubias M, Pak MD, Wei A (1992) An essential “set” of K+ channels conserved in flies, mice and humans. Trends Neurosci 15:161–166.

Salvador-Recatalà V, Gallin WJ, Abbruzzese J, Ruben PC, Spencer AN (2006) A potassium channel (Kv4) cloned from the heart of the tunicate Ciona intestinalis and its modulation by a KChIP subunit. J Exp Biol 209:731–747.

Sanghera MK, Trulson M., German DC (1984) Electrophysiological properties of mouse dopamine neurons: In vivo and in vitro studies. Neuroscience 12:793–801.

Sauer B (1987) Functional expression of the cre-lox site-specific recombination system in the yeast Saccharomyces cerevisiae. Mol Cell Biol 7:2087–2096.

Sauer B, Henderson N (1988) Site-specific DNA recombination in mammalian cells by the Cre recombinase of bacteriophage P1. Proc Natl Acad Sci U S A 85:5166–5170.

Saunders A, Johnson CA, Sabatini BL (2012) Novel recombinant adeno-associated viruses for Cre activated and inactivated transgene expression in neurons. Front Neural Circuits 6:47.

Saunders BT, Robinson TE (2012) The role of dopamine in the accumbens core in the expression of Pavlovian-conditioned responses. Eur J Neurosci 36:2521–2532.

Savitz JB, Drevets WC (2013) Neuroreceptor imaging in depression. Neurobiol Dis 52:49–65.

Sawaguchi T, Matsumura M, Kubota K (1990) Effects of dopamine antagonists on neuronal activity related to a delayed response task in monkey prefrontal cortex. J Neurophysiol 63:1401–1412.

Schiemann J, Schlaudraff F, Klose V, Bingmer M, Seino S, Magill PJ, Zaghloul KA, Schneider G, Liss B, Roeper J (2012) K-ATP channels in dopamine substantia nigra neurons control bursting and novelty-induced exploration. Nat Neurosci 15:1272–1280.

Schmidt R, Berke JD (2017) A Pause-then-Cancel model of stopping: evidence from basal ganglia neurophysiology. Philos Trans R Soc London B Biol Sci 372.

Schmitt KC, Reith MEA (2010) Regulation of the dopamine transporter: aspects relevant to psychostimulant drugs of abuse. Ann N Y Acad Sci 1187:316–340.

Schmitz Y, Schmauss C, Sulzer D (2002) Altered dopamine release and uptake kinetics in mice lacking D2 receptors. J Neurosci 22:8002–8009.

Schultz W (1986) Responses of midbrain dopamine neurons to behavioral trigger stimuli in the monkey. J Neurophysiol 56:1439–1461.

Schultz W (1997) Dopamine neurons and their role in reward mechanisms. Curr Opin Neurobiol 7:191–197.

Schultz W (2007) Behavioral dopamine signals. Trends Neurosci 30:203–210.

Schultz W (2016a) Dopamine reward prediction-error signalling: a two-component response. Nat Rev Neurosci 17:183–195.

Schultz W (2016b) Reward functions of the basal ganglia. J Neural Transm 123:679–693.

Schultz W, Apicella P, Ljungberg T (1993) Responses of monkey dopamine neurons to reward and conditioned stimuli during successive steps of learning a delayed response task. J Neurosci 13:900–913.

Schultz W, Carelli RM, Wightman RM (2015) Phasic dopamine signals: from subjective reward value to formal economic utility. Curr Opin Behav Sci 5:147–154.

Schultz W, Dayan P, Montague PR (1997) A Neural Substrate of Prediction and Reward. Science (80-) 275:1593–1599.

Schwarting RK, Huston JP (1996) The unilateral 6-hydroxydopamine lesion model in behavioral brain research. Analysis of functional deficits, recovery and treatments. Prog Neurobiol 50:275–331.

Schwenk J, Baehrens D, Haupt A, Bildl W, Boudkkazi S, Roeper J, Fakler B, Schulte U (2014) Regional diversity and developmental dynamics of the AMPA-receptor proteome in the mammalian brain. Neuron 84:41–54.

Schwenk J, Zolles G, Kandias NG, Neubauer I, Kalbacher H, Covarrubias M, Fakler B, Bentrop D (2008) NMR analysis of KChIP4a reveals structural basis for control of surface expression of Kv4 channel complexes. J Biol Chem 283:18937–18946.

Seamans JK, Yang CR (2004) The principal features and mechanisms of dopamine modulation in the prefrontal cortex. Prog Neurobiol 74:1–57.

Serôdio P, Rudy B (1998) Differential Expression of Kv4 K+ Channel Subunits Mediating Subthreshold Transient K+ (A-Type) Currents in Rat Brain. 79:1081–1091.

Sesack SR, Grace AA (2010) Cortico-Basal Ganglia Reward Network: Microcircuitry. Neuropsychopharmacology 35:27–47.

Sesack SR, Hawrylak VA, Matus C, Guido MA, Levey AI (1998) Dopamine axon varicosities in the prelimbic division of the rat prefrontal cortex exhibit sparse immunoreactivity for the dopamine transporter. J Neurosci 18:2697–2708.

Seutin V, Engel D (2010) Differences in Na+ Conductance Density and Na+ Channel Functional Properties Between Dopamine and GABA Neurons of the Rat Substantia Nigra. J Neurophysiol 103.

Shabel SJ, Proulx CD, Trias A, Murphy RT, Malinow R (2012) Input to the lateral habenula from the basal ganglia is excitatory, aversive, and suppressed by serotonin. Neuron 74:475–481.

Sharpe MJ, Chang CY, Liu MA, Batchelor HM, Mueller LE, Jones JL, Niv Y, Schoenbaum G (2017) Dopamine transients are sufficient and necessary for acquisition of model-based associations. Nat Neurosci 20:735–742.

Shen W, Flajolet M, Greengard P, Surmeier DJ (2008) Dichotomous Dopaminergic Control of Striatal Synaptic Plasticity. Science (80-) 321:848–851.

Shepherd GM (1974) The synaptic organization of the brain : an introduction. Oxford University Press.

Shepherd GM (2011) The Microcircuit Concept Applied to Cortical Evolution: from Three-Layer to Six-Layer Cortex. Front Neuroanat 5:30.

Shibata R, Misonou H, Campomanes CR, Anderson AE, Schrader LA, Doliveira LC, Carroll KI, Sweatt JD, Rhodes KJ, Trimmer JS (2003) A fundamental role for KChIPs in determining the molecular properties and trafficking of Kv4.2 potassium channels. J Biol Chem 278:36445–36454.

Shulman JM, Chen K, Keenan BT, Chibnik LB, Fleisher A, Thiyyagura P, Roontiva A, McCabe C, Patsopoulos NA, Corneveaux JJ, Yu L, Huentelman MJ, Evans DA, Schneider JA, Reiman EM, De Jager PL, Bennett DA (2013) Genetic susceptibility for Alzheimer disease neuritic plaque pathology. JAMA Neurol 70:1150–1157.

Simmons D V, Petko AK, Paladini CA (2017) Differential Expression of Long Term Potentiation among Identified Inhibitory Inputs to Dopamine Neurons. J Neurophysiol.

Simon H, Le Moal M, Stinus L, Calas A (1979) Anatomical relationships between the ventral mesencephalic tegmentum — A 10 region and the locus coeruleus as demonstrated by anterograde and retrograde tracing techniques. J Neural Transm 44:77–86.

Sims JE, Smith DE (2010) The IL-1 family: regulators of immunity. Nat Rev Immunol 10:117.

Sippy T, Lapray D, Crochet S, Petersen CCH (2015) Cell-Type-Specific Sensorimotor Processing in Striatal Projection Neurons during Goal-Directed Behavior. Neuron 88:298–305.

Skinner BF (1938) The behavior of organisms: an experimental analysis.

Sklar P et al. (2008) Whole-genome association study of bipolar disorder. Mol Psychiatry 13:558–569.

Smith LM, Ebner FF, Colonnier M (1980) The thalamocortical projection inPseudemys turtles: A quantitative electron microscopic study. J Comp Neurol 190:445–461.

Solanto M V (1998) Neuropsychopharmacological mechanisms of stimulant drug action in attention-deficit hyperactivity disorder: a review and integration. Behav Brain Res 94:127–152.

Spielewoy C, Gonon F, Roubert C, Fauchey V, Jaber M, Caron MG, Roques BP, Hamon M, Betancur C, Maldonado R, Giros B (2000a) Increased rewarding properties of morphine in dopamine-

transporter knockout mice. Eur J Neurosci 12:1827–1837.

Spielewoy C, Roubert C, Hamon M, Nosten-Bertrand M, Betancur C, Giros B (2000b) Behavioural disturbances associated with hyperdopaminergia in dopamine-transporter knockout mice. Behav Pharmacol 11:279–290.

Stamatakis AM, Stuber GD (2012a) Optogenetic strategies to dissect the neural circuits that underlie reward and addiction. Cold Spring Harb Perspect Med 2.

Stamatakis AM, Stuber GD (2012b) Activation of lateral habenula inputs to the ventral midbrain promotes behavioral avoidance. Nat Neurosci 15:1105–1107.

St Onge JR, Ahn S, Phillips AG, Floresco SB (2012) Dynamic fluctuations in dopamine efflux in the prefrontal cortex and nucleus accumbens during risk-based decision making. J Neurosci 32:16880–16891.

Stauffer WR, Lak A, Schultz W (2014) Dopamine reward prediction error responses reflect marginal utility. Curr Biol 24:2491–2500.

Steffens DC, Wagner HR, Levy RM, Horn KA, Krishnan KRR (2001) Performance feedback deficit in geriatric depression. Biol Psychiatry 50:358–363.

Steinberg EE, Keiflin R, Boivin JR, Witten IB, Deisseroth K, Janak PH (2013) A causal link between prediction errors, dopamine neurons and learning. Nat Neurosci 16:966–973.

Stelly CE, Pomrenze MB, Cook JB, Morikawa H (2016) Repeated social defeat stress enhances glutamatergic synaptic plasticity in the VTA and cocaine place conditioning. Elife 5.

Stephenson-Jones M, Kardamakis AA, Robertson B, Grillner S (2013) Independent circuits in the basal ganglia for the evaluation and selection of actions. Proc Natl Acad Sci U S A 110:E3670-9.

Stephenson-Jones M, Samuelsson E, Ericsson J, Robertson B, Grillner S (2011) Evolutionary Conservation of the Basal Ganglia as a Common Vertebrate Mechanism for Action Selection. Curr Biol 21:1081–1091.

Stephenson-Jones M, Yu K, Ahrens S, Tucciarone JM, van Huijstee AN, Mejia LA, Penzo MA, Tai L-H, Wilbrecht L, Li B (2016) A basal ganglia circuit for evaluating action outcomes. Nature 539:289–293.

Stopper CM, Tse MTL, Montes DR, Wiedman CR, Floresco SB (2014) Overriding Phasic Dopamine Signals Redirects Action Selection during Risk/Reward Decision Making. Neuron 84:177–189.

Storm JF (1988) Temporal integration by a slowly inactivating K+ current in hippocampal neurons. Nature 336:379–381.

Strausfeld NJ, Hirth F (2013) Deep Homology of Arthropod Central Complex and Vertebrate Basal Ganglia. Science (80-) 340:157–161.

Stuart GJ, Spruston N (2015) Dendritic integration: 60 years of progress. Nat Neurosci 18:1713–1721.

Subramaniam M, Althof D, Gispert S, Schwenk J, Auburger G, Kulik A, Fakler B, Roeper J (2014a) Mutant alpha-synuclein enhances firing frequencies in dopamine substantia nigra neurons by oxidative impairment of A-type potassium channels. J Neurosci 34:13586–13599.

Subramaniam M, Kern B, Vogel S, Klose V, Schneider G, Roeper J (2014b) Selective increase of in vivo firing frequencies in DA SN neurons after proteasome inhibition in the ventral midbrain. Eur J Neurosci 40:2898–2909.

Sugam JA, Day JJ, Wightman RM, Carelli RM (2012) Phasic Nucleus Accumbens Dopamine Encodes Risk-Based Decision-Making Behavior. Biol Psychiatry 71:199–205.

Sullivan PF, Lin D, Tzeng J-Y, van den Oord E, Perkins D, Stroup TS, Wagner M, Lee S, Wright FA, Zou F, Liu W, Downing AM, Lieberman J, Close SL (2008) Genomewide association for schizophrenia in the CATIE study: results of stage 1. Mol Psychiatry 13:570–584.

Sulzer D, Cragg SJ, Rice ME (2016) Striatal dopamine neurotransmission: Regulation of release and uptake. Basal Ganglia 6:123–148.

Sunsay C, Rebec G V (2014) Extinction and reinstatement of phasic dopamine signals in the nucleus accumbens core during Pavlovian conditioning. Behav Neurosci 128:579–587.

Surmeier DJ, Carrillo-Reid L, Bargas J (2011) Dopaminergic modulation of striatal neurons, circuits, and assemblies. Neuroscience 198:3–18.

Surmeier DJ, Ding J, Day M, Wang Z, Shen W (2007) D1 and D2 dopamine-receptor modulation of striatal glutamatergic signaling in striatal medium spiny neurons. Trends Neurosci 30:228–235.

Surmeier DJ, Plotkin J, Shen W (2009) Dopamine and synaptic plasticity in dorsal striatal circuits controlling action selection. Curr Opin Neurobiol 19:621–628.

Sutton MA, Schuman EM (2006) Dendritic Protein Synthesis, Synaptic Plasticity, and Memory. Cell 127:49–58.

Sutton RS (1988) Learning to predict by the methods of temporal differences. Mach Learn 3:9–44.

Sutton RS, Barto AG (1981) Toward a modern theory of adaptive networks: expectation and prediction. Psychol Rev 88:135–170.

Sutton RS, Barto AG (1998) Reinforcement learning : an introduction. MIT Press.

Swanson JM, Kinsbourne M, Nigg J, Lanphear B, Stefanatos GA, Volkow N, Taylor E, Casey BJ, Castellanos FX, Wadhwa PD (2007) Etiologic Subtypes of Attention-Deficit/Hyperactivity Disorder: Brain Imaging, Molecular Genetic and Environmental Factors and the Dopamine Hypothesis. Neuropsychol Rev 17:39–59.

Takeda H, Tsuji M, Matsumiya T (1998) Changes in head-dipping behavior in the hole-board test reflect the anxiogenic and/or anxiolytic state in mice. Eur J Pharmacol 350:21–29.

Tang Y-Q, Zhou J-H, Yang F, Zheng J, Wang K (2014) The tetramerization domain potentiates Kv4 channel function by suppressing closed-state inactivation. Biophys J 107:1090–1104.

Tang Y-QQ, Liang P, Zhou J, Lu Y, Lei L, Bian X, Wang K (2013) Auxiliary KChIP4a suppresses A-type K+ current through Endoplasmic Reticulum (ER) retention and promoting closed-state inactivation of Kv4 channels. J Biol Chem 288:14727–14741.

Tarfa RA, Evans RC, Khaliq ZM (2017) Enhanced sensitivity to hyperpolarizing inhibition in mesoaccumbal relative to nigrostriatal dopamine neuron subpopulations. J Neurosci.

Taylor Tavares J V., Clark L, Furey ML, Williams GB, Sahakian BJ, Drevets WC (2008) Neural basis of abnormal response to negative feedback in unmedicated mood disorders. Neuroimage 42:1118–1126.

Tecuapetla F, Jin X, Lima SQ, Costa RM (2016) Complementary Contributions of Striatal Projection Pathways to Action Initiation and Execution. Cell 166:703–715.

Tempel BL, Papazian DM, Schwarz TL, Jan YN, Jan LY (1987) Sequence of a probable potassium channel component encoded at Shaker locus of Drosophila. Science 237:770–775.

Tepper JM, Lee CR (2007) GABAergic control of substantia nigra dopaminergic neurons. In, pp 189–208.

Tesauro G (1992) Practical issues in temporal difference learning. Mach Learn 8:257–277.

Thiele SL, Chen B, Lo C, Gertler TS, Warre R, Surmeier JD, Brotchie JM, Nash JE (2014) Selective loss of bi-directional synaptic plasticity in the direct and indirect striatal output pathways accompanies generation of parkinsonism and l-DOPA induced dyskinesia in mouse models. Neurobiol Dis 71:334–344.

Thomsen M, Hall FS, Uhl GR, Caine SB (2009) Dramatically Decreased Cocaine Self-Administration in Dopamine But Not Serotonin Transporter Knock-Out Mice. J Neurosci 29:1087–1092.

Thorndike EL (1898) Animal intelligence: An experimental study of the associative processes in animals. Psychol Rev Monogr Suppl 2:i-109.

Tian J, Huang R, Cohen JY, Osakada F, Kobak D, Machens CK, Callaway EM, Uchida N, Watabe-Uchida M (2016) Distributed and Mixed Information in Monosynaptic Inputs to Dopamine Neurons. Neuron 91:1374–1389.

Tian J, Uchida N (2015) Habenula Lesions Reveal that Multiple Mechanisms Underlie Dopamine Prediction Errors. Neuron 87:1304–1316.

Tieu K (2011) A guide to neurotoxic animal models of Parkinson's disease. Cold Spring Harb Perspect Med 1:a009316.

Tobler PN, Dickinson A, Schultz W (2003) Coding of Predicted Reward Omission by Dopamine Neurons in a Conditioned Inhibition Paradigm. J Neurosci 23.

Tobler PN, Fiorillo CD, Schultz W (2005) Adaptive Coding of Reward Value by Dopamine Neurons. Science (80-) 307:1642–1645.

Tolman EC (1948) Cognitive maps in rats and men. Psychol Rev 55:189–208.

Torregrossa MM, Taylor JR (2013) Learning to forget: manipulating extinction and reconsolidation processes to treat addiction. Psychopharmacology (Berl) 226:659–672.

Torres GE, Gainetdinov RR, Caron MG (2003) Plasma membrane monoamine transporters: structure, regulation and function. Nat Rev Neurosci 4:13–25.

Treichler FR, Hall JF (1962) The relationship between deprivation weight loss and several measures of activity. J Comp Physiol Psychol 55:346–349.

Tronche F, Casanova E, Turiault M, Sahly I, Kellendonk C (2002) When reverse genetics meets physiology: the use of site-specific recombinases in mice. FEBS Lett 529:116–121.

Truchet B, Manrique C, Sreng L, Chaillan FA, Roman FS, Mourre C (2012) Kv4 potassium channels modulate hippocampal EPSP-spike potentiation and spatial memory in rats. Learn Mem 19:282–

293.

Tucker KR, Huertas MA, Horn JP, Canavier CC, Levitan ES (2012) Pacemaker Rate and Depolarization Block in Nigral Dopamine Neurons: A Somatic Sodium Channel Balancing Act. J Neurosci 32.

Tukey JW (John W (1977) Exploratory data analysis. Addison-Wesley Pub. Co.

Turrigiano G (2012) Homeostatic synaptic plasticity: local and global mechanisms for stabilizing neuronal function. Cold Spring Harb Perspect Biol 4:a005736.

Tye KM, Deisseroth K (2012) Optogenetic investigation of neural circuits underlying brain disease in animal models. Nat Rev Neurosci 13:251–266.

Tye KM, Mirzabekov JJ, Warden MR, Ferenczi EA, Tsai H-C, Finkelstein J, Kim S-Y, Adhikari A, Thompson KR, Andalman AS, Gunaydin LA, Witten IB, Deisseroth K (2012) Dopamine neurons modulate neural encoding and expression of depression-related behaviour. Nature 493:537–541.

Ubl B, Kuehner C, Kirsch P, Ruttorf M, Diener C, Flor H (2015) Altered neural reward and loss processing and prediction error signalling in depression. Soc Cogn Affect Neurosci 10:1102–1112.

Uhl GGR, Liu Q-RQ, Drgon T, Johnson C, Walther D, Rose JE, David SSP, Niaura R, Lerman C (2008) Molecular genetics of successful smoking cessation: convergent genome-wide association study results. Arch Gen Psychiatry 65:683.

Ungless MA, Grace AA (2012) Are you or aren't you? Challenges associated with physiologically identifying dopamine neurons. Trends Neurosci 35:422–430.

Ungless MA, Magill PJ, Bolam JP (2004) Uniform Inhibition of Dopamine Neurons in the Ventral Tegmental Area by Aversive Stimuli. Science (80-) 303:2040–2042.

Ungless MA, Whistler JL, Malenka RC, Bonci A (2001) Single cocaine exposure in vivo induces long-term potentiation in dopamine neurons. Nature 411:583–587.

Vaccarino F, Franklin KB (1982) Self-stimulation and circling reveal functional differences between medial and lateral substantia nigra. Behav Brain Res 5:281–295.

Valenti O, Gill KM, Grace AA (2012) Different stressors produce excitation or inhibition of mesolimbic dopamine neuron activity: response alteration by stress pre-exposure. Eur J Neurosci 35:1312–1321.

Vallone D, Picetti R, Borrelli E (2000) Structure and function of dopamine receptors. Neurosci Biobehav Rev 24:125–132.

van Zessen R, Phillips JL, Budygin EA, Stuber GD (2012) Activation of VTA GABA Neurons Disrupts Reward Consumption. Neuron 73:1184–1194.

van Enkhuizen J, Henry BL, Minassian A, Perry W, Milienne-Petiot M, Higa KK, Geyer MA, Young JW (2014) Reduced dopamine transporter functioning induces high-reward risk-preference consistent with bipolar disorder. Neuropsychopharmacology 39:3112–3122.

Vaughan RA, Foster JD (2013) Mechanisms of dopamine transporter regulation in normal and disease states. Trends Pharmacol Sci 34:489–496.

Venter JC et al. (2001) The Sequence of the Human Genome. Science (80-) 291.

Vernon J, Irvine EE, Peters M, Jeyabalan J, Giese KP (2016) Phosphorylation of K+ channels at single residues regulates memory formation. Learn Mem 23:174–181.

Vetulani J (2013) Early maternal separation: a rodent model of depression and a prevailing human condition. Pharmacol Rep 65:1451–1461.

Viggiano D, Ruocco LA, Sadile AG (2003) Dopamine phenotype and behaviour in animal models: in relation to attention deficit hyperactivity disorder. Neurosci Biobehav Rev 27:623–637.

Volkow ND, Koob GF, McLellan AT (2016) Neurobiologic Advances from the Brain Disease Model of Addiction Longo DL, ed. N Engl J Med 374:363–371.

Volkow ND, Wang G, Fowler JS, Logan J, Gerasimov M, Maynard L, Ding Y, Gatley SJ, Gifford A, Franceschi D (2001) Therapeutic doses of oral methylphenidate significantly increase extracellular dopamine in the human brain. J Neurosci 21:RC121.

Waelti P, Dickinson A, Schultz W (2001) Dopamine responses comply with basic assumptions of formal learning theory. Nature 412:43–48.

Wahlsten D (2010) Mouse behavioral testing : how to use mice in behavioral neuroscience. Academic.

Walsh RN, Cummins RA (1976) The Open-Field Test: a critical review. Psychol Bull 83:482–504.

Waltz JA, Schweitzer JB, Gold JM, Kurup PK, Ross TJ, Jo Salmeron B, Rose EJ, McClure SM, Stein EA (2009) Patients with Schizophrenia have a Reduced Neural Response to Both Unpredictable and Predictable Primary Reinforcers. Neuropsychopharmacology 34:1567–1577.

Wang JQ, McGinty JF (1996) D1 and D2 receptor regulation of preproenkephalin and preprodynorphin mRNA in rat striatum following acute injection of amphetamine or methamphetamine. Synapse 22:114–122.

Wang M, Vijarayaghavan S, Goldman-Rakic PS (2004) Selective D2 Receptor Actions on Working Memory. Science (80-) 303:853–856.

Wang Z, Kai L, Day M, Ronesi J, Yin HH, Ding J, Tkatch T, Lovinger DM, Surmeier DJ (2006) Dopaminergic Control of Corticostriatal Long-Term Synaptic Depression in Medium Spiny Neurons Is Mediated by Cholinergic Interneurons. Neuron 50:443–452.

Watabe-Uchida M, Zhu L, Ogawa SK, Vamanrao A, Uchida N (2012) Whole-Brain Mapping of Direct Inputs to Midbrain Dopamine Neurons. Neuron 74:858–873.

Watanabe M, Kodama T, Hikosaka K (1997) Increase of extracellular dopamine in primate prefrontal cortex during a working memory task. J Neurophysiol 78:2795–2798.

Watanabe S, Hoffman DA, Migliore M, Johnston D (2002) Dendritic K+ channels contribute to spike-timing dependent long-term potentiation in hippocampal pyramidal neurons. Proc Natl Acad Sci U S A 99:8366–8371.

Wattler S, Kelly M, Nehls M (1999) Construction of gene targeting vectors from lambda KOS genomic libraries. Biotechniques 26:1150–1156, 1158, 1160.

Wayment HK, Schenk JO, Sorg BA (2001) Characterization of Extracellular Dopamine Clearance in the Medial Prefrontal Cortex: Role of Monoamine Uptake and Monoamine Oxidase Inhibition. J Neurosci 21.

Weber P, Ohlendorf D, Wendoloski J, Salemme F (1989) Structural origins of high-affinity biotin binding to streptavidin. Science (80-) 243.

Wei A, Covarrubias M, Butler A, Baker K, Pak M, Salkoff L (1990) K+ current diversity is produced by an extended gene family conserved in Drosophila and mouse. Science 248:599–603.

Weißflog L, Scholz CJ, Jacob CP, Nguyen TT, Zamzow K, Groß-Lesch S, Renner TJ, Romanos M, Rujescu D, Walitza S, Kneitz S, Lesch KP, Reif A (2013) KCNIP4 as a candidate gene for personality disorders and adult ADHD. Eur Neuropsychopharmacol 23:436–447.

Whiteford HA, Degenhardt L, Rehm J, Baxter AJ, Ferrari AJ, Erskine HE, Charlson FJ, Norman RE, Flaxman AD, Johns N, Burstein R, Murray CJ, Vos T (2013) Global burden of disease attributable to mental and substance use disorders: findings from the Global Burden of Disease Study 2010. Lancet 382:1575–1586.

Williams S, Goldman-Rakic PS (1998) Widespread origin of the primate mesofrontal dopamine system. Cereb Cortex 8:321–345.

Willuhn I, Burgeno LM, Everitt BJ, Phillips PEM (2012) Hierarchical recruitment of phasic dopamine signaling in the striatum during the progression of cocaine use. Proc Natl Acad Sci U S A 109:20703–20708.

Wilson CJ, Callaway JC (2000) Coupled oscillator model of the dopaminergic neuron of the substantia nigra. J Neurophysiol 83:3084–3100.

Wilson CJ, Park MR (1989) Capacitance compensation and bridge balance adjustment in intracellular recording from dendritic neurons. J Neurosci Methods 27:51–75.

Wilson CJ, Young SJ, Groves PM (1977) Statistical properties of neuronal spike trains in the substantia nigra: Cell types and their interactions. Brain Res 136:243–260.

Winton-Brown TT, Fusar-Poli P, Ungless MA, Howes OD (2014) Dopaminergic basis of salience dysregulation in psychosis. Trends Neurosci 37:85–94.

Wise RA (1981) Intracranial self-stimulation: mapping against the lateral boundaries of the dopaminergic cells of the substantia nigra. Brain Res 213:190–194.

Wise RA (2002) Brain Reward Circuitry: Insights from Unsensed Incentives. Neuron 36:229–240.

Witten IBB, Steinberg EEE, Lee SYY, Davidson TJJ, Zalocusky KAA, Brodsky M, Yizhar O, Cho SLL, Gong S, Ramakrishnan C, Stuber GDD, Tye KMM, Janak PHH, Deisseroth K (2011) Recombinase-driver rat lines: Tools, techniques, and optogenetic application to dopamine-mediated reinforcement. Neuron 72:721–733.

Wolfart J, Neuhoff H, Franz O, Roeper J (2001) Differential expression of the small-conductance, calcium-activated potassium channel SK3 is critical for pacemaker control in dopaminergic midbrain neurons. J Neurosci 21:3443–3456.

Wolfart J, Roeper J (2002) Selective coupling of T-type calcium channels to SK potassium channels prevents intrinsic bursting in dopaminergic midbrain neurons. J Neurosci 22:3404–3413.

Wong DF, Wagner HN, Tune LE, Dannals RF, Pearlson GD, Links JM, Tamminga CA, Broussolle EP,

Ravert HT, Wilson AA, Toung JK, Malat J, Williams JA, O'Tuama LA, Snyder SH, Kuhar MJ, Gjedde A (1986) Positron emission tomography reveals elevated D2 dopamine receptors in drug-naive schizophrenics. Science 234:1558–1563.

Xiao L, Priest MF, Nasenbeny J, Lu T, Kozorovitskiy Y (2017) Biased Oxytocinergic Modulation of Midbrain Dopamine Systems. Neuron.

Xu W, Cohen-Woods S, Chen Q, Noor A, Knight J, Hosang G, Parikh S V, De Luca V, Tozzi F, Muglia P, Forte J, McQuillin A, Hu P, Gurling HM, Kennedy JL, McGuffin P, Farmer A, Strauss J, Vincent JB (2014) Genome-wide association study of bipolar disorder in Canadian and UK populations corroborates disease loci including SYNE1 and CSMD1. BMC Med Genet 15:2.

Yagishita S, Hayashi-Takagi A, Ellis-Davies GCR, Urakubo H, Ishii S, Kasai H (2014) A critical time window for dopamine actions on the structural plasticity of dendritic spines. Science 345:1616–1620.

Yamada T, McGeer PL, Baimbridge KG, McGeer EG (1990) Relative sparing in Parkinson's disease of substantia nigra dopamine neurons containing calbindin-D28K. Brain Res 526:303–307.

Yamamoto S, Seto ES (2014) Dopamine dynamics and signaling in Drosophila: an overview of genes, drugs and behavioral paradigms. Exp Anim 63:107–119.

Yan Y, Nabeshima T (2009) Mouse model of relapse to the abuse of drugs: Procedural considerations and characterizations. Behav Brain Res 196:1–10.

Yang F, Feng L, Zheng F, Johnson SW, Du J, Shen L, Wu C, Lu B (2001) GDNF acutely modulates excitability and A-type K(+) channels in midbrain dopaminergic neurons. Nat Neurosci 4:1071–1078.

Yavich L, Forsberg MM, Karayiorgou M, Gogos JA, Männistö PT (2007) Site-Specific Role of Catechol-O-Methyltransferase in Dopamine Overflow within Prefrontal Cortex and Dorsal Striatum. J Neurosci 27.

Yin H, Zhuang X, Balleine B (2006) Instrumental learning in hyperdopaminergic mice. Neurobiol Learn Mem 85:283–288.

Yin HH, Mulcare SP, Hilário MRF, Clouse E, Holloway T, Davis MI, Hansson AC, Lovinger DM, Costa RM (2009) Dynamic reorganization of striatal circuits during the acquisition and consolidation of a skill. Nat Neurosci 12:333–341.

York DH (1973) Motor responses induced by stimulation of the substantia nigra. Exp Neurol 41:323–330.

Youdim MBH, Edmondson D, Tipton KF (2006) The therapeutic potential of monoamine oxidase inhibitors. Nat Rev Neurosci 7:295–309.

Yttri EA, Dudman JT (2016) Opponent and bidirectional control of movement velocity in the basal ganglia. Nature 533:402–406.

Yu C, Gupta J, Chen J-F, Yin HH (2009) Genetic deletion of A2A adenosine receptors in the striatum selectively impairs habit formation. J Neurosci 29:15100–15103.

Zaborszky L, Vadasz C (2001) The Midbrain Dopaminergic System: Anatomy and Genetic Variation in Dopamine Neuron Number of Inbred Mouse Strains. Behav Genet 31:47–59.

Zaghloul KA, Blanco JA, Weidemann CT, McGill K, Jaggi JL, Baltuch GH, Kahana MJ (2009) Human Substantia Nigra Neurons Encode Unexpected Financial Rewards. Science (80-) 323.

Zhang X, Bearer EL, Boulat B, Hall FS, Uhl GR, Jacobs RE (2010) Altered Neurocircuitry in the Dopamine Transporter Knockout Mouse Brain Manzoni OJ, ed. PLoS One 5:e11506.

Zhang Y, MacLean JN, An WF, Lanning CC, Harris-Warrick RM (2003) KChIP1 and Frequenin Modify shal-Evoked Potassium Currents in Pyloric Neurons in the Lobster Stomatogastric Ganglion. J Neurophysiol 89:1902–1909.

Zhou J, Tang Y, Zheng Q, Li M, Yuan T, Chen L, Huang Z, Wang K (2015) Different KChIPs Compete for Heteromultimeric Assembly with Pore-Forming Kv4 Subunits. Biophys J 108:2658–2669.

Zhou Y, Suzuki Y, Uchida K, Tominaga M (2013) Identification of a splice variant of mouse TRPA1 that regulates TRPA1 activity. Nat Commun 4:2399.

Zhuang X, Oosting RS, Jones SR, Gainetdinov RR, Miller GW, Caron MG, Hen R (2001) Hyperactivity and impaired response habituation in hyperdopaminergic mice. Proc Natl Acad Sci U S A 98:1982–1987.

Ziegler S, Pedersen ML, Mowinckel AM, Biele G (2016) Modelling ADHD: A review of ADHD theories through their predictions for computational models of decision-making and reinforcement learning. Neurosci Biobehav Rev 71:633–656.

Zweifel LS et al. (2009) Disruption of NMDAR-dependent burst firing by dopamine neurons provides

selective assessment of phasic dopamine-dependent behavior. Proc Natl Acad Sci 106:7281–7288.

Zweifel LS, Argilli E, Bonci A, Palmiter RD (2008) Role of NMDA Receptors in Dopamine Neurons for Plasticity and Addictive Behaviors. Neuron 59:486–496.

Curriculum Vitae

Personal details

Name: Kauê Machado Costa
Date of birth: August 29th 1989
Place of birth: Belém, Pará, Brazil

Education

2013-2018 **PhD in Neuroscience**
Institute of Neurophysiology, Goethe University; Frankfurt am Main, Germany
International Max Planck Research School for Neural Circuits, Max Planck Institute for Brain Research; Frankfurt am Main, Germany
Mentor: **Dr. Jochen Roeper**

2010-2012 **Master's degree in Physiology**
School of Medicine of Ribeirão Preto, University of São Paulo, Ribeirão Preto, Brazil
Mentor: **Dr. Benedito Honório Machado**

2006-2010 **Bachelor's degree in Biological Sciences**
Institute of Biological Sciences, Federal University of Pará, Belém, Brazil
Mentor: **Dr. Manoel da Silva Filho**

Fellowships and employment

2013-Current **Graduate research assistant**, Goethe University (Germany)

2012-2013 **Doctoral graduate fellowship**, Max Planck Society (Germany)

2010-2012 **Master graduate fellowship**, Coordination for Improvement of Higher Education Personnel (Brazil)

2006-2010 **Undergraduate Scientific Initiation fellowship,** National Council for Scientific and Technological Development (Brazil)

Additional research experience

2013 **Graduate internship**, Department of Neural Systems and Coding, Max Planck Institute for Brain Research, Frankfurt am Main, Germany
Mentor: **Dr. Gilles Laurent**

2012 **Voluntary internship,** School of Medicine of Ribeirão Preto, University of São Paulo, Ribeirão Preto, Brazil
Mentor: **Dr. Norberto Garcia Cairasco**

Awards

2017 **Trainee Professional Development Award;** Society for Neuroscience, USA

Best oral presentation award; Barcelona Young Neuroscientists Symposium, Spain

2016 **Exceptional poster presentation award;** 95th Annual meeting of the German Physiological Society, Germany

2012 **Exceptional poster presentation award;** 16th Brazilian Symposium of Cardiovascular Physiology, Brazil

2011 **Exceptional poster presentation award;** 15th Brazilian Symposium of Cardiovascular Physiology, Brazil

2010 **Honor award for the highest academic achievement in the Biological Sciences' bachelor program;** Federal University of Pará, Brazil

2008 **Exceptional poster presentation award;** 23rd Annual Meeting of the Brazilian Federation of Experimental Biology Societies, Brazil

2006 **Honor award for first place in the admissions ranking for the Biological Sciences' bachelor program;** Federal University of Pará, Brazil

2003 **Honor award for academic achievement;** Sistema de Ensino Universo, Brazil

José Márcio Ayres award for young naturalists; Emílio Goeldi Museum, Brazil

Grants and funding

2017 **Travel grant;** to attend the 47th Annual Society for Neuroscience Meeting (USA); granted by the Vereinigung von Freunden und Förderern der Goethe-Universität, Germany

Travel grant; to attend the Barcelona Young Neuroscientists Symposium (Spain); granted by the symposium organizing committee, Spain

Specialized training

2014 **Ion Channel and Synaptic Transmission Summer Course;** Cold Spring Harbor Laboratory, Cold Spring Harbor, USA

2013 **Writing in the Sciences;** Stanford University (online course)

Certified Course on Laboratory Animal Science: FELASA Category B; Berliner Fortbildungen, Berlin, Germany

2009 **Summer Course of Physiology;** Department of Physiology, School of Medicine of Ribeirão Preto, University of São Paulo, Ribeirão Preto, Brazil

Winter Course of Comparative Physiology; Department of Physiology, Institute of Biosciences, University of São Paulo, São Paulo, Brazil

Short courses and workshops

2017 **Voice and Body Coaching: Communicating with Confidence and Accuracy;** Goethe Graduate Academy, Goethe University, Frankfurt am Main, Germany

2016 **Data Science and Data Skills for Neuroscientists;** Society for Neuroscience, San Diego, USA

2015 **Scientific Paper Writing: Special Focus on Life and Medical Sciences;** Goethe Graduate Academy, Goethe University, Frankfurt am Main, Germany

2014 **Short Course Statistics (R-Course);** Goethe Graduate Academy, Goethe University, Frankfurt am Main, Germany

Using NEURON to Model Cells and Networks; Society for Neuroscience, Washington D.C., USA

2013 **Personality Based Communication for Academics;** Goethe Graduate Academy, Goethe University, Frankfurt am Main, Germany

2012 **Writing a Review Paper;** Goethe Graduate Academy, Goethe University, Frankfurt am Main, Germany

Publications

Journal articles

2017 Messer M., Costa K.M., Roeper J, Schneider G. **Multi-scale detection of rate changes in spike trains with weak dependencies.** Journal of Computational Neuroscience, 42(2), 187–201, 2017. DOI:10.1007/s10827-016-0635-3

de Macedo M.S.F.C., Costa K.M., da Silva Filho M. **Voice disorder in systemic lupus erythematosus**. PLoS One, 12(4): e0175893, 2017. DOI: 10.1371/journal.pone.0175893

2014 Costa K.M. **The Effects of Aging on Substantia Nigra Dopamine Neurons.** The Journal of Neuroscience, 34 (46), 15133-15134, 2014. DOI: 10.1523/JNEUROSCI. 3739-14.2014

Costa K.M., Accorsi-Mendonça D., Moraes D.J. and Machado B.H. **Evolution and physiology of neural oxygen sensing.** Frontiers in Physiology, 5:302, 2014. DOI: 10.3389/fphys.2014.00302

Moraes D.J.A., Bonagamba L.G.H., Costa K.M, Costa-Silva J.H., Zoccal D.B., Machado B.H. **Short-term sustained hypoxia induces changes in the coupling of sympathetic and respiratory activities in rats.** The Journal of Physiology, 592: 2013–2033, 2014. DOI: 10.1113/jphysiol.2013.262212

Granjeiro É.M., Marroni S.S., Dias D.P.M., Bonagamba L.G.H., Costa K.M., do Santos J.C., Oliveira J.A.C., Machado B.H., Garcia-Cairasco N. **Behavioral and Cardiorespiratory Responses to Bilateral Microinjections of Oxytocin into the Central Nucleus of Amygdala of Wistar Rats, an Experimental Model of Compulsion**. PLoS One 9(7): e99284, 2014. DOI:10.1371/journal.pone.0099284

Lourenço B.M., Costa K.M., da Silva Filho M. **Voice Disorder in Cystic Fibrosis Patients**. PLoS One, 9(5): e96769, 2014. DOI:10.1371/journal.pone.0096769

2013 Costa K.M., Moraes D.J.A., Machado B.H. **Acute inhibition of glial cells in the NTS does not affect respiratory and sympathetic activities in rats exposed to chronic intermittent hypoxia**. Brain Research, 1496, p. 36-48, 2013. DOI: 10. 1016/j.brainres.2012.12.003.

da Silva Filho M., Santos D.V., Costa K.M. **A new low cost wide-field illumination method for photooxidation of intracellular fluorescent markers**. PLoS One, 8(2): e56512, 2013. DOI:10.1371/journal.pone.0056512.

2012 Tejada J.[1], Costa K.M.[1], Bertti P.[1], Garcia-Cairasco N. **The epilepsies: Complex challenges needing complex solutions.** Epilepsy & Behavior. Volume 26, Issue 3, 212-228, 2013. DOI: 10.1016/j.yebeh.2012.09.029

[1] Joint first authorship

Santos D.V., Costa K.M., Vaz M.C.G., da Silva Filho M. **Relations between dendritic morphology, spatial distribution and firing patterns in Layer I neurons**. Brazilian Journal of Medical and Biological Research, 45(12), p.1221-1233, 2012. DOI: 10.1590/S0100-879X2012007500137

2010 Costa J.C., Costa K.M., Nascimento J. L. M. **Scopolamine- and diazepam-induced amnesia are blocked by systemic and intraseptal administration of substance P and choline chloride**. Peptides, 31(9), p.1756-1760, 2010. DOI: 10.1016/j.peptides.2010.06.008

Machado B.H., Moraes D.J.A., Costa K.M. **Highlights in basic autonomic neurosciences: Glia and neuromodulation**. Autonomic Neuroscience: Basic & Clinical, 156(1-2), p.1-4, 2010. DOI: 10.1016/j.autneu.2010.06.005

Published conference proceedings

2017 Kovacheva L., Costa K.M., Farassat N., Roeper J. **Behavioral and electrophysiological changes after a unilateral intrastriatal 6-hydroxydopamine lesion in mice**. 96th Annual Meeting of the German Physiological Society, Greiswald. Acta Physiologica, 219, s711: 125-125

Accorsi-Mendonça D., Almado C.E.L., Bonagamba L.G.H., Costa K.M., Castania J.A., Costa-Silva J.H., Zoccal D.B., Moraes D.J.A., Machado B.H. **Neural Mechanisms Involved in Autonomic and Respiratory Changes in Rats, Submitted to Short-Term Sustained Hypoxia**. 6th Chronic Hypoxia Symposium, La Paz. Wilderness & Environmental Medicine , 28(1): e4

2016 Costa K.M., Messer M., Subramaniam M., Schneider G., Roeper J. **Spike train pause detection in midbrain dopamine neurons: identifying the selective effects of KChIP4 knockout.** 95th Annual Meeting of the German Physiological Society, Lübeck. Acta Physiologica, Acta Physiologica, 216, s707: 95

Kovacheva L., Costa K.M., Farassat N., Roeper J. **Full recovery of spontaneous turning bias in an unilateral Intrastriatal 6-OH-dopamine mouse model of Parkinson.** 95th Annual Meeting of the German Physiological Society, Lübeck. Acta Physiologica, 216, s707: 92-93

2014 Costa K.M., Kashiotis A.M., Roeper J. **In vivo recordings in KChIP4 knockout mice reveals a selective role for slowly inactivating A-type channels in the duration of firing pauses in dopaminergic VTA neurons.** 93rd Annual Meeting of the German Physiological Society, Mainz. Acta Physiologica, 210, s695:70-70

2013 Zoccal D.B., Moraes D.J.A., Bonagamba L.G.H., Costa K.M., Costa-Silva J.H., Machado B.H. **Active expiration and sympathetic overactivity induced by short-term sustained hypoxia in rats.** Experimental Biology, Boston, 2013. The FASEB Journal, 27:1207.2

2011 Costa K.M., Moraes D.J.A., Machado B.H. **Do glial cells in the NTS play a role in autonomic and respiratory control in rats?** Joint Meeting ISAN/AAS, Búzios Autonomic Neuroscience: Basic and Clinical, 163, p.76-77

Academic production related to this thesis

Publications

2017 Messer M., Costa K.M., Roeper J, Schneider G. **Multi-scale detection of rate changes in spike trains with weak dependencies.** Journal of Computational Neuroscience, 42(2), 187–201, 2017. DOI:10.1007/s10827-016-0635-3

First author poster presentations

2018 Costa K.M., Roeper J. **Alternative Splicing of KCNIP4 in Dopamine VTA Neurons Controls the Dynamics of Learning from Reward Omission**. Basal Ganglia Gordon Research Conference, Ventura, CA, USA

2017 Costa K.M., Roeper J. **Alternative splicing of KCNIP4 in dopamine VTA neurons controls the dynamics of learning from reward omission.** 47th Annual Society for Neuroscience Meeting, Washington DC, USA, 2017.

2016 Costa K.M., Messer M., Subramaniam M., Schneider G., Roeper J. **Spike train pause detection in midbrain dopamine neurons: identifying the selective effects of KChIP4 knockout.** 95th Annual Meeting of the German Physiological Society, Lübeck, Germany, 2016. **(Exceptional Poster presentation award)**

Costa K.M., Kashioitis A.M., Schneider G., Subramaniam M., Roeper J. **KChIP4: a biophysical amplifier of inhibition in mesolimbic dopamine neurons**. 46th Annual Society for Neuroscience Meeting, San Diego, USA

2014 Costa K.M., Kashioitis A.M., Schneider G., Subramaniam M., Roeper J. **Selective dynamic range compression of in vivo firing of dopamine VTA neurons in KChIP4 knockout mice.** 44th Annual Society for Neuroscience Meeting, Washington DC, USA

Oral presentations and talks

2018 **Alternative Splicing of KCNIP4 in Dopamine VTA Neurons Controls the Dynamics of Learning from Reward Omission**. Basal Ganglia Gordon Research Seminar, Ventura, CA, USA

2017 **KChIP4a: a biophysical modulator of learning from disappointment**. Barcelona Young Neuroscientists Symposium, Barcelona, Spain **(Best oral presentation award).**

KChIP4a: a biophysical modulator of learning from disappointment Young Investigators Colloquium, Frankfurt am Main, Germany

2016 **KChIP4a: a biophysical modulator of learning from disappointment**. Invited talk to the Schoenbaum Lab, NIDA/NIH, Baltimore, USA

KChIP4a: a biophysical modulator of learning from disappointment. Invited talk to the Uchida Lab, Harvard University, Cambridge MA

KChIP4a: a biophysical modulator of learning from disappointment. Invited talk to the Lammel Lab, UC Berkeley, Berkeley, USA

2014 **Selective dynamic range compression of in vivo firing of dopamine VTA neurons in KChIP4 knockout mice.** Invited talk to the Kandel Lab, Columbia University, New York, USA

***In vivo* recordings in KChIP4 knockout mice reveals a selective role for slowly inactivating A-type channels in the duration of firing pauses in dopaminergic VTA neurons.** 93rd Annual Meeting of the German Physiological Society, Mainz, Germany

“In conclusion, it appears that nothing can be more improving to a young naturalist, than a journey in distant countries.”

— Charles Darwin, Voyage of the Beagle